

MODELLING OF RAINFALL GENERATED RUNOFF AND SEDIMENT YIELD

A THESIS

*Submitted in partial fulfilment of the
requirements for the award of the degree*

of

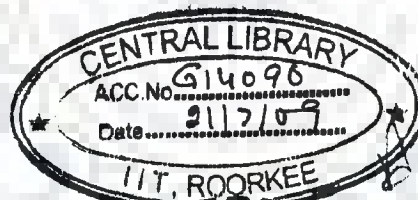
DOCTOR OF PHILOSOPHY

in

WATER RESOURCES DEVELOPMENT

By

PUSHPENDRA KUMAR SINGH



DEPARTMENT OF WATER RESOURCES DEVELOPMENT & MANAGEMENT

INDIAN INSTITUTE OF TECHNOLOGY ROORKEE

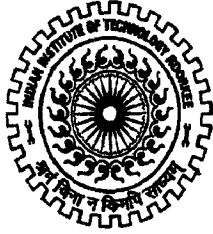
ROORKEE-247 667 (INDIA)

DECEMBER, 2007



©INDIAN INSTITUTE OF TECHNOLOGY ROORKEE, ROORKEE, 2007
ALL RIGHT RESERVED

INDIAN INSTITUTE OF TECHNOLOGY ROORKEE ROORKEE



CANDIDATE'S DECLARATION

I hereby certify that the work which is being presented in the thesis entitled **MODELLING OF RAINFALL GENERATED RUNOFF AND SEDIMENT YIELD** in the partial fulfilment of the requirements for the award of the Degree of Doctor of Philosophy and submitted in the Department of Water Resources Development and Management of the the Indian Institute of Technology Roorkee, Roorkee is an authentic record of my own work carried out during the period from January 2004 to December 2007 under the supervision of Dr. U. C. Chaube, Professor, and Dr. S. K. Mishra, Assistant Professor, Department of Water Resources Development and Management, Indian Institute of Technology Roorkee, Roorkee.

The matter presented in this thesis has not been submitted by me for the award of any other degree in this or any other Institute.

Bingh

(PUSHPENDRA KUMAR SINGH)

This is to certify that the above statement made by the candidate is correct to the best of our knowledge.

(S. K. Mishra)
(S. K. Mishra)
Supervisor

U. C. Chaube
(U. C. Chaube)
Supervisor

Date: 24.12.2007

The Ph. D. Viva-Voce examination of **Mr. Pushpendra Kumar Singh**, Research Scholar, has been held on...11.08.2008.

(S. K. Mishra)
11.08.08
Signature of Supervisors

(Pushpendra Kumar Singh)
Signature of External Examiner

ABSTRACT

Rainfall-runoff-sediment yield modeling is integral to water resources planning, development and management, flood control, environmental impact assessment, erosion and sediment control, water quality modeling and watershed management. A multitude of models are available in hydrologic literature to address the issues related with the runoff and sediment yield modeling. The Soil Conservation Service Curve Number (SCS-CN) method is one of the popular event-based models widely used for estimation of direct runoff for a given storm rainfall event from small watersheds. The method has witnessed myriad applications including those which were not originally intended. Similarly, the synthetic unit hydrograph (SUH) methods are widely used for estimating design flood for ungauged catchments, and for partial data availability conditions. The SUH methods are of paramount importance for developing countries, for majority of the small basins are ungauged. The sediment graph models are particularly used for estimation of time distributed sediment yield and play a significant role in water quality modeling and effectiveness of watershed management programmes. The increased awareness of environmental quality and an efficient control of non-point source pollution have further increased the need for sediment graph models. The present study is undertaken to explore the new/modified or improved versions of SCS-CN method, SUH methods, and sediment graph models on a more sound hydrological perception and a stronger mathematical foundation to perform their prescribed tasks successfully and efficiently.

Revised Soil Moisture Accounting Procedure in SCS-CN Methodology

Recent past has witnessed various improvements/modifications to the existing SCS-CN methodology. Based on certain issues, however, a need of further improvement has been felt for better results. The soil moisture accounting (SMA) procedure that lies behind the SCS-CN methodology is one of them. Introduced by Williams and LaSeur (1976), SMA procedure was employed by Mishra et al. (2004a) to address the variability due to antecedent rainfall and associated soil moisture amount in terms of antecedent moisture condition (AMC). Based on SMA procedure, Michel et al. (2005) proposed a renewed SCS-CN

methodology to overcome the inconsistencies associated with the existing SCS-CN method, including the incorrect parameterization. However, the proposed methodology contains some structural inconsistencies from SMA view point. Specifically, it relies on the existing SCS-CN method, which lacks SMA accountability in the basic proportionality concept or $C = S_r$ concept (Mishra and Singh, 2003a), where C is the runoff coefficient, S_r is the degree of saturation. Secondly, the methodology does not have any expression for estimation of initial soil moisture V_0 and threshold soil moisture or intrinsic parameter S_a . Hence, the present study revisits the existing SCS-CN method for its underlying SMA procedure and provides simple expressions for V_0 and S_a . This revision led to the development of revised version of the Michel et al. model, named as SMA inspired event-based SCS-CN model. Based on the revised SMA procedure, the present study also proposes SMA inspired continuous SCS-CN model parallel to continuous model of Michel et al.

The performance of SMA inspired event-based SCS-CN model, event model of Michel et al., and the existing SCS-CN method has been evaluated by applying them to event rainfall-runoff data of 35 small watersheds of United States. In these applications, the proposed SMA inspired event-based model performs the best, and the existing SCS-CN method performs poorest of all. Further, the performance of SMA inspired continuous SCS-CN model and continuous model of Michel et al. is evaluated by applying both to daily rainfall-runoff data of Hemavati watershed (India). Based on Nash and Sutcliffe (NS) (1970) efficiency criterion, both the models perform equally well for continuous hydrologic simulation; the proposed model however performs marginally better than the Michel et al. model.

Extended Hybrid Model for Synthetic Unit Hydrograph (SUH) Derivation

The unavailability or partial availability of the required rainfall-runoff data in quality and quantity largely initiated the development of SUH methods. However, the efforts still continue for development of new/improved models for synthetic unit hydrograph (SUH) derivation. For example, Bhunya et al. (2005) proposed a hybrid model (HM) for SUH derivation. Though the proposed HM model can be taken as an improvement over the widely used Nash (1957) model, it also has few concerns, which require to be attended for a credible

application. First it ignores the concept of translation, which is essential for describing a dynamic system, and secondly it lacks in its generality. The present study proposes a conceptually sound and theoretically improved extended hybrid model (EHM) by introducing the concept of translation. The proposed EHM model explicitly considers the cascaded approach of Nash (1957) and the hybrid approach of Bhunya et al. (2005) for SUH derivation. The study also proposes a general expression for EHM model. Both EHM and HM models are applied to the short-term data of five catchments (small to medium) ranging from 21 km² to 452.25 km². It is found that the quantitative performance of EHM model in terms of standard error (STDER) and relative error (RE) enhances upon the HM model for the larger catchments. The Nash model performs poorer than both EHM and HM models. Further, a structural diagnosis of the general expression of EHM shows that HM and Nash models are the only specific cases of the earlier one.

Chi-square and Fréchet Distributions for SUH derivation

The probability distribution functions (pdfs) as synthetic unit hydrograph (SUH) is a well accepted technique among the hydrologists. Probably, the similarity between pdf of a distribution with area under the pdf curve to be unity and a conventional unit hydrograph are the two important features of a pdf useful for SUH derivation. The present study explores the potential of one-parameter Chi-square and two-parameter Fréchet distributions for SUH derivation using Horton order ratios (Rodriguez-Iturbe and Valdes, 1979) in comparison to widely used two-parameter Gamma distribution (2PGD) model (Rosso, 1984). Analytical methods are proposed for parameter estimation of the two distributions. Using random generation scheme, the suitability of proposed analytical methods is checked, and it is found that the proposed analytical methods can be used successfully for their intended task. Further, an attempt has been made to search for the possible similarity among the three pdfs, viz., one parameter Chi-square distribution (CSD), two-parameter Fréchet distribution (2PFD), and two-parameter Gamma distribution (2PGD). The three pdfs are applied to two Indian catchments for limited data availability conditions. The results show that SUHs obtained by one parameter CSD and 2PFD are well comparable with those obtained by 2PGD model.

SCS-CN Method Based Sediment Graph Models

The conceptual sediment graph models are popular for estimation of time distribution of sediment yield (sediment graph computation) as well as the total sediment yield due to a particular storm event from a catchment. The present study attempts to develop new conceptual sediment graph models based on three popular and extensively used models/methods (here termed as sub-models), viz., Nash-based IUSG (Nash, 1957), SCS-CN method, and Power law (Novotny and Olem, 1994). Four sediment graph models (SGM₁-SGM₄), corresponding to four different cases are proposed. For SGM₁, both the initial soil moisture V_0 and initial abstraction I_a are assumed to be zero, i.e. $V_0 = 0$ and $I_a = 0$. For SGM₂, $V_0 = 0$, but $I_a \neq 0$; For SGM₃, $V_0 \neq 0$ and $I_a = 0$; and for SGM₄, $V_0 \neq 0$ and $I_a \neq 0$. The proposed sediment graph models take due consideration to the major runoff and, in turn, the sediment yield producing watershed characteristics such as soil type, land use, hydrologic condition, antecedent moisture, and rainfall characteristics. On the basis of number of parameters, SGM₁ is the simplest one, and SGM₄ the most complex sediment graph model. The proposed sediment models are applied to the observed short-term sediment yield data of Nagwan watershed. Goodness-of-fit (GOF) results show that the proposed sediment graph models matched closely with the observed sediment graphs and the total sediment yield computed by them is in close agreement with the observed sediment yield for the three storm events. The results indicate that both components of hydrologic cycle affect both the sediment graph derivation and sediment yield computation, and the proposed models are most sensitive to the exponent of the Power law, β , than the other parameters. The workability of simplest SGM₁ model is further evaluated using the short-term sediment yield data of Ramganga catchment. The resulting higher values of model efficiencies and lower values of RE of peak sediment flow rate Q_{ps} and total sediment yield Q_s further supports the suitability of the proposed sediment graph model for computation of time distributed sediment yield and total sediment yield as well.

Keywords: SCS-CN method, Soil moisture accounting, Synthetic unit hydrograph, Probability distribution function, Sediment graph, Rainfall-runoff-sediment yield.

ACKNOWLEDGEMENT

At very first instant, the author bows his head with a lot reverence to Him who is omnipresent, omnipotent and omniscient and is the cause behind every effect.

It is my great pleasure in expressing my profound indebtedness and heartfelt gratitude and reverence to my supervisors Dr. U. C. Chaube, Professor, and Dr. S. K. Mishra, Assistant Professor, Department of Water Resources Development and Management, for their invaluable guidance, constant encouragement, moral support and wholehearted co-operation, and ever valuable help during this research work.. Their painstaking efforts in going through the manuscript, and personal interest into the research work can not be described in words.

I remain extremely indebted with gratitude to my supervisor Dr. S. K. Mishra, for his guidance at each step, meticulous observations, creative suggestions, and invaluable help during this research work.

I am highly grateful and indebted to Dr. P. K. Bhunya, Scientist, National Institute of Hydrology Roorkee, for his ever valuable help during this research work and motivation for generating research abilities and interests.

I wish to express my gratitude to the respected family of my supervisor Dr. U. C. Chaube for extending their love, blessings, and moral encouragement during the course of research work.

I am highly indebted to the respected family of my supervisor Dr. S. K. Mishra, Mrs. Mishra Bhabhi Ji, Maa Ji, daughters Sivangi and Surbhi for their ever lasting love, blessings, and moral encouragement.

I am very much thankful to Dr. M. K. Jain, Assistant Professor, Department of Hydrology, Indian Institute of Technology Roorkee, Dr. R. P. Pandey, Dr. J. V. Taygi, Scientists, National Institute of Hydrology Roorkee, for their esteemed help and constant encouragement.

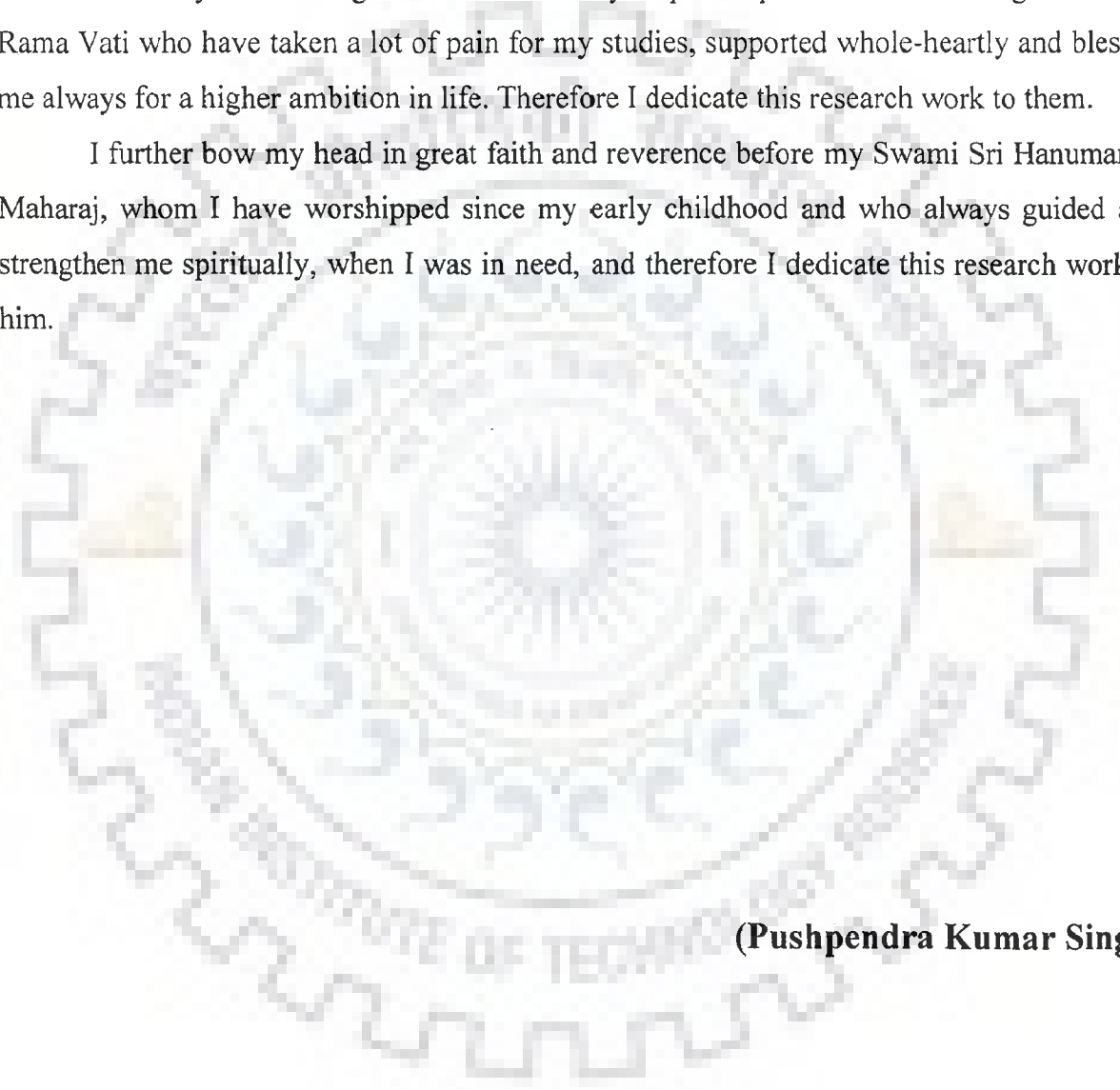
I thankfully acknowledge the help by the fellow research scholars Mr. Harsh Vardhan Trivedi, Mr. Pradeep Kumar, Mr. Tejwant Singh Brar, Mr. Dhananjay Deshmukh, Mr. S. R. Yadav, Mr. Bhaskar Nikam, Mr. H. G. Gundekar, Mr. Soban S. Rawat, Mrs. K. P. Samal, and other will-wishrs for their direct and/or indirect help at various stages of this research work.

I wish to express my gratitude and warm sentiments to my elder brother Amrendra and Bhabhi Ji; my younger brothers Ram Ji, Hari Om, and Alok, for their love and continuous encouragement, moral support and help during the course of research work.

It gives me immense pleasure to express my special thanks to my wife Rakhi Singh, whose continuous loving care, emotional support, and wholehearted co-operation helped me a lot to complete this research work efficiently, and therefore I dedicate this research work to her.

I bow my head with great reverence to my respected parents Sri Ram Singh and Smt. Rama Vati who have taken a lot of pain for my studies, supported whole-heartly and blessed me always for a higher ambition in life. Therefore I dedicate this research work to them.

I further bow my head in great faith and reverence before my Swami Sri Hanuman Ji Maharaj, whom I have worshipped since my early childhood and who always guided and strengthen me spiritually, when I was in need, and therefore I dedicate this research work to him.



(Pushpendra Kumar Singh)

TABLE OF CONTENTS

Chapter No.	Title	Page No.
	Candidate's Declaration	
	Abstract	i
	Acknowledgement	v
	Table of Contents	vii
	List of Figures	xii
	List of Tables	xvi
	List of Symbols	xviii
1	INTRODUCTION	1
1.1	RUNOFF MODELING	1
1.2	SEDIMENT YIELD MODELING	2
1.3	RESEARCH OBJECTIVES	2
1.4	ORGANIZATION OF THESIS	3
2	REVIEW OF LITERATURE	5
2.1	SCS-CN METHOD	5
2.1.1	Historical Background	5
2.1.2	Theoretical Background	7
2.1.3	Advantages and Limitations	10
2.1.4	Watershed Characteristics Affecting CN Estimation	12
2.1.5	CN Estimation Methods	14
2.1.6	Applications	16
2.1.7	Remarks	28
2.2	SYNTHETIC UNIT HYDROGRAPH (SUH) METHODS	29
2.2.1	Background	29
2.2.2	Popular Synthetic Unit Hydrograph Methods	30

2.2.3	Conceptual Synthetic Unit Hydrograph Methods	35
2.2.4	Geomorphologic Instantaneous Unit Hydrograph (GIUH) Based SUH Methods	39
2.2.5	Probability Distribution Function Based SUH Methods	44
2.2.6	Remarks	47
2.3	SEDIMENT GRAPH BASED SEDIMENT YIELD MODELING	48
2.3.1	Background	48
2.3.2	Sediment Yield Process	49
2.3.3	Approaches of Sediment Yield Modeling	50
2.3.4	Selection of an Appropriate Model	52
2.3.5	Popular Sediment Graph models	53
2.3.6	Remarks	62
2.4	SUMMARY	62
3	STUDY AREA AND DATA USED	64
3.1	EVENT RAINFALL-RUNOFF DATA	64
3.2	DAILY RAINFALL-RUNOFF DATA	67
3.3	SHORT-TERM RAINFALL-RUNOFF DATA	67
3.3.1	Chaukhutia Catchment	67
3.3.2	Gormel Ermenek Creek Catchment	70
3.3.3	Bridge Catchment no. 253	70
3.3.4	Kothuwatari Catchment	70
3.3.5	Shanchuan Catchment	71
3.3.6	Myntdu-Leska Catchment	71
3.4	SHORT-TERM SEDIMENT YIELD DATA	71
3.4.1	Nagwan Watershed	71
3.4.2	Chaukhutia Catchment	75

4	PROCEDURE FOR ACCOUNTING SOIL MOISTURE IN SCS-CN	77
	METHODOLOGY	
4.1	BACKGROUND	77
4.2	MATHEMATICAL FORMULATION	78
4.2.1	SMA Inspired Event Based SCS-CN Model	78
4.2.2	SMA Inspired Continuous SCS-CN Model	92
4.3	APPLICATION	94
4.3.1	SMA Based Event-Aggregated and Existing SCS-CN Models	94
4.3.2	Procedure Adopted for Models Application	94
4.3.3	Marquardt Constrained Least Square Approach	95
4.3.4	Goodness of Fit	95
4.3.5	Performance Evaluation of SMA Based Event-Aggregated and Existing SCS-CN Models	96
4.3.6	SMA Based Continuous SCS-CN Models	96
4.3.7	Performance Evaluation of SMA Based Continuous SCS-CN Models	99
4.4	SUMMARY	103
5	EXTENDED HYBRID MODEL FOR SYNTHETIC UNIT	104
	HYDROGRAPH DERIVATION	
5.1	BACKGROUND	104
5.2	EXTENDED HYBRID MODEL (EHM) FORMULATION	105
5.3	APPLICATION	110
5.3.1	Parameter Estimation	111
5.4	DISCUSSION OF RESULTS	112
5.4.1	Performance of the Models	113
5.4.2	Sensitivity Analysis	120
5.5	SUMMARY	124

6	CHI-SQUARE AND FRÉCHET DISTRIBUTIONS FOR SUH DERIVATION	125
6.1	BACKGROUND	125
6.2	STATISTICAL DISTRIBUTIONS	126
6.2.1	One-Parameter Chi-Square Distribution	126
6.2.2	Two-Parameter Fréchet Distribution	128
6.3	VALIDITY OF ANALYTICAL ESTIMATION METHODS	130
6.3.1	One-Parameter Chi-square Distribution	130
6.3.2	Two-Parameter Fréchet Distribution	131
6.4	SENSITIVITY OF DISTRIBUTION PARAMETERS	131
6.4.1	One-Parameter Chi-square Distribution	131
6.4.2	Two-Parameter Fréchet Distribution	135
6.5	SIMILARITY BETWEEN THE THREE DISTRIBUTIONS	135
6.6	APPLICATION OF MODELS	137
6.6.1	For Bridge Catchment	138
6.6.2	For Myntdu-Leska Catchment	139
6.7	PERFORMANCE OF MODELS	141
6.8	SUMMARY	142
7	SCS-CN METHOD BASED SEDIMENT GRAPH MODELS	143
7.1	BACKGROUND	143
7.2	MATHEMATICAL FORMULATION	144
7.2.1	Sub-models	144
7.2.1.1	Nash Based IUSG	144
7.2.1.2	SCS-CN Method	148
7.2.1.3	Power Law	149
7.2.2	Case Specific Formulations	150
7.2.2.1	SGM ₁ : Initial soil moisture (V_0) = 0 and Initial abstractions (I_a) = 0	150
7.2.2.2	SGM ₂ : Initial soil moisture (V_0) = 0 and Initial abstractions $I_a \neq 0$	151

7.2.2.3	SGM ₃ : Initial Soil moisture (V_0) \neq 0 and Initial abstractions (I_a) = 0	152
7.2.2.4	SGM ₄ : Initial soil moisture (V_0) \neq 0 and Initial abstractions (I_a) \neq 0	153
7.3	MODEL APPLICATION AND TESTING	154
7.3.1	Parameter Estimation	155
7.3.2	Performance Analysis	155
7.3.3	Sensitivity Analysis	157
7.4	RESULTS AND DISCUSSION	157
7.4.1	Parameter Estimation	157
7.4.2	Comparative Performance of Models	158
7.4.3	Sensitivity of Parameters	163
7.5	FURTHER APPLICATION OF SGM ₁	168
7.6	SUMMARY	174
8	SUMMARY AND CONCLUSIONS	175
8.1	REVISED SOIL MOISTURE ACCOUNTING PROCEDURE IN SCS-CN METHODOLOGY	176
8.2	SYNTHETIC UNIT HYDROGRAPH (SUH) METHODS	177
8.2.1	Extended Hybrid Model (EHM)	177
8.2.2	Chi-square and Fréchet Distributions for SUH derivation	177
8.3	SCS-CN METHOD BASED SEDIMENT GRAPH MODELS	178
8.4	MAJOR RESEARCH CONTRIBUTIONS OF THE STUDY	179
8.5	FUTURE SCOPE	181
	REFERENCES	182
	APPENDICES	202
	PUBLICATIONS FROM THE THESIS	223

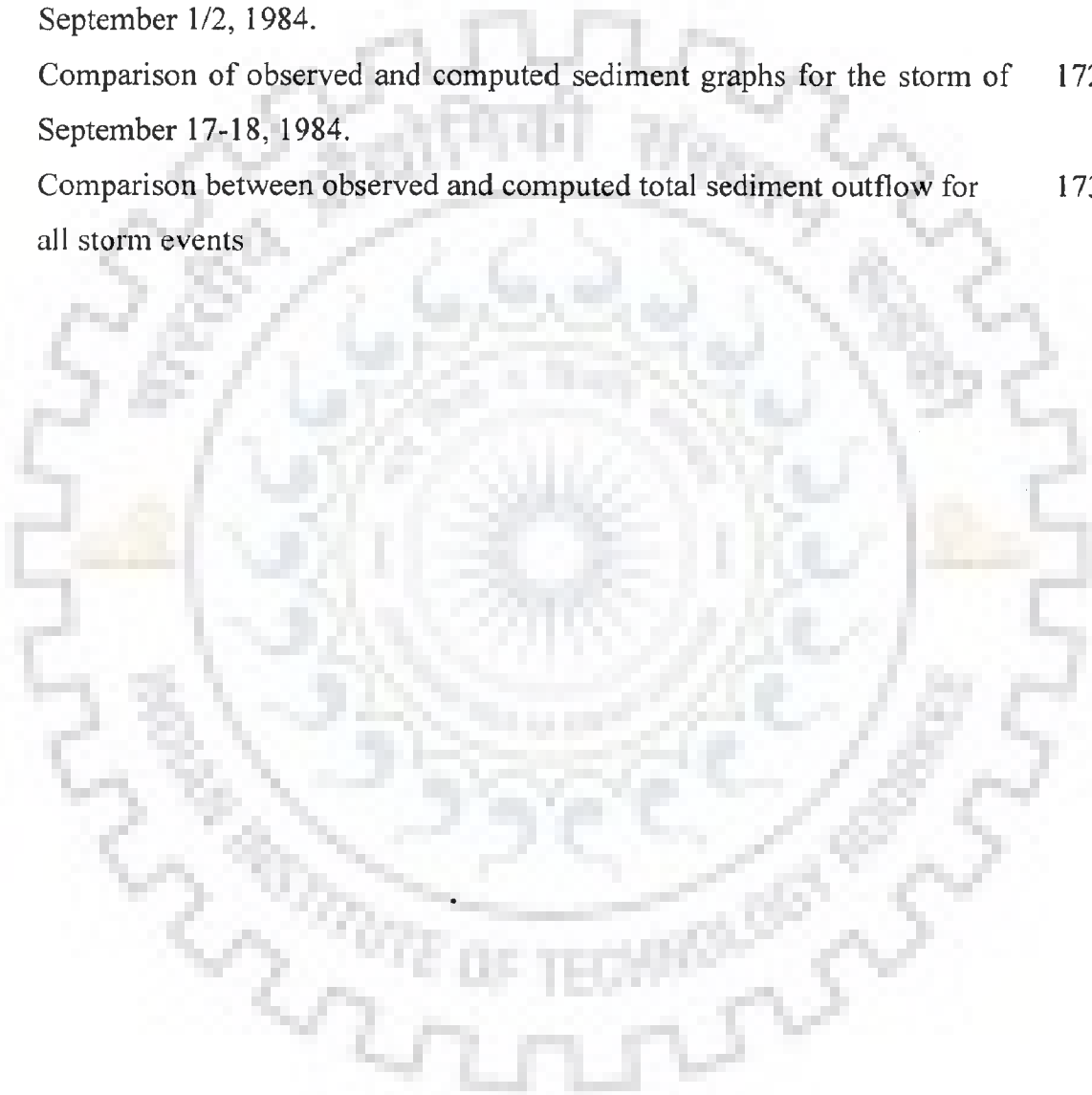
LIST OF FIGURES

Figure No.	Title	Page No.
2.1	Proportionality Concept	8
2.2	Determination of CN for AMC I through AMC III using Existing SCS- CN method	14
3.1	Map of USDA-ARS experimental Watersheds	65
3.2	Map of River Hemavati up to Sakleshpur	68
3.3	Location of Chaukhutia watershed in Ramganga reservoir catchment	69
3.4	Index map Bridge no. 253 of Tyria stream catchment, Narmada River, India	72
3.5	Index Map of Myntdu-Leska catchment	73
4.1	Conceptual soil-water-air system of a soil profile	81
4.2	Feasible limits of V-variation for $q \geq 0$	81
4.3	Schematic diagram showing the generalized behavior of the proposed continuous sub-model accounting soil moisture based on modified SCS- CN method	86
4.4	Feasible variation of q/p with V/S_b . Third parameter = S_a/S_b	87
4.5	Proportionality between direct surface runoff rate and rainfall intensity	88
4.6	Schematic of the proposed event-aggregated SMA procedure for various antecedent moisture levels	90
4.7	Fitting of SMA based Proposed and Michel et al models for continuous hydrologic simulation to the data of Hemavati watershed for the year- 1975 (Jan.1 st to Dec. 30, 1975).	100
4.8	Fitting of SMA based Proposed and Michel et al models for continuous hydrologic simulation to the data of Hemavati watershed for the year- 1976 (Jan.1 st to Dec. 30, 1976).	101

4.9	Fitting of SMA based Proposed and Michel et al models for continuous hydrologic simulation to the data of Hemavati watershed for the year-1977 (Jan.1 st to Dec. 30, 1977).	101
4.10	Fitting of SMA based Proposed and Michel et al models for continuous hydrologic simulation to the data of Hemavati watershed for the year-1977 (Jan.1 st to Dec. 30, 1978).	102
4.11	Fitting of SMA based Proposed and Michel et al models for continuous hydrologic simulation to the data of Hemavati watershed for the year-1977 (Jan.1 st to Dec. 30, 1979).	102
5.1	Representation of basin system by series of n hybrid units	106
5.2	Agreement between observed and estimated one-hour-unit hydrographs for Chaukhutia catchment	114
5.3	Agreement between observed and estimated two-hour-unit hydrographs for Gormel Ermenek Creek catchment	114
5.4	Agreement between observed and estimated one-hour-unit hydrographs for Bridge catchment no. 253	115
5.5	Agreement between observed and estimated unit hydrographs for Kothuwatari watershed of Tilaiya dam catchment	115
5.6	Agreement between observed and estimated unit hydrographs for Shanchuan catchment	116
5.7	Variation of DSTDER with catchment area	118
5.8	Agreement between observed and estimated peak flow rates	119
5.9	Variation of relative error in peak flow rates with catchment area	120
5.10	Sensitivity of peak flow rates with Translation	123
5.11	Agreement between observed and estimated two-hour-unit hydrographs for Gormel Ermenek Creek catchment	123
6.1	pdf shapes for of One-parameter Chi-square distribution (CSD) ($\tau = 3$) and Two-parameter Fréchet distribution (2PFD) ($c = 2, \alpha = 5$), and Two parameter Gamma distribution (2PGD) ($n = 3, K = 2$).	127

6.2a	Best-fit-line between estimated and actual τ of one parameter CSD	132
6.2b	Best-fit-line between estimated and actual c of 2PFD	133
6.2c	Best-fit-line between estimated and actual α of 2PFD	134
6.3a	Sensitivity to parameter m of one parameter CSD	134
6.3b	Sensitivity to parameter c of 2PFD	136
6.3c	Sensitivity to parameter α of 2PFD	136
6.4	Comparison of observed and computed UHs using three different pdfs for Bridge catchment no. 253. The figures in bracket give the corresponding STDER.	140
6.5	Comparison of observed and computed UHs using three different pdfs for Myntdu-Leska catchment. The figures in bracket give the corresponding STDER.	141
7.1	Schematic representation of Nash based IUSG sub-model	145
7.2	Comparison of observed and computed sediment graphs for the storm of July 6, 1989	159
7.3	Comparison of observed and computed sediment graphs for the storm of July 20, 1989	160
7.4	Comparison of observed and computed sediment graphs for the storm of July 28, 1989	161
7.5	Comparison between observed and computed Sediment yield using SGM ₁ -SGM ₄ models	164
7.6	Models sensitivity to α	165
7.7	Models sensitivity to β	165
7.8	Models sensitivity to k	166
7.9	Models sensitivity to θ	166
7.10	Models sensitivity to λ	167
7.11	Models sensitivity to n_s	167
7.12	Comparison of observed and computed sediment graphs for the storm of July 17, 1983.	170

7.13	Comparison of observed and computed sediment graphs for the storm of August 21/22, 1983.	170
7.14	Comparison of observed and computed sediment graphs for the storm of July 15, 1984.	171
7.15	Comparison of observed and computed sediment graphs for the storm of August 18/19, 1984.	171
7.16	Comparison of observed and computed sediment graphs for the storm of September 1/2, 1984.	172
7.17	Comparison of observed and computed sediment graphs for the storm of September 17-18, 1984.	172
7.18	Comparison between observed and computed total sediment outflow for all storm events	173



6.2a	Best-fit-line between estimated and actual τ of one parameter CSD	132
6.2b	Best-fit-line between estimated and actual c of 2PFD	133
6.2c	Best-fit-line between estimated and actual α of 2PFD	134
6.3a	Sensitivity to parameter m of one parameter CSD	134
6.3b	Sensitivity to parameter c of 2PFD	136
6.3c	Sensitivity to parameter α of 2PFD	136
6.4	Comparison of observed and computed UHs using three different pdfs for Bridge catchment no. 253. The figures in bracket give the corresponding STDER.	140
6.5	Comparison of observed and computed UHs using three different pdfs for Myntdu-Leska catchment. The figures in bracket give the corresponding STDER.	141
7.1	Schematic representation of Nash based IUSG sub-model	145
7.2	Comparison of observed and computed sediment graphs for the storm of July 6, 1989	159
7.3	Comparison of observed and computed sediment graphs for the storm of July 20, 1989	160
7.4	Comparison of observed and computed sediment graphs for the storm of July 28, 1989	161
7.5	Comparison between observed and computed Sediment yield using SGM ₁ -SGM ₄ models	164
7.6	Models sensitivity to α	165
7.7	Models sensitivity to β	165
7.8	Models sensitivity to k	166
7.9	Models sensitivity to θ	166
7.10	Models sensitivity to λ	167
7.11	Models sensitivity to n_s	167
7.12	Comparison of observed and computed sediment graphs for the storm of July 17, 1983.	170

6.4	Parameters of the three distributions for the partial data condition for the study areas	140
7.1	Unit sediment graph characteristics of the storm events of Nagwan watershed	158
7.2	Optimized parameter values for Nagwan watershed	158
7.3	Goodness of fit of models in terms of Model efficiency and Relative error	162
7.4	Unit sediment graph characteristics of storm events of Chaukhtutia watershed	169
7.5	Optimized parameter values for Chaukhtutia watershed	169
7.6	Goodness of fit statistics	169



LIST OF SYMBOLS

\overline{Q}_{obs}	Mean of the observed runoff
\overline{L}_w	Mean length of stream of order w
\overline{A}_w	Mean area of basin of order w
α and β	coefficient and exponent of power relationship
A	Potential maximum erosion
a and b	Coefficient and exponent of the power equation of Gray method
AMC I	AMC corresponding to dry condition
AMC II	AMC corresponding to normal condition
AMC III	AMC corresponding to wet condition
A_w	Area of the watershed
b	Empirical index value of Mockus method
C	Runoff coefficient
CN _I , CN _{II} , and CN _{III}	CN corresponding to AMC I, AMC II, and AMC III, respectively
C_T and C_p	Nondimensional constants of Snyder's method
D	Differential operator
	Rainfall-excess duration
E	Pan evaporation
F	Actual infiltration
f	Infiltration rate at any time t
f_c	Final infiltration rate
F_c	Static portion of infiltration
f_0	Initial infiltration rate at time t=0
i_0	Uniform rainfall intensity
I_a	Initial abstractions
i_e	Effective rainfall intensity
k	Infiltration decay constant
K	Storage coefficient

K_1 and K_2	Storage coefficient of first and second reservoirs (hr)
K_s	Sediment storage storage coefficient
L	Length of main stream
L_{CA}	Distance from the watershed outlet to a point on the main stream nearest to the center of the area of the watershed in km or miles;
n	Number of linear reservoirs
N	Total number of hydrograph ordinates
n_s	Number of linear reservoirs of IUSG model
N_w	Number of streams of the order w
P_5	5-day antecedent rainfall amount
Q	direct surface runoff
$Q(t)$	Direct runoff rate
Q_{com}	Computed runoff
Q_{obs}	Observed runoff
Q_p	Peak flow rate
Q_{ps}	Peak sediment outflow rate
Q_s	Total sediment outflow
$Q_s(t)$	Sediment outflow rate
R_A	Area ratio
R_B	Bifurcation ratio
R_L	Length ratio
S	Potential maximum retention Storage coefficient
s	Laplace transform coefficient
S_a	Threshold value of soil moisture storage
S_b	Absolute potential maximum retention
S_l	Potential maximum retention corresponding to AMC I
S_r	Degree of saturation
T	Translation time of channel
t_B	Time base
t_L	Lag time

t_p	Time to peak
t_{ps}	Time to peak sediment flow rate
V	Moisture storage at any time t during the storm event
v	Average peak flow velocity or characteristic velocity
V_0	Initial soil moisture storage level
V_a	Volume of air
V_w	Volume of water
w	Weightage factor used to estimate STDER
	Stream order
W_{50} and W_{75}	UH width at 50% and 75% of peak flow rate
Y	Amount of mobilized sediment
Y_T	Total amount of mobilized sediment
α, c	location and shape parameters of 2PFD
β	A non-dimensional term
	A parameter
Γ	Gamma function
θ	a constant equal to the ratio of V_0 and S ;
λ	Initial abstraction coefficient
λ' and γ	Shape and scale parameter of Gray method
τ	Parameter of Chi-square distribution

ABBREVIATIONS

2PFD	Two-Parameter Fréchet Distribution
2PGD	Two-Parameter Gamma Distribution
ABFI	Antecedent Base Flow Index
AMC	Antecedent Moisture Contition
ANN	Artificial Neural Network
ANSWERS	Areal Non-Point Source Watershed Environment Response Simulation
API	Antecedent Precipitation Index
ASCE	American Society of Civil Engineers

ASRC	Annual Storm Runoff Coefficient
CN	Curve Number
COD	Coefficient of Determination
CREAMS	Chemicals, Runoff, and Erosion from Agricultural Management Systems
CSD	Chi-Square Distribution
DR	Delivery Ratio
DRH	Direct Runoff Hydrograph
DSG	Direct Sediment Graph
EHM	Extended Hybrid Model
ERH	Effective Rainfall Hyetograph
GIS	Geographic Information System
GIUH	Geomorphological Instantaneous Unit Hydrograph
GOF	Goodness-of-Fit
HEC-HMS	Hydrologic Engineering Centre-Hydrologic Modeling System
HM	Hybrid Model
HSPF	Hydrologic Simulation Package Fortran
IAHS	International Association of Hydrological Sciences
IUH	Instantaneous Unit Hydrograph
IUSG	Instantaneous Unit Sediment Graph
KINEROS	Kinematic Runoff and Erosion Model
LC	Linear Channel
LR	Linear Reservoir
MUSLE	Modified Universal Soil Loss Equation
NEH	National Engineering Handbook
NRCS	Natural Resources Conservation Service
NS	Nash and Sutcliffe
PANC	Pan Coefficient
pdf	Probability Distribution Function
PET	Potential Evapotranspiration
PUB	Predictions in Ungauged Basins

RE	Relative Error
RUSLE	Revised Universal Soil Loss Equation
SCD	Soil Conservation Department
SCS	Soil Conservation Service
SCS-CN	Soil Conservation Service Curve Number
SEDIMOT	Sedimentology Simulation Model
SGM	Sediment Graph Model
SGM ₁	Sediment Graph Model 1
SGM ₂	Sediment Graph Model 2
SGM ₃	Sediment Graph Model 3
SGM ₄	Sediment Graph Model 4
SHE	System Hydrologique European
SMA	Soil Moisture Accounting
SMI	Soil-Moisture-Index
SSG	Synthetic Sediment Graph
STDER	Standard Error
SUH	Synthetic Unit Hydrograph
SVL	Soil-Vegetation-Landuse
SWAT	Soil and Water Assesment Tool
UH	Unit Hydrograph
USACE	United States Army Corps of Engineers
USDA-ARS	United States Department of Agriculture-Agricultural Research Service
USDAHL	United States Department of Hydrograph Laboratory
USG	Unit Sediment Graph
USLE	Universal Soil Loss Equation
WMY	Water Yield Model

CHAPTER-1

INTRODUCTION

“Water is the most abundant substance on the earth, the principal constituent of all living things, and a major force constantly shaping the surface of earth. It is also a key factor in air-conditioning the earth for human existence and in influencing the progress of civilization” (Chow et al., 1988). The supply of water available for our use is limited by nature. Although there is plenty of water on earth, it is not always available at the right place, at the right time and of the right quality. Hydrology has evolved as a science in response to the need to understand the complex water systems of the earth and helps to solve water problems. It is a subject of great importance for people and their environment. Mishra and Singh (2003a) defined hydrology as: “Hydrology is the science of water that deals with the space-time-frequency characteristics of the quantity and quality of waters of the earth with respect to their occurrence, distribution, movement, storage, and development”. It plays a fundamental role in addressing a range of issues related to environmental and ecological management and societal development. One of these issues of permanent importance is the rainfall-runoff-sediment yield modeling, which, in particular, is used in water resources assessment, flood control, evaluation of impact of climate change, environmental impact assessment, water resources planning and management, erosion and sediment control, non point source pollution, water quality modeling and watershed management.

1.1 RAINFALL-RUNOFF MODELING

Rainfall-runoff models are employed in a wide spectrum of areas ranging from watershed management to engineering design (Singh, 1995). At the field scale, the runoff models are used for planning and design soil conservation practices, irrigation water management, wetland restoration, stream restoration, and water-table management. On the other hand, at large scale, these are used for flood forecasting, flood protection projects, floodplain management, and water-supply forecasting. The popular Soil Conservation Service Curve Number (SCS-CN) method and the Synthetic Unit Hydrograph (SUH) methods can be successfully employed to address the aforementioned assignments. Both the

models have attracted a great deal of attention of hydrologic research community in the recent past, including potential for their improvement.

1.2 SEDIMENT YIELD MODELING

The quantitative analysis of sediment is essential for estimation of total sediment outflow from a storm or its variation with time. Both being important in water quality modeling, the time distributed sediment flow estimates (sediment graphs) are useful in designing efficient sediment control structures for maximum trap efficiency. On the other hand, the estimation of time distributed sediment is also essential if the sediment is transporting the pollutants that are toxic at high concentrations as without sediment graphs, only the average sediment rate for the storm can be determined. For this, the instantaneous unit sediment graph (IUSG) or unit sediment graph (USG) based models are widely used. The literature suggests scope for their advancement.

1.3 RESEARCH OBJECTIVES

Literature review shows possibility as well as necessity for improvements in SCS-CN, SUH, and sediment graph models in rainfall-runoff-sediment yield study. This study is undertaken with the following specific objectives:

1. To propose an event-based SMA-inspired SCS-CN procedure using the $C = S_r$ concept for runoff estimation.
2. To propose a continuous hydrologic simulation model using SMA-inspired SCS-CN procedure for runoff estimation.
3. To test both the models on a large set of field data.
4. To develop an extended hybrid model (EHM) for SUH derivation by representing the basin system as series of hybrid units, where each hybrid unit consists of two linear reservoirs (LR) connected by a linear channel (LC) in a specific order i.e. (LR-LC-LR).

5. To evaluate the workability of EHM in comparison to hybrid model (HM) (Bhunya et al., 2005) using field data.
6. To explore the potential of one-parameter Chi-square distribution and two-parameter Fréchet distribution to describe the complete shape of SUH using Horton order ratios of a catchment on the basis of a geomorphologic model of catchment response.
7. To evaluate the workability of the above distribution-based approach used for SUH derivation and compare it with the existing Gamma synthetic method (Rosso, 1984) for the limited data condition.
8. To propose new conceptual sediment graph models (SGMs) based on coupling of popular and extensively used methods, viz., Nash model based IUSG, SCS-CN method, and Power law.
9. To evaluate/compare the workability of the proposed SGMs using field data.

1.4 ORGANIZATION OF THESIS

The thesis is arranged in eight chapters as follows:

Chapter One: The first chapter introduces the problem, briefly describes the present state-of-the-art knowledge, and outlines the research objectives.

Chapter Two: This chapter presents a critical review of literature available in the field of runoff and sediment yield modeling related with the present study. To accomplish this, the chapter is divided mainly into three sections dealing with SCS-CN method for runoff modeling; synthetic unit hydrograph methods and conceptual models used for synthetic unit hydrograph derivation; SCS-CN method and sediment graph models for estimation of sediment yield.

Chapter Three: This chapter describes the study area considered for different studies as well as the corresponding types of data used. The types of data are lumped, event rainfall-runoff data; daily rainfall-runoff data; hyetographs and hydrographs; and sediment graphs.

Chapter Four: This chapter focuses on the short (event-based) and long-term (daily) hydrologic modeling aspects of the SCS-CN methodology to propose an event-based SMA-inspired SCS-CN procedure using the $C = S_r$ concept and a continuous hydrologic simulation model using SMA-inspired SCS-CN procedure for runoff estimation, and to test both the models on a large set of data derived from the catchments of United States and India.

Chapter Five: In this chapter, the hybrid model (HM) is extended by inserting a linear channel between the two reservoirs to account for translation, to develop an extended hybrid model (EHM) for SUH derivation by representing the basin system as series of hybrid units, where each hybrid unit consists of two linear reservoirs (LR) connected by a linear channel (LC) in a specific order i.e. (LR-LC-LR). Further, a generalized form of EHM is also derived. Lastly, the EHM and HM models are compared for their performance on field data of small to medium catchments.

Chapter Six: In this chapter, the potential of one-parameter Chi-square and two-parameter Fréchet distributions for SUH derivation is explored. An analytical approach is used to estimate the distribution parameters; and the UH parameters, viz., peak discharge, time to peak etc. are estimated using Horton ratios given by Rodriguez-Iturbe and Valdes (1979). Finally, the workability of these pdfs for SUH derivation is compared with the existing Gamma synthetic method of Rosso (1984) using the data of two Indian catchments for limited data availability condition.

Chapter Seven: In this chapter, four sediment graph models (SGM_1 , SGM_2 , SGM_3 , and SGM_4) are developed based on popular and extensively methods viz. (i) Nash based IUSG; (ii) SCS-CN method; and (iii) Power law. The suitability of models is checked using the field data. Based on quantitative approach, the models are analyzed for their sensitivity to changes in various parameters on the output. Further, the simplest sediment graph model SGM_1 is applied to another set of the field data for its workability.

Chapter Eight: This chapter presents summary, important conclusions drawn from the study, major research contributions of the study, and scope for future research work.

CHAPTER-2

REVIEW OF LITERATURE

This chapter is mainly divided into three sections. The first section deals with the Soil Conservation Service Curve Number (SCS-CN) methodology; the second section with synthetic unit hydrograph (SUH) methods and conceptual models; and the third with the sediment yield modeling, particularly the sediment graph modeling approach.

2.1 SCS-CN METHOD

A multitude of methods/models are available in hydrologic literature to simulate the complex process of rainfall-runoff in a watershed. One of the most widely used methods is the SCS-CN method (SCS, 1956). It computes the volume of surface runoff for a given rainfall event from small agricultural, forest, and urban watersheds (SCS, 1986). The method is simple to use and requires basic descriptive inputs that are converted to numeric values for estimation of watershed direct runoff volume (Bonta, 1997). A “curve number” that is descriptive of runoff potential of watershed is required in the method. The method is widely used by engineers and hydrologists and watershed managers as a simple watershed model, and as the runoff estimating component in more complex watershed models. In words of Ponce and Hawkins (1996) “The SCS-CN method is a conceptual model of hydrologic abstraction of storm rainfall, supported by empirical data. Its objective is to estimate direct runoff volume from storm rainfall depth, based on a curve number CN”. A review pertinent to the methodology with respect to its origin and vast areas of applications is presented here, as follows.

2.1.1 Historical Background

In year 1954, the United States Department of Agriculture, Soil Conservation Service (now called the Natural Resources Conservation Service (NRCS)) developed a unique procedure known as Soil Conservation Service Curve Number (SCS-CN) method for

estimating direct runoff from storm rainfall. The SCS-CN method (SCS, 1956, 1964, 1971, 1972, 1993) is a rainfall-runoff model widely used to estimate direct storm runoff from total event rainfall (Mishra et al., 2005). The method has since witnessed myriad applications all over the world. The method, which is basically empirical, was developed to provide a rational basis for estimating the effects of land treatment/landuse changes upon runoff resulting from storm rainfall. Because of its simplicity, it has been used through the spectrum of the hydrology, even for the range of the problems not originally intended to solve. According to Garen and Moore (2005) “.....the reason for the wide application of curve number method includes its simplicity, ease of use, widespread acceptance, and the significant infrastructure and institutional momentum for this procedure within NRCS. To the date, there has been no alternative that possesses so many advantages, which is why it has been and continues to be commonly used, whether or not it is, in an strict scientific sense, appropriate....”.

The methodology is the result of more than 20 years of studies of rainfall-runoff relationships carried out during the late 1930s and early 1940s for small rural watersheds, and the works of several investigators including Mockus (1949), Sherman (1949), Andrews (1954), and Ogrosky (1956). The passage of watershed protection and Flood Prevention Act (Public Law 83-566) in August 1954 was the major catalyst for the origin of methodology and it led to the recognition of methodology at the federal level. The data collected from experimental watersheds were, however, found to be scant and covering only a marginal fraction of the conditions affecting the rainfall-runoff process in watersheds (Andrews, 1954). Therefore, thousands of infiltrometer tests on field plots were conducted to develop a rational method for estimating runoff under various cover conditions. Following Sherman (1949) to plot direct runoff versus storm rainfall, Mockus (1949) proposed that the estimation of direct runoff for ungauged watersheds depends on soils, landuse, antecedent rainfall, duration of storm and rainfall amount associated, and average annual temperature and date of storm. Mockus (1949) communed these factors into an empirical index value b and proposed following relationship between storm rainfall depth P and direct runoff Q as (Mishra and Singh, 1999a):

$$Q = P(1 - 10^{-bP}) \quad (2.1)$$

Further, Mockus realized that Eq. (2.1) gave better results for short storms than the larger ones and for mixed-cover rather than the single cover watersheds. Andrews (1954) independently grouped the infiltrometer data collected from Texas, Oklahoma, Arkansas, and Louisiana, and developed a graphical rainfall-runoff procedure taking into account the soil texture, type and amount of cover, and conservation practices, combined into what is referred to as soil-cover complex or soil-vegetation-landuse (SVL) complex (Miller & Cronshey, 1989). According to Rallison and Miller (1982) the Mockus empirical P-Q rainfall-runoff relationship and Andrews's SVL complex were the building blocks of the existing SCS-CN method documented in Section-4, National Engineering Handbook (NEH-4) (Hydrology, 1985).

2.1.2 Theoretical Background

The SCS-CN method is based on the water balance equation and two fundamental hypotheses. The first hypothesis equates the ratio of actual amount of direct surface runoff Q to the total rainfall P (or maximum potential surface runoff) to the ratio of actual infiltration (F) to the amount of the potential maximum retention S . The second hypothesis relates the initial abstraction (I_a) to the potential maximum retention (S), also described as the potential post initial abstraction retention (McCuen, 2002). Expressed mathematically,

(a) Water balance equation

$$P = I_a + F + Q \quad (2.2)$$

(b) Proportional equality (First hypothesis)

$$\frac{Q}{P - I_a} = \frac{F}{S} \quad (2.3)$$

(c) I_a - S relationship (Second hypothesis)

$$I_a = \lambda S \quad (2.4)$$

The values of P , Q , and S are given in depth dimensions, while the initial abstraction coefficient λ is dimensionless. Though the original method was developed in U.S. customary units (in.), an appropriate conversion to SI units (cm) is possible (Ponce, 1989). In a typical case, a certain amount of rainfall is initially abstracted as interception, infiltration, and surface storage before runoff begins, and a sum of these is termed as ‘initial abstraction’.

The first (or fundamental) hypothesis (Eq. 2.3) is primarily a proportionality concept (Mishra and Singh, 2003a). Fig. 2.1 graphically represents this proportionality concept. Apparently, as $Q \rightarrow (P - I_a)$, $F \rightarrow S$. This proportionality enables dividing $(P - I_a)$ into two components: surface water Q and sub-surface water F for given watershed characteristics.

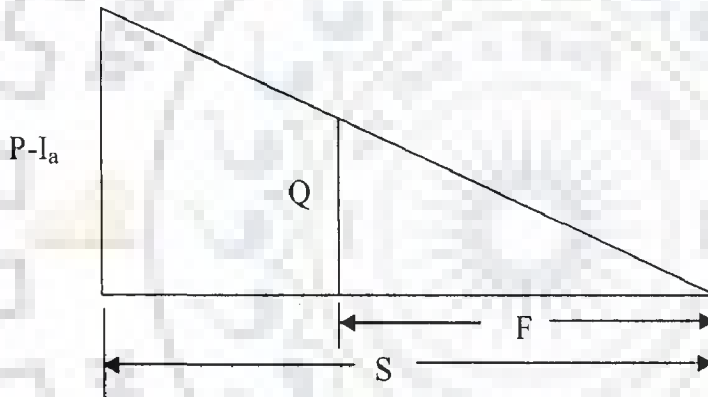


Fig. 2.1. Proportionality concept of the existing SCS-CN method

The parameter S of the SCS-CN method depends on soil type, land use, hydrologic condition, and antecedent moisture condition (AMC). The initial abstraction coefficient λ is frequently viewed as a regional parameter depending on geologic and climatic factors (Boszany, 1989; Ramasastry and Seth, 1985). The existing SCS-CN method assumes λ to be equal to 0.2 for practical applications. Many other studies carried out in the United States and other countries (SCD, 1972; Springer et al., 1980; Cazier and Hawkins, 1984; Ramasastry and Seth, 1985; Bosznay, 1989) report λ to vary in the range of (0, 0.3). However, as the initial abstraction component accounts for the short-term losses such as interception, surface

storage, and infiltration before runoff begins, λ can take any value ranging from 0 to ∞ (Mishra and Singh, 1999a). A study of Hawkins et al. (2001) suggested that value of $\lambda = 0.05$ gives a better fit to data and would be more appropriate for use in runoff calculations.

The second hypothesis (Eq. 2.4) is a linear relationship between initial abstraction I_a and potential maximum retention S . Coupling Eqs. (2.2) and (2.3), the expression for Q can be written as:

$$Q = \frac{(P - I_a)^2}{P - I_a + S} \quad (2.5)$$

Eq. (2.5) is the general form of the popular SCS-CN method and is valid for $P \geq I_a$; $Q = 0$ otherwise. For $\lambda = 0.2$, the coupling of Eqs. (2.4) and (2.5) results

$$Q = \frac{(P - 0.2S)^2}{P + 0.8S} \quad (2.6)$$

Eq. (2.6) is the popular form of existing SCS-CN method. Thus, the existing SCS-CN method with $\lambda = 0.2$ is a one-parameter model for computing surface runoff from daily storm rainfall.

Since parameter S can vary in the range of $0 \leq S \leq \infty$, it is mapped onto a dimensionless curve number CN , varying in a more appealing range $0 \leq CN \leq 100$, as:

$$S = \frac{1000}{CN} - 10 \quad (2.7)$$

where S is in inches. The difference between S and CN is that the former is a dimensional quantity (L) whereas the later is non-dimensional. $CN = 100$ represents a condition of zero potential maximum retention ($S = 0$), that is, an impermeable watershed. Conversely, $CN = 0$ represents a theoretical upper bound to potential maximum retention ($S = \infty$), that is an infinitely abstracting watershed. However, the practical design values validated by experience lie in the range (40, 98) (Van Mullem, 1989). It is to explicitly mention here

that CN has no intrinsic meaning; it is only a convenient transformation of S to establish a 0-100 scale (Hawkins, 1978).

2.1.3 Advantages and Limitations

The Soil Conservation Service Curve number (SCS-CN) method (SCS, 1956) is one of the most popular techniques for computing direct surface runoff from a rainstorm event (Ponce and Hawkins, 1996; Mishra and Singh, 2003b; Mishra et al., 2006a,b; Michel et al., 2005; and Sahu et al., 2007). Well established in hydrologic, agriculture, and environmental engineering, its popularity is rooted in its convenience, simplicity, authoritative origins, and responsiveness to four readily available catchment properties: soil type, land use/treatment, surface condition, and antecedent moisture condition.

The method though appealing to many practicing hydrologists by its overwhelming simplicity, contains some unknowns and inconsistencies (Chen, 1982). Due to its origin and evolution as agency methodology, which effectively isolated it from rigors of peer review, other than the information contained in NEH-4, which was not intended to be exhaustive no complete account of the methods foundation is available to date. Ponce and Hawkins (1996) critically examined this method, clarified its conceptual and empirical basis, delineated its capabilities, limitations, uses, and identified areas of research in the SCS-CN methodology. Following are the major advantages associated with the existing SCS-CN methodology.

1. It is simple, predictable, stable, and lumped conceptual model.
2. It relies on only one parameter CN.
3. Well suited for ungauged catchments.
4. Well established in hydrologic, agriculture, and environmental engineering.
5. Simple enough in application to handle the real world problems.
6. The only agency methodology that features readily grasped and reasonably well documented environmental inputs.
7. Perhaps it is the single methodology available, which is used widely in majority of the computer based hydrologic simulation models used currently (Singh, 1995).

8. Its responsiveness to four readily grasped catchment properties: soil type, land use/treatment, surface condition, and antecedent moisture condition.
9. It requires only a few basic descriptive inputs that are convertible to numeric values for estimation of direct surface runoff.
10. The method does best in agricultural sites, for which it was originally intended, and extended to urban sites.

The disadvantages associated with the existing methodology are summarized below.

1. Lack of clear guidance on how to vary antecedent moisture condition.
2. The discrete relationship between CN and AMC classes permits sudden jump in CN, and hence corresponding quantum jump in calculated runoff.
3. Lack of assumptions in development of NEH-4 table.
4. Application of the method to the catchments with area greater than 250 km² should be viewed with caution.
5. Since the method was developed for United States using regional data, some caution is recommended for its use in other geographic or climatic regions.
6. The method has no explicit provisions for spatial scale effects on the CN.
7. The method is not suitable for long-term hydrologic simulation.
8. Choice of fixing the initial abstraction coefficient $\lambda = 0.2$. Thus preempting the regionalization based on geologic and climatic conditions.
9. The method does not have any expression of time and ignores the impact of rainfall intensity and its temporal distribution.
10. The method does not have any expression for antecedent moisture which plays a significant role in runoff generation process. Rather adjustments are made for it using the empirical mapping relationship.
11. The method performs poorly on the forest sites.

2.1.4 Watershed Characteristics Affecting CN Estimation

Before dealing with the watershed characteristics which affect the curve number estimation or in turn the storm runoff, it is appropriate here to quote the following (Hawkins, 1975): “.....that errors in CN may have much more consequences on runoff estimation than errors of similar magnitude in storm rainfall P....”. This says enough about the importance of accurate CN estimation. Major watershed characteristics such as soil type, land use/treatment classes, hydrologic soil group, hydrologic condition, and the most important one antecedent moisture condition play a significant role in accurate CN estimation.

The Soil Conservation Service classified the soils into four hydrologic soil groups as A, B, C, and D on the basis of their infiltration and transmission rates (Mishra and Singh, 2003a). The soils in group A have high infiltration rates, even when thoroughly wetted and consisting chiefly of well to excessive drained sands or gravels. These soils have high rate of water transmission and low runoff potential. The soils in group B have moderate infiltration rates, when thoroughly wetted and exhibit a moderate rate of water transmission. The soil with moderate deep to deep, moderate well to well drained, e.g. shallow loess and sandy loam soils fall in group B. The soils in group C have low infiltration rates when thoroughly wetted and consisting chiefly of soils with a layer that impedes downward movement of water. The soils in group D have very low infiltration rates when thoroughly wetted, consisting of chiefly clay soils with high swelling potential. These soils exhibit a very slow rate of water transmission. NEH-4 provides a list of more than 4000 soils of the United States of America. Thus the hydrologic soil group of a watershed significantly affects the CN or the runoff potential of the watershed, and it increases as the soil group changes from group A to group D, and vice versa.

The hydrologic condition of an agricultural watershed is defined to be Poor, Fair, and Good on the basis of percent area of grass cover. A watershed having larger acreage of grass cover is said to be in good hydrologic condition and vice versa. A Good hydrologic condition is an indicative of lesser runoff potential and more infiltration than does the Poor hydrologic condition. Correspondingly, the curve number will be the highest for the Poor, average for the Fair, and lowest for the Good hydrologic condition.

In words of Hawkins et al. (1985) that “.....the antecedent moisture condition (AMC) is one of the most influential watershed characteristics in determining curve number (CN)”..... The Soil Conservation Service defines antecedent moisture condition (AMC) as an index of the watershed wetness (Hjelmfelt, 1991). Mishra et al. (2003a, 2004a) defined the AMC as the initial moisture condition of the soil prior to occurrence of rainstorm. As a result, three concepts are presented in hydrologic literature to identify AMC: (i) the antecedent precipitation index (API); (ii) antecedent base flow index (ABFI); and (iii) the soil-moisture-index (SMI). The API concept is based on the amount of antecedent rainfall, where the term antecedent ranges from 5 to 30 days. The National Engineering Handbook (SCS, 1971) uses the antecedent 5-day rainfall as API for three AMCs as AMC I through AMC III. AMC I refers to dry condition of watershed with antecedent 5-day rainfall of less than 1.3 cm and 3.6 cm, respectively for dormant and growing seasons. Similarly AMC II represents normal or average condition of watershed with antecedent 5-day rainfall varying from 1.3 to 2.8 cm and 3.6 to 5.3 cm, respectively, for dormant and growing seasons. For AMC III, which refers to wet condition of the watershed, the antecedent 5-day rainfall is more than 2.8 mm and 5.3 mm, respectively, for dormant and growing seasons. These three dry, wet, and normal conditions of the watershed statistically correspond to respective 90%, 10%, and 50% cumulative probability of exceedance of runoff depth for a given rainfall (Hjelmfelt et al., 1982). In AMC II description, it is however not clear if this is a quantitative or a qualitative definition, and if quantitative, what should be averaged (Hjelmfelt, 1991). The concept of ABFI is based on the amount of antecedent base flow, which is seldom used in practice. Furthermore, the antecedent base flow, which is a delayed response, may not be representative of the soil moisture due to the antecedent precipitation. The concept of soil moisture index (SMI) is generally used in long-term hydrologic simulation, where soil moisture is accounted for water balance (Gosain et al., 2006). Such simulations utilize evapotranspiration, and thus, incorporate other climatic factors, such as daily temperature, solar radiation, etc. Sarkar and Singh (2007) studied the soil moisture index variation with evapotranspiration.

2.1.5 CN Estimation Methods

Despite widespread use of SCS-CN methodology, the accurate estimation of parameter CN is a topic of discussion among hydrologists and water resources community (Hawkins, 1978; Hawkins, 1979; Hjelmfelt, 1980; Hawkins, 1984; McCuen, 2002; Springer et al., 1980; Hjelmfelt, 1991; Simanton et al., 1996; Steenhuis et al., 1995; Bonta, 1997; Chen, 1982; Pone and Hawkins, 1996; Mishra and Singh, 1999a; Mishra and Singh, 2002a; Sahu et al., 2005; and Mishra and Singh, 2006). Originally CNs were developed using daily rainfall-runoff records corresponding to the maximum annual flows from gauged watersheds for which information on their soils, cover, and hydrologic condition was available (SCS, 1972). The rainfall (P)-runoff (Q) data were plotted on the arithmetic paper having a grid of plotted curve number, as shown in Fig. 2.2.

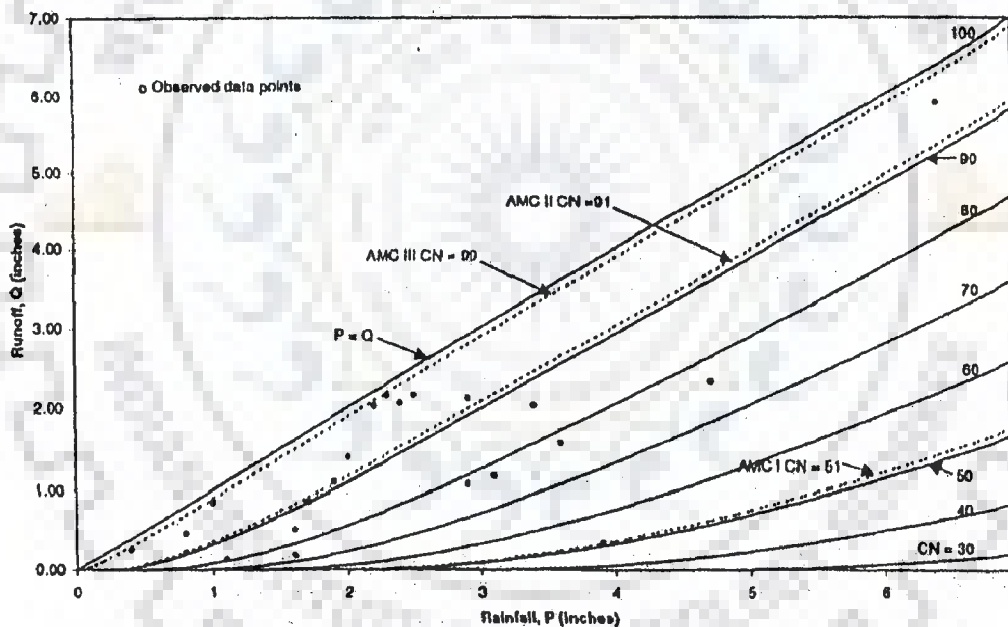


Fig.2.2. Determination of CN for AMC I through AMC III using existing SCS-CN method

The CN corresponding to the curve that separated half of the plotted data from the other half was taken as the median curve number for the watershed. Thus the developed curve numbers represented the averages or median site values for soil groups, cover, and hydrologic

condition and corresponds to AMC II (CN_{II}). The upper enveloping curve was taken to correspond to AMC III (CN_{III}) and the lower curve to AMC I (CN_I). The average condition was taken to mean average response, which was later extended to imply average soil moisture condition (Miller and Cronshey, 1989). Depending on 5-day antecedent rainfall, CN_{II} is convertible to CN_I and CN_{III} using the relationships given by Sobhani (1975); Hawkins et al. (1985); Chow et al. (1988); Neitsch et al. (2002) (Table 2.1); and directly from the NEH-4 tables (SCS, 1972; McCuen, 1982, 1989; Ponce, 1989, Singh, 1992; and Mishra and Singh, 2003a), and these are applicable to ungauged watersheds.

Table 2.1 Popular AMC dependent CN conversion formulae

Method	AMC I	AMC III
Sobhani (1975)	$CN_I = \frac{CN_{II}}{2.334 - 0.01334CN_{II}}$	$CN_{III} = \frac{CN_{II}}{0.4036 + 0.005964CN_{II}}$
Hawkins et al. (1985)	$CN_I = \frac{CN_{II}}{2.281 - 0.01281CN_{II}}$	$CN_{III} = \frac{CN_{II}}{0.427 + 0.00573CN_{II}}$
Chow et al. (1988)	$CN_I = \frac{4.2CN_{II}}{10 - 0.058CN_{II}}$	$CN_{III} = \frac{23CN_{II}}{10 + 0.13CN_{II}}$
Neitsch et al. (2002)	$CN_I = CN_{II} - \frac{20(100 - CN_{II})}{\{100 - CN_{II} + \exp[2.533 - 0.0636(100 - CN_{II})]\}}$	$CN_{III} = CN_{II} \exp\{0.00673(100 - CN_{II})\}$

However, to estimate the average CN values (CN_{II}) mathematically from the rainfall (P)-runoff (Q) data of a gauged watershed, Hawkins (1993) suggested S (or CN) computation using the expression

$$S = 5 \left[P + 2Q - \sqrt{Q(4Q + 5P)} \right] \quad (2.8)$$

Eq. (2.8) can be easily derived from Eq. (2.6).

Another approach to estimate CN from rainfall (P)-runoff (Q) data is the rank-order method (Hjelmfelt, 1980), where the P-Q data are sorted out and rearranged on rank-order basis to

have equal return periods. However, the individual runoff values are not necessarily associated with the causative rainfall values (Hawkins, 1993). Bonta (1997) evaluated the potential of derived distributions to determine curve numbers from measured P-Q data, treating them as separate distributions. The derived distribution method resulted in fewer variable estimates of CN for a wide range of sample sizes than the methods of Hawkins (1993) and Hjelmfelt (1980). The derived-distribution method also identifies watershed as 'standard', 'violent,' and 'complacent' similar to Hawkins (1993). The derived-distribution method has potential even when data availability is limited. Schneider & McCuen (2005) developed a new Log-normal frequency method to estimate curve numbers from measured P-Q data. The developed method was found to be more accurate than the rank-order method and by Eq. (2.8). Recently, Mishra and Singh (2006) investigated the variation of CN with AMC and developed a new power relationship between the S (or CN) and the 5-day antecedent rainfall. The developed CN-AMC relationship is applicable to gauged as well as ungauged watershed and eliminates the problem of sudden jump from one AMC level to other.

2.1.6 Applications

Since its inception the method has witnessed myriad and variety of applications to the fields not originally intended, due to the reason of its simplicity, stability and accountability for most runoff producing watershed characteristics: Soil type, land use treatment, surface condition, and antecedent moisture condition. Recently Singh and Frevert (2002) edited a book titled "Mathematical Models of Small Watershed Hydrology and Applications", in which at least 6 of the 22 chapters have mathematical models of watershed hydrology based on SCS-CN approach. This reflects the robustness and lasting popularity of SCS-CN methodology.

A considerable amount of literature on the method has been published and the method has undergone through various stages of critical reviews several times (Rallison, 1980; Chen, 1982; Ponce and Hawkins, 1996; and Mishra and Singh, 2003a). Rallison (1980) provided detailed information about the origin and evaluation of the methodology and highlighted major concerns to its application to the hydrology and water resources problems it was

designed to solve and suggested future research areas. Chen (1982) evaluated the mathematical and physical significance of methodology for estimating the runoff volume. A sensitivity analysis shows that the errors in CN have more serious consequences on runoff estimates than the errors of similar magnitude in initial abstraction or rainfall.

Though primarily intended for event-based rainfall-runoff modeling of the ungauged watersheds, the SCS-CN method has been applied successfully in the realm of hydrology and watershed management and environmental engineering, such as long-term hydrologic simulation (Huber et al., 1976; Williams and LaSeur, 1976; Hawkins, 1978; Knisel, 1980; Woodward and Gburek, 1992; Pandit and Gopalakrishnan, 1996; Choi et al., 2002; and Mishra and Singh, 2004a; and Geetha et al., 2007); prediction of infiltration and rainfall-excess rates (Aron et al., 1977; Mishra and Singh, 2002a, 2004b); metal partitioning (Mishra et al., 2004b,c); sediment yield modeling (Mishra and Singh, 2003a; Mishra et al., 2006a); and determination of sub-surface flow (Yuan et al., 2001). The method has also been successfully applied to distributed watershed modeling (White, 1988; Moglen, 2000; and Mishra and Singh, 2003a). Thus the vast applicability reflects the method's status among the hierarchy of hydrologic models.

Yu (1998) examined one of the most critical assumptions of the SCS-CN method, 'The proportionality concept or the ratio of the actual retention to the potential maximum retention is equal to the ratio of actual runoff to potential runoff,' and developed relationships between rainfall and runoff exactly similar to the SCS-CN method based on two simple but reasonable assumptions that the spatial variation of infiltration capacity has an exponential distribution and the lumped variation of rainfall follows an exponential distribution. A theoretical justification based on the frequency distribution also allows an independent validation of the SCS-CN method. Grove et al. (1998) studied the feasibility of distributed curve number approach compared to composite approach for estimation of runoff depths using SCS-CN method. The distributed approach may have an advantage for analysis of urbanizing watersheds with the proliferation of remote sensing and geographic information systems. Mishra & Singh (1999a) discussed the origin and heritage of the existing SCS-CN methodology in a sound analytical environment. They derived analytically the existing SCS-CN method from the empirical method of Mockus (1949) and proposed a modified SCS-CN

method along with a general form of the modified SCS-CN method. The expressions of Q for modified as well as general form of modified SCS-CN method are given as:

(i) Modified Form of SCS-CN method

$$Q = \frac{P^2}{(S + 0.5P)} \quad (2.9)$$

(ii) General Form of Modified SCS-CN method

$$Q = \frac{P^2}{(S + aP)} \quad (2.10)$$

where $a = \frac{1}{2} - \frac{S}{P} + \sqrt{\frac{1}{4} + \frac{S}{P}}$. Subsequently, a modification to the S-CN mapping was also developed by introducing a new parameter S_b in order to maintain range of CN values from 50 -100. The new S-CN relation is expressed as:

$$\frac{S}{S_b} = \frac{100}{CN} - 1 \quad (2.11)$$

where S_b is the absolute potential maximum retention. S and S_b are in inches and S varies from 0 to S_b .

Williams & LaSeur (1976) were probably the first to introduce the concept of Soil Moisture Accounting (SMA) procedure to develop a Water Yield Model (WYM) based on the existing SCS-CN methodology. The model was based on the notion that CN varied continuously with soil moisture, and thus considering many values of CN instead of only three (CN_I , CN_{II} , CN_{III}). The model computes a soil moisture index depletion parameter that forces an agreement between the measured and predicted average annual runoff. The developed model has following advantages:

1. It is a one-parameter model and uses a 1-day time interval.
2. It eliminates sudden jump in the CN-values while changing from one AMC to the other.
3. It requires simple inputs as: (i) CN_{II} estimate for the study watershed; (ii) measured monthly runoff; (iii) daily rainfall; and (iv) average monthly lake evaporation, and only outputs runoff volume.
4. It can be applied to the nearby ungauged watershed by adjusting the curve number for the ungauged watershed in proportion to ratio of the AMC II curve number to the average predicted curve number for the gauged watershed.

The model however has some perceived limitations and disadvantages:

1. The model utilizes an arbitrary assigned value of 20 inches for absolute potential maximum retention S_t .
2. The model assumes a physically unrealizable decay of soil moisture with the lake evaporation.
3. In spite of utilizing soil moisture accounting (SMA) concept in model formulation, the model still relies on the existing SCS-CN method for runoff calculation, which itself needs to be addressed for the issues related with the proportionality concept.
4. The iterative procedure required for the adjustment of the soil moisture index depletion parameter to match the measured and predicted average annual runoff and thus, loses the physical soundness.
5. Due to faulty assumption of decay of soil moisture with the lake evaporation, the model describes the variation of direct runoff Q with P analogous to F , and thus, contrasts the existing SCS-CN methodology (Mishra and Singh, 2003a).

Hawkins (1978) outlined serious flaws associated with the CN and AMC relationship as given in NEH-4 table, some of them are: (i) the discrete relationship between CNs and AMC class leads to sudden jump in CN and corresponding quantum jump in calculated runoff; (ii) the lack of assumptions in development of NEH-4 table, and thus, no physical reasoning or reconciliation with reality. Keeping in view, he developed a daily flow simulation model

based on SCS-CN method by accounting for the site moisture using the volumetric concept.

A brief description of the model is given here, as follows:

Expressing the existing SCS-CN method (Eq. 2.6) in the form:

$$Q = P - S \left(1.2 - \frac{S}{P + 0.8S} \right) \quad (2.12)$$

It can be observed that the maximum possible difference (as $P \rightarrow \infty$) between P and Q is 1.2 S.

Let us denote it by S_T as:

$$S_T = 1.2 S \quad (2.13)$$

An analysis of Eq. (2.13) results in: $S_T = S + 0.2 S = S + I_a$. Hence, the general expression for S_T can be given as:

$$S_T = (S + I_a) \quad (2.14)$$

For any time t, the coupling of Eq. (2.7) and (2.13) results

$$S_{T(t)} = 1.2 \left(\frac{1000}{CN_t} - 10 \right) \quad (2.15)$$

For next one time step i.e. $(t + \Delta t)$, $S_{T(t + \Delta t)}$ can be expressed as:

$$S_{T(t + \Delta t)} = S_{T(t)} + [ET - (P - Q)]_{(t, t + \Delta t)} \quad (2.16)$$

Similar to Eq. (2.15), an expression for $S_{T(t + \Delta t)}$ with $CN_{(t + \Delta t)}$ can be expressed as:

$$S_{T(t + \Delta t)} = 1.2 \left(\frac{1000}{CN_{t + \Delta t}} - 10 \right) \quad (2.17)$$

Equating the right hand side terms of Eqs. (2.16) and (2.17), an expression for $CN_{t+\Delta t}$ can be derived as:

$$CN_{t+\Delta t} = \frac{1200}{\frac{1200}{CN_t} + [ET - (P - Q)]_{(t, t+\Delta t)}} \quad (2.18)$$

Hence, if (i) CN_t for the first time step and (ii) P , Q , and ET for the next time step (Δt) are known, then Eq. (2.18) can be used to compute $CN_{t+\Delta t}$ for the next time step and sequentially, the daily Q from Eq. (2.6). The model has following advantages:

1. The model accounts for the site moisture on continuous basis and thus eliminates the problem of sudden jump in CN .
2. The model is easier to apply than is WYM (William and LaSeur, 1976).
3. The SMA procedure followed in model development is hydrologically sounder than WYM.

However, the model has following disadvantages of concern:

1. The foundation of model lies on the existing SCS-CN method which does not consider the initial soil moisture in the basic proportional equality.
2. The model assumes that the SCS-CN method is based on the (I_a+S) scheme, whereas I_a is separate from S .
3. Though the developed model eliminates the unwanted sudden jump in CN estimation, the model still uses the conventional empirical S-CN mapping relationship for computing the CN for the various time steps.
4. According to conceptual soil-water-air system of a soil profile (Mishra and Singh, 2003a), the general expression for the maximum possible difference (or absolute potential maximum retention) between P and Q should be $(S_b = S+I_a+V_0)$ (Michel et al., 2005), rather than $(S_T = S+I_a)$. This clearly indicates the negligence of initial soil moisture in the model formulation.

Pandit and Gopalakrishnan (1996) developed a continuous simulation model using existing SCS-CN method for computing annual pollutant loads based on annual storm runoff

coefficient (ASRC) and degree of perviousness/ imperviousness of watershed. The model is very simple and specifically useful for small urban watersheds characterized by the percent imperviousness. However, it allows sudden jumps in CN values, ignores evapotranspiration, drainage contribution, and watershed routing.

Mishra et al. (2004a) discussed the inherent sources of variability associated with the curve number procedure such as spatial and temporal variation of rainfall and variation of CNs with the antecedent moisture. The variability due to antecedent moisture is widely recognized in terms of AMCs and employs the concepts of antecedent precipitation index (API); antecedent base flow index (ABFI); and soil-moisture index (SMI) to identify the antecedent moisture condition. The antecedent moisture is the leading factor for the CN variability and has led to statistical (Hjelmfelt, 1980; Hawkins, 1993, 1996; Bonta, 1997; McCuen, 2002) and stochastic (Hjelmfelt, 1982; Bhunya et al., 2003a) considerations of the curve number. Furthermore, the incorporation of antecedent moisture in the existing SCS-CN method in terms of three AMC levels permits unreasonable sudden jumps in the CN-variation. To circumvent the aforementioned variability due to antecedent moisture, a modified form of Mishra-Singh (MS) (2002b) model using the $C = S_r$ concept was developed by incorporating the antecedent moisture or initial soil moisture (V_0) in the basic proportionality of the existing SCS-CN method as:

$$\frac{Q}{P - I_a} = \frac{F + V_0}{S + V_0} \quad (2.19)$$

which upon substituting into Eq. (2.2) leads to

$$Q = \frac{(P - I_a)(P - I_a + V_0)}{(P - I_a + S + V_0)} \quad (2.20)$$

Here, V_0 is computed as:

$$V_0 = \frac{(P_5 - 0.2S_1)S_1}{(P_5 + 0.8S_1)} \quad (2.21)$$

where P_5 is the antecedent 5-d precipitation amount, and S_1 is the potential maximum retention corresponding to AMC I. Eq. (2.21) assumes the watershed to be dry 5 days before the onset of the rain storm. Putting $S_1 = S + V_0$ in Eq. (2.21) and solving for V_0 results

$$V_0 = 0.5 \left[-1.2S + \sqrt{0.64S^2 + 4P_5 S} \right] \quad (2.22)$$

Here, + sign before the square root is retained for V_0 to be greater than or equal to zero. A generalized form of Eq. (2.22) can be given as:

$$V_0 = 0.5 \left[-(1 + \lambda S) + \sqrt{(1 - \lambda)^2 S^2 + 4P_5 S} \right] \quad (2.23)$$

where $\lambda = 0.2$. Eqs. (2.23), (2.22), & (2.20) constitute the modified MS model.

A comparison between the existing SCS-CN method and modified MS model shows that the latter one performs better and it can be recommended for real world applications. The modified version of MS model has only one-parameter similar to existing SCS-CN method and obviates the sudden jump in CN corresponding to change in the antecedent moisture condition. Further a catchment area based evaluation of MS model and its modified version (Mishra et al., 2005) shows that the modified version performed better than the existing method. However, the developed model has few points of concern as: (i) the model is based on the $(I_a + S)$ scheme, whereas I_a is separate from S ; (ii) no explicit relationship between I_a and V_0 , it is of common experience that I_a relies on interception, surface storage, and infiltration (Ponce and Hawkins, 1996) and all these factors are highly dependent on initial soil moisture; (iii) the relationship $S_1 = S + V_0$ is valid only for $I_a = 0$ (Chen, 1982), and needs further attention; and (iii) the model is not suitable for long term hydrologic simulation.

Mishra et al. (2003b) addressed various issues pertaining to the SCS-CN method such as: (i) partial-area contributing concept; (ii) estimation of CNs from the recorded rainfall and runoff

data; (iii) the CNs variability associated with antecedent moisture; and (iv) variability due to temporal and spatial variation of rainfall. Accordingly they suggested a modified SCS-CN method based on $C = S_r$ concept accounting for the static portion of infiltration and the antecedent moisture and provided a simple spread sheet estimation of the potential maximum retention S from P and Q data, and 5-day antecedent precipitation (P_5). The modified SCS-CN method is expressed as:

$$Q = \frac{(P - I_a - F_c)(P - I_a - F_c + V_0)}{P - I_a - F_c + V_0 + S} \quad \text{for } P \geq I_a + F_c \quad (2.24)$$

$$= 0 \quad \text{otherwise}$$

and V_0 is computed by the expression

$$V_0 = \frac{(P_5 - I_a)S_i}{P_5 - I_a + S_i} \quad (2.25)$$

where F_c is the static portion of infiltration. The method was found to perform well on the same data sets as used in the National Engineering Handbook (SCS, 1971). However, the model has following limitations as: (i) it requires a prior knowledge of minimum infiltration rate; (ii) more complex than the existing SCS-CN method.

Mishra & Singh (2004a) provided a brief review of the long term hydrologic simulation models such as Hydrologic Simulation Package Fortran (HSPF), United States Department of Hydrograph Laboratory (USDAHL) (Holtan and Lopez, 1971), Water Yield Model (WYM) (William and LaSeur, 1976), models of Hawkins (1978) and Pandit and Gopalakrishnan (1996), Systeme Hydrologique European (SHE) (Abbott et al., 1986a,b), and Hydrologic Engineering Centre-Hydrologic Modeling System (HEC-HMS) (HEC, 2000) in terms of their architecture and structure, degree of complexity of inputs, time interval used in simulation, and their applicability particularly in the context of developing countries. They developed a four parameter "Versatile SCS-CN Model" to remove the inconsistencies and

complexities associated with the existing models of long term hydrologic simulation. The model obviates the sudden jumps in CN values, exclusively considers the soil moisture budgeting on continuous basis, evapotranspiration, and watershed routing procedures. These characteristics make the model versatile. However, the versatile model contains higher number of parameters and does not distinguish between the intrinsic parameter and initial condition of watershed.

Mishra & Singh (2004b) established the criterion for the applicability of SCS-CN method and extended the SCS-CN concept to derivation of a time distributed runoff model, expressible as:

$$Q(t) = \left\{ 1 - \frac{1}{(1 + kt - \lambda)^2} \right\} i_e A_w \quad (2.26)$$

where $Q(t)$ is the rainfall-excess rate (L^3T^{-1}); i_e is the effective rainfall intensity (LT^{-1}); A_w is the catchment area (L^2); and k and λ are the infiltration decay constant and initial abstraction coefficient, respectively. The rainfall-excess rates obtained through Eq. (2.26) are routed through the single linear reservoir mechanism to compute the outflow at the basin outlet. Mishra and Singh (2004b) also derived SCS-CN based infiltration model, expressed as:

$$f = f_c + \frac{i_0 - f_c}{(1 - \lambda + kt)^2} \quad (2.27)$$

where f is the infiltration rate (LT^{-1}) at any time t ; f_c is the final infiltration rate (LT^{-1}); i_0 is the uniform rainfall intensity; λ is the initial abstraction coefficient; and k is the decay parameter (T^{-1}).

Michel et al. (2005) highlighted the major inconsistencies associated with age-old but most popular SCS-CN methodology, some of them are: (i) it ignores the initial soil moisture, i.e. the moisture storage at the beginning of the storm event in its formulation; (ii) it is applicable only for the end of the storm event, i.e. it is silent in-between the storm event; (iii) there

exists confusion between intrinsic parameter and initial condition of watershed; and (iv) the relationship between the initial abstraction I_a and the potential maximum retention S is not justifiable, although presenting uniqueness in terms of parameter i.e. *one* parameter model characteristics. To tackle these inconsistencies they introduced a renewed SCS-CN procedure based on soil moisture accounting (SMA) procedure, while keeping the acknowledged efficiency of the original methodology as follows:

(i) Hypothesis: that the SCS-CN method is valid not only at the end of storm point but also at any instant during a storm. Thus, P and Q can be differentiated with time t as $\left(\frac{dP}{dt}, \frac{dQ}{dt}\right)$.

(ii) Formulation of SMA store: which would absorb that part of the rainfall not transformed into runoff by the SCS-CN water balance equation (Eq. 2.2) (this part of the rainfall = $(F+I_a)$ in the original method) as:

$$V = V_0 + (P - Q) \quad (2.28)$$

where V_0 is the soil moisture storage level at the beginning of the storm event, V is the moisture storage at any time t during the storm event, and P is the accumulated rainfall up to the time t , and Q is the corresponding runoff. Interestingly, V_0 was ignored in the original SCS-CN methodology, but at the end of storm event the quantity $(V-V_0)$ corresponds to (I_a+F) of the original methodology (for $P > I_a$). However, this SMA procedure is based on the notion that the higher the moisture store level, the higher the fraction of rainfall that is converted into runoff, i.e. if moisture store is full, all the rainfall will transform into runoff.

(iii) On the basis of first hypothesis and SMA procedure, they clarified the confusion between intrinsic parameter and initial condition and conceptualized a new intrinsic parameter $S_a = V_0 + I_a$, independent of the initial condition, and renamed as threshold moisture.

(iv) On the basis of the SMA procedure and changed parameterization, they formulated a coherent and hydrologically sound procedure for the three different cases as follows:

$$\text{for } V_0 \leq S_a - P \quad Q = 0 \quad (2.29)$$

$$\text{for } S_a - P < V_0 < S_a \quad Q = \frac{(P + V_0 - S_a)^2}{P + V_0 - S_a + S} \quad (2.30)$$

$$\text{for } S_a \leq V_0 \leq S_b \quad Q = P \left(1 - \frac{(S_b - V_0)^2}{S^2 + P(S_b - V_0)} \right) \quad (2.31)$$

where $S_b = (S + V_0 + I_a) = (S + S_a)$. It is quite interesting to note that Eq. (2.31) corresponds to $I_a < 0$, the case not included in the original SCS-CN method.

Michel et al (2005) further proposed a continuous sub-model based on their SMA procedure as:

$$q = p \left(\frac{V - S_a}{S} \right) \left(2 - \frac{V - S_a}{S} \right) \quad \text{for } V \geq S_a \quad (2.32)$$

$$= 0 \quad \text{otherwise} \quad (2.33)$$

In an endeavor to simplify, the threshold moisture S_a was taken as a set fraction of S ($= 0.33S$), and antecedent conditions tentatively taken into account by replacing V_0 by a fraction of S i.e. $0.33S$, $0.61S$, and $0.87S$ to accommodate the three AMCs i.e. AMC I, AMC II, and AMC III, respectively. On substituting the designated values of V_0 and S_a into Eq. (2.31), the resulting expressions are given as:

$$\text{for AMC I } (V_0 = 0.33S) \quad Q = P \frac{P}{P + S} \quad (2.34)$$

$$\text{for AMC II } (V_0 = 0.61S) \quad Q = P \frac{(0.48S + 0.72P)}{(S + 0.72P)} \quad (2.35)$$

$$\text{for AMC III } (V_0 = 0.87S) \quad Q = P \frac{(0.79S + 0.46P)}{(S + 0.46P)} \quad (2.36)$$

These event-based SCS-CN-inspired models were found to be specifically sound for the condition, $V_0 \geq S_a$, the condition not encountered in the original method. However, the procedure ignores the case $V_0 < S_a$, with probability of less than 0.1, which corresponds to the existing SCS-CN method (Eq. 2.30). Though the above renewed SCS-CN procedure is founded on a sounder perception of SMA procedure, there exists some inconsistencies as below:

1. the whole procedure is based on the existing SCS-CN methodology, which in itself does not account for the initial soil moisture (V_0) in its basic proportionality ($C = S_r$) concept, which forms the basis of the methodology.
2. the continuous SMA model yields 'zero' runoff for the condition $V \leq S_a$, where S_a is the threshold moisture, and it may not be justifiable as the flow may still appear in the form of interflow.
3. the choice of fixing $S_a = S/3$ or $0.33S$, which can be expressed as $S_a = (0.2S + 0.13S)$ or $I_a = 0.2S$ and $V_0 = 0.13 S$. Here, S = potential maximum retention. This shows that relationship $S_a = S/3$ will not always be valid, it rather holds only for $V_0 = 0.13 S$, which does not fall into any of their AMC description.
4. a tentative replacement of V_0 by a set fraction of S to accommodate the three AMCs seems to be a forced assumption and is not mathematically supported.

2.1.7 Remarks

Within the tremendous literature available on applications of SCS-CN methodology in surface water hydrology, a relevant review dealing with its origin, theoretical and historical background, nature, advantages and limitations, issues pertaining to structural foundation, including the CN vs AMC description and SMA procedure, and advanced applications of methodology including the areas other than originally intended have been presented and discussed for their merits and demerits. Some of its critics suggest it to be obsolete, a remnant of outdated technology, and needs overhaul or outright replacement (Smith and Eggert, 1978; Van-Mullem, 1989). Yuan et al. (2001) applied the methodology for sub-surface drainage study. On the other hand, Mishra and Singh (2004a,b), and Mishra et al. (2006a) extended the methodology to long term hydrologic simulation, time distributed

runoff modeling, and event based sediment yield modeling, respectively. Recently Michel et al. (2005) highlighted the structural inconsistencies associated with the methodology and proposed a renewed SCS-CN procedure that retains its simplicity and, in all likelihood, the potential efficiency of the original model. However, there still exist some inconsistencies, further reflecting the need of improvement.

2.2 SYNTHETIC UNIT HYDROGRAPH (SUH) METHODS

The SUH methods are of great significance in determination of flood peak and runoff volume, especially from ungauged watersheds. The qualifier “*synthetic*” denotes that UH is obtained without using watershed’s rainfall-runoff data (Bhunya et al., 2003b). These synthetic or artificial unit hydrographs are characterized by their simplicity and ease in construction. They require less amount of data and yield a smooth and single-valued shape corresponding to unit runoff volume, which is essential for UH derivation.

2.2.1 Background

The unit hydrograph concept proposed by Sherman (1932) for estimating the storm runoff hydrograph at the gauging site in a watershed corresponding to a rainfall hyetograph is still a widely accepted and admired tool in hydrologic analysis and synthesis. This was one of the first tools available to hydrologic community to determine the complete shape of the hydrographs rather than the peak discharges only (Todini, 1988). As the unit hydrograph concept needed the observed rainfall-runoff data at the gauging site for hydrograph generation, the paucity of these data sparked the idea of synthetic unit hydrograph (SUH) concept. The beginning of SUH concept can be traced back to the model (distribution graph) proposed by Bernard (1935) to synthesize the UH from watershed characteristics, rather than the rainfall-runoff data (Singh, 1988). The methods used for derivation of unit hydrographs in catchments where there is a limited amount of data and for catchments with no data i.e. ungauged catchments will be discussed here under four sections: (i) Popular Synthetic Unit Hydrograph methods; (ii) Conceptual methods of Synthetic Unit Hydrograph; (iii)

Geomorphologic Unit Hydrograph (GIUH) based synthetic Unit Hydrograph methods; and
 (iv) Probability Distribution Function based Synthetic Unit Hydrograph methods.

2.2.2 Popular Synthetic Unit Hydrograph Methods

In practice, a SUH is derived from a few salient points of the UH by manually fitting a smooth curve. The methods of Snyder (1938), Taylor and Schwarz (1952), Soil Conservation Service (SCS, 1957), Gray (1961), and Espey and Winslow (1974) are a few examples among others, which utilize empirical equations to estimate salient points of the hydrograph, such as peak flow (Q_p), lag time (t_L), time base (t_B), and UH widths at $0.5Q_p$ and $0.75Q_p$. Thus, a great degree of subjectivity is involved in such manual fittings. In addition, these fitted curves require simultaneous adjustments for the area under SUH to represent unit runoff volume. In spite of their limitations, these methods are widely used for SUH derivations in ungauged watersheds. In this chapter some of the commonly used popular SUH methods e.g., Snyder's method (Snyder, 1938), Soil Conservation Service method (SCS, 1957), and Gray method (Gray, 1961) will be discussed.

(a) Snyder's Method

For the first time Snyder (1938) established a set of empirical relationships, which relate the watershed characteristics, such as A_w = area of the watershed (square miles); L = length of main stream (miles); and L_{CA} = the distance from the watershed outlet to a point on the main stream nearest to the center of the area of the watershed (miles) with the three basic parameters of the UH (i.e. t_L = lag time to peak (hr); Q_p = peak flow rate (ft^3/s); and t_B = base time (days), to describe the shape of the UH, expressed as:

$$t_L = C_T (LL_{CA})^{0.3} \quad (2.37)$$

$$Q_p = 640 \left(\frac{A_w C_P}{t_L} \right) \quad (2.38)$$

$$t_B = 3 + 3 \left(\frac{t_L}{24} \right) \quad (2.39)$$

where C_T and C_P are nondimensional constants, varying from 1.8 to 2.2 and 0.56 to 0.69, respectively. Eqs. (2.37) to (2.39) hold good for rainfall-excess duration (or unit duration = T_D (hr)) as:

$$T_D = \frac{t_L}{5.5} \quad (2.40)$$

If the duration of rainfall-excess, say D (hr), is different from T_D , a revised lag time t_{LR} (hr) is estimated from

$$t_{LR} = t_L + \frac{(D - T_D)}{4} \quad (2.41)$$

These relationships (Eqs. 2.37 to 2.41) provide a complete shape of SUH. Since one can sketch many SUHs through the three known characteristic points (i.e. t_L , Q_P , and t_B), with its specific criteria i.e. area under the SUH to be unity. To overcome with this ambiguity associated with the Snyder's method, the U.S. Army Corps of Engineers (USACE, 1940) developed empirical equations between widths of SUH at 50% and 75% of Q_P i.e. W_{50} and W_{75} respectively as a function of $(Q_P/A_w) = q_p$, expressible as:

$$W_{50} = \frac{830}{q_p^{1.1}} \quad (2.42)$$

$$W_{75} = \frac{470}{q_p^{1.1}} \quad (2.43)$$

where W_{50} and W_{75} are in units of hour. Thus one can sketch a smooth curve through the seven points (t_L , t_B , Q_P , W_{50} , and W_{75}) relatively in an easier way with less degree of

ambiguity and to have the area under the SUH unity. However, this procedure is also tedious and involves great degree of subjectivity and errors due to manual fitting of the points and simultaneous adjustments for the area under the SUH. In summary, the major inconsistencies associated with the method are:

1. the manual fitting of the characteristic points involves great degree of subjectivity and trial and error, and may involve error.
2. the constants C_T and C_P vary over wide range and from region to region, and may not be equally suitable for all the regions.
3. the time base t_B (Eq. 2.39) is always greater than three days (Raudkivi, 1979), which reflects the method's applicability for fairly large watersheds only (Langbein, 1947; Taylor and Schwarz, 1952; Gray 1961).

(b) SCS Method

The SCS method (SCS, 1957, 1972) of the United States Department of Agriculture (USDA) uses a specific average dimensionless unit hydrograph derived from the analysis of large number of natural UHs for the watersheds of varying size and geographic locations, to synthesize the UH (Singh, 1988). The method assumes the triangular shape of dimensionless unit hydrograph in order to define time base, t_B , in terms of time to peak, t_p , and time to recession, t_r , and to compute runoff volume (V_R) and peak discharge q_p as:

$$V_R = \frac{(q_p t_B)}{2} = \frac{1}{2} q_p (t_p + t_r); t_r = 1.67 t_p \quad (2.44)$$

$$q_p = 0.749 \left(\frac{V_R}{t_p} \right) \quad (2.45)$$

where q_p is in mm/hr/mm (or inch/hr/inch) and can be related to Q_p as equal to Q_p/A_w per unit depth of rainfall-excess; V_R is in mm (or inch); t_p and t_r are in hrs. To determine the complete shape of SUH from the nondimensional (q/q_p vs t/t_p) hydrograph, the time to peak and peak flow rate are computed as:

$$t_p = t_L + \left(\frac{D}{2}\right) \quad (2.46)$$

$$Q_p = 484 \left(\frac{A_w}{t_p}\right) \quad (2.47)$$

where t_L = lag time from centroid of excess-rainfall to peak discharge (Q_p) (hour); D = the excess-rainfall duration (unit duration) (hour); Q_p = peak discharge in ft^3/s ; and A_w = area in square miles. The lag time (t_L) can be estimated from the watershed characteristics using curve number (CN) procedure as:

$$t_L = \frac{L^{0.8} (2540 - 22.86\text{CN})^{0.7}}{14104\text{CN}^{0.7} S_{av}^{0.5}} \quad (2.48)$$

where t_L = in hours; L = hydraulic length of watershed (m); CN = curve number ($50 \leq 95$); and S_{av} = average catchment slope in (m/m). Thus with known Q_p , t_p , and specified dimensionless UH, the SUH can be developed smoothly. However, the inconsistencies associated with the method can be enumerated as follows:

1. since the SCS method fixes the ratio of time base to time to peak (t_b/t_p) for triangular UH equal to 2.67 (or 8/3), ratios other than this may lead to the other shapes of the UH. In particular, the larger ratio implies the greater catchment storage. Therefore, since the SCS method fixes the ratio (t_b/t_p), it should be limited to midsize watersheds in the lower end of the spectrum (Ponce, 1989).
2. the SCS method is one of the popular methods for synthesizing the UH for only small watersheds of less than 500 square miles (Wu, 1969; Wang and Wu, 1972; and McCuen and Bondelid, 1983).

(c) Gray's Method

Gray (1961) developed a dimensionless graph (empirical in nature) procedure based on two-parameter gamma distribution function and watershed characteristics to derive a SUH. The geometry of dimensionless graph is expressed as:

$$Q_{t/P_R} = \frac{25.0(\gamma')\lambda'}{\Gamma(\lambda')} \left(e^{-\gamma' t/P_R} \right) \left(\frac{t}{P_R} \right)^{(\lambda'-1)} \quad (2.49)$$

where Q_{t/P_R} = % flow/0.25 P_R at any given t/P_R value; P_R = the time from beginning of surface runoff to the occurrence of peak discharge (minutes); γ' = a dimensionless parameter = γP_R ; λ' = shape parameter = $1 + \gamma'$; γ = scale parameter; Γ = gamma function.

In words of Gray (1961), "Each graph was adjusted with the ordinate values expressed in percentage flow based on a time increment equal to $1/4$ the period of rise, P_R . The empirical graphs described in this manner were referred to as dimensionless graphs". He defined the ratio $1/\gamma = P_R/\gamma'$ as the storage factor, a measure of the storage property of watershed or the travel time required for water to pass through a given reach, and related it with the watershed characteristics in the form of a power equation as:

$$\frac{P_R}{\gamma'} = a \left(\frac{L}{\sqrt{S_M}} \right)^b \quad (2.50a)$$

where a and b are the coefficient and exponent of the power equation. Eq. (2.50a) was applied to 33 watersheds comprising of three regional groups: (i) Nebraska-Western Iowa; (ii) Central Iowa-Missouri-Illinois and Wisconsin; and (iii) Ohio, to estimate a and b . Finally, for each group Eq. (2.50a) is expressed as:

For Nebraska-Western Iowa: -
$$\frac{P_R}{\gamma'} = 7.40 \left(\frac{L}{\sqrt{S_M}} \right)^{0.498} \quad (2.50b)$$

For Central Iowa-Missouri-Illinois and Wisconsin: -
$$\frac{P_R}{\gamma'} = 9.27 \left(\frac{L}{\sqrt{S_M}} \right)^{0.562} \quad (2.50c)$$

For Ohio: -
$$\frac{P_R}{\gamma'} = 11.40 \left(\frac{L}{\sqrt{S_M}} \right)^{0.531} \quad (2.50d)$$

where the ratio P_R/γ' is in minutes; L = length of main stream in miles; S_M is the slope of main stream in %. Finally, Gray developed a regression relationship between the period of rise P_R and dimensionless parameter γ' as

$$\frac{P_R}{\gamma'} = \frac{1}{\frac{2.676}{P_R} + 0.0139} \quad (2.51)$$

Thus, Eqs. (2.49) to (2.51) are used to develop the dimensionless UH, and consequently the SUH. One of the best finding of the study is that the two-parameter gamma distribution can be used successfully to describe the synthetic unit hydrograph. However, the empirical relationships (Eqs. 2.50-2.51) are watershed size specific, and should be used with in the area limits for which these are developed (Gray, 1961).

2.2.3 Conceptual Synthetic Unit Hydrograph Methods

In this section the popular conceptual models of Clark (1945); Nash (1958, 1959); and Hybrid model (HM) of Bhunya et al. (2005) are discussed.

(a) Clark's Model

The Clark IUH model is based on the concept that IUH can be derived by routing unit excess-rainfall in the form of a time area diagram through a single linear reservoir. For derivation of IUH the Clark model uses two parameters viz. time of concentration (T_c) in hours and storage coefficient (K) in hours of a single linear reservoir in addition to the time-area diagram. The governing equation of the Clark IUH model is expressed as (Kumar et al., 2002):

$$u_i = CI_i + (1 - C)u_{i-1} \quad (2.52)$$

where $u_i = i^{\text{th}}$ ordinate of IUH; C and $(1-C)$ = the routing coefficients; and $C = \Delta t / (K + 0.5\Delta t)$; Δt = computational interval in hours; $I_i = i^{\text{th}}$ ordinate of time-area diagram. Finally a unit hydrograph of desired duration (D) can be derived using the following equation

$$U_i = \frac{1}{N} (0.5I_{i-N} + u_{i-N+1} + \dots + u_{i-1} + 0.5u_i) \quad (2.53)$$

where $U_i = i^{\text{th}}$ ordinate of unit hydrograph of D -hour duration and computational interval Δt hours; $N = \text{number of computational intervals in } D\text{-hours} = D/\Delta t$. Eq. (2.53) can also be used to derive flood hydrograph in ungauged catchments. One of the approaches popularly used by field engineers is through regionalization of Clark parameters K and C . For example, HEC-1 (1990) evaluates the two parameters of Clark's model for determining the representative UH for a catchment. The computed parameters are given in the form of $K/(T_c + K)$, which can be used for developing a regional relationship by relating it to physical characteristics of different catchments in a homogeneous region. This regional relationship can then be used to compute the Clark model parameters for an ungauged catchment which is then used to derive the UH. Alternatively, data of gauged catchments in a region can be used to develop regional relationship that yields either of the parameters for an ungauged catchment in the region. However, some of the inconsistencies associated with Clark's model are of concern such as (i) the entire hydrograph recession is represented by a single recession constant, while a recession constant that varies with time is implicitly incorporated into Nash model (Nash, 1958). HEC-1 uses Snyder's C_p and t_p to optimize the parameters (T_c and K) of Clark's UH. In addition to this, it requires for application. This is a limitation of Clark's UH to be used as an SUH.

(b) Nash Model

In a series of publications, Nash (1957, 1958, 1959, and 1960) developed a conceptual model based on a cascade of n equal linear reservoirs with equal storage

coefficient K for derivation of the IUH for a natural watershed. The analytical form of the model is expressed as:

$$q(t) = \frac{1}{K\Gamma(n)} \left(\frac{t}{K}\right)^{n-1} e^{-\frac{t}{K}} \quad (2.54)$$

where $q(t)$ is the depth of runoff per unit time per unit effective rainfall and K is the storage coefficient of the reservoirs in units of hours. The parameters n and K are often termed, respectively, as the shape and scale parameters. It is noteworthy that parameter n is dimensionless and K has the unit of time. The area under the curve defined by Eq. (2.54) is unity. Thus the rainfall-excess and direct surface runoff depths are equal to unity. The IUH (Eq. 2.54) is used to derive the resultant flood hydrograph for a given input rainfall. To estimate n and K , Nash (1960) related the first and the second moments of the IUH with important physical characteristics for some English catchments as follows:

$$m_1 = 27.6A_w^{0.03}S_0^{-0.3} = \frac{1}{K\Gamma(n)} \int_0^{\infty} \left(\frac{t}{K}\right)^{n-1} e^{-\frac{t}{K}} (t) dt = n K \quad (2.55a)$$

$$m_2 = 1.0m_1^{-0.2}S_0^{-0.1} = \frac{1}{K\Gamma(n)} \int_0^{\infty} \left(\frac{t}{K}\right)^{n-1} e^{-\frac{t}{K}} (t^2) dt = n(n+1) K^2 \quad (2.55b)$$

where m_1 and m_2 are the first and the second moments of the IUH about the origin, A_w is the catchment area in square miles, and S_0 is the overland slope. Eqs. (2.55) can be used to compute the parameters of Eq. (2.54). Once the parameters are evaluated from available A_w and S_0 , the complete IUH can be derived using Eq. (2.54). Thus, this is one of the approaches for deriving IUH for ungauged catchments. It may be noted here that IUH can be extended to a UH for the catchment using existing conventional procedures (Ponce, 1989; Bras, 1990; Singh, 1992). It is observed that Eq. (2.54) is nothing but the two-parameter gamma distribution (2PGD). Use of two-parameter gamma distribution for representing the SUH has long hydrologic history that started with Edson (1951), and subsequently followed by Croley

(1980), Aron and White (1982), Haan et al. (1994), and Bhunya et al. (2003b, 2004, 2007a). A detail review of these studies on gamma distribution along with some popular probability distributions as SUH is discussed in the forthcoming section.

(c) Hybrid Model (HM)

To overcome the inconsistencies associated with the Nash model such as: (i) the number of linear reservoirs 'n' should desirably be an integer value, generally comes out to be a fractional value when derived from observed data (Singh, 1988); and (ii) a single linear reservoir of Nash model (n=1) yields an IUH that follows extreme Poisson distribution without a rising limb, or $t_p = 0$. Hence, to simulate a complete IUH with rising limb (or $t_p > 0$) the Nash model requires a minimum of two reservoirs connected in series. Building on this idea, Bhunya et al. (2005) developed a hybrid model for derivation of synthetic unit hydrograph by splitting Nash single linear reservoir into two serially connected reservoirs of unequal storage coefficient (one hybrid unit) to have a physically realistic response. The hybrid unit concept is similar to one generally used in chemical engineering for defining a unit of chemical system (Kafarov, 1976). The analytical form of the model for two hybrids units in series is expressed as:

$$Q_2(t) = \frac{1}{(K_1 - K_2)^2} \left[\left(te^{-\frac{t}{K_1}} + te^{-\frac{t}{K_2}} \right) - \frac{2K_1K_2}{(K_1 - K_2)} \left(e^{-\frac{t}{K_1}} - e^{-\frac{t}{K_2}} \right) \right] \quad (2.56)$$

where $Q_2(t)$ = the output from the second hybrid unit (mm/ /hr/mm); and K_1 and K_2 = the storage coefficient of first and second reservoirs (hr), respectively, of each hybrid unit. From Eq. (2.56) one can get easily the expression for time to peak flow rate (t_p) for the condition at $t = t_p$, $Q_2(t) = Q_p$ or $dQ_2(t)/dt = 0$. Eq. (2.56) is nothing but the output response function for the second hybrid unit due to a unit impulse perturbation at the inlet of first hybrid unit, and defines the complete shape of IUH. Eq. (2.56) has two parameters, i.e., K_1 and K_2 . They developed empirical relationships to estimate K_1 and K_2 from known peak flow rate (q_p) and time to peak (t_p). However, for ungauged conditions, q_p and t_p were estimated through Snyder

method (Snyder, 1938) and SCS method (SCS, 1957). The hybrid model was found to work significantly better than the most widely used methods such as Snyder, SCS, and Nash model (two-parameter gamma distribution function) when tested on the data of Indian and Turkey catchments for partial (known q_p and t_p) and no data availability (ungauged) conditions.

2.2.4 Geomorphologic Instantaneous Unit Hydrograph (GIUH) Based SUH Methods

Linking quantitative geomorphology with basin hydrologic characteristics can provide a simple way to understand the hydrologic behavior of different basins, particularly the ungauged ones. The quantitative study of channel networks was originated by Horton (1945). He developed a system for ordering streams networks and derived laws relating the stream numbers, stream lengths, and catchment area associated with streams of different order. The quantitative expressions of Horton's laws are (Rodriguez-Iturbe and Valdes, 1979):

Law of stream number

$$N_w / N_{w+1} = R_B \quad (2.57)$$

Law of stream length

$$\bar{L}_w / \bar{L}_{w-1} = R_L \quad (2.58)$$

Law of stream areas

$$\bar{A}_w / \bar{A}_{w-1} = R_A \quad (2.59)$$

where N_w is the number of streams of the order w , \bar{L}_w is the mean length of stream of order w , and \bar{A}_w is the mean area of basin of order w . R_B , R_L , and R_A represent the bifurcation

ratio, length ratio, and area ratio whose values in nature are normally between 3 and 5 for R_B , between 1.5 and 3.5 for R_L , and between 3 and 6 for R_A .

Several attempts have been made to establish relationships between the parameters of the models for ungauged catchments, and the physically measurable watershed characteristics (Bernard, 1935; Snyder, 1938; Taylor and Schwarz, 1952; Gray, 1961; and Boyd et al., 1979 & 1987). In this regard, the pioneering works of Rodriguez-Iturbe and Valdes (1979), Valdes et al. (1979), and Rodriguez-Iturbe et al. (1979), which explicitly integrate the geomorphology details and the climatological characteristics of a basin, in the framework of travel time distribution, are a boon for stream flow synthesis in ungauged basins or partial information on storm event data. Gupta et al. (1980) examined the above approach and reformulated, simplified and generalized it. Rosso (1984) parameterized the Nash model in terms of Horton order ratios of a catchment based on the geomorphologic model of a catchment. Rinaldo and Rodriguez- Iturbe (1996) and Rodriguez-Iturbe and Rinaldo (1997) expressed the pdf of travel times as a function of the basin forms characterized by the stream networks and other landscape features. Chutha and Dooge (1990) reformulated the GIUH on a deterministic platform rather than on Markov and statistical mechanics approaches. Kirshen and Bras (1983) studied the effect of linear channel on GIUH. Al-Wagdany and Rao (1997) investigated the dependency of average velocity of GIUH on climatic and basin geomorphologic parameters and found that the average velocity of varies inversely with effective rainfall depth. Cudenec et al. (2004) provided the geomorphological explanation of the UH concept based on the statistical physics reasoning (similar to Maxwell's reasoning) that considers a hydraulic length symbolic space, built on self similar lengths of the components, and derived the theoretical expressions of the probability density functions of the hydraulic length and of the lengths of all the components in form of gamma pdf in terms of geomorphological parameters. Allam and Balkhair (1987) discussed several issues related to the probabilistic and hydraulic structure of the GIUH concept. Jain et al. (2000), Jain and Sinha (2003), Sahoo et al. (2006), and Kumar et al. (2007) applied geographic information system (GIS) supported GIUH approach for estimation of design flood. Similarly the works of Bérod et al. (1995), Sorman (1995), Bhaskar et al. (1997), Yen and Lee (1997), Hall et al. (2001), and Fleurant et al. (2006) based on GIUH approach for estimation of design flood from gauged as well as ungauged basins

are noteworthy. Some of the pertinent works related with GIUH approach are discussed here as follows.

Rodriguez-Iturbe and Valdes (1979) expressed the initial state probability of one droplet of rainfall in terms of geomorphological parameters as well as the transition state probability matrix. The final probability density function of droplets leaving the highest order stream into the trapping state is nothing but the GIUH. An exponential holding time mechanism, equivalent to that of a linear reservoir, was assumed. The expression derived by Rodriguez-Iturbe and Valdes (1979) yields full analytical, but complicated expressions for the instantaneous unit hydrograph (IUH). They suggested that it is adequate to assume a triangular instantaneous unit hydrograph and only specify the expressions for the time to peak and peak value of the IUH. These expressions are obtained by regression of the peak as well as time to peak of IUH derived from the analytic solutions for a wide range of parameters with that of the geomorphologic characteristics and flow velocities. The model was parameterized in terms of Horton's order laws (Horton 1945) of drainage network composition and Strahler's stream ordering scheme (Strahler 1957). The expressions for peak flow (q_p) and time to peak (t_p) of the IUH are given as:

$$q_p = \left(\frac{1.31}{L} \right) R_L^{0.43} v \quad (2.60)$$

and

$$t_p = 0.44 \left(\frac{L}{v} \right) R_B^{0.55} R_A^{-0.55} R_L^{-0.38} \quad (2.61)$$

where L is the length of main channel or length of highest order stream in kilometers, v is the average peak flow velocity or characteristic velocity in m/s, q_p and t_p are in units of hr^{-1} and hr, respectively. Rodriguez-Iturbe and Valdes (1979) defined a non-dimensional term β as the product of q_p (Eq. 2.60) and t_p (Eq. 2.61) as:

$$\beta = 0.584 \left(\frac{R_B}{R_A} \right)^{0.55} R_L^{0.05} \quad (2.62)$$

It is observed from Eq. (2.62) that β is independent of velocity v and length of highest order stream or scale variable L , thereby, on the storm characteristics and hence is a function of only the catchment characteristics. Alternatively, Eqs. (2.60) and (2.61) can be expressed as (Rosso, 1984):

$$q_p = 0.364R_L^{0.43}vL^{-1} \quad (2.63)$$

and

$$t_p = 1.584(R_B/R_A)^{0.55}R_L^{-0.38}v^{-1}L \quad (2.64)$$

where q_p , t_p , L and v must be in coherent units. The UH parameters given by Eqs. (2.60) and (2.61) can be used in Snyder's method, SCS method or Gray's method to develop a SUH in ungauged catchments as discussed in earlier sections. The following text describes the Geomorphologic UH based 2PGD Model (Nash Model).

The possibility of preserving the form of the SUH through a two-parameter gamma pdf was analyzed by Rosso (1984), where Nash model parameters were related to Horton's order ratios using Eq. (2.62). For this, the problem has been approached by equating the dimensionless products of the peak and time to peak resulting from the two formulations. The mean and variances of two-parameter gamma pdf (Eq. 2.54) are described as:

$$\text{Mean } (\mu) = n K; \text{ variance } (\sigma^2) = n K^2 \quad (2.65)$$

where K is the scale parameter [T], n is the shape parameter, and $\Gamma ()$ is the gamma function. Chow (1964) relates n and K as:

$$K = t_p / (n-1) \quad (2.66)$$

From Eq. (2.54) one can easily get the expression relating K and n for the condition at $t = t_p$, $q(t) = q_p$ or $dq(t)/dt = 0$.

On substituting K from Eq. (2.66) into Eq. (2.54) one gets the expression for q_p as:

$$q_p = \frac{(n-1)^{(n-1)} e^{-(n-1)}}{t_p \Gamma(n-1)} \quad (2.67)$$

Alternatively, the product $q_p t_p$ can be combined into the following simpler form:

$$\beta = q_p t_p = \frac{(n-1)^{(n-1)} e^{-(n-1)}}{\Gamma(n-1)} \quad (2.68)$$

Rosso used an iterative computing scheme and proposed the following equations for n and K by equating the expressions of β (Eqs. 2.62 and 2.68) as:

$$n = 3.29(R_B / R_A)^{0.78} R_L^{0.07} \quad (2.69)$$

and

$$K_* = 0.70[R_A / (R_B R_L)]^{0.48} \quad (2.70)$$

where $K_* = KvL^{-1}$ is a dimensionless scale parameter. Thus, for an observed v , the parameters of the 2GPD and the shape of the UH can be computed from the geomorphological parameters of the catchment. Further the author tested the capability of Eqs. (2.69) and (2.70) on five Italian catchments to predict the parameters of the Nash model against some traditional regression formulae such as Nash (1960), Wu (1963), and De Vito (1975). It was found that the present approach improves substantially the capability of predicting the parameters of the Nash model with respect to the others. Some of the important findings associated with the study can be summarized as:

1. the form of the IUH derived from the GUH model of catchment response can be satisfactorily preserved by a two-parameter gamma pdf, and the gamma pdf can

be successfully parameterized in terms of Horton's order ratios, i.e., physically meaningful and easily determined quantities.

2. for the Nash model of catchment response the shape parameter of the IUH only depends on the Horton's order ratios and can therefore be predicted from catchment geomorphology. This notion indicates the applicability of the proposed approach to the ungauged catchments as well.
3. for the Nash model the scale parameter of catchment response depends both on geomorphology and on stream flow velocity.

From the above study it seems that under the same framework a similar approach can also be applied to other suitable probability distribution functions for ungauged catchments.

2.2.5 Probability Distribution Function Based SUH Methods

Due to similarity in the shape of the statistical distributions and a conventional unit hydrograph, several attempts have been made in the past to use their probability density functions (pdfs) for derivation of the SUH. For example, Gray (1961), Sokolov et al. (1976), Croley (1980), Aron and White (1982), Haktanir and Sezen (1990), Yue et al. (2002), and Nadarajah (2007) are to name but are only a few of them. Singh (2000) transmuted the popular SUHs, such as those of Snyder, the SCS, and Gray into the Gamma distribution. Bhunya et al. (2003b & 2004) utilized two-parameter Gamma distribution (2PGD) and three-parameter Beta distribution function (3PBD) in deriving SUH for Indian as well as Turkey catchments. More recently, Bhunya et al. (2007a) explored the potential of four popular pdfs, i.e., two-parameter Gamma, three-parameter Beta, two-parameter Weibull, and one-parameter Chi-square distribution to derive SUH. Some of the recent research work related with the use of distribution functions as SUH is discussed here as follows.

Croley (1980) developed synthetic hydrograph by fitting two-parameter gamma distribution for different set of boundary conditions: (t_p, q_p) , (t_p, t_i) or (q_p, t_i) . These boundary conditions are used to estimate the parameters n and K of the distribution. The general expression for the synthetic hydrograph is expressed as:

$$q(t) = \frac{V_R}{K\Gamma(n)} \left(\frac{t}{K}\right)^{n-1} e^{-\frac{t}{K}} \quad (2.71)$$

where V_R is defined as:

$$\int_0^{\infty} q(t) dt = V_R \quad (2.72)$$

where t_i is the point of inflection [T], q_p is the peak discharge per unit area per unit effective rainfall [T^{-1}], and t_p is the time to peak [T]. It is interesting to note that if V_R corresponds to the volume of runoff produced by a unit depth of rainfall excess uniformly applied both spatially over the watershed area and temporarily over the storm duration, then $q(t)$ (Eq. 2.71) is by definition, the "unit hydrograph" for that area and for that storm duration. It can be converted easily into hydrographs corresponding to other rainfall excess depths and storm durations by using the available linear superposition techniques (Linsley et al., 1975; Croley, 1977). The methodology provides a line of initiation to work with probability distribution functions for synthetic unit hydrograph derivation for ungauged catchments.

Haktanir and Sezen (1990) explored the suitability of two-parameter gamma and three-parameter beta distributions as synthetic unit hydrographs for Anatolia catchments in Turkey. The analytical expressions for scale-adjusted gamma and beta distributions as SUH are expressed as:

(i) Gamma Synthetic Unit Hydrograph

$$Q(t) = (A_w/0.36) \frac{1}{K\Gamma(n)} (t/K)^{n-1} e^{-t/K} \quad (2.73)$$

where $Q(t)$ = the flow rate of the gamma SUH at time t in $m^3/s/cm$; A_w = watershed area in km^2 ; t = time in hours; and n and K are same as discussed above.

(ii) Beta Synthetic Unit Hydrograph

$$Q(t) = (A_w/0.36) \left[t^{r-1} (b-t)^{p-r-1} \right] / [B b^{p-1}] \quad (2.74)$$

where B is given as

$$B = [\Gamma(r)\Gamma(p-r)]/\Gamma(p) \quad (2.75)$$

where $Q(t)$ = the flow rate of Beta SUH at time t in $m^3/s/cm$; r and p = the shape parameters; b = scale parameter in hours. The parameters of both distributions were estimated by using classical Newton iterative algorithm. They found both the distributions to fit reasonably well to observed unit hydrographs.

Bhunya et al. (2003b) introduced a simplified version of two-parameter gamma distribution to derive a synthetic unit hydrograph more conveniently and accurately than the popular Snyder, SCS, and Gray methods. The analytical form of the distribution is represented by Eq. (2.54). They also defined a non-dimensional term $\beta = q_p t_p$ (Eq. 2.68) same as to Rosso (1984) to relate n and β . Since the exact solution of n in terms of β from Eq. (2.68) is not possible, they developed simpler relationships between n and β to obtain the simplified versions of gamma distribution. The developed relationships are given as:

$$n = 5.53\beta^{1.57} + 1.04 \quad \text{for } 0.01 < \beta < 0.35; \text{ COD} = 1 \quad (2.76a)$$

and

$$n = 6.29\beta^{1.998} + 1.157 \quad \text{for } \beta \geq 0.35; \text{ COD} = 1 \quad (2.76b)$$

Thus, for known values of β , n can be estimated from Eq. (2.76) and K from Eq. (2.66). In addition, it eliminates the cumbersome trial and error solution of Eq. (2.68) to estimate n and K . One thousand sets of (n, β) values with n ranging from 1 to 40.0 and β ranging from 0.01 to 2.5 were considered for developing the relationships (Eqs. 2.76a,b). The major findings

are: (i) n can be expressed mathematically in terms of β in a simple but accurate form; (ii) the parameter n and dimensionless term β are dependent not only on the physical characteristics of the watershed, but also on its storage characteristics; and (iii) The present approach worked better than the Snyder, SCS, and Gray methods.

Bhunya et al. (2007a) explored the potential of four popular pdfs, viz., two-parameter Gamma, three-parameter Beta, two-parameter Weibull, and one-parameter Chi-square distribution to derive SUH. They developed simple analytical and numerical relationships to compute the distribution parameters, and checked their validity using simulation and field data. Some of the important conclusions drawn from the study were:

1. given two points on the UH, e.g., time to peak and peak flow, these pdfs can be used to describe the shape of the unit hydrograph, and they perform better than the existing synthetic methods, i.e. methods suggested by Snyder (1938), SCS (1957), and Gray (1961).
2. the proposed analytical solutions for parameter estimations are simple to use, and gives accurate results of the actual pdf parameters.
3. among the four pdfs analyzed in the study, the Beta and Weibull distributions are more flexible in description of SUH shape as they skew on both sides similar to a UH, and on the basis of their application to field data.

2.2.6 Remarks

The synthetic unit hydrograph (SUH) approach is a powerful tool to estimate flood peak, time to peak, and the complete shape of unit hydrograph for ungauged catchments. The SUH methods developed so far can be categorized as (i) the empirical methods of Snyder, SCS, and Taylor and Schwartz methods; (ii) the conceptual models of Clark and Nash, and Bhunya et al. (2005); (iii) the GIUH based methods of Rodriguez-Iturbe and Valdes (1979), Gupta et al. (1980), Rosso (1984), etc.; and (iv) the probability distribution functions based methods of Gray, (1961), Sokolov et al., (1976), and Croley (1980), Haktanir and Sezen (1990), Bhunya et al. (2003b, 2004, 2007a), and Nadarajah (2007), etc. Though the empirical methods of Snyder and SCS are widely used for SUH derivation, but have several

inconsistencies with them. The conceptual model of Nash defines the standard shape of UH using the minimum number of parameters. However, there exists not many improvements over these conceptual models in recent past and their applications to prediction of design flood in ungauged catchments are limited. Recently Bhunya et al. (2005) proposed a Hybrid model (HM), which can be taken as an improvement over the Nash model. However, the HM model also lacks the concept of translation, which is essential for describing a dynamic system. Various researchers like Gray (1961), Sokolov et al. (1976), and Croley (1980), Haktanir and Sezen (1990), Singh (2000), and Bhunya et al. (2004, 2005, 2007a) used the statistical properties of gamma and other probability distributions to derive the complete shape of UH for ungauged catchments. This approach avoids subjective sketching of UH shape in order to satisfy the constraint of unit volume. With GIUH techniques, it has become possible to compute some salient parameters of an ungauged catchment from geomorphological catchment characteristics. This can be used to get the complete shape of SUH using the methods, such as those due to Rosso (1984).

2.3 SEDIMENT GRAPH BASED SEDIMENT YIELD MODELING

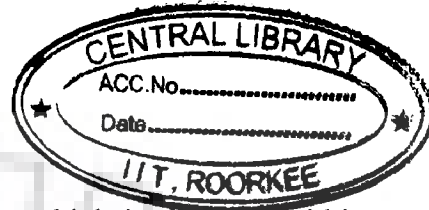
Sediment yield is defined as the total sediment outflow from a watershed or a drainage basin, measurable at a point of reference and in a specific period of time (ASCE, 1970). Sediment yield from a watershed is the output form of an erosion process, and is difficult to estimate as it arises from a complex interaction of various hydro-geological processes, and the knowledge of the actual process and extent of suspended material is far less detailed (Juyal and Shastry, 1991; Sharda et al., 2002). Since the present study deals mainly with the sediment graph based sediment yield modeling, a detailed review on the available sediment graph models is presented here. However, before this, a brief introduction about the basic concepts and theories associated with the sediment yield modeling is in order.

2.3.1 Background

Estimates of sediment yield are required for solution of number of problems such as design of dams and reservoirs, transport of pollutants, river morphology, design and planning

reflect watershed sediment yield processes. The process of sediment yield generally involves: (i) detachment and transportation of soil particles by rainfall, (ii) the detachment and transport of soil particles by runoff, and (iii) eventually deposition of soil particles. The sediment yield process may be considered to consist of two phases: (i) the upland phase and (ii) the lowland stream or the channel phase (Bennet, 1974).

(a) Upland Phase



The upland phase occurs on an upland area, which is the area within a watershed where runoff is predominantly overland flow (Foster and Meyer, 1975). The rainfall characteristics play an important role in determining sediment yield in the upland phase. Major factors affecting the sediment yield in this phase are (Singh, 1989): (i) soil characteristics, (ii) climate, (iii) vegetation, (iv) topography, and (v) human activities. The upland phase is further divided mainly into three stages, i.e. sheet, rill, and gully erosion, which are followed by one another in time and to some extent in space, and collectively these stages are called as the source of erosion.

(b) Channel Phase

The channel phase receives sediment from the upland phase. A channel is defined as a well-defined watercourse flowing through a valley in which the material composing of the valley has been deposited by the stream in the past (Bennett, 1974). Factors like velocity and depth of flow, channel slope, wash load, water temperature, hydraulic roughness, discharge, and cross-sectional area are some of the pertinent variables affecting sediment yield in the channel phase.

2.3.3 Approaches of Sediment Yield Modeling

The various approaches of sediment-yield modeling have been recently discussed by a number of researchers. For example, Woolhiser and Renard (1980) and Singh et al. (1988) addressed the stochastic aspects of modelling sediment yield, and Moore and Clarke (1983)

of soil conservation practices, design of stable channels, determination of the effects of basin management, and non-point source pollution estimates. Increased awareness of environmental quality and desire to control non-point-source pollution has significantly increased the need of sediment yield estimates (Singh, 1989).

A number of sediment yield models have been developed to address the wide-ranging soil and water resources problems. Williams (1981) classified the models on the basis of the problem intended to be solved, like (i) erosion-control planning, (ii) water resources planning and design, and (iii) water quality planning. The complexity of the model in terms of the formulation is usually dictated by the nature of the problem. For example, erosion-control planning for agricultural field, construction sites, reclaimed mines, and forest management requires the simplest models. The only estimate needed in such applications is the average annual soil loss for various erosion-control systems. On the other hand, sediment yield estimates required for designing structures ranging from temporary sediment basins at construction sites to large dams and for evaluating the effects of hydraulic works on flood plain and channel degradation and deposition need to be sufficiently accurate, and hence need more complex models. Similarly, sediment yield models required to determine water quality depend on the water quality parameter to be modeled. For example, the sediment carrying highly toxic chemicals, high concentrations of pesticides and fertilizer, needed a short time step to define changes in the concentration during rainfall-runoff events.

G14090

2.3.2 Sediment Yield Process

The suspended sediment loads in a stream are the result of processes of erosion and transport within the drainage basin area (Einstein, 1964). Supply and removal of suspended solids depends upon the form and structure of the drainage area, vegetative cover as well as upon the climatic conditions (Nippes, 1971; Juyal and Katiyar, 1991). The sediment transported in a stream is sub-divided into two categories, according to dominant mode of transport, suspended sediment load, and bed load (Kumar and Rastogi, 1987). Several authors (Chow, 1964; Graf, 1971; Shen, 1971) have estimated that bed load contributions to the total sediment yield is usually small and may in some cases be neglected from total yield calculations. Therefore, in many areas suspended sediment yields may be considered to

the probabilistic approach. Moore (1984) proposed a dynamic model of sediment yield, and Renard (1980) discussed erosion and sediment yield modeling from rangeland. Wischmeier and Smith (1978) developed an empirical model (USLE) to estimate average annual soil loss from small watersheds. The model has since been the subject of exhaustive research and a number of modifications, viz., MUSLE (Williams, 1975); USLE-M (Kinnell and Risse, 1988); and RUSLE (Renard et al., 1994). Anderson (1954, 1962) developed regression equations relating sediment yield to watershed and climatic characteristics, and Güldal and Müftüoğlu (2001) developed a non-linear functional model “2D Unit Sediment Graph” to predict the suspended sediment yield. Kothyari et al. (1994, 1996) utilized time-area concept coupled with sediment delivery ratio (DR) to estimate the sediment yield. Kothyari et al. (1997) utilized kinematic method to estimate the temporal variation of sediment yield. Tayfur et al. (2003) and Kisi et al. (2006) applied fuzzy logic approach for suspended sediment yield modeling. Raghuwanshi et al. (2006) utilized artificial neural network (ANN) technique to model sediment yield from small agricultural watersheds. Further there are plenty of models available in literature, which are based on the solution of fundamental equations describing stream flow and sediment transport and associated nutrient generation in a catchment. These models utilize cell or grid based discretization of catchments, e.g., CREAMS (Knisel, 1980); ANSWERS (Beasley et al., 1980); SEDIMOT (Wilson et al., 1984); KINEROS (Woolhiser et al., 1990); SWAT (Arnold et al., 1998); and WEHY (Kavvas et al., 2004, 2006) are a few of them. Rendon-Herrero (1978); Williams (1978); Singh et al. (1982), Singh (1989, 1992); Chen and Kuo (1986); Kumar and Rastogi (1987); Das and Agarwal (1990); Raghuwanshi et al. (1994, 1996); and Sharma and Murthy (1996) utilized the unit sediment graph (USG)/instantaneous unit sediment graph (IUSG) concepts to model the suspended sediment from a watershed. Recently Mishra et al. (2006a) developed SCS-CN based sediment yield models.

Thus, a wide range of models (concepts) exist for modeling sediment yield and associated pollutants. However, these models differ in terms of complexity, processes considered, and the data required for model calibration and its use. In general there is no ‘best’ model valid for all applications. The most appropriate model will depend on the intended use and the characteristics of the catchment being considered. Other factors affecting the choice of a model for an application include:

1. Data requirements of the model including the spatial and temporal variation of model inputs and outputs;
2. The accuracy and validity of the model including its underlying assumptions;
3. The components of the model, reflecting the model capabilities;
4. The objectives of the model user(s), including the ease of use of the model, the scales at which model outputs are required and their form;

2.3.4 Selection of an Appropriate Model

Since each model type serves a particular purpose, and has suitability for specific conditions in terms of (i) input availability; (ii) quality of output desired; and (iii) availability of computational facilities. For example, if the average annual sediment yield or sediment transport is to be estimated, empirical models are better. On the other hand, if the sediment is carrying highly toxic pollutants, or in other words, the water quality is to be assessed, then conceptual models or sediment graph models have no alternative. If one desires to identify the erosion-prone areas within the watershed and process-oriented output, and sufficient computational facilities and modern techniques like Remote Sensing and GIS are available, then one has no choice except to adopt the process-based models (Park et al., 2004; Eldho et al., 2006). Thus, the choice of a particular type of model mainly depends on the user, the problem to be addressed, and the facilities available. However, simpler models tend to be more robust, thus providing more stable performance than the more complicated models. The complicated models with large numbers of processes considered and associated parameters inherit the risk of having a high degree of uncertainty associated with the model inputs which are translated through to the model outputs (Chaves and Kojiri, 2007). These uncertainties may negate the benefit of having a more realistic representation of the processes. However, the ultimate factor determining a model's value is its simplicity relative to its explanatory power (Steeffel and Van Cappellan, 1998).

2.3.5 Popular Sediment Graph Models

The sediment graphs are needed to predict pollutant concentrations in streams and reservoirs. This need was not generally recognized until the recent development of water quality models. Previously, sediment prediction techniques were designed to estimate sediment yield for individual storms, average annual sediment yield or sediment transport. The sediment graphs were not essential because the prediction techniques were primarily for reservoir design. The time distribution of the sediment transport rate within a storm provides useful information for solving variety of problems. It can be used for water-quality modeling, design of efficient sediment-control structures, study of transport of pollutants attached to the sediment, and also in the development of sediment-routing procedures (similar to flood routing hydrographs) besides the total sediment yield (Raghuwanshi et al., 1994). Without a sediment graph, only the average sediment rate for the storm can be determined. The average sediment yield is not adequate for estimating dynamic sediment load and pollutants load during the storm.

According to Bennett (1974), a small portion (less than one-fourth) of the eroded sediment is delivered to the receiving bodies (e.g. sea, inland lakes, streams, etc.) while the remaining is deposited in their way. The major part of the annual sediment discharge is transported in a short period of time by a few storms during which the discharge of the stream is continuously changing. Therefore temporal variations of the stream sediment discharge (sediment graph) studies are very important. It indicates the importance of sediment graph based studies in the area of sedimentation. The first attempt at applying a linear model in sedimentation was made by Johnson (1943) for derivation of distribution graphs of suspended sediment concentrations. Since then, the topic has been at the forefront of the hydrology and water resources research activities (Rendon-Herrero, 1974, 1978; Renard and Laursen, 1975; Bruce et al., 1975; Williams, 1978; Singh et al., 1982; Chen and Kuo, 1986; Singh and Woolhiser, 2002; Merritt et al., 2003; Aksoy and Kavvas, 2006). A detailed review on the available models of sediment graph is in order.

Rendon-Herrero (1974, 1978) developed a method for the estimation of total sediment discharge from a storm or its variation with time or both. For that he defined the unit

sediment graph (USG) analogous to the unit hydrograph (UH) as “the sediment graph resulting due to 1.0 ton distributed uniformly over the watershed area for a given duration”. In order to develop sediment graphs with this USG for a particular storm event, one has to estimate the mobilized sediment during the event. For this he developed the regression relationships between the effective rainfall and mobilized sediment to get the mobilized sediment for a known effective rainfall corresponding to an event. The developed methodology depends on (i) the amount of excess rainfall per storm and (ii) the assumption that the sediment graph and hydrograph for a given excess rainfall resembles a parallel nature. The unit sediment graph ordinates are determined through the relationship expressible as:

$$q_s(t) = \frac{Q_s(t)}{Y} \quad (2.77)$$

where $q_s(t)$ is the unit sediment graph ordinate in km^2/hr , $Q_s(t)$ is the ordinate of direct sediment graph in tons/hr, and Y is the amount of mobilized sediment in tons/ km^2 .

The methodology is advantageous in the sense that it is easy to apply, is based on stronger conceptual and theoretical bases, and lays the foundation for further research based on USG concept. However, it has certain limitations too as: (i) it is not applicable to ungauged watersheds; (ii) the method does not explicitly accounts for the major runoff and sediment producing characteristics of watersheds in their mathematical formulation, rather than depends fully on the observed runoff and sediment graph data.

Bruce et al. (1975) developed a sediment graph model based on erosion and transport capacity, but several parameters must be optimized by using gauged data. However, if these parameters could be replaced by physical descriptors, the model might be quite useful for ungauged watershed. Renard and Laursen (1975) computed sediment graphs by multiplying the storm hydrograph flow rates by concentrations predicted using a sediment transport model. The approach may be adequate for areas where the transport model is applicable, if the parameters can be determined successfully. However, the model neglects the watershed

cover, land slope, and conservation practices. This limits the applicability of model for field uses as well as on ungauged watersheds.

Williams (1978) discussed the applicability and limitations of the available conceptual models such as those due to Rendon- Herrero (1974, 1978), Renard and Laursen (1975), and Bruce et al. (1975) for computing sediment graphs and developed a sediment graph model based on instantaneous unit sediment graph (IUSG) useful for ungauged watersheds. However, the method has following limitations of concern: (i) the assumption that IUSG varies linearly with source runoff volume is questionable, (ii) the dimensions are found to be inconsistent when the sediment graphs are predicted by convoluting the IUSG with source runoff, (iii) the curve numbers estimated through the Water Yield Model (WMY) may not be true representative of watershed curve numbers as discussed above, and (iv) the large number model parameters pose further difficulties in practical applications (Kumar and Rastogi, 1987).

Chen and Kuo (1986) developed a “new rigorous synthetic procedure” to generate synthetic sediment graphs for ungauged watersheds. The procedure is based on a one-hour unit sediment graph (USG) concept which was defined as “the direct sediment graph (DSG) resulting from one unit of effective sediment (mobilized sediment) of a storm of one-hour duration generated uniformly over the basin at a uniform rate. Well known to the fact that linearity and time invariance are the bases for the development of the unit hydrograph; the same was used to derive the unit sediment graphs for ungauged watersheds. Once the one hour unit sediment graph is developed, the one hour sediment graph of a storm for a specific watershed can be generated by convoluting the one hour unit sediment graph with the mobilized sediment of one hour duration provided that the rainfall records and characteristics of soil and watershed are known. The steps involved in the model development are summarized below:

1. Develop regression relationships between effective rainfall (ER) (mm/km^2), mobilized sediment (Y) (tons/km^2), effective rainfall intensity (ERI) (mm/hr), and effective sediment erosion intensity (ESEI) (tons/hr) of the form

$$Y = a(\text{ER})^b \quad (2.78)$$

and

$$ESEI = \alpha(ERI)^\beta \quad (2.79)$$

where a , b , α , and β are the regression coefficients, which are estimated using the observed hourly rainfall, stream flow and suspended sediment data. However, for one-hour duration of the storm, $ER = ERI$ and $Y = ESEI$. These regression relationships are based on the assumptions that (i) the sediment erosion intensities are directly related to the rainfall intensities, (ii) the duration of rainfall and of soil erosion due to rainfall is the same, (iii) the high rainfall intensities yield high sediment erosion intensities, (iv) the effective sediment erosion occurs during the same period of effective rainfall, and (v) there is no sediment erosion if there is no rainfall.

2. Estimate the average one hour USG from the observed sediment graph data and estimate peak sediment discharge (q_{ps}) (hr^{-1}), base time (t_s) (hr), and time to peak sediment discharge (t_{ps}) (hr).
3. Correlate the known quantities (dependent variable) q_{ps} , t_s , and t_{ps} with the soil properties and watershed characteristics (independent variable) as:

$$\left. \begin{array}{l} q_{ps} \\ t_{ps} \\ t_s \end{array} \right\} = f(A_w, L, S, E, S_E) \quad (2.80)$$

where S_E = soil erodibility; A_w , L , S , and E = watershed area, main channel length, main channel slope, mean basin elevation, respectively.

4. Lastly, the regression relationships developed at step (1)-(3) are utilized to get the synthetic sediment graph for the ungauged watershed.

The developed procedure is advantageous in the sense that it (i) is easy to apply, (ii) rests on the fundamental principles of system hydrology, and (iii) is well applicable to the ungauged watersheds. However, there are some inconsistencies such as: (i) entire procedure depends

upon the regressional equations, which are not the analytical functions, and therefore, may lead to erroneous results, and (iii) ignores the routing concept.

Kumar and Rastogi (1987) developed a conceptual model of an IUSG for predicting sediment graphs from a watershed. The IUSG was defined as the distribution of sediment from an instantaneous burst of rainfall producing one unit of mobilized sediment. A regression relationship was developed between the mobilized sediment and effective rainfall to estimate the mobilized sediment for the event the sediment graph is desired. The developed regression relationship is expressible as:

$$Y = 1.17ER^{1.974} \quad r^2 = 0.6701 \quad (2.81)$$

where Y is the mobilized sediment in tons/km², ER is the effective rainfall in mm/km², and r^2 is the coefficient of determination. This equation entails the estimation of mobilized sediment on the basis of known effective rainfall. Finally the sediment graphs were predicted by convolution of an IUSG with mobilized sediment. The distinguished features of the model are: (i) it has less number of parameters, (ii) it is based on a stronger conceptual base, and (iii) it is easy to apply to real world problems. The most striking feature of the model is that it paves the way for applicability of various probability distribution functions (pdfs) to the sediment graph based studies. However, the model possesses various inbuilt inconsistencies, some of them are: (i) it does not explicitly consider the major runoff and sediment producing characteristics of watershed, viz., soil, land use, vegetation, and hydrologic condition in their mathematical formulation; (ii) it utilizes the regression relationship between effective rainfall and mobilized sediment to estimate the mobilized sediment for the storm the sediment graph is desired, it does not always produce the satisfactory results (Raghuwanshi et al., 1994); and (iii) it is not applicable to predict sediment graphs from ungauged watersheds.

Raghuwanshi et al. (1994) extended the linear time-invariant (LTI) system model of an IUH based on translation and attenuation functions of rainfall excess as outlined by Clark (1945) to model the catchment response in terms of an IUSG. The mobilized sediment was taken as input to get the sediment graph as the output from the model. For each storm event, for which

the sediment graph is desired, the mobilized sediment was determined by the same procedure as followed by Chen and Kuo (1986) and Kumar and Rastogi (1987). Finally, IUSG model was developed by routing the time-area histogram of the mobilized sediment through a linear reservoir using the Muskingum routing procedure. The model has a strong conceptual foundation as it relies on the popular time-area concept (Clark, 1945) and uses Muskingum routing procedure to compute the sediment graph. However, the model has some limitations and inconsistencies of concern, some of them are: (i) model does not explicitly account for the watershed's geomorphological characteristics, hydrological and meteorological characteristics; (ii) mathematically, the model formulation does not consider the factors which can show the effects of soil conservation practices on the sediment yield from the watersheds; and (iii) the model can not be applied to the limited data condition availability or to ungauged watersheds.

Raghuvanshi et al. (1996) applied the basic principles of linearity and time-invariance to develop the unit sediment graph (USG) and series graph (SG) for predicting temporal distribution of wash load (sediment graph) from a hilly watershed. They defined the unit sediment graph as the sediment graph resulting from one ton of sediment distributed uniformly over the catchment area for an effective duration. The ordinates of the individual USG were determined using Eq. (2.77). Finally, the sediment graphs were obtained by convolving mobilized sediment and effective rainfall with unit sediment graph and series graph ordinates, respectively, for a given storm event. Further, a regression relationship between the effective rainfall and mobilized sediment were developed to estimate the mobilized sediment for the storm event the sediment graph is needed.

Sharma and Murthy (1996) developed a conceptual IUSG-based catchment model, similar to Kumar and Rastogi (1987) for sediment graph prediction from arid upland basins by routing mobilized sediments through a series of linear reservoirs. In the model, the effective rainfall was related to sediment transport through the linear reservoir concept, similar to that originally outlined by Nash (1957). The model parameters were determined from storm sediment graphs (instead of storm runoff hydrographs) and were used to characterize the shape of IUSG. The mobilized sediment was related with the effective rainfall through a

regression relationship similar to Eq. (2.81) to get the amount of mobilized sediment during a storm event for which the sediment graph is desired.

Kothyari et al. (1996) discussed the advantages and limitations of distributed and empirical models of sediment yield, such as the distributed models are based on the grid-based subdivision of catchments and these provide an appropriate means of representing spatial diversity across a catchment and are well suited to recent developments in GIS analysis and automated procedures for calculating morphometric characteristics based on digital elevation models (DEM). However, they require the coordinated use of various sub-models related to meteorology, hydrology, hydraulics, and soil and as a result the number of parameters may be as high as 50, e.g., in the case of WEPP model (Bradford, unpublished lecture notes, 1988), which makes the limited applicability of the models. Secondly, the lumped empirical models such as USLE (Wischmeier and Smith, 1978), MUSLE (Williams, 1975) or RUSLE (Renard et al., 1991) combined erosion from all processes over a catchment into one equation. Though these models are in frequent use in many parts of world but are found not to produce satisfactory results. To enhance the prediction capability of sediment yield models, they developed a sediment delivery ratio (DR) coupled time-area curve procedure for modeling temporal variation of sediment yield as well as the total yield. The model was based on the assumption that the time-area curve of a catchment can be used to obtain the catchment response to an input.

Lee and Singh (1999) enumerated the possible sources of errors in the sediment yield models, some of them are: (i) inadequacy of the model itself, (ii) parameter uncertainty, (iii) errors in data utilized for parameter estimation, and (iii) inadequate understanding of the watershed sediment yield process to the long extent. Building on the idea that the errors in the prediction of sediment yield due to uncertainty caused by the physical processes involved, the model, and the input data are reduced if the model is coupled with the Kalman filter, they developed a sediment graph model by coupling IUSG model with it. The Kalman filter technique is based on the state space-time domain formulation of the process involved and uses the observation system to measure the state estimator. The state space formulation exclusively permits the physical, conceptual, and black box models to be cast within the

mathematical framework of two equations: (i) a system equation and (ii) a measurement equation. The process of filtering is a mathematical operation which utilizes the past data or measurement of a dynamic system in order to make more accurate statements about the present, future or past state of the system that could have been made using information from a single direct measurement. The Kalman filter determines the state vector of the process model using two ways: (i) the observation data and (ii) the model parameters. A comparative study between the observed sediment graphs and the sediment graphs estimated by IUSG model and IUSG model coupled Kalman filter shows that sediment graphs estimated by the latter model are in close agreement with the observed sediment graphs than the former model. In summary, the Kalman filter allows the IUSG to vary in time, increases the accuracy of the IUSG model, and reduces the physical uncertainty of the sediment yield processes. From application view point, however, the Kalman filter based IUSG model has some limitations: (i) it requires the formidable computations and (ii) the Kalman filter assumes that the dynamic system's noise properties are known exactly.

Lee and Singh (2005) proposed a tank model of sediment yield consisting of three tanks to estimate the sediment graphs and hydrographs from the watershed. In the tank model each tank represents a specific runoff component e.g. the first tank represents the surface runoff component, the second tank represents the intermediate runoff (or inter flow) component and the third tank represents the ground water runoff component (base flow component). The model is based on the conceptualization that the sediment of the first tank infiltrates into the second tank and the sediment of the second tank infiltrates into the third tank. Thus, the sediment yield due to intermediate runoff and groundwater runoff results when the water due to interflow and groundwater flow appears on the soil surface. The sediment yield of each tank is computed by multiplying the total sediment yield by the sediment yield coefficients and the total sediment yield is obtained by the product of the runoff of each tank and the sediment concentration in that tank. The sediment concentration of the first tank is computed from its storage and sediment concentration distribution, the sediment concentration of the next lower tank is obtained by its storage and the sediment infiltration of the upper tank, and so on. The sediment concentration distribution within each tank caused by the incremental source runoff (or effective-runoff) is obtained by IUSG and a sediment routing function. An

application of the tank model of sediment yield and IUSG model to an upland watershed in northwestern Mississippi shows that sediment graphs computed by the tank model are in good agreement with the observed sediment graphs than those computed by IUSG model. The developed model explicitly gives due considerations to the sediment yield due to intermediate flow and ground water flow. However, the model does not account for the runoff and sediment producing watershed characteristics such as soil type, land use, hydrologic condition, etc. in its formulation.

Mishra et al. (2006a) coupled the popular SCS-CN method with USLE for modeling rainfall generated sediment yield from a watershed. The coupling is based on the following hypotheses: (i) the runoff coefficient C is equal to the degree of saturation S_r , (ii) the potential maximum retention S can be expressed in terms of USLE parameters, and (iii) the sediment delivery ratio DR is equal to the runoff coefficient C . Based on the above hypotheses, they developed a generalized sediment yield model expressed as:

$$Y = \left[\frac{(1 - \lambda_1)[P - \lambda S + V_0]}{P + (1 - \lambda)S + V_0} + \lambda_1 \right] A \quad (2.82)$$

where Y = sediment yield, A = the potential maximum erosion, P = total rainfall, S = potential maximum retention, V_0 = initial soil moisture, and λ_1 is the initial flush coefficient. An application of the developed models to large set of rainfall-runoff-sediment yield data shows that the computed sediment yield is in good agreement with the observed values. The important inferences drawn from the study are: (i) the models, being conceptual in nature, enjoy all the simplicity in applications than the rigorous physical models do, (ii) the popular SCS-CN methodology is equally useful for sediment yield modeling with the same spirit and efficiency as that in runoff applications, (ii) it is possible to determine the potential erodible depth of a watershed using USLE and NEH-4 tables, (iii) the sediment yield depends on the amount of infiltration, and (iv) the initial soil moisture, similar to SCS-CN based runoff applications, play a significant role in case of sediment yield modeling. Despite of having a hydrologically sound procedure and a firm mathematical base, the models are not applicable for modeling time-distributed suspended sediment yield or sediment graph applications.

2.3.6 Remarks

The sediment graph models are powerful tools for modeling time-distributed sediment yield in streams and reservoirs. These models are particularly important if the sediment carries pollutants that are toxic at high concentrations. The sediment graph models provide useful information for solving variety of problems such as in (i) water-quality modeling, (ii) design of efficient sediment-control structures, (iii) study of transport of pollutants attached to the sediment, and (iv) the development of sediment-routing procedures (similar to flood routing hydrographs) besides the total sediment yield. This reflects the significance of sediment graph models in the realm of sedimentation. The sediment graph models developed so far are either (i) based on regression foundations (Chen and Kuo, 1986; Kumar and Rastogi, 1987; Raghuwanshi et al., 1994), which make their specific or limited applicability, or (ii) based on lengthy and complicated procedure, which uses two or more models to simulate each component individually (Williams, 1978). However, the conceptual model of Kumar and Rastogi (1987) follows a well established procedure of Nash (1957). Recently Mishra et al. (2006a) developed SCS-CN based sediment yield models, which are not applicable for sediment graph based applications. Their model accounts for most of the watershed characteristics, which may affect the yield.

2.4 SUMMARY

The literature available on the origin, theoretical and historical background, nature, advantages and limitations, and advanced applications of SCS-CN method was critically reviewed. Issues pertaining to structural foundation of the method, including SMA procedure and CN vs AMC description were discussed. The renewed SCS-CN procedure of Michel et al. (2005) still possesses certain structural inconsistencies. These are needed to be attended on $C = S_r$ concept for an enhanced performance of the SCS-CN methodology. The SUH methods, viz., the empirical methods, the conceptual models, the GIUH based methods, and the pdf based models were reviewed critically for their advantages and limitations. The methods of Snyder and SCS involve great subjectivity in SUH derivation. The conceptual HM model ignores the concept of translation essential for describing a dynamic system. The

use of pdfs for SUH derivation is getting wider acceptability as it avoids subjective sketching of UH shape in order to satisfy the constraint of unit volume and GIUH technique facilitates to compute salient points of UH from catchment geomorphology. This facilitates to get the complete shape of SUH. Sediment yield generation and modeling approaches were discussed. Popular sediment graph models were reviewed critically for their advantages and limitations. Majority of them either utilize the regression foundations (which make their specific/limited applicability) or the lengthy and complicated procedures using two or more models to simulate each component individually. Secondly they ignore the sediment producing watershed characteristics such as soil type, land use, hydrologic condition, and antecedent moisture.

Given the present status of the works carried out for estimation of runoff using SCS-CN method, derivation of SUHs for estimation of flood from ungauged catchments, and conceptual models of sediment graph, the following can be attempted:

1. To further revisit the renewed SCS-CN methodology of Michel et al. (2005) for its inconsistencies on a stronger mathematical platform and hydrologically sounder perception and compare both with the existing SCS-CN methodology using a large data set.
2. To extend the Hybrid Model (HM) of Bhunya et al. (2005) for SUH derivation to account for concept of translation, which is essential for describing a dynamic system (Ponce, 1989), and develop a generalized form of the extended hybrid model (EHM) similar to Dooge (1959) and Nash (1959). Further check the suitability of EHM and HM using storm data.
3. To explore the suitability of Chi-square and Fréchet distributions combined with Horton's order ratios to develop SUH. Further check their suitability against the 2PGD method of Rosso (Rosso, 1984) using field data.
4. To develop sediment graph models based on popular IUSG concept similar to IUH concept of Nash (1957) and popular SCS-CN method, and apply these models to field data.

CHAPTER-3

STUDY AREA AND DATA USED

Three types of data are used in the present study as follows:

- (i) Event and daily rainfall-runoff data
- (ii) Short-term time distributed rainfall-runoff data
- (iii) Short-term time distributed sediment yield data

The event based rainfall runoff data are used for testing the the workability of SMA based event-based SCS-CN inspired models; daily data used for testing the workability of SMA inspired continuous SCS-CN models; the short-term time distibuted rainfall-runoff data comprising of hourly (or fraction) event based unit hydrograph data for testing the suitability of synthetic unit hydrograph methods; and the short-term time distributed sediment yield data, mainly sediment graph data, for evaluation of the suitability of the proposed sediment graph models for sediment graph and total sediment yield computations.

3.1 EVENT RAINFALL-RUNOFF DATA

A large event rainfall-runoff data set is derived from the United States Department of Agriculture-Agricultural Research Service (USDA-ARS) data base, which is a collection of rainfall and stream flow data from small agricultural watersheds of the United States of America (Fig. 3.1). The data base is available on <http://www.ars.usda.gov/arsdb.html> as well as on <http://hydrolab.arsusda.gov/arswater.html>. In the present study, rainfall-runoff data of 9197 events from 35 watersheds of areas varying from 0.17 to 53.42 ha are used to test the workability of the SCS-CN inspired models. Table 3.1 shows the watershed no., area, location, latitude and longitude, and the no. of events available for each watershed. Appendix A shows the typical rainfall-runoff and antecedent precipitation (P_5) data set for a US watershed (no. 9004).

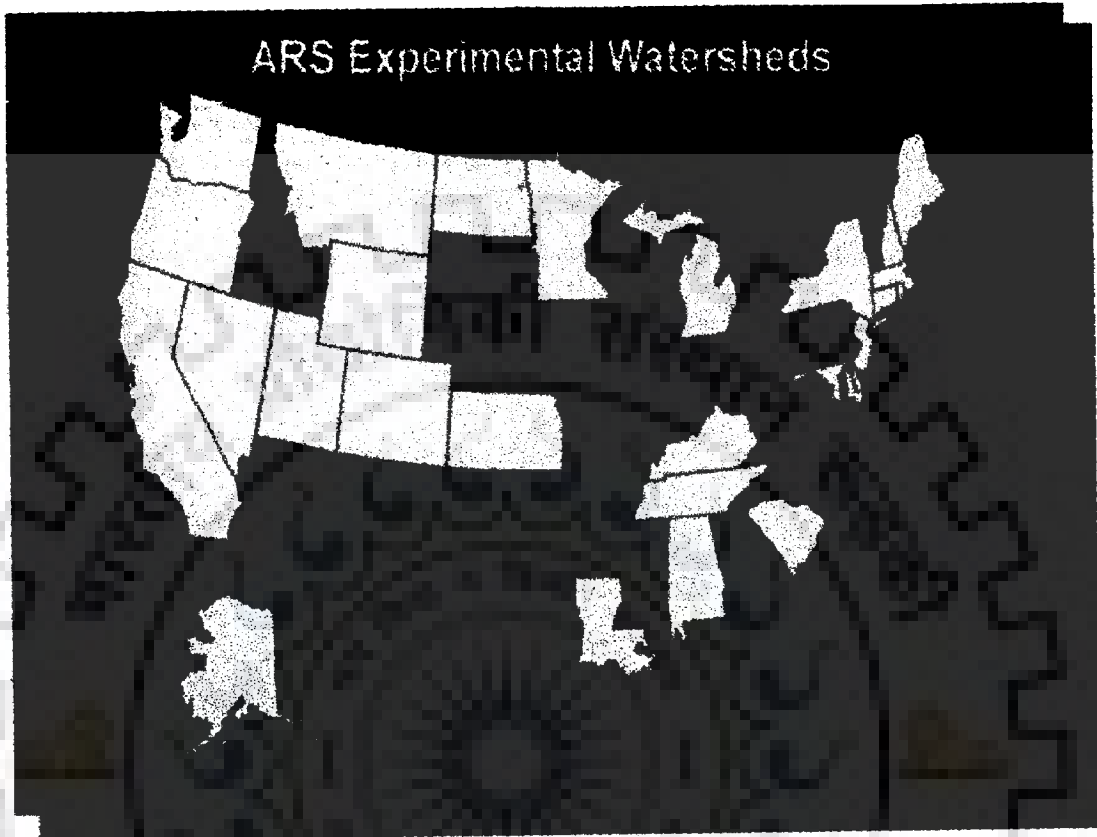


Fig. 3.1 Map of USDA-ARS experimental watersheds (Source: <http://hydrolab.arsusda.gov/arswater.html>)

Table 3.1 Summary of US watersheds and their characteristics

Sl. No.	Watershed No.	Area (ha)	Location	Latitude	Longitude	No. of Events
1	9004	23.96	Americus/Georgia	32 ^o 13'08''	84 ^o 21'48''	94
2	16010	40.47	Klingerstown/Pennsylvania	-	-	325
3	17001	11.02	Edwardsville/Illinois	38 ^o 52'45''	89 ^o 54'14''	586
4	17002	20.21	Edwardsville/Illinois	38 ^o 52'45''	89 ^o 54'24''	546
5	17003	5.08	Edwardsville/Illinois	38 ^o 52'27''	89 ^o 54'08''	137
6	26010	0.55	Coshocton/Ohio	40 ^o 22'23''	81 ^o 47'20''	879
7	26013	0.68	Coshocton/Ohio	40 ^o 22'11''	81 ^o 47'39''	572
8	26014	0.26	Coshocton/Ohio	40 ^o 21'56''	81 ^o 47'49''	695
9	26016	0.59	Coshocton/Ohio	40 ^o 22'04''	81 ^o 46'50''	358
10	26018	0.48	Coshocton/Ohio	40 ^o 22'04''	81 ^o 46'56''	106
11	26031	49.37	Coshocton/Ohio	40 ^o 23'29''	81 ^o 48'40''	77
12	26863	0.17	Coshocton/Ohio	40 ^o 22'15''	81 ^o 47'49''	197
13	34002	1.95	Cherokee/Oklahoma	36 ^o 44'0''	98 ^o 23'06''	247
14	34006	0.71	Cherokee/Oklahoma	36 ^o 44'0''	98 ^o 23'06''	275
15	34007	0.81	Cherokee/Oklahoma	36 ^o 44'0''	98 ^o 23'06''	262
16	34008	1.91	Cherokee/Oklahoma	36 ^o 44'0''	98 ^o 23'06''	231
17	35001	13.52	Guthrie/ Oklahoma	35 ^o 49'12''	97 ^o 23'18''	158
18	35002	1.3	Guthrie/ Oklahoma	35 ^o 49'12''	97 ^o 23'18''	151
19	35003	1.27	Guthrie/ Oklahoma	35 ^o 49'12''	97 ^o 23'18''	107
20	35008	3.68	Guthrie/ Oklahoma	35 ^o 49'12''	97 ^o 23'18''	129
21	35010	6.35	Guthrie/ Oklahoma	35 ^o 49'12''	97 ^o 23'18''	113
22	35011	38.36	Guthrie/ Oklahoma	35 ^o 49'12''	97 ^o 23'18''	99
23	37001	6.76	Stillwater/ Oklahoma	36 ^o 21'0''	97 ^o 04'0''	195
24	37002	37.23	Stillwater/ Oklahoma	36 ^o 21'0''	97 ^o 04'0''	388
25	42010	7.97	Riesel/Texas	31 ^o 27'12''	96 ^o 53'0''	224
26	42012	53.42	Riesel/Texas	31 ^o 28'30''	96 ^o 52'46''	277
27	42013	32.33	Riesel/Texas	31 ^o 28'30''	96 ^o 52'54''	36
28	42014	6.6	Riesel/Texas	31 ^o 28'26''	96 ^o 53'09''	273
29	42015	16.19	Riesel/Texas	31 ^o 28'08''	96 ^o 52'49''	128
30	42016	8.42	Riesel/Texas	31 ^o 28'22''	96 ^o 52'54''	293
31	42017	7.53	Riesel/Texas	31 ^o 28'31''	96 ^o 53'10''	237
32	42037	4.57	Riesel/Texas	31 ^o 28'36''	96 ^o 52'39''	181
33	42038	2.27	Riesel/Texas	31 ^o 28'11''	96 ^o 52'55''	158
34	42039	4.01	Riesel/Texas	31 ^o 27'56''	96 ^o 53'07''	237
35	42040	4.57	Riesel/Texas	31 ^o 27'57''	96 ^o 53'08''	226

3.2 DAILY RAINFALL-RUNOFF DATA

In the present study, the daily rainfall-runoff data of Hemawati catchment are used for testing the workability of SMA inspired continuous SCS-CN models. The daily rainfall-runoff data from January 1, 1975, to December 31, 1979, were available for use. The Hemavati catchment (area = 600 km²) up to Sakleshpur is a sub-catchment of River Cauvery (Fig. 3.2). It lies between 12^o55' and 13^o11' North latitudes and 75^o29' and 75^o51' East longitudes in the southwest part of Karnataka State in India. The upper part of the catchment is hilly with an average elevation of 1240 m above the mean sea level (msl) and the lower part forms a plain terrain with an average elevation of 890 m above msl. It traverses a total length of about 55.13 km up to Sakleshpur. Its topography can be broadly divided into three parts: (i) low land (valley lands), (ii) semi-hilly (gently sloping lands), and (iii) hilly (hill ranges of steep to moderate slopes). The average rainfall of the basin for the period 1942-71 is 2972 mm. Appendix B shows the typical rainfall-runoff and evaporation data for the year 1975.

3.3 SHORT-TERM RAINFALL-RUNOFF DATA

In the present study, the short-term rainfall-runoff data (comprising of UH data and watershed characteristics) of the following watersheds is used.

3.3.1 Chaukhutia Catchment

The Chaukhutia catchment (area = 452.25 km²) (Fig. 3.3) is located in the Pauri Garhwal district of Uttarakhand state, lies between 79^o 31' to 79^o 46' 15" East longitude and 29^o 12' 15" to 30^o 6' N latitude. The storm data were taken from Verma and Rastogi (2002) for the analysis. These data were collected from the Divisional Forest Office Ranikhet (India). The average annual precipitation is 1467 mm, which varies from 1208 mm to 1744 mm at different locations. The elevation of the catchment ranges from 929 to 3144 m above

mean sea level. The details of catchment and unit hydrograph characteristics are given in Table 3.2.

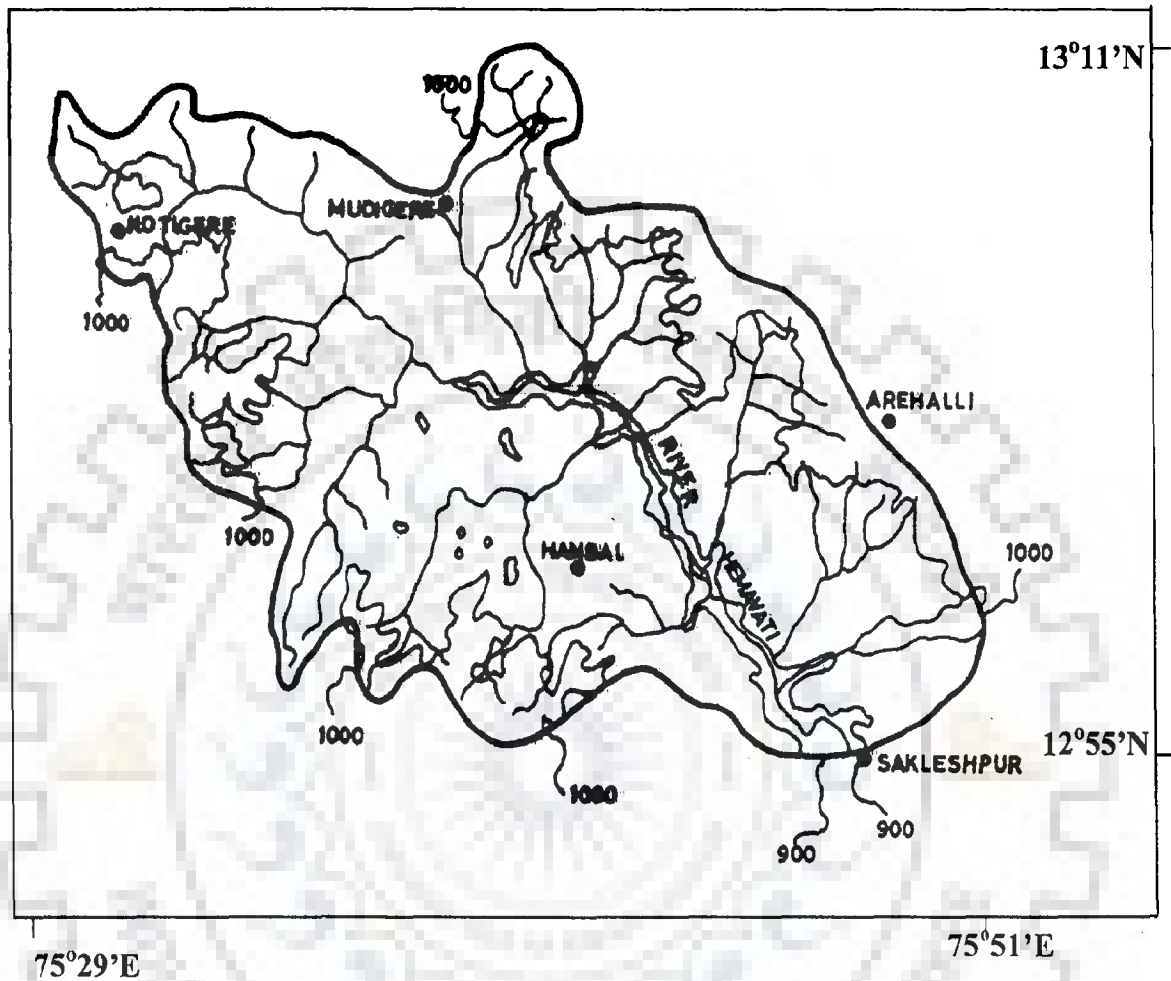


Fig. 3.2 Map of River Hemavati up to Sakleshpur (Source: Mishra and Singh, 2004a)

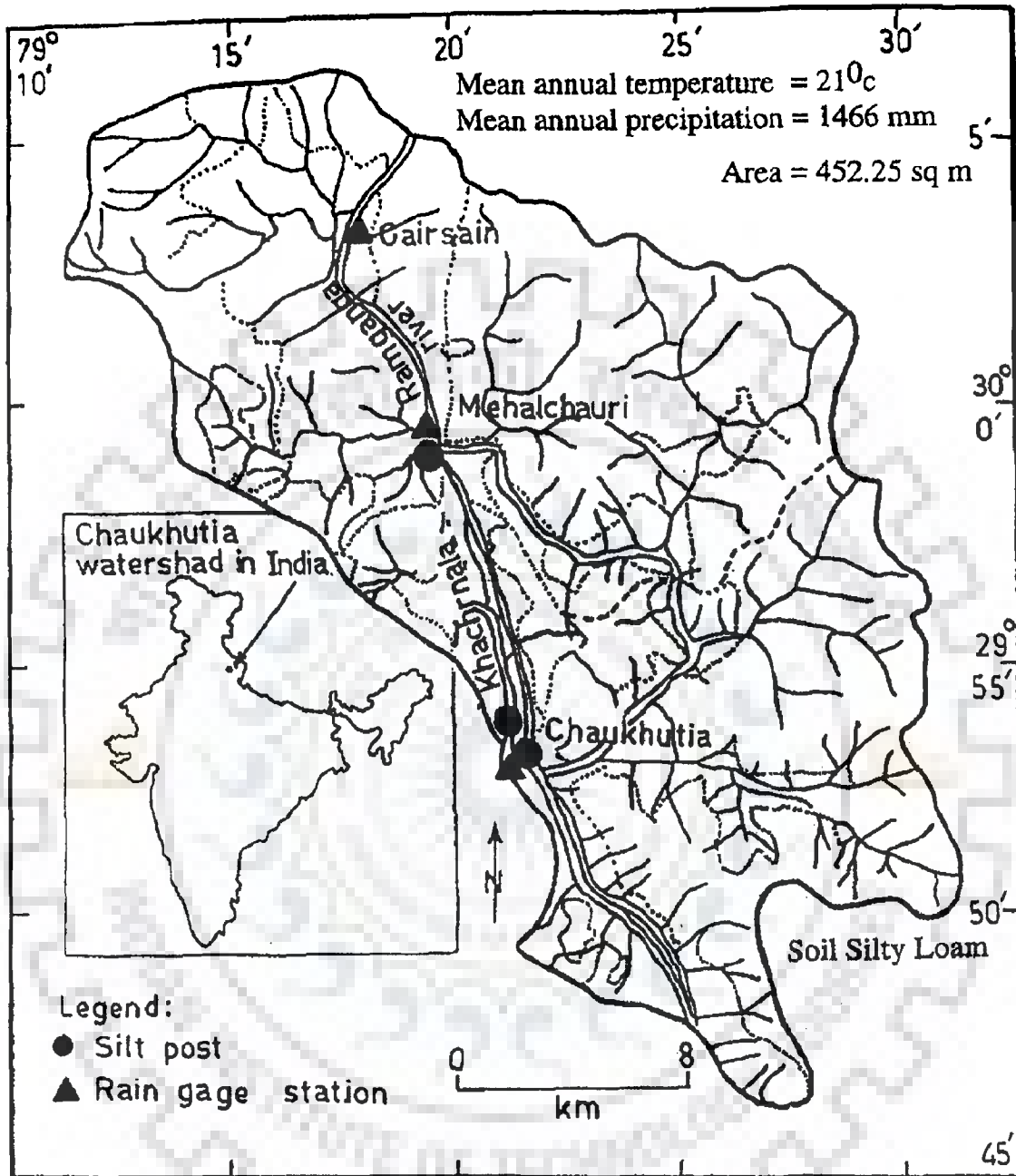


Fig. 3.3 Location of Chaukhutia watershed in Ramganga reservoir catchment (Source: Kumar and Rastogi, 1987; Raghuwanshi et al. 1994)

3.3.2 Gormel Ermenek Creek Catchment

The storm data for the analysis were taken from Haktanir and Sazen (1990) of Gormel Ermenek Creek catchment (area = 141.5 km²) in Anatolia (Turkey). The study catchment is situated in the south east of Turkey. Data were collected from the reports of the office of General Directorate of Electric Works Planning (1985), which is a State Office set up for the evaluation of characteristics of the Turkish rivers, mainly for their hydroelectric potential. The details of catchment and unit hydrograph characteristics are given in Table 3.2.

3.3.3 Bridge Catchment no. 253

The storm data for the analysis were taken from Bhunya et al. (2005) of Bridge catchment no. 253 (area = 114.22 km²) is a railway bridge on the Tyria stream of Narmada River at Gondia-Jabalpur railway line (Fig. 3.4). For UH derivation using Collins (1939) method in the present study, the direct surface runoff hydrograph for the catchment was computed using linear base flow separation technique (Singh, 1988). The details of catchment and unit hydrograph characteristics are given in Table 3.2.

3.3.4 Kothuwatari Catchment

The Kothuwatari catchment (area = 27.93 km²) is a sub-catchment of Tilaiya dam catchment of upper Damodar Valley Corporation (DVC), Hazaribagh, India. The catchment is situated at the South-Eastern part of the Tilaiya dam catchment between 24° 12' 27" and 24° 16' 54" North latitudes and 85° 24' 18" and 85° 28' 10" East longitudes. In the year 1991, the catchment was selected for 'Watershed Management' under the "Indo-German Bilateral Project (IGBP)" for assessing the effects of soil conservation measures on runoff and wash load. The storm data were obtained from the Soil Conservation Department (SCD) of Damodar Valley Corporation (DVC), Hazaribagh, India. The UH data for the catchment were taken from Singh (2003). The details of catchment and unit hydrograph characteristics are given in Table 3.2.

3.3.5 Shanchuan Catchment

The Shanchuan catchment (area = 21 km²) is located in Loess Plateau and Sichan Province China. The data for the present study were taken from Wang et al. (1992). The details of catchment and unit hydrograph characteristics are given in Table 3.2.

3.3.6 Myntdu-Leska Catchment

The Myntdu-Leska river catchment (Fig. 3.5) is located in Jaintia hills district of Meghalaya, in the northeastern part of India, in the southern slope of the State adjoining Bangladesh. Its geographic location extends from 92°15' to 92° 30' E longitude and 25° 10' to 25° 17' N latitude. The area is narrow and steep, lying between central upland falls of the hills of Meghalaya. The catchment area is about 350 km² and elevations range from about 1372 m to 595 m above mean sea level. The UH data for the catchment were taken from Bhunya (2005). The details of catchment and unit hydrograph characteristics are given in Table 3.2.

Based on the availability of catchments geomorphological data, the Bridge catchment no. 253 and Myntdu-Leska catchments are utilized to test the suitability of Fréchet and Chi-square distributions combined with Horton's order ratios to derive a synthetic unit hydrograph. Table 3.3 shows the catchment's relevant geomorphological data and UH characteristics.

3.4 SHORT-TERM SEDIMENT YIELD DATA

In the present study, the short-term sediment yield data of the following watersheds are used.

3.4.1 Nagwan Watershed

The Nagwan watershed (area = 92.46 km²) is located in the Upper Damodar Valley of Hazaribagh district in Jharkhand (India). The watershed lies between 85° 16' 41" and 85° 23'

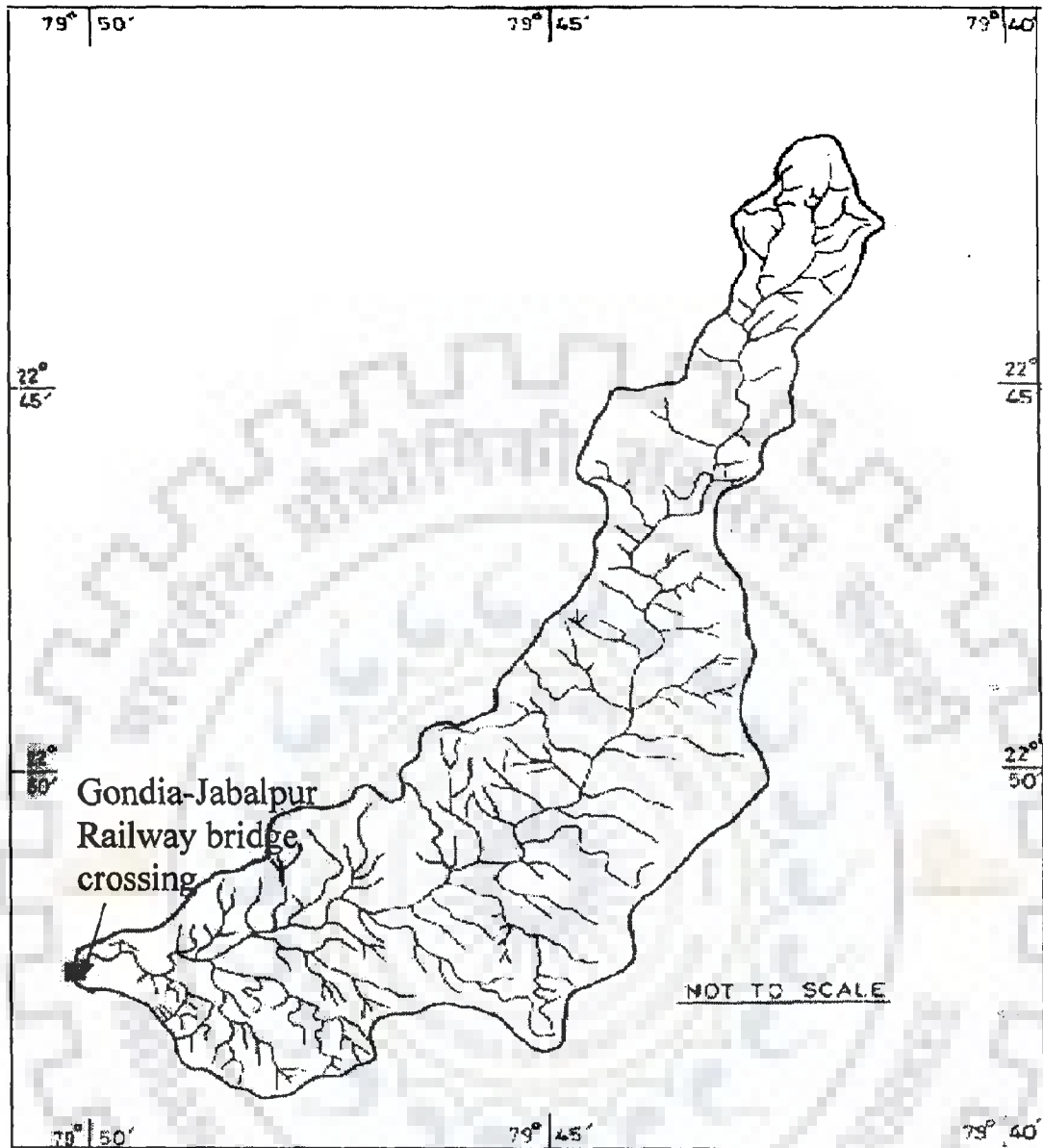


Fig. 3.4 Index map Bridge no. 253 of Tyria stream catchment, Narmada River, India (Source: Bhunya, 2005)

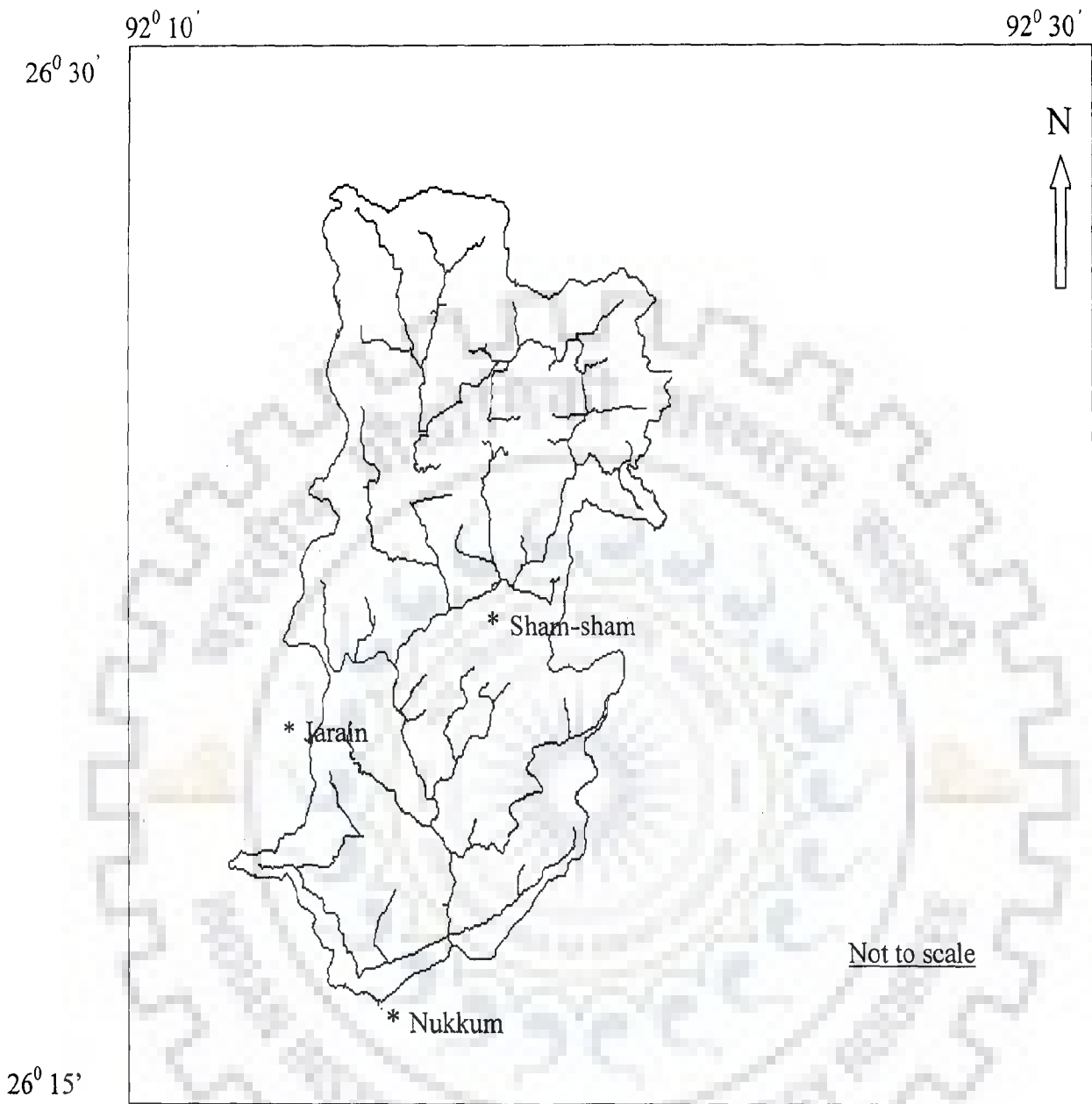


Fig. 3.5 Index Map of Myntdu-Leska catchment (Source: Bhunya, 2005)

Table 3.2 Summary of unit hydrographs and catchment characteristics used for EHM and HM models

Catchments	Flood Event	Area (km ²)	Q _p (m ³ /s)	t _p (hr)
Chaukhutia (India)	29-8-1985	452.25	51.13	2.00
Gormel Ermenek Creek (Turkey)	Haktanir & Sazen (1990)	141.50	5.48	6.00
Bridge catchment no. 253 (India)	03-08-1996	114.22	5.46	5.00
Kothuwatari (India)	23/24-08-1994	27.93	4.34	1.00
Shanchuan (China)	15-8-1966	21.00	15.05	0.25

Table 3.3 Summary of unit hydrographs and catchment geomorphologic characteristics used for 2PFD and one parameter CSD

Catchments	Catchment characteristics					UH characteristics	
	A _w (km ²)	L (km)	R _A	R _B	R _L	Q _p (m ³ /s)	t _p (hr)
Bridge catchment no. 253	114.22	35.4	5.55	4.28	1.91	5.46	5
Myntdu-Leska	350	52.0	4.61	4.27	2.12	11.8	5

Table 3.4 Summary of sediment graph characteristics of Nagwan watershed

Sl. No.	Date of storm	Q_s (kN)	Q_{ps} (kN/hr)	t_{ps} (hr)
1	July 6, 1989	21315	4621	3.5
2	July 20, 1989	70075	11069	4.5
3	July 28, 1989	31833	5459	4.5

50" E longitudes and between 23° 59' 33" and 24° 05' 37" N latitudes. The major soil type is silty clay but sandy loam, clay loam, loam and loamy sand soils are also found in the watershed. The watershed was gauged under a collaborative project 'Indo-German Bilateral Project (IGBP)' by Damodar Valley Corporation (DVC) and a German agency, namely, Deutsche Gessllschaft für Technische Zusammenarbeit (GTZ) (SWC&D, 1991–1996). The sediment graph data corresponding to three storm events were derived for the present study as shown in Table 3.4. The base sediment flow of the sediment graphs was separated in a manner similar to the separation of the base flow of the runoff hydrographs used by Chow (1964).

3.4.2 Chaukhutia Catchment

The physiographic characteristics of the catchment have been discussed in section 3.3.1. The sediment samples were taken at Chaukhutia flow gauging station using a one liter bottle sampler at an interval of 2-4 h, during the rising and falling limbs, at peak, and also during the recession of the events. Sample collection in the midstream and at different depths was not possible during the torrential flow. Therefore, these were collected, as far as it was possible to move in the stream from the river bank. The sediment graph data corresponding to six storm events were derived for the present study as shown in Table 3.5. The base sediment flow of the sediment graph was separated in a manner similar to that discussed in section 3.4.1. For the present study, the sediment graph data were taken from Kumar and Rastogi (1987) and Raghuwanshi et al. (1994, 1996).

Table 3.5 Summary of sediment graph characteristics of Chaukhutia catchment

Sl. No.	Date of storm	Q_s (tons)	Q_{ps} (tons/hr)	t_{ps} (hr)
1	July 17, 1983	2698	1025	2
2	August 21/22, 1983	2070	875	2
3	July 15, 1984	3145	1250	2
4	August 18/19, 1984	2105	850	2
5	September 1/2, 1984	1205	475	2
6	September 17/18, 1984	963	392	2



CHAPTER-4

PROCEDURE FOR ACCOUNTING SOIL MOISTURE IN SCS-CN METHODOLOGY

4.1 BACKGROUND

Modelling of the event-based rainfall-runoff process has significant importance in Hydrology. It has been fundamental to a range of applications in hydrological practices since the first documentation of hydrology by P. Perreault in 1674 (Linsley, 1982). One of the most commonly used methods to estimate the volume of surface runoff for a given rainfall event is the Soil Conservation Service Curve Number (SCS-CN) method (SCS, 1956, 1964, 1971, 1993), which has now been renamed as Natural Resource Conservation Service Curve Number (NRCS-CN) method. The method is simple, easy to understand, and useful for ungauged watersheds. It accounts for the major runoff producing watershed characteristics, viz., soil type, land use/treatment, surface condition, and antecedent moisture conditions (AMCs). The methodology has been a topic of much discussion in hydrologic community. Owing to spatial and temporal variability of rainfall, quality of measured rainfall-runoff data, and the variability of antecedent rainfall and the associated soil moisture amount, the SCS-CN method however exhibits variability in runoff computation. The most cognizant source of variability is commonly recognized as the AMC (Ponce and Hawkins, 1996; Mishra et al., 2006b).

The existing SCS-CN method consists of two external components (Mishra and Singh, 2003a): (i) initial soil moisture before the start of rainfall and (ii) initial abstractions. The existing SCS-CN method ignores the initial soil moisture storage. Much more the assumption of initial soil moisture storage equal to zero in computation of potential maximum retention 'S' from the rainfall-runoff data of a gauged watershed exhibits contradicting features in respect of the SCS-CN application to gauged and ungauged watersheds. It has led to the development of the concepts of (i) statistical error bands; (ii) ordering of rainfall-runoff data (Hjelmfelt, 1980; Hawkins, 1993; McCuen, 2002); and (iii) derived distribution (Bonta, 1997).

The runoff prediction using SCS-CN method can be improved considerably by incorporating Soil Moisture Accounting (SMA) procedure (Williams and LaSeur, 1976). The SMA concept is based on the notion that the higher the initial moisture storage level,

the higher the fraction of rainfall converted into runoff. Building on this idea, Michel et al. (2005) proposed a renewed SCS-CN procedure to overcome the inconsistencies associated with the existing SCS-CN method. They also introduced a continuous hydrologic simulation model based on the new procedure. However, the renewed procedure also has voids of concern as discussed in section 2.1.6.

Thus, it may be inferred that the original method as well as the renewed procedure of Michel et al. needs to be further examined on a sounder perception of the SMA procedure, and formulated to explain the issues related with AMCs, S_a and S . The present work therefore focuses on both event-based and long-term hydrologic modeling aspects of the SCS-CN methodology with the following objectives: (a) to develop an event-based SMA-inspired SCS-CN model, (b) to develop a long-term SMA-inspired SCS-CN model, and (c) to test both the models on a large set of data from the catchments of United States and India.

4.2 MATHEMATICAL FORMULATION

4.2.1 SMA Inspired Event Based SCS-CN Model

The original SCS-CN method (SCS, 1956) is applicable only at the end point of the storm, or indirectly time independent, but it has long been applied to the cumulative rainfall at a number of points within the cumulative rainfall hyetograph to yield the rainfall-excess hyetograph (ASCE, 1996). However, if the SCS-CN method is to be used within a continuous watershed model, the application of the method cannot be restricted to the total storm runoff depth only. Therefore, it is quite reasonable to hypothesize that the SCS-CN method is valid not only at the end of storm point but also at any instant during a storm. Thus, P and Q can be differentiated with time t as $\left(\frac{dP}{dt}, \frac{dQ}{dt}\right)$.

Mathematically, since the existing SCS-CN method (Eq. 2.5) does not yield a zero value of Q for $P < I_a$, its derivative may exhibit a mathematical problem and may be treated by imposing a similar condition, as shown later. Furthermore, the basic SCS-CN hypothesis (Eq. 2.3) does not explicitly account for the initial soil moisture i.e. the soil moisture storage level at the beginning of the storm event (Mishra and Singh, 2003a&b,

2004a). Therefore, to account for the initial soil moisture storage, the basic hypothesis (Eq. 2.3) can be modified as (Mishra & Singh, 2002b, 2003a&b):

$$\frac{Q}{P - I_a} = \frac{F + V_0 + I_a}{S + V_0 + I_a} \quad (4.1)$$

where V_0 is the initial soil moisture storage level. Combining Eqs. (2.2) and (4.1) one gets

$$Q = \begin{cases} \frac{(P + V_0)(P - I_a)}{P + S + V_0} & \text{if } P > I_a \\ 0 & \text{Otherwise} \end{cases} \quad (4.2)$$

Eq. (4.2) is the modified form of the existing SCS-CN method and is derived after incorporating the initial soil moisture storage in the basic hypothesis (Eq. 2.3) or $C = S_r$ concept. Mathematically, equation (4.2) is an improved form of the existing SCS-CN method (Eq. 2.5). However, since the condition $P < I_a$ yields a negative runoff, it can be safely taken as zero.

Now, before proceeding to develop continuous sub-model similar to Michel et al., it is necessary here to understand the conceptual soil-water-air system of a soil profile to have sounder perception of SMA and intrinsic nature of parameters. If V_0 is the soil moisture storage level at the beginning of the storm event, V is the moisture storage at any time t during the storm event, and P is the accumulated rainfall up to the time t , and Q is the corresponding runoff. Consistent with the derivation of Michel et al., an expression for V can be derived as follows:

Differentiation of Eq. (2.2) with time 't' yields

$$\frac{dP}{dt} = \frac{dQ}{dt} + \frac{dI_a}{dt} + \frac{dF}{dt} \quad (4.3)$$

Defining $dP/dt = p$, $dQ/dt = q$, for $I_a = \text{constant}$, and $dI_a/dt = 0$, Eq. (4.3) can be written as

$$p - q = \frac{dF}{dt} \quad (4.4)$$

where dF/dt is similar to dV/dt . Replacing dF/dt with dV/dt in Eq. (4.4) one gets

$$\frac{dV}{dt} = p - q \quad (4.5)$$

Integration of Eq. (4.5) with the limits at $t = 0, V = V_0$, and at $t = t, V = V$, yields

$$V = V_0 + (P - Q) \quad (4.6)$$

Eq. (4.6) is same as Eq. (2.28). Initially, Eq. (4.6) was given by Michel et al., now we have its complete mathematical description derived from water balance equation (Eq. 2.2), but on considering the initial soil moisture.

Consistent with Michel et al., V_0 was ignored in the original SCS-CN method, and its effect on S can be described by taking $I_a = 0$ and assuming V_0 as shown in Fig. 4.1. In this figure the sum of volume of air (V_a) and volume of water ($V_w = V_0$) represents the volume of voids, expressed mathematically as:

$$V_v = V_a + V_0 \quad (4.7)$$

In such a situation, V_a in Eq. (4.7) represents the SCS-CN parameter, the potential maximum retention, S , and V_v represents the absolute potential maximum retention, S_b , which is a constant for a particular watershed (Mishra and Singh, 1999a).

For $I_a \neq 0$ Eq. (4.7) can be rewritten as:

$$V_v = V_a + (V_0 + I_a) \quad (4.8)$$

Replacing different terms of Eq. (4.8) by their suitable notations, viz., $V_v = S_b, V_a = S, S_a = (V_0 + I_a)$ results into the following:

$$S_b = S + S_a \quad (4.9)$$

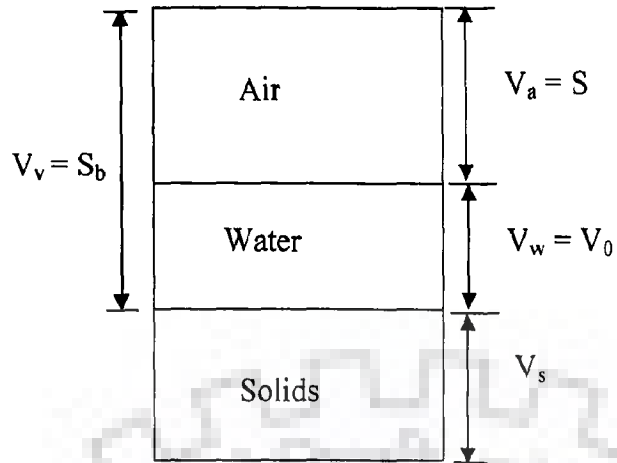


Fig. 4.1 Conceptual soil-water-air system of a soil profile

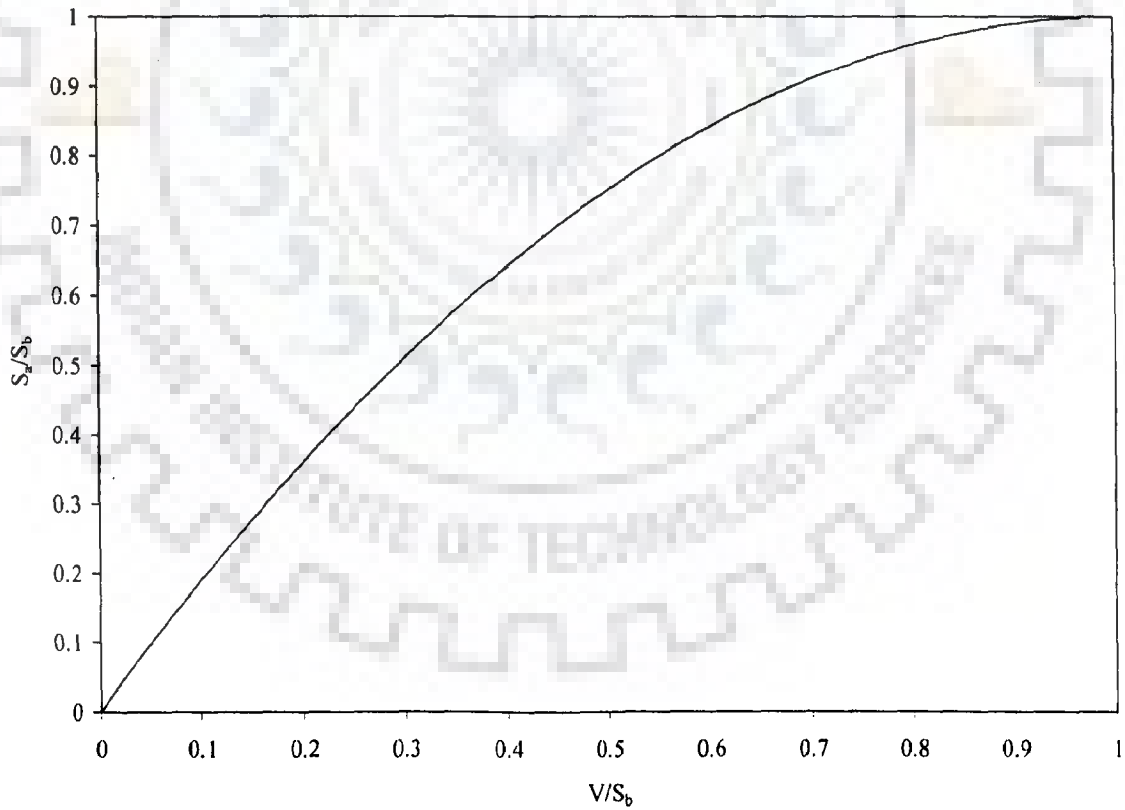


Fig. 4.2 Feasible limits of V-variation for $q \geq 0$

Eq. (4.9) shows the dependency of S on both S_b and S_a . This further strengthens the intrinsic nature of the parameters. Putting the value of Q from Eq. (4.2) into Eq. (4.6), the moisture storage level at any time t can be expressed as:

$$V = V_0 + P - \left[\frac{(P + V_0)(P - I_a)}{P + S + V_0} \right] \quad (4.10)$$

Eq. (4.10) will be used to present Eq. (4.2) in the form of continuous soil moisture accounting (SMA) sub-model i.e. rate of runoff (q) as a function of rate of rainfall, p, moisture storage level, V, and basin parameters.

Substituting Q from Eq. (4.2) into $q = \frac{dQ}{dt}$, as above, and differentiating gives,

$$q = p \left[\frac{(P + V_0 + S)(2P + V_0 - I_a) - (P + V_0)(P - I_a)}{(P + S + V_0)^2} \right] \quad (4.11)$$

P can be obtained from Eq. (4.10) as:

$$P = \frac{[V_0 I_a - (V_0 + S)(V - V_0)]}{(V - V_0) - (S + I_a)} \quad (4.12)$$

Substitution of P into Eq. (4.11) leads to defining different terms of equation as follows:

$$(P + V_0 + S) = \frac{S(S + S_a)}{S + S_a - V}, \quad (4.13a)$$

$$(2P + V_0 - I_a) = \frac{V(S + S_a) - S_a(S + S_a)}{S + S_a - V}, \quad (4.13b)$$

$$(P + V_0) = \frac{SV}{S + S_a - V}, \quad (4.13c)$$

$$(P - I_a) = \frac{(S + S_a)(V - S_a)}{S + S_a - V}, \quad (4.13d)$$

and

$$(P + S + V_0)^2 = \frac{S^2(S + S_a)^2}{(S + S_a - V)^2} \quad (4.13e)$$

Putting these terms into Eq. (4.11) and then simplifying finally results into

$$q = p \left[\frac{VS + (V - S_a)(S_b - V)}{SS_b} \right] \quad (4.14)$$

where all S_b , S , and S_a are constant for a given watershed and storm. Eq. (4.14) contains three terms in numerator viz., VS , $(V - S_a)$ and $(S_b - V)$. If all these terms are positive, the equation yields a non-negative runoff 'q'. As seen, VS and $(S_b - V)$ are always non-negative. The second term $(V - S_a)$ may however take any value, positive or negative, depending on $V > S_a$ or $V < S_a$. From hydrologic view point, only two extreme conditions for runoff 'q' are possible, viz., $q \geq 0$ and $q \leq p$, and therefore, are worth analyzing, as follows.

First Condition ($q \geq 0$)

On putting q from Eq. (4.14) into the first condition, $q \geq 0$, one obtains

$$p \left[\frac{VS + (V - S_a)(S_b - V)}{SS_b} \right] \geq 0 \quad (4.15)$$

or

$$V^2 - 2VS_b + S_aS_b \leq 0 \quad (4.16)$$

The solution of which can be given as:

$$V \leq S_b \left[1 - \sqrt{1 - \frac{S_a}{S_b}} \right] \quad (4.17)$$

It follows that $V \leq S_b$ and since V can not be less than zero, it can range $(0, S_b)$ as shown in Fig. 4.2, which is a physically realizable condition.

Second Condition ($q \leq p$)

On putting q from Eq. (4.14) into the second condition, $q \leq p$, one obtains

$$p \left[\frac{VS + (V - S_a)(S_b - V)}{SS_b} \right] \leq p \quad (4.18)$$

or

$$2VS_b^2 - V^2 - S_b^2 \leq 0 \quad (4.19)$$

or

$$S_b^2 + V^2 - 2VS_b \geq 0 \quad (4.20)$$

The solution of Eq. (4.20) can be given as:

$$[S_b - V]^2 \geq 0 \quad (4.21)$$

It yields $V \leq S_b$, which is a feasible solution. Thus, Eq. (4.14) can be re-written as follows:

$$\checkmark q = p \left[\frac{VS + (V - S_a)(S_b - V)}{SS_b} \right] \quad V \leq S_b \left[1 - \sqrt{1 - \frac{S_a}{S_b}} \right] \quad (4.22)$$

= 0

otherwise

Now, four explicit conditions viz., $V < S_a$, $V = S_a$, $V > S_a$, and $V = S_b$, can be distinguished from Soil Moisture Accounting (SMA) view point, as shown in Fig. 4.3.

In order to physically interpret the first two conditions i.e. $V < S_a$, $V = S_a$, Eq. (4.22) is further expressed in non-dimensional form as

$$\frac{q}{p} = \frac{V}{S_b} + \left(\frac{V}{S_b} - \frac{S_a}{S_b} \right) \left(1 - \frac{V}{S_b} \right) / \left(1 - \frac{S_a}{S_b} \right) \quad (4.23)$$

Eq. (4.23) is represented graphically (Fig.4.4) for the feasible variation of q/p with V/S_b and S_a/S_b . It is observed that even when $V < S_a$, q is not zero. Similarly for the condition $V = S_a$, Eq. (4.23) reduces to:

$$q = p \left(\frac{S_a}{S_b} \right) \text{ or } \frac{q}{p} = \left(\frac{S_a}{S_b} \right) \quad (4.24)$$

Eq. (4.24) describes a proportionality of direct surface runoff rate and rainfall intensity (Fig. 4.5), similar to the basic proportionality of the existing SCS-CN method (Eq. 2.5). It follows that when $V = S_a$ and $S_a \rightarrow S_b$ (i.e. soil is fully saturated initially), $q \rightarrow p$, which is close to reality. However, the proportionality condition (Eq. 4.24) was not encountered in the Michel et al. model due to considering the existing SCS-CN method in the development of continuous sub-model i.e. ignoring the concept of SMA in the basic proportionality concept. Equations (4.23) and (4.24) hydrologically represents the presence of some runoff (though in fractions) in the form of interflow, when the moisture storage is equal to or less than the threshold value, i.e. S_a .

For $V > S_a$, q can be computed from Eq. (4.22), and for $V = S_b$ (maximum capacity of moisture storage), Eq. (4.22) yields $q = p$. At this stage no more rainfall can enter the soil moisture storage, or $\frac{dV}{dt} = 0$ from Eq. (4.6). Table 4.1 compares these expressions with those of Michel et al. for all the four conditions encountered (i.e., $V < S_a$, $V = S_a$, $V > S_a$, and $V = S_b$). To this end, we have developed the continuous sub-model (Eq. 4.22), expressed in terms of rainfall and runoff rates, i.e., variables p and q , not P and Q as in the original SCS-CN method (Eq. 2.5). However, this situation can be tackled by coupling Eq. (4.6) with Eq. (4.22). But before this, one must check the consistency of Eq. (4.2) for

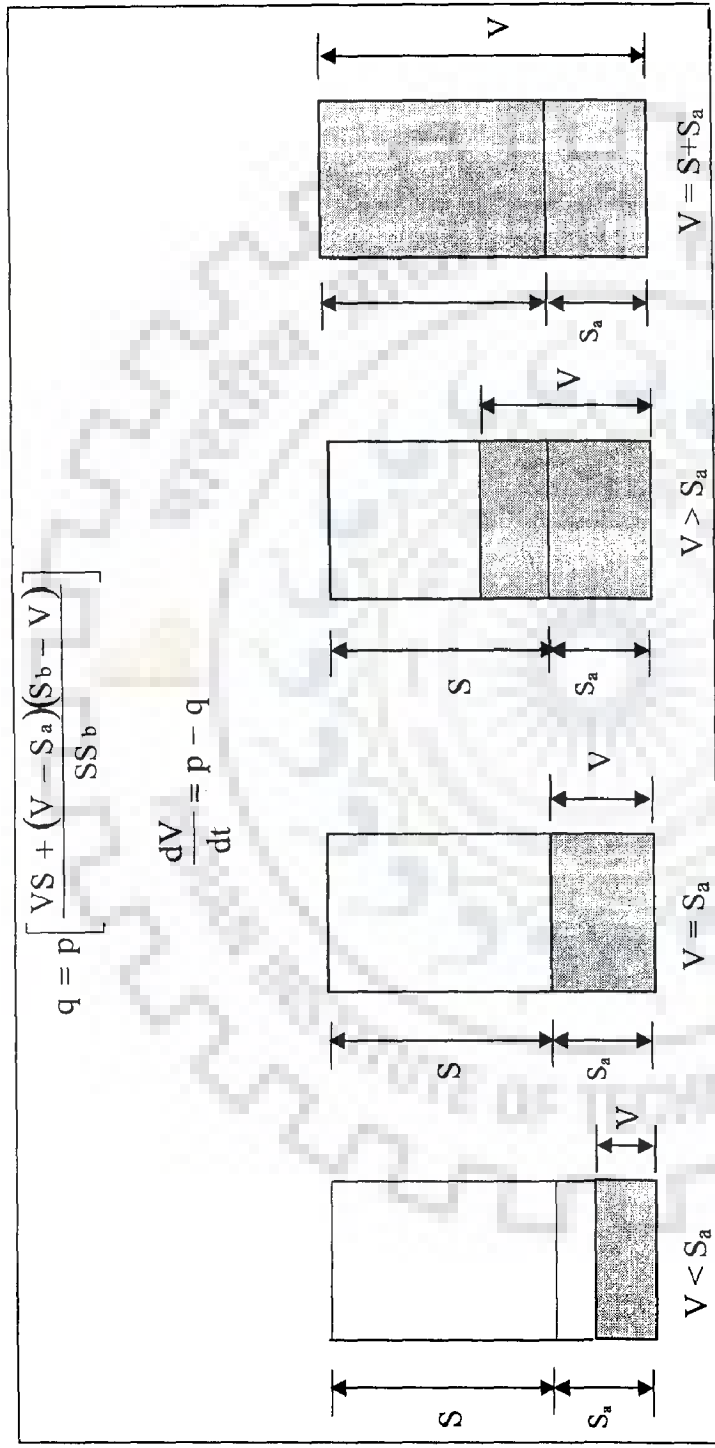


Fig. 4.3 Schematic diagram showing the generalized behavior of the proposed continuous sub-model accounting soil moisture based on modified SCS-CN method

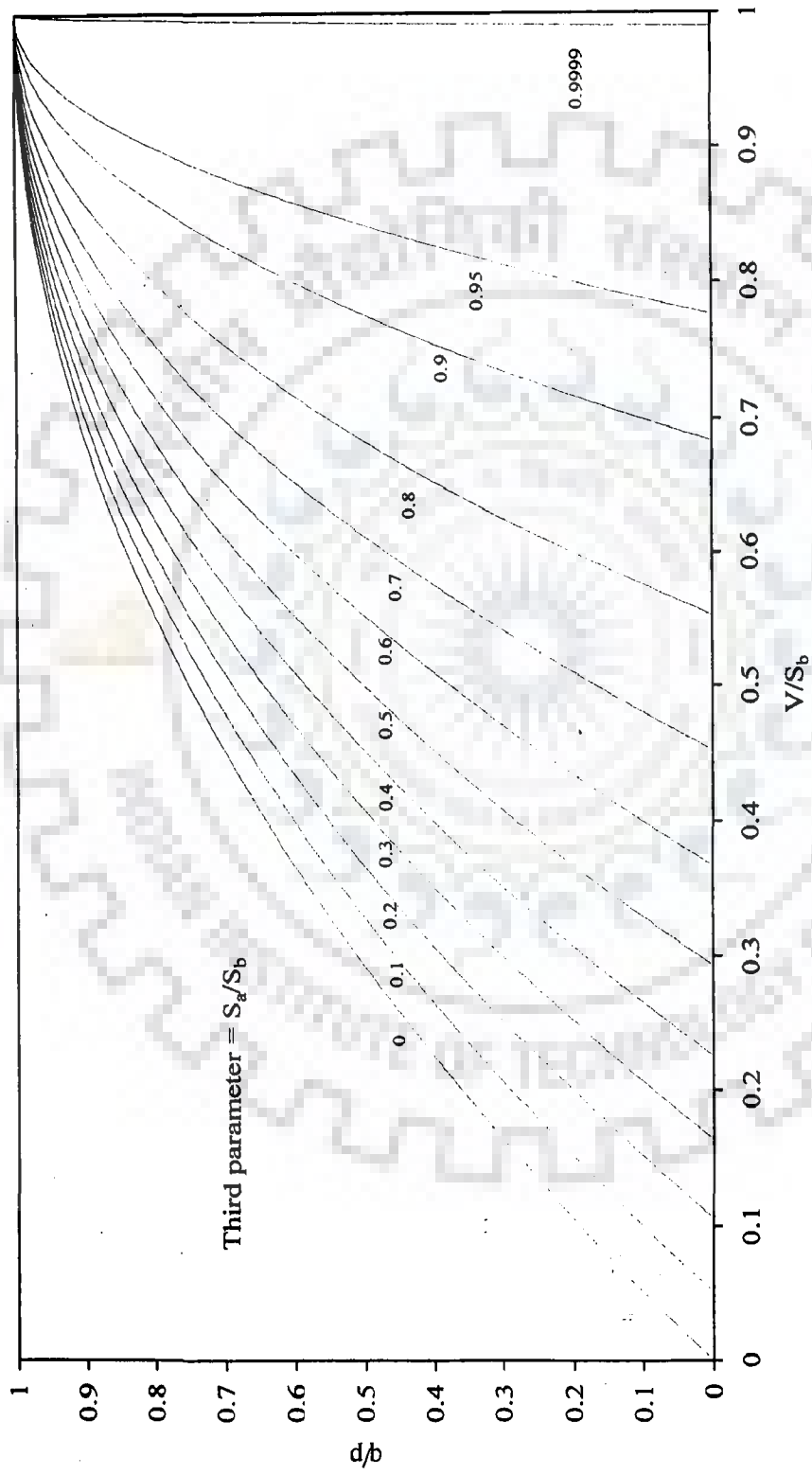


Fig. 4.4 Feasible variation of q/p with V/S_b . Third parameter = S_d/S_b

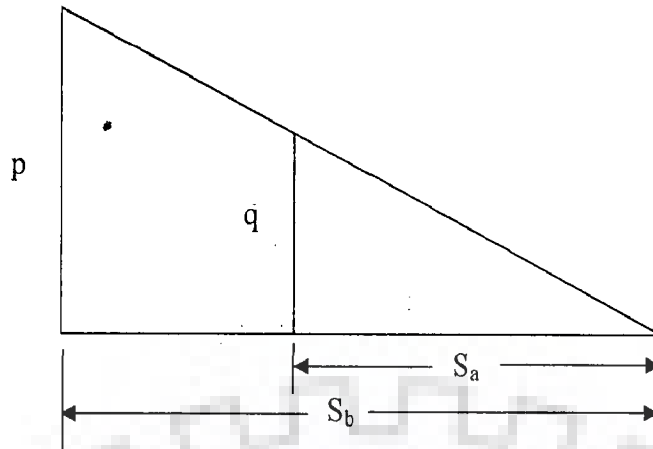


Fig. 4.5 Proportionality between direct surface runoff rate and rainfall intensity

Table 4.1 Summary of continuous sub-models of runoff q for different values of moisture storage V

Soil moisture storage (V)	Proposed	Michel et al.
$V < S_a$	$q = p \left[\frac{VS - (V - S_a)(S_b - V)}{SS_b} \right]$	$q = 0$
$V = S_a$	$q = p \left(\frac{S_a}{S_b} \right)$	$q = 0$
$S_a < V < S_b$	$q = p \left[\frac{VS + (V - S_a)(S_b - V)}{SS_b} \right]$	$q = p \left(\frac{V - S_a}{S} \right) \left(2 - \frac{V - S_a}{S} \right)$
$V = S_b$	$q = p$	$q = p$

its SMA foundation, as it considers V_0 in proportionality ($C = S_r$) concept or basic hypothesis (Eq. 2.3). This can be accomplished by replacing I_a from Eq. (4.2) by V_0 and S_a , as follows:

$$Q = \frac{(P + V_0)(P + V_0 - S_a)}{P + S + V_0} \quad \text{for } P + V_0 > S_a \quad (4.25)$$

$$= 0 \quad \text{otherwise}$$

If soil is fully saturated before the start of a storm event, i.e., $V_0 = S_b$, then Q should be equal to P . Thus, putting $V_0 = S_b$ in Eq. (4.25), one gets:

$$Q = \frac{(P + S_b)(P + S_b - S_a)}{P + S + S_b} \quad (4.26)$$

Alternatively, Eq. (4.26) can be expressed as

$$Q = P + \frac{SS_b}{P + S + S_b} \quad (4.27)$$

It can be inferred from Eq. (4.27) that Q is greater than P for the condition, $V_0 = S_b$. This indicates towards the mathematical inconsistency in the modified form of existing SCS-CN method (Eq. 4.2), and needs to be addressed on complete SMA foundation. For this, the only way to obtain the mathematically consistent formulation is to recalculate the formula for cumulative runoff (Q) and cumulative rainfall (P) by coupling Eq. (4.6) with Eq. (4.22), similar to Michel et al., as indicated above. However, three cases, illustrated in Fig.4.6, arise from the presence of V_0 and S_a , as follows:

First case: when $V_0 < S_a - P$ or $P < I_a$ i.e. rainfall P is not large enough to meet I_a requirement then $Q = 0$

Second case: when $V_0 < S_a$, but $(P + V_0) > S_a$ i.e. $S_a - P < V_0 < S_a$, then the generated runoff (Q) can be computed using Eq. (4.2).

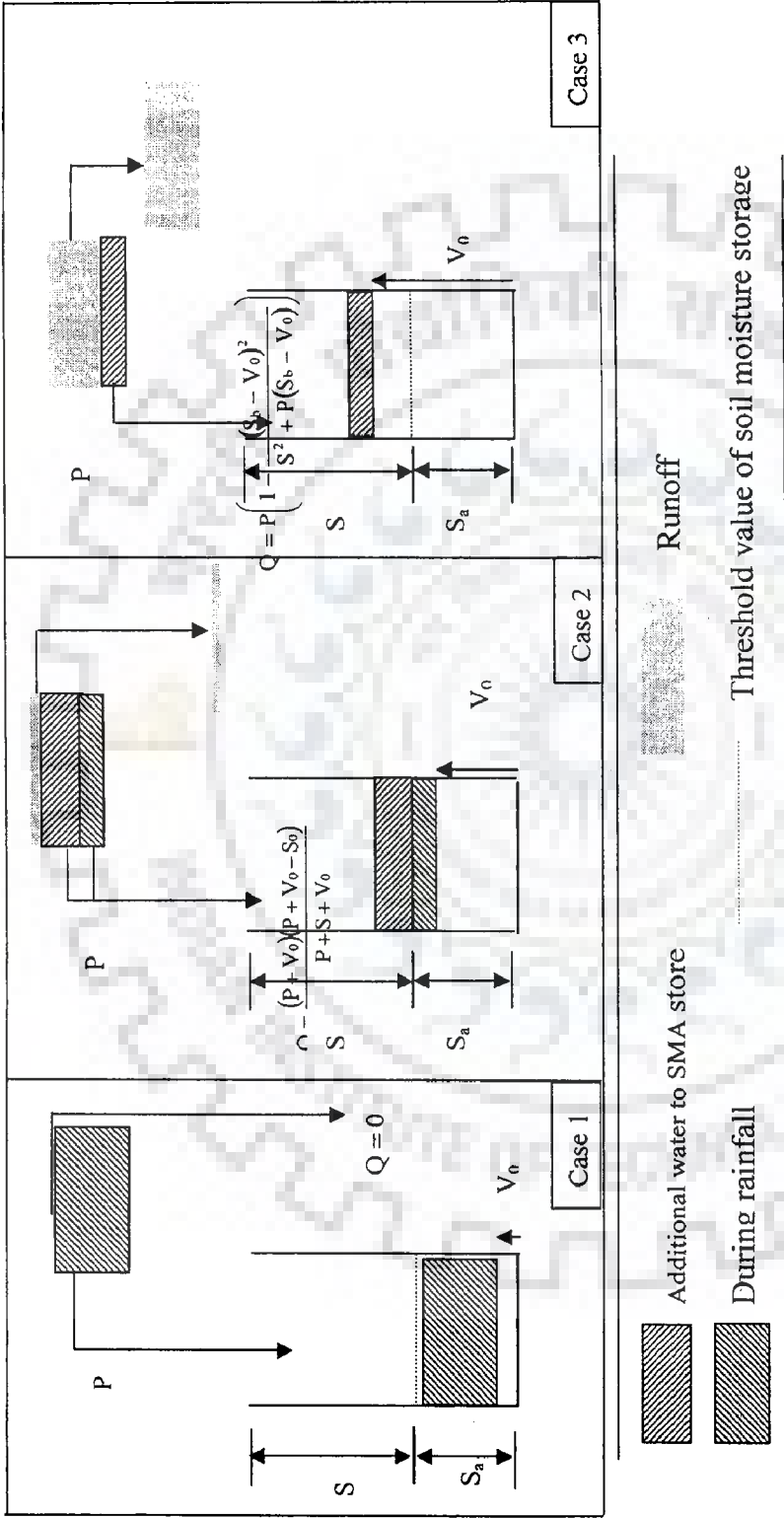


Fig. 4.6 Schematic of the proposed event-aggregated SMA procedure for various antecedent moisture levels

Third Case: when V_0 is greater than S_a but less than S_b i.e. $S_a \leq V_0 \leq S_b$, then substituting q from Eq. (4.22) into Eq. (4.2) one gets

$$\frac{dV}{dt} = p - p \left[\frac{VS + (V - S_a)(S_b - V)}{SS_b} \right] \quad (4.28)$$

or

$$\frac{dV}{dt} = p \left[1 - \frac{VS + (V - S_a)(S_b - V)}{SS_b} \right] \quad (4.29)$$

After re-arranging, Eq. (4.29) is expressible as:

$$\frac{dV}{dt} = p \left[1 - \frac{V}{S_b} + \left(\frac{V}{S_b} - \frac{S_a}{S_b} \right) \left(1 - \frac{V}{S_b} \right) / \left(1 - \frac{S_a}{S_b} \right) \right] \quad (4.30)$$

or

$$\frac{dV}{dt} = p \left[\frac{(S_b - V)^2}{SS_b} \right] \quad (4.31)$$

Again, re-arranging Eq. (4.31) and applying appropriate lower and upper limits of integration, one gets:

$$\int_{V=V_0}^V \frac{dV}{(S_b - V)^2} = \int_{t=0}^t \frac{p dt}{SS_b} \quad (4.32)$$

On integrating Eq. (4.32), we get

$$\frac{1}{(S_b - V)} - \frac{1}{(S_b - V_0)} = \frac{P}{SS_b} \quad (4.33)$$

Now, substituting V from Eq. (4.6) into Eq. (4.33) and rearranging leads to

$$\frac{(P - Q)}{[(S_b - V_0) - (P - Q)](S_b - V_0)} = \frac{P}{SS_b} \quad (4.34)$$

Eq. (4.34) can be further simplified as:

$$Q = P \left(1 - \frac{(S_b - V_0)^2}{SS_b + P(S_b - V_0)} \right) \quad (4.35)$$

It is observed from Eq. (4.35) that if $V_0 = S_b$, then $Q = P$, consistent both mathematically and physically.

Finally, the event-based models corresponding to the three cases can be summarized below as:

$$V_0 < S_a - P \quad Q = 0 \quad (4.36)$$

$$S_a - P < V_0 < S_a \quad Q = \frac{(P + V_0)(P + V_0 - S_a)}{P + S + V_0} \quad (4.37)$$

$$S_a \leq V_0 \leq S_b \quad Q = P \left(1 - \frac{(S_b - V_0)^2}{SS_b + P(S_b - V_0)} \right) \quad (4.38)$$

Here, it is to be noted that the third case, i.e., $V_0 \geq S_a$ corresponds to $I_a \leq 0$, was not included in the original SCS-CN method. Thus, the set of equations (Eqs. 4.36 to 4.38), framed under the three cases, represents a hydrologically more rational and sound procedure, which should replace the existing SCS-CN method, and is an improvement over Michel et al. model. Table 4.2 summarizes the proposed SCS-CN model, Michel et al. model, and the existing SCS-CN method for the three conditions.

4.2.2 SMA Inspired Continuous SCS-CN Model

As discussed above, Eq. (4.22) describes only a part of the SMA based continuous model since it lacks the component of soil moisture depletion (i.e. the evapotranspiration), which occurs during the inter-storm periods. Accordingly, a

Table 4.2 Comparison of event-aggregated SMA procedure based SCS-CN model for various antecedent moisture levels

Sl. No.	Case	Proposed model	Michel et al. model
I	$V_0 \leq S_a - P$	$Q = 0$	$Q = 0$
II	$S_a - P < V_0 < S_a$	$Q = \frac{(P + V_0)(P + V_0 - S_a)}{P + S + V_0}$	$Q = \frac{(P + V_0 - S_a)^2}{P + V_0 - S_a + S}$
III	$S_a \leq V_0 \leq S_b$	$Q = P \left(1 - \frac{(S_b - V_0)^2}{SS_b + P(S_b - V_0)} \right)$	$Q = P \left(1 - \frac{(S_b - V_0)^2}{S^2 + P(S_b - V_0)} \right)$

complete SMA based continuous model would essentially comprise of Eq. (4.22) along with an expression for evapotranspiration. In the present study, similar to the ‘Versatile SCS-CN model’ proposed by Mishra and Singh (2004a), the potential evapotranspiration was computed as:

$$PET = PANC * E \quad (4.39)$$

where PANC is the pan coefficient and E is the pan evaporation during Δt period or time interval (=1-day in present case). Pan evaporation depends on several meteorological factors, such as temperature, humidity, wind speed, and solar radiation. PANC however depends on vegetative cover and season and is thus a function of the time of the year and varies between 0 and 1. Accordingly the dynamic relationship for V (Eq. 4.5) can be modified as:

$$\frac{dV}{dt} = p - q - PET \quad (4.40)$$

Thus, Eqs. (4.22), (4.39) & (4.40) constitute the proposed SMA inspired continuous SCS-CN model. Similarly, Eqs. (2.32), (4.39) & (4.40) constitute the continuous SCS-CN model developed by Michel et al.

4.3 APPLICATION

4.3.1 SMA Based Event-Aggregated and Existing SCS-CN Models

The proposed event-based SCS-CN model (Eqs. 4.36-4.38), Michel et al. model (Eqs. 2.29-2.31), and existing SCS-CN method (Eq. 2.6) were applied to a large rainfall-runoff data set derived from the U.S. Department of Agriculture-Agricultural Research Service (USDA-ARS) data base, as discussed in Chapter 3. In the present study, rainfall-runoff data of 9359 events from 35 watersheds having area varying from 0.71 to 53.42 ha are used (Table 3.1).

4.3.2 Procedure Adopted for Models Application

The proposed as well as Michel et al. event-based SCS-CN models have three parameters, viz., V_0 , S , and S_a . For proposed model, parameter V_0 was estimated by a simple but efficient and hydrologically rational relationship (Mishra et al. 2006b):

$$V_0 = \alpha \sqrt{P_5 S} \quad (4.41)$$

where α is a coefficient, and P_5 is the 5-day antecedent rainfall amount. The advantage of such an expression is that it relates physically V_0 to P_5 and S , in the sense that a higher P_5 or S will have a higher value of V_0 . Moreover, it obviates the sudden jump of V_0 with S or CN. Since Michel et al. model does not have any expression for V_0 estimation, the same expression (Eq. 4.41) is used for V_0 estimation.

Similarly, the parameter S_a of proposed model was estimated by a linear relationship between S_a and S , given as

$$S_a = \beta S \quad (4.42)$$

where β is a coefficient. However, for Michel et al model S_a is taken as a set fraction of S ($= 0.33S$). For existing SCS-CN method (SCS, 1956; McCuen, 1982; Ponce and Hawkins, 1996; and Mishra and Singh, 1999a), which is based on I_a - λ relationship and

three AMC conditions (NEH-4 procedure), λ was taken as 0.2 (a standard value). Finally, Marquardt (Marquardt, 1963) constrained least-square approach was utilized to estimate the coefficients α , β , and parameter S.

4.3.3 Marquardt Constrained Least Square Approach

Marquardt (1963) provided an elegant and improved version of the non-linear method originally proposed by Levenberg (1944). The method primarily provides a smooth variation between the two extremes of the inverse-Hessian method and the steepest descent method. The later is used when the trial solution is far from the minimum and it tends continuously towards the former as the minimum is approached. The details of the approach are given in Mishra and Singh (2003a).

4.3.4 Goodness of Fit

The goodness-of-fit of the models was evaluated using the Nash and Sutcliffe (NS) (1970) efficiency criterion as:

$$NS = 1 - \frac{\sum (Q_{obs} - Q_{com})^2}{\sum (Q_{obs} - \overline{Q_{obs}})^2} \times 100 \quad (4.43)$$

where Q_{obs} is the observed runoff, Q_{com} and $\overline{Q_{obs}}$ stand for computed and the mean of the observed runoff, respectively. The efficiency varies on the scale of 0-100. It can also assume a negative value if $\sum (Q_{obs} - Q_{com})^2 > \sum (Q_{obs} - \overline{Q_{com}})^2$, implying that the variance in the observed and computed runoff values is greater than the model variance. In such a case, the mean of the observed data fits better than does the proposed model. The efficiency of 100 implies that the computed values are in perfect agreement with the observed data. Recently, McCuen et al. (2006) found that NS efficiency is a very good criterion for assessing the comparative performance of hydrologic models.

4.3.5 Performance Evaluation of SMA Based Event-Aggregated and Existing SCS-CN Models

As discussed above, the NS efficiencies resulting from the application of SMA based event-aggregated SCS-CN models, viz., the proposed SCS-CN model, Michel et al. model, and existing SCS-CN method (Eq. 2.6) are shown in Table 4.3. For convenience sake, the proposed event-aggregated SCS-CN model is designated as Model 1, Michel et al. model as Model 2, and existing SCS-CN method as Model 3. The performance was evaluated by assigning ranks (i – iii) to the above three models in the order of their NS efficiency-based merit in applications to the data set of a watersheds. The rank i corresponds to the maximum efficiency, and rank iii to the minimum. For evaluating the overall performance of these models in all applications, each rank was assigned a grade 2-0 (at an interval of 1, i.e., 2-1-0), respectively, and the assigned grades were added to rank these models in the order of their overall performance. Such type of ranking and grading system has been applied successfully by Mishra and Singh (1999a). Based on NS efficiencies shown in Table 4.3, the ranks of Models in each application and assigned overall ranks (I-III) from the overall score obtained by each model are shown in Table 4.4. It is observed from the table that Model 1 scores the highest marks 65 followed by Model 2 with 41, and Model 3 with 0 mark out of the maximum 70. Accordingly Models 1, 2, and 3 can be ranked as I through III, respectively. Alternatively Model 1 performs the best, followed by Model 2, and Model 3. Thus, the results show that the performance of Model 1 (proposed model) is much better than Model 2 (Michel et al. model), and Model 3 (existing SCS-CN method) performs poorest in the present application. Similar inferences can be drawn from the results shown graphically in Appendix G.

4.3.6 SMA Based Continuous SCS-CN Models

The proposed SMA inspired continuous SCS-CN model (Eqs. (4.22), (4.39) & (4.40)) and the continuous SCS-CN model of Michel et al. (Eqs. (2.32), (4.39) & (4.40)) were applied to five year daily rainfall-runoff and evaporation data set of the Hemavati watershed. It is noteworthy here that the threshold value of soil moisture (S_a) was taken as 0.33S in Michel et al. application, whereas in application of the proposed model it was estimated using Eq. (4.42).

Table 4.3 Statistic of Goodness of fit

			NS efficiency of SMA inspired Event-aggregated and Existing SCS-CN Models		
Sl. No.	Watershed No.	Area (ha)	Model 1	Model 2	Model 3
1	9004	23.96	76.63	74.88	46.83
2	16010	40.47	41.71	31.00	7.94
3	17001	11.02	78.77	78.15	3.56
4	17002	20.21	78.90	78.12	1.48
5	17003	5.08	74.83	75.15	-2.45
6	26010	0.55	63.26	57.63	-17.26
7	26013	0.68	34.57	23.20	-10.14
8	26014	0.26	65.24	62.40	-6.99
9	26016	0.59	54.59	47.57	-4.56
10	26018	0.48	77.77	71.60	-5.08
11	26031	49.37	27.41	11.71	-85.98
12	26863	0.17	85.94	85.37	-26.66
13	34002	1.95	65.86	62.83	1.96
14	34006	0.71	60.42	57.31	-5.99
15	34007	0.81	66.90	65.15	-2.52
16	34008	1.91	54.83	52.26	-3.00
17	35001	13.52	81.70	81.19	-16.96
18	35002	1.3	74.89	67.60	-27.24
19	35003	1.27	83.18	83.38	-16.19
20	35008	3.68	79.92	77.19	19.80
21	35010	6.35	79.41	78.39	7.44
22	35011	38.36	46.28	45.52	-6.39
23	37001	6.76	59.81	59.15	-11.85
24	37002	37.23	62.40	62.30	6.17
25	42010	7.97	75.01	72.08	-27.00
26	42012	53.42	73.35	72.43	-14.02
27	42013	32.33	83.14	82.88	-53.69
28	42014	6.6	70.53	67.31	-15.70
29	42015	16.19	72.60	72.10	-9.68
30	42016	8.42	74.32	72.66	-11.84
31	42017	7.53	76.65	76.14	-14.03
32	42037	4.57	75.58	76.13	0.21
33	42038	2.27	69.87	69.62	-25.42
34	42039	4.01	68.45	68.56	-12.54
35	42040	4.57	63.09	63.51	-15.82

Table 4.4 Performance Evaluation of Models

			Rank and Score based on NS efficiency		
Sl. No.	Watershed No.	Area (ha)	Model 1	Model 2	Model 3
1	9004	23.96	i (2)	ii (1)	iii (0)
2	16010	40.47	i (2)	ii (1)	iii (0)
3	17001	11.02	i (2)	ii (1)	iii (0)
4	17002	20.21	i (2)	ii (1)	iii (0)
5	17003	5.08	ii (1)	i (2)	iii (0)
6	26010	0.55	i (2)	ii (1)	iii (0)
7	26013	0.68	i (2)	ii (1)	iii (0)
8	26014	0.26	ii (2)	i (2)	iii (0)
9	26016	0.59	i (2)	ii (1)	iii (0)
10	26018	0.48	i (2)	ii (1)	iii (0)
11	26031	49.37	i (2)	ii (1)	iii (0)
12	26863	0.17	i (2)	ii (1)	iii (0)
13	34002	1.95	i (2)	ii (1)	iii (0)
14	34006	0.71	i (2)	ii (1)	iii (0)
15	34007	0.81	i (2)	ii (1)	iii (0)
16	34008	1.91	i (2)	ii (1)	iii (0)
17	35001	13.52	i (2)	ii (1)	iii (0)
18	35002	1.3	i (2)	ii (1)	iii (0)
19	35003	1.27	ii (1)	i (2)	iii (0)
20	35008	3.68	i (2)	ii (1)	iii (0)

(continued...)

Table 4.4 Performance Evaluation of Models

21	35010	6.35	i (2)	ii (1)	iii (0)
22	35011	38.36	i (2)	ii (1)	iii (0)
23	37001	6.76	i (2)	ii (1)	iii (0)
24	37002	37.23	i (2)	ii (1)	iii (0)
25	42010	7.97	i (2)	ii (1)	iii (0)
26	42012	53.42	i (2)	ii (1)	iii (0)
27	42013	32.33	i (2)	ii (1)	iii (0)
28	42014	6.6	i (2)	ii (1)	iii (0)
29	42015	16.19	i (2)	ii (1)	iii (0)
30	42016	8.42	i (2)	ii (1)	iii (0)
31	42017	7.53	i (2)	ii (1)	iii (0)
32	42037	4.57	ii (1)	i (2)	iii (0)
33	42038	2.27	i (2)	ii (1)	iii (0)
34	42039	4.01	ii (1)	i (2)	iii (0)
35	42040	4.57	ii (1)	i (2)	iii (0)
Total Score			65	41	0
Overall Rank			I	II	III

*(No. in bracket indicates the grade (2-0 scale) assigned to the models on rank basis)

4.3.7 Performance Evaluation of SMA Based Continuous SCS-CN Models

Consistent with the work of Mishra and Singh (2004a), the daily rainfall- excess rates computed by the proposed and Michel et al. continuous SCS-CN models were

routed through the watershed using single linear reservoir scheme to obtain the direct surface runoff at the outlet. Here, it is noted that for $V < S_a$ condition, q is taken as zero. Finally, the application results are shown in Figs. 4.7 through 4.11. The figures show that the computed peaks of the hydrographs, in general, fairly match the observed ones. Further, the models performance was evaluated using Eq. (4.41), and the averaged NS efficiency was found to be 82.56% and 81.87%, respectively, for proposed and Michel et al. models. The efficiency statistic indicates that both the models perform equally well for continuous hydrologic simulation; the proposed model however performs marginally better than the Michel et al. model.

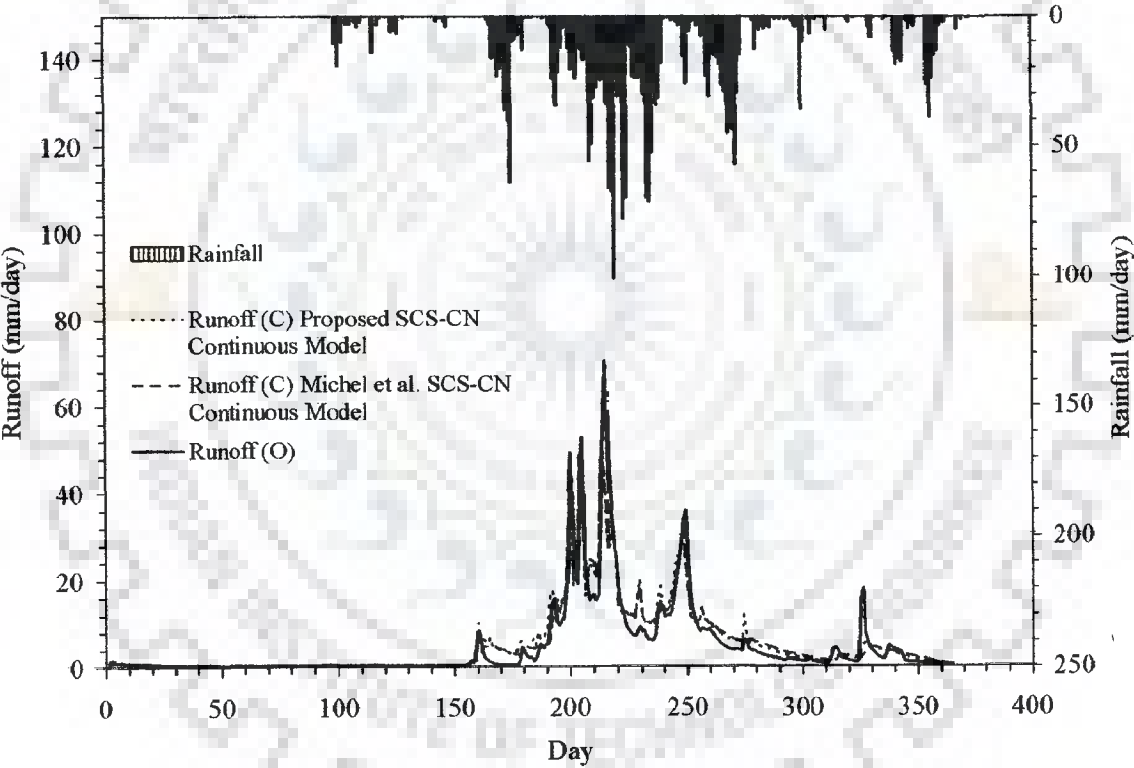


Fig. 4.7 Fitting of SMA based Proposed and Michel et al. models for continuous hydrologic simulation to the data of Hemavati watershed for the year-1975 (Jan.1st to Dec. 30, 1975)

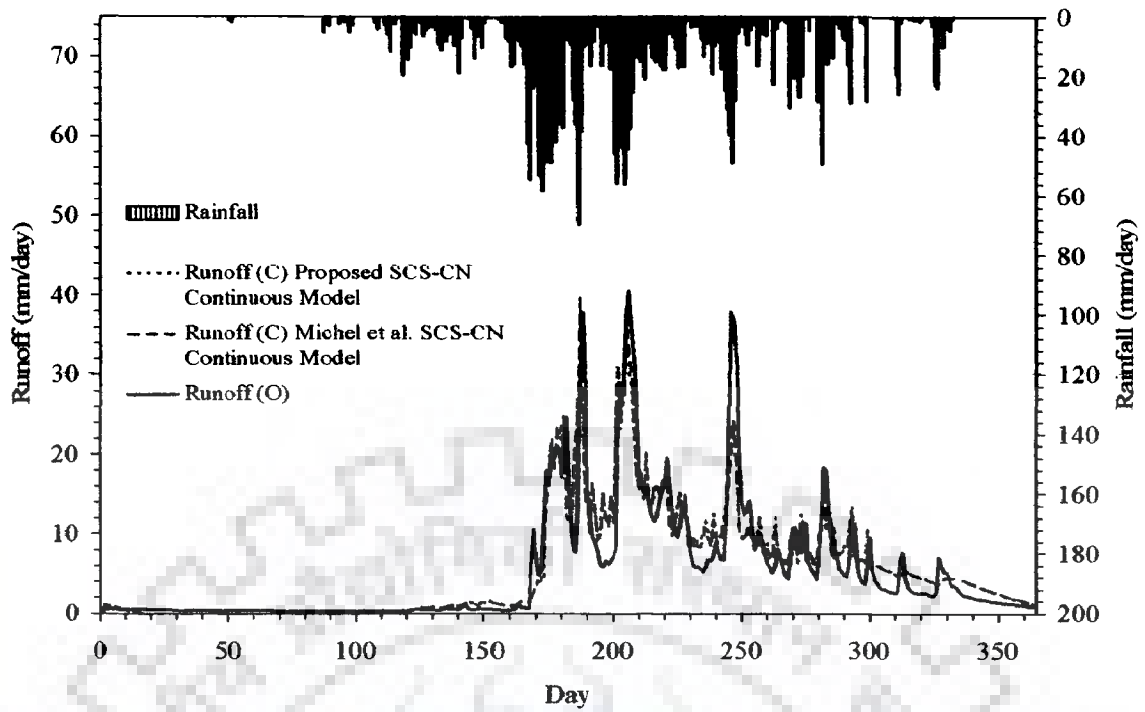


Fig. 4.8 Fitting of SMA based Proposed and Michel et al. models for continuous hydrologic simulation to the data of Hemavati watershed for the year-1976 (Jan.1st to Dec. 30, 1976)

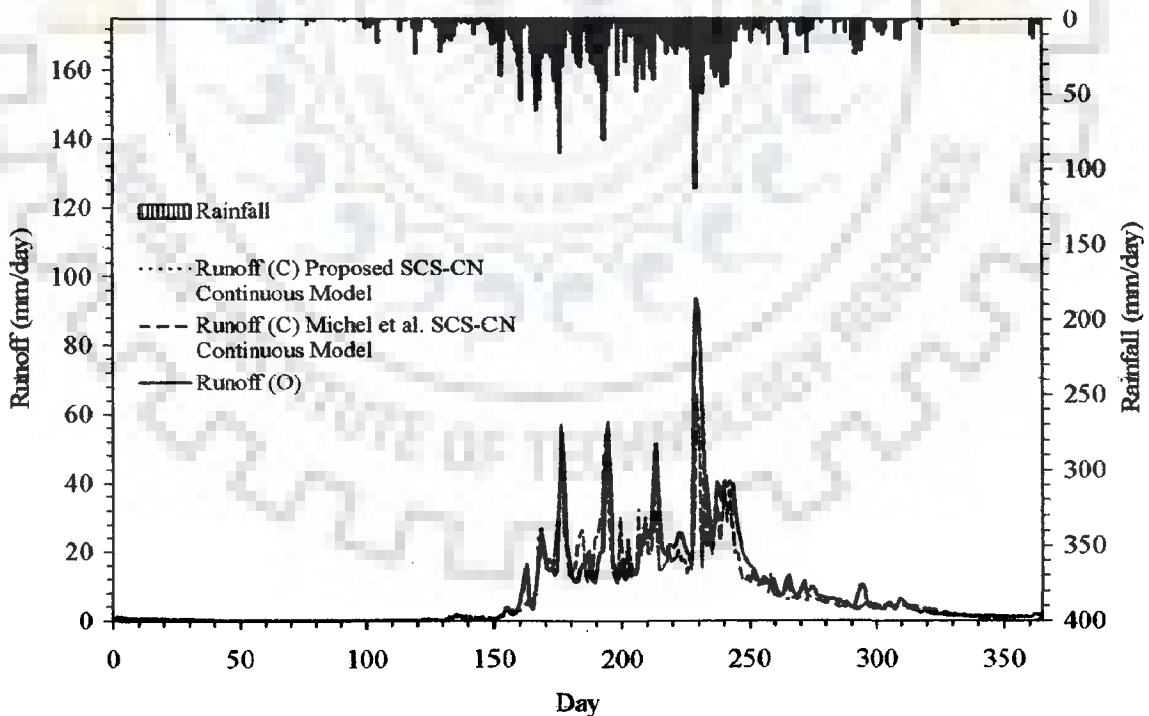


Fig. 4.9 Fitting of SMA based Proposed and Michel et al. models for continuous hydrologic simulation to the data of Hemavati watershed for the year-1977 (Jan.1st to Dec. 30, 1977)

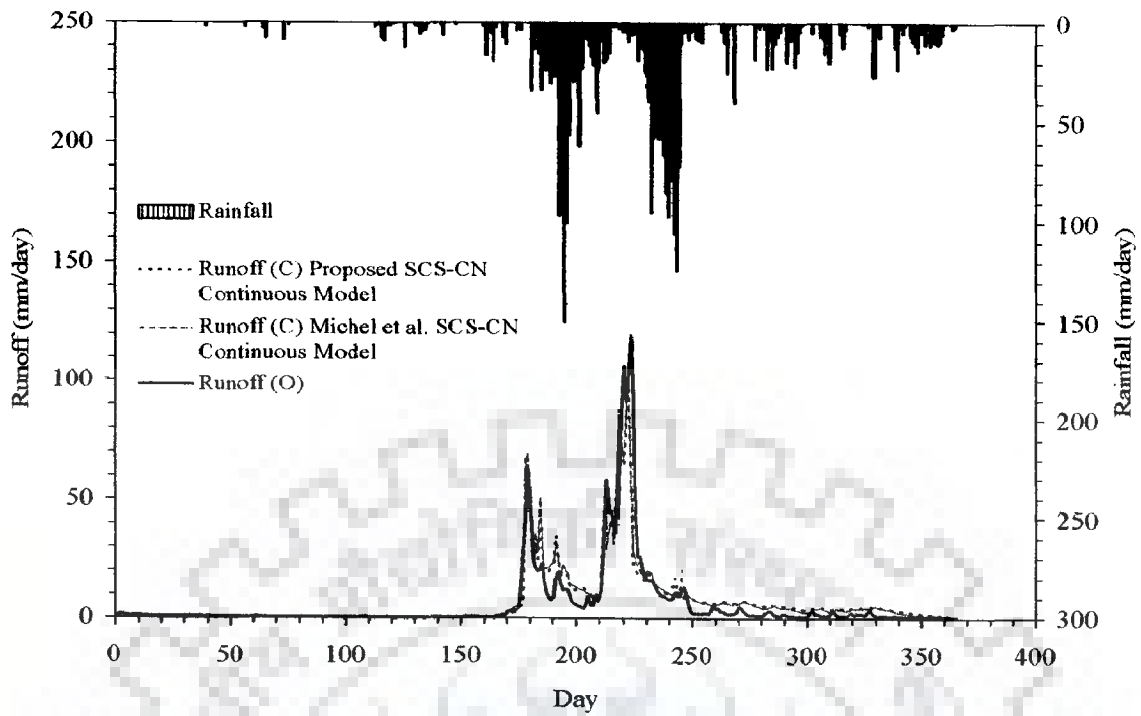


Fig. 4.10 Fitting of SMA based Proposed and Michel et al. models for continuous hydrologic simulation to the data of Hemavati watershed for the year-1977 (Jan.1st to Dec. 30, 1978)

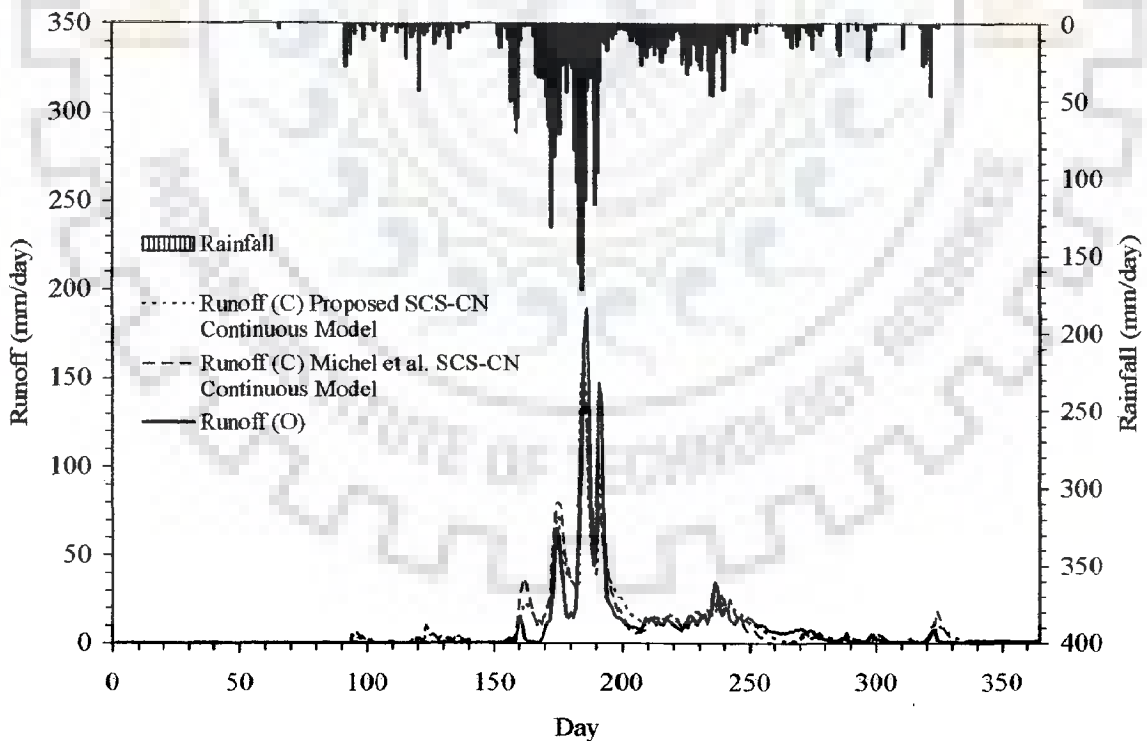


Fig. 4.11 Fitting of SMA based Proposed and Michel et al. models for continuous hydrologic simulation to the data of Hemavati watershed for the year-1979 (Jan.1st to Dec. 30, 1979)

4.4 SUMMARY

A revisit to the SCS-CN method for its underlying SMA procedure led to a revised version of Michel et al. model. The revision based on a stronger mathematical platform and hydrologically sounder perception. Using the data of 35 watersheds of United States, the event-aggregated proposed model, Michel et al. model, and the original SCS-CN method were compared for their performance. In these applications the proposed procedure was found to be more accurate than the others, and the original SCS-CN method poorest of all. The results obtained herein reflected the appropriateness of inclusion of initial soil moisture in the $C = S_r$ concept in particular and in SCS-CN's proportionality hypothesis in general. The study also proposed a continuous hydrologic simulation model parallel to the Michel et al. model, and the results indicated that both performed equally well, when applied to daily rainfall-runoff data of Hemavati watershed; the proposed model however performed marginally better than the Michel et al. model.

CHAPTETR-5

EXTENDED HYBRID MODEL FOR SYNTHETIC UNIT HYDROGRAPH DERIVATION

5.1 BACKGROUND

The need for a synthetic method to develop unit hydrograph has inspired many studies (Kull^{and Feld}1998). For deriving the SUH analytically, the two parameter gamma distribution is most commonly used in various forms depending on the values of peak flow rate and time to peak. Furthermore, the instantaneous unit hydrograph (IUH) is better suited for mathematically expressing the ERH and DRH relationship in a catchment (Jeng and Coon, 2003).

Based on the concept of IUH, Nash (1957) developed a conceptual model of a drainage basin as series of n number of identical linear reservoirs in series. Later Dooge (1959) improved the Nash (1957) model by introducing translation time into the cascades that was ignored earlier. However, the model was not amenable to practical applications (Chow 1964). To overcome this difficulty Singh (1964) derived the IUH using a nonlinear model considering the overland and channel flow components separately. More recently, Bhunya et al. (2005) highlighted the major inconsistencies (Chapter 2) associated with the Nash model and developed a hybrid model (HM) to address these inconsistencies. However, the model has few points of concern, as discussed in Chapter 1 ~~to chapter 2.~~

Thus, to overcome the inconsistencies associated with the hybrid model (HM), the present study extends the HM by inserting a linear channel between the two reservoirs to account for translation. While simulating the process of rainfall-runoff in the proposed model, the storage effects of the channel are ignored or, in other words, only the pure translational effects of channel are considered. Thus, the objectives of the present chapter are: (i) to develop an extended hybrid model (EHM) for SUH derivation by representing the basin system as series of hybrid units, where each hybrid unit consists of two linear reservoirs (LR) connected by a linear channel (LC) in a specific order i.e. (LR-LC-LR); (ii) to derive a generalized form of EHM and to show analytically that the HM and Nash models are the specific forms of the earlier one; and (iii) check workability of EHM in comparison to HM and Nash models using field data of catchments ranging from small to medium range to check the workability.

5.2 EXTENDED HYBRID MODEL (EHM) FORMULATION

Assuming K_1 and K_2 in the units of hours to be the storage coefficients of the first and second linear reservoirs, respectively, and T [hr] as the translation time of linear channel, the outflow due to an unit input is deduced as follows.

For an instantaneous unit excitation of rainfall $[\delta(t)]$ at the inlet of the first hybrid unit, let the response at the outlet of the first unit be $Q_1(t)$ (Fig 51). It is noted that the time is reckoned since the appearance of the input at the inlet boundary of the first unit. Using the concept that the output of the preceding unit forms variable input to the succeeding unit, the unit response function for any given input is derived as follows:

First hybrid unit

The mass balance in the first reservoir for an infinitely small time can be employed as:

$$\delta(t) - Q(t) = \frac{dS_1(t)}{dt} \quad (5.1)$$

where $\delta(t)$ = a unit impulse input at the inlet of the first reservoir, defined as: $\delta(t) = 1$ for $t = 0$; and $\delta(t) = 0$ for $t > 0$; $Q(t)$ = variable outputs from the first reservoir; and $S_1(t)$ = storage for the first reservoir.

As storage of the linear reservoir is defined as $S_1(t) = K_1 Q(t)$, its substitution in Eq. (5.1) yields

$$K_1 \frac{dQ(t)}{dt} + Q(t) = \delta(t) \quad (5.2)$$

By utilizing the operator notation, $D = d/dt$, alternatively Eq. (5.2) can be expressed as (Singh, 1992):

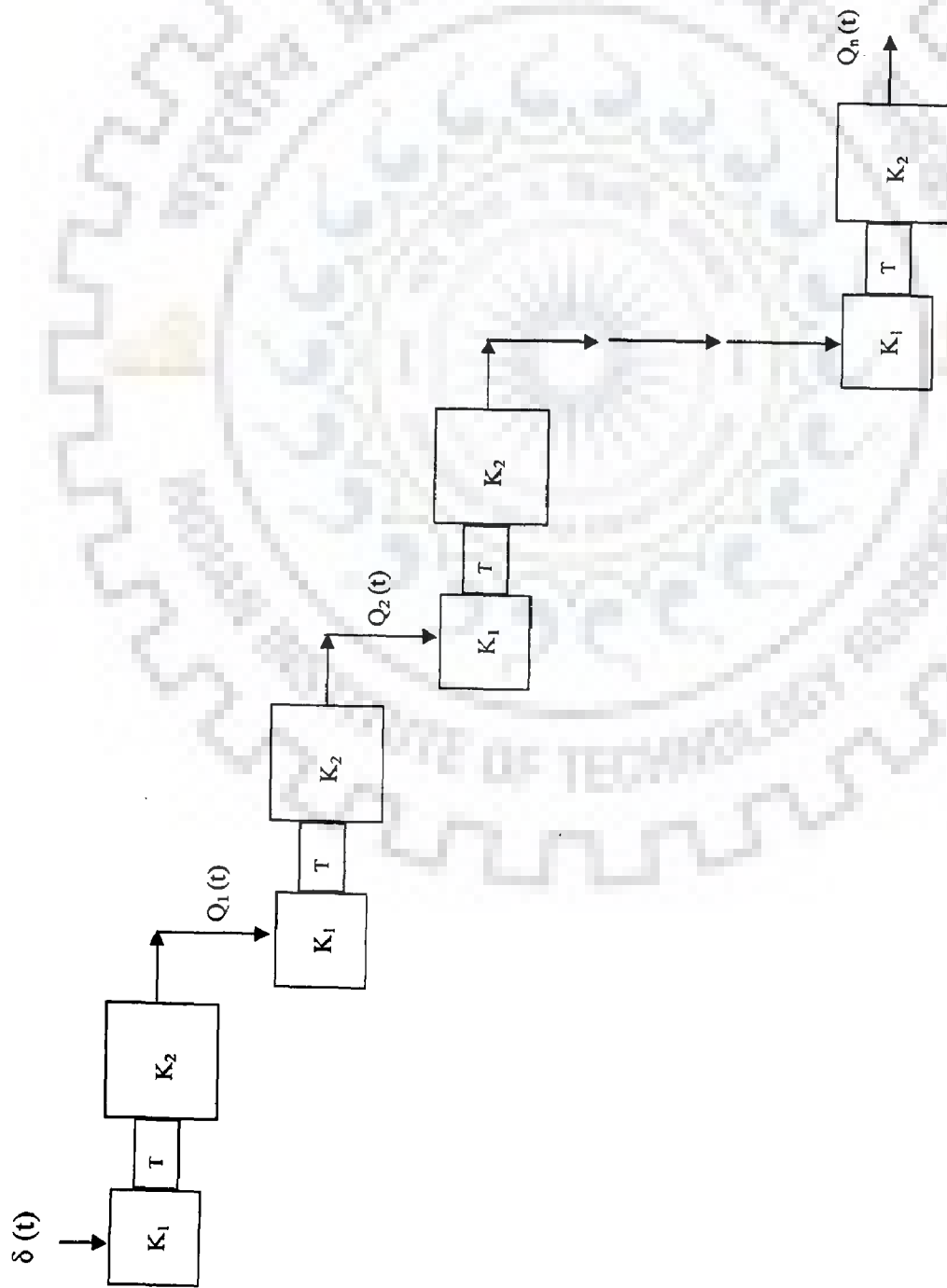


Fig.5.1 Representation of basin system by series of n hybrid units

$$Q(t) = \frac{1}{(1 + K_1 D)} \delta(t) \quad (5.3)$$

Thus, Eq. (5.3) acts as the inflow for the linear channel. As the process of converting rainfall-excess into runoff is a mixture of storage and translation actions in the catchment, a linear channel is introduced for accounting the translational effects similar to Dooge (1959) as it translates the inflow hydrograph without changing the shape. Thus, the linear channel shifts the scale equal to its translation time and therefore the outflow from the channel incorporates the channel effects, i.e. delay time or translation time, and can be expressed as:

$$Q(t) = \frac{1}{(1 + K_1 D)} \delta(t - T) \quad (5.4)$$

Here, the outflow from the linear channel (Eq. 5.4) forms an input to the second reservoir of storage coefficient K_2 . Using the mass balance equation, the expression for the second reservoir can be given as:

$$I(t) - Q_1(t) = \frac{dS_2(t)}{dt} \quad (5.5)$$

where $Q_1(t)$ = output from the first hybrid unit; $I(t)$ = variable input to the second reservoir = $Q(t)$ = output from the channel; and $S_2(t)$ is the storage for the second reservoir, defined as $S_2(t) = K_2 Q_1(t)$.

Substituting $S_2(t) = K_2 Q_1(t)$ and $I(t) = Q(t)$ in Eq. (5.5) gives

$$\left[K_2 \frac{dQ_1(t)}{dt} + Q_1(t) \right] = [Q(t)] \quad (5.6)$$

The Laplace transform of Eq. (5.6) gives

$$Q_1(s) = \frac{e^{-Ts}}{(1 + K_1 s)(1 + K_2 s)} \quad (5.7)$$

where s = Laplace transform coefficient and $Q_1(s)$ is the Laplace transform of $Q_1(t)$.

The inverse Laplace transform of Eq. (5.7) gives

$$Q_1(t) = \frac{1}{(K_1 - K_2)} \left[\exp\left(\frac{T-t}{K_1}\right) - \exp\left(\frac{T-t}{K_2}\right) \right] \text{ for } t \geq T \quad (5.8)$$

$$= 0 \quad \text{otherwise}$$

It may be noted here that Eq. (5.8) holds good for $K_2 > K_1$, otherwise $Q_1(t)$ becomes a negative quantity, which is not practical. The routing of flow downstream causes attenuation leading to reduction of magnitude of peak flow and, in turn, wave celerity and, therefore, K_2 has to be greater than K_1 (Mishra and Singh, 1999b). The response at the outlet of the first hybrid unit due to unit impulse excitation at its inlet is represented by Eq. (5.8). Further, if (i) $K_2 = 0$, $T = 0$ and $K_1 = K$, Eq. (5.8) converts to the solution of the Nash's single linear reservoir ($n = 1$) (Singh, 1988), and (ii) for $T = 0$, Eq. (5.8) converts to the hybrid model (Bhunya et al., 2005) for a single hybrid unit. For given K_1 , K_2 and T , the distribution of Eq. (5.8) describes time to peak, peak value, and distinct rising and falling limbs, fundamental to the description of an IUH. Eqs. (5.7) and (5.8) are similar to the model proposed by Singh (1964).

Thus, Eq. (5.8) is an improved version of the Nash (1959, 1960) and Bhunya et al. (2005) models and its time to peak (t_p) is given by:

$$t_p = T + \left(\frac{K_1 K_2}{K_2 + K_1} \right) \quad (5.9)$$

The peak flow rate can be expressed as:

$$Q_{(tp)} = \frac{1}{(K_1 - K_2)} \left[\exp\left\{ -\frac{K_2 \ln \frac{K_1}{K_2}}{(K_1 - K_2)} \right\} - \exp\left\{ -\frac{K_1 \ln \frac{K_1}{K_2}}{(K_1 - K_2)} \right\} \right] \quad (5.10)$$

Second hybrid unit

For extension to the second hybrid unit, consider two serially connected hybrid units, where the output from the first hybrid unit forms the variable input to the second hybrid

unit. The output from the second unit $Q_2(t)$ can be derived using convolution of variable output from the first unit with the unit impulse response function of the second unit using convolution theorem (Singh, 1988) as follows:

$$Q_2(t) = \int_0^t I(\tau)Q_1(t-\tau)d\tau \quad (5.11)$$

where $I(\tau)$ = variable inputs to the second unit or variable outputs from the first unit; $Q_1(t-\tau)$ = unit impulse response function for variable 't' or unit impulse response function of the first unit, which equals $Q_1(t-\tau)$ if storage coefficients are identical; and τ = a dummy time variable. The Laplace transform of Eq. (5.11) can be expressed as (Singh, 1988):

$$Q_2(s) = I(s) Q_1(s) \quad (5.12)$$

where $I(s)$ is Laplace transform of the variable input to the second unit. The output from the second hybrid unit can be given as:

$$Q_2(t) = \frac{1}{(K_1 - K_2)^2} \left\{ e^{-\frac{(t-2T)}{K_1}} \left[t - 2 \left(T + \frac{K_1 K_2}{(K_1 - K_2)} \right) \right] + e^{-\frac{(t-2T)}{K_2}} \left[t - 2 \left(T - \frac{K_1 K_2}{(K_1 - K_2)} \right) \right] \right\} \quad (5.13)$$

for $t \geq 2T$
otherwise

= 0

Mathematically Eq. (5.13) is an improved version of both Nash (1957, 1958) and Bhunya et al. (2005) models for two equal linear reservoirs and two hybrid units in series respectively, as shown below.

Nash Model [Eq. (5.13)]

On substituting $K_2 = 0$, $K_1 = K$, and $T = 0$ in Eq. (5.13) results

$$Q_2(t) = \frac{1}{K^2} e^{-\frac{t}{K}}(t) \quad (5.14)$$

Alternatively Eq. (5.14) can be expressed as:

$$Q_2(t) = \frac{1}{K\Gamma(2)} \left(\frac{t}{K} \right)^{2-1} e^{-\frac{t}{K}} \quad (5.15)$$

Eq. (5.15) is the Nash model for $n = 2$. Similarly, putting $T = 0$ in Eq. (5.13) and after little simplification, one obtains

$$Q_2(t) = \frac{1}{(K_1 - K_2)^2} \left[\left(te^{-\frac{t}{K_1}} + te^{-\frac{t}{K_2}} \right) - \frac{2K_1K_2}{(K_1 - K_2)} \left(e^{-\frac{t}{K_1}} - e^{-\frac{t}{K_2}} \right) \right] \quad (5.16)$$

where Eq. (5.16) is the expression of hybrid model (HM) (Eq. 2.56) for two hybrid units in series ($n = 2$). A more generalized form of the extended hybrid model (EHM) is presented here and its equivalence with the Nash model is discussed in Appendices C and D.

Eq. (5.13) represents the output response function for the second unit due to a unit impulse excitation at the inlet of the first unit. Its time to peak ($t_{p(2)}$) is given by

$$t_{p(2)} = 2T + \frac{(K_1K_2)(K_1 + K_2)(K_1 - K_2)^2}{K_1^4 + K_2^4} \quad (5.17)$$

A similar expression for $Q_{p(2)}(t)$ in terms of K_1 and K_2 can be obtained by coupling Eqs. (5.13) and (5.17).

5.3 APPLICATION

The extended hybrid model (EHM) is applied to derive SUH taking data of five catchments (Table 3.2). The five catchments (small to medium) range from 21 km² to 452.25 km². Box and Jenkins (1970) and Quimpo (1967) stated that a *second order* model is often considered adequate to model the catchment behavior. Following Bhunya et al. (2005), It is conceptually more rational to use more than one hybrid unit (preferably two) than a fractional value for simulation of real data. Thus, consistent with the work of

Bhunya et al. (2005), during the course of analysis each catchment is simulated by two hybrid units.

5.3.1 Parameter Estimation

EHM consists of the parameters K_1 , K_2 , and T . In the present study, the values of first two parameters are evaluated first and then these are used to evaluate T using a trial and error approach. The detail procedure is given as follows:

Step(I)

The first step is based on the Buckingham π theorem and random number generation procedure. It provides fairly accurate estimates of the parameters. The three nondimensional groups α , β , and λ are formed, taking q_p , t_p , K_1 , and K_2 , as variables, and L and T as repeating variables, as follows:

$$\alpha = \frac{K_2}{K_1} \quad (5.18)$$

$$\beta = q_p t_p \quad (5.19)$$

$$\lambda = \frac{t_p}{K_2} \quad (5.20)$$

where β is the form factor that quantifies the hydrograph peakedness or, in turn, the index showing the shape of the hydrograph, α , is related with the storage index; and λ reflects the positive and negative skewedness of the hydrograph. Finally, the empirical relationships for K_1 and K_2 estimation are given by (Bhunya et al., 2005):

$$K_2 = \frac{\beta t_p}{9.4452(\beta)^3 - 8.2173(\beta)^2 + 4.306(\beta) - 0.4466} \quad (5.21)$$

$$K_1 = \frac{K_2}{-0.2073(\lambda)^3 + 1.772(\lambda)^2 - 5.2535(\lambda) + 7.1051} \quad (5.22)$$

Thus, from the known values of q_p [1/hr] and t_p [hr] corresponding to an observed UH for a catchment, the parameters 'K₁' and 'K₂' can be estimated by Eqs. (5.18)- (5.22). Further, the estimated values of K₁ and K₂ were substituted into Eq. (5.17) to get an approximated value of 'T' for the study catchments due to a particular storm event considered.

Step (II)

The K₁, K₂, and T parameters estimated in the first step were substituted into the extended hybrid model (EHM) (Eq. 5.13) and hybrid model (HM) (Eq. 5.16) to obtain UH. Here, the ordinates of EHM for the condition $t \leq nT$ were always negative. Similar to Singh (1964), first of all a trial and error T-value was selected to derive the ordinates of the proposed model. Since 'q_p' and 't_p' are salient points of UH, the time to peak and peak flow rate due to both the models were matched by trial and error, and the results are given in Table 5.1. Furthermore, the estimated values of T, K₁, and K₂ are considered to be satisfactory if (i) the peak flow rate, q_p, of the observed UH approximates the computed value; (ii) the times to peak, t_p, of the observed and estimated UHs are more or less the same; and (iii) the fit of the observed and estimated UHs is satisfactory (Singh, 1964). It is observed from Table 5.1 that the empirical method proposed by Bhunya et al. (2005) for estimating the parameters (K₁ and K₂) of HM is equally applicable for estimating parameters of EHM, and provides a unique base for selecting the most appropriate values of K₁, K₂, and T for both the models. It may be argued that another set of T, K₁, and K₂ values might yield a comparable fit of the UHs.

5.4 DISCUSSION OF RESULTS

First of all, the parameters of EHM and HM were estimated using both the approaches and using the data of five catchments (Table 3.2). Then the estimated unit hydrographs were compared with the observed ones. The performances of the models were judged on the basis of visual appraisal and goodness of fit in terms of standard error

(STDER) and relative error (RE). A sensitivity analysis of EHM is then performed, in order to assess the dependability of the peak flow rate (Q_p) on the parameters T, K_1 , and K_2 as discussed in the following sections.

Table 5.1 Estimation of K_1 , K_2 and T parameters

Sl. No.	Catchment	Method of Bhunya et al. & Eq. (5.16) [Step I]			Trial & Error method [Step II]		
		K_1 (hr)	K_2 (hr)	T (hr)	K_1 (hr)	K_2 (hr)	T (hr)
1	Chaukhutia	0.374	0.601	0.462	0.252	0.599	0.119
2	Gormel Ermenek Creek	1.120	1.720	0.905	1.250	1.650	0.500
3	Bridge catchment no.253	0.947	1.35	0.442	1.15	1.36	0.110
4	Kothuwatari	0.250	0.540	0.450	0.275	0.480	0.050
5	Shanchuan	0.0585	0.110	0.116	0.063	0.099	0.005

5.4.1 Performance of the Models

The model performance was assessed on the basis of (i) visual agreement among the various hydrographic components i.e. rising segment, time to peak, peak flow rates, and recession segment of the unit hydrographs, and (ii) the goodness of fit between the unit hydrographs, in terms of standard error (STDER) and relative error (RE).

For visual assessment, the resulting UHs of both the models were compared with the observed UHs as illustrated in Figs. 5.2-5.6. These figures represent the agreement between the UHs in order of largest to smallest catchment areas. Fig. (5.2) shows the EHM to exhibit a closer agreement in the rising segment and peak flow rate of the UH than does the HM, but works poorly for the recession segment. However, as the catchment area decreases the HM closely matches the rising segment than the EHM does, and vice versa, for the recession segment (Figs. 5.3-5.6).

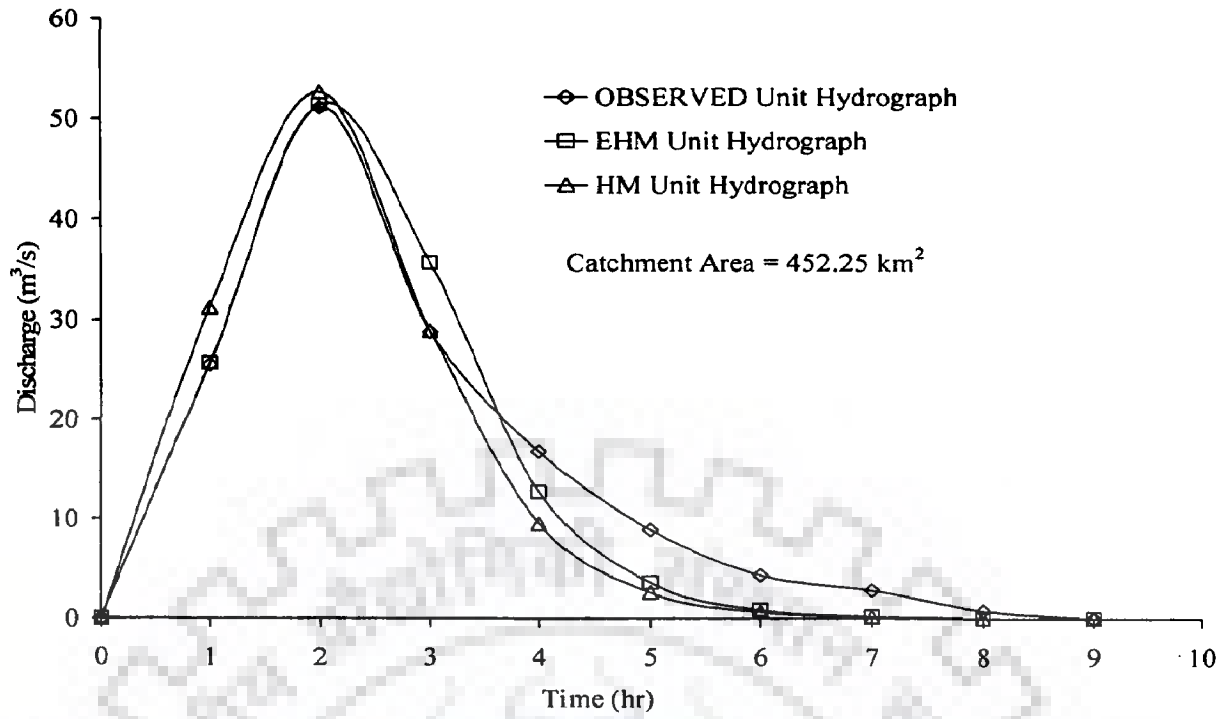


Fig. 5.2 Agreement between observed and estimated one-hour-unit hydrographs for Chaukhtia catchment

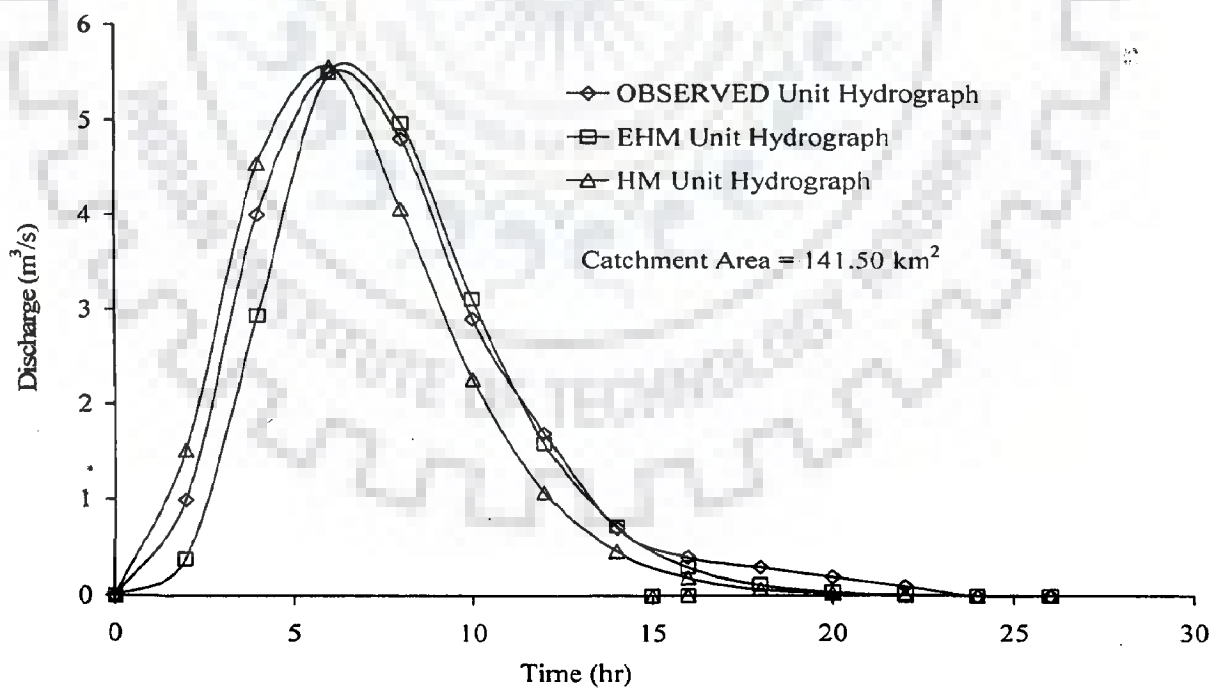


Fig. 5.3 Agreement between observed and estimated two-hour-unit hydrographs for Gormel Ermenek Creek catchment

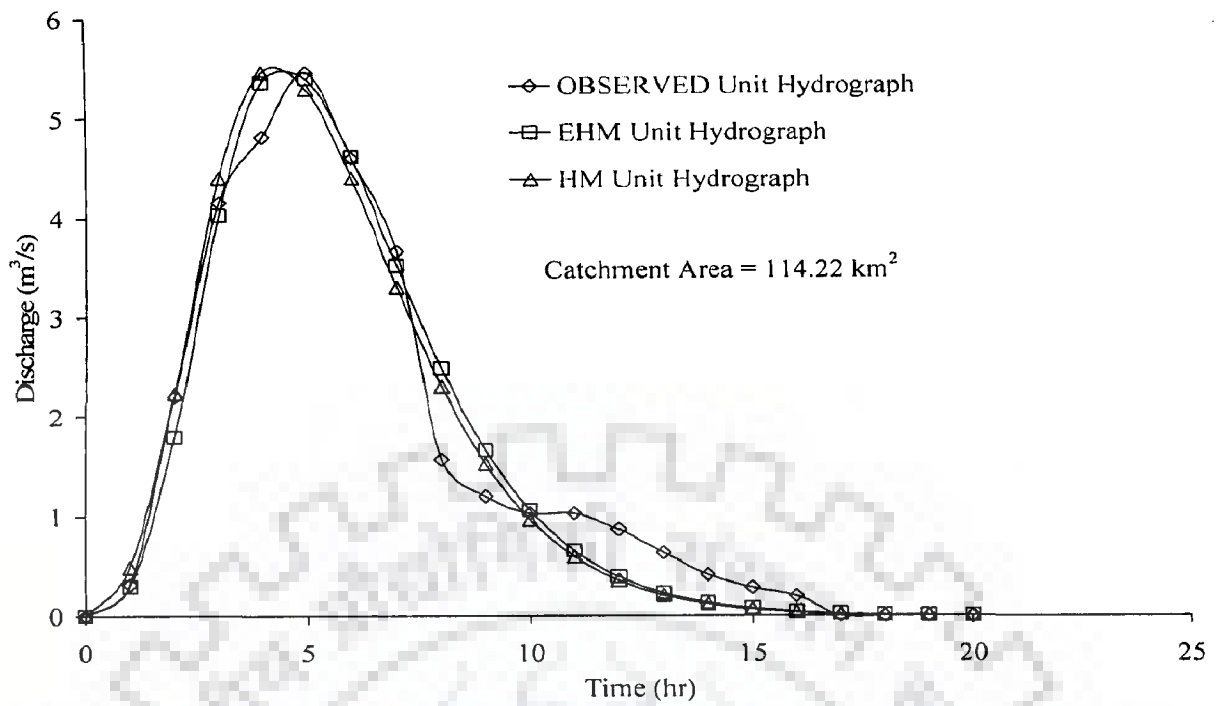


Fig. 5.4 Agreement between observed and estimated one-hour-unit hydrographs for Bridge catchment no. 253

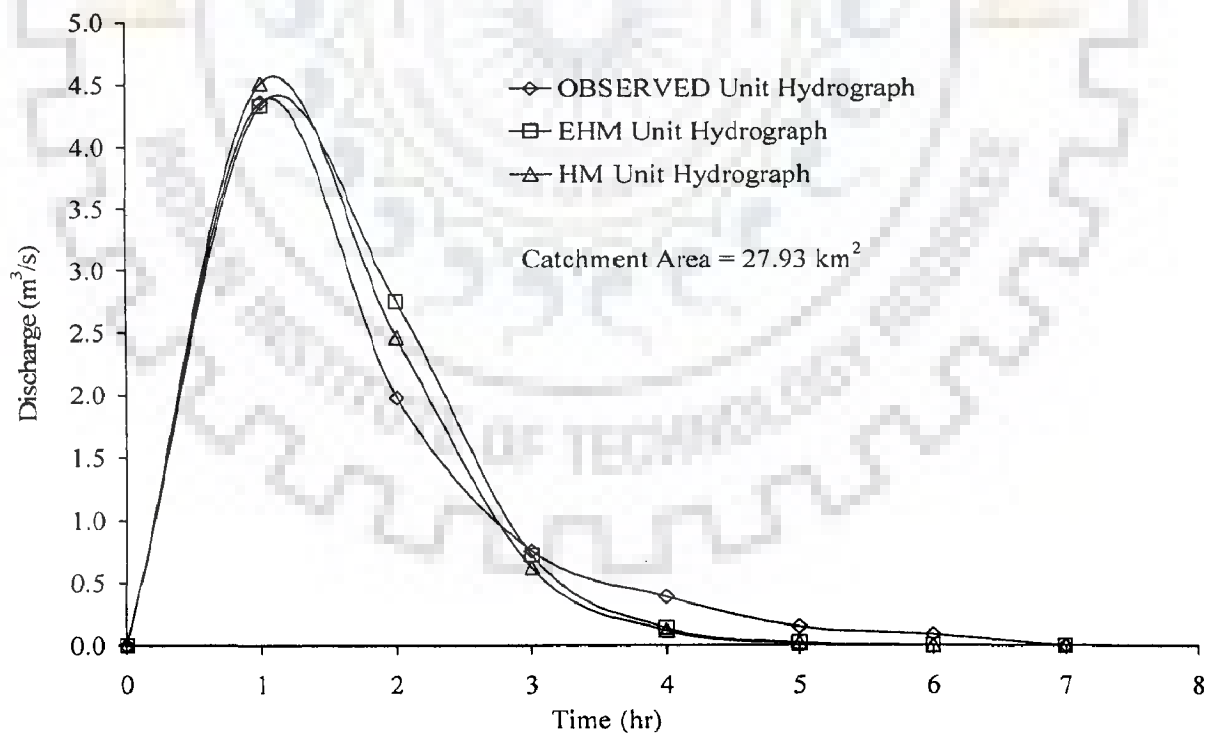


Fig. 5.5 Agreement between observed and estimated unit hydrographs for Kothuwatari watershed of Tilaiya dam catchment

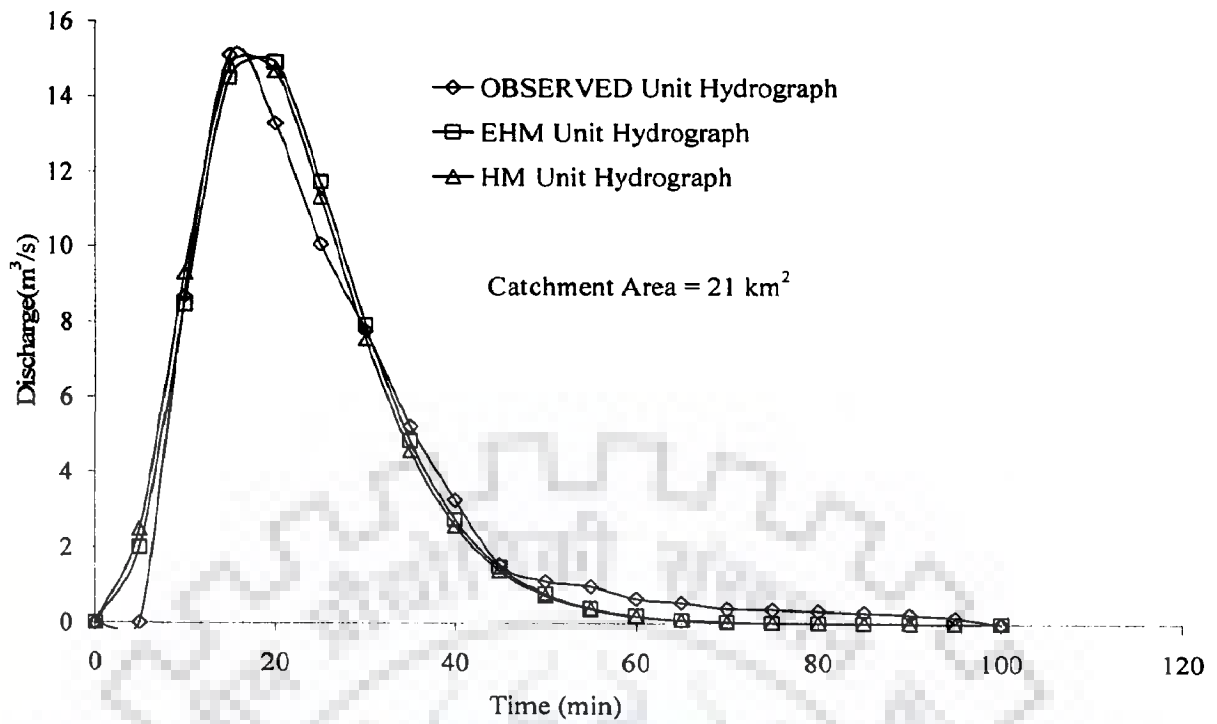


Fig. 5.6 Agreement between observed and estimated unit hydrographs for Shanchuan catchment

The goodness of fit in terms of standard error (STDER) (USACE, 1990) can be expressed as:

$$STDER = \left[\frac{\sum_{i=1}^N (Q_{oi} - Q_{ci})^2 w_i}{N} \right]^{\frac{1}{2}} \quad (5.23)$$

$$w_i = \frac{(Q_{oi} + Q_{av})}{2Q_{av}} \quad (5.24)$$

where w_i = weighted value of the i^{th} UH ordinate, Q_{oi} = i^{th} ordinate of the observed UH; Q_{ci} = i^{th} ordinate of the computed UH, and N = total number of UH ordinates. However, STDER is used only to compare the performance of two or more methods, and it does not indicate a good or bad/poor fit (Bhunya et al., 2005). Table 5.2 shows the STDER due to EHM and HM along with the variation of the difference in standard error (DSTDER) with the catchment area.

Table 5.2 Goodness of fit in terms of STDER

Sl. No.	Catchment	Area (km ²)	STDER		DSTDER
			EHM	HM	
1	Chaukhutia	452.25	3.56	3.95	-0.39
2	Gormel Ermenek Creek	142.00	0.42	0.46	-0.04
3	Bridge catchment no.253	114.22	0.34	0.35	-0.01
4	Kothuwatari	27.93	0.35	0.25	0.10
5	Shanchuan	21.00	0.44	0.82	0.06

It can be inferred from Table 5.2 that the STDER for EHM is less than that due to HM as the catchment area increases, and vice versa. This trend shows that EHM performs better than HM as the catchment area increases and vice versa, indicating the significance of incorporating translation in the EHM. However, EHM as well as HM results in higher STDER for the largest and the smallest catchments, e.g. for the Chaukhutia catchment (area = 452.25 km²), STDER = 3.56 and 3.95, respectively; and for Shanchuan catchment (area = 21 km²), STDER = 0.88 and 0.82 respectively. The variation of DSTDERs with the catchment area due to both the models is shown in Fig. (5.7) to further assess the variation in the model performance with catchment area, where DSTDERs ranges from -0.39 (for Chaukhutia catchment, area = 452.25 km²) to 0.06 (for Shanchuan catchment, area = 21 km²). It is observed from Fig. (5.7) that the DSTDER increases negatively with an increase in catchment area. This reflects that (i) as the catchment area increases, STDER due to both the models will be higher; and (ii) the STDER due to the EHM will be lower than the HM, showing performance of the EHM better than the HM.

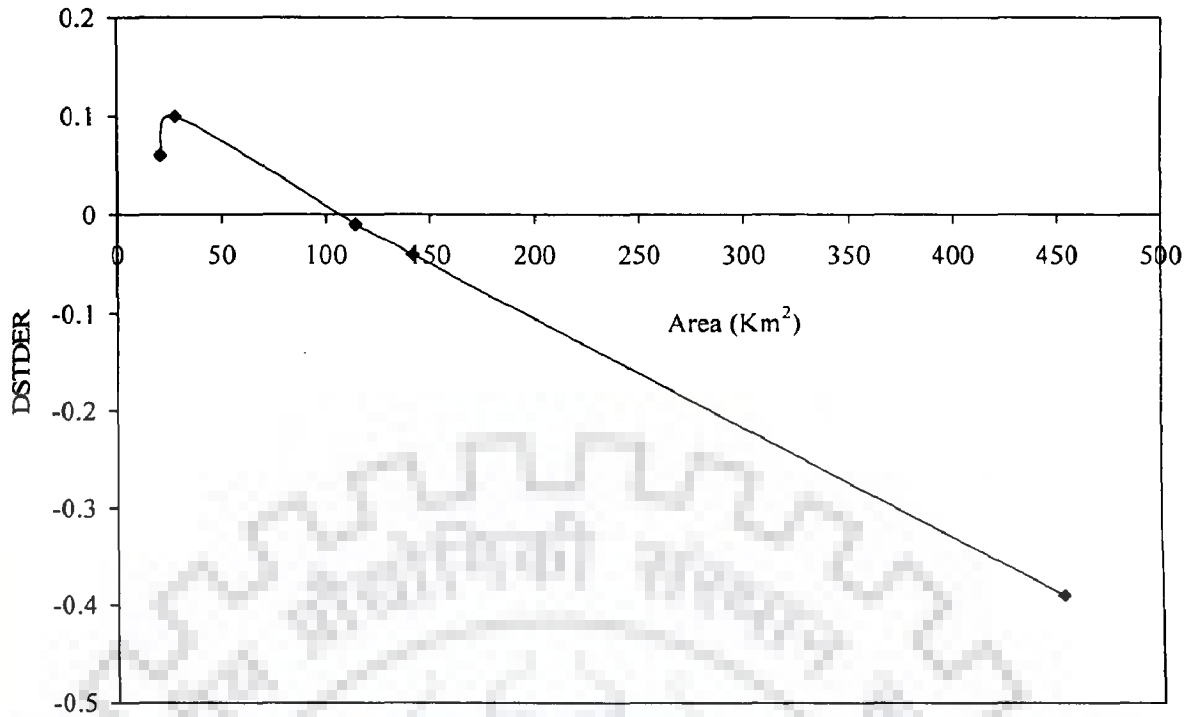


Fig. 5.7 Variation of DSTDER with catchment area

Further, the relative error (RE) can be expressed as:

$$RE (\%) = \frac{Q_{p[OBS]} - Q_{p[COM]}}{Q_{p[OBS]}} \times 100 \quad (5.25)$$

where $Q_{p[OBS]}$ = peak flow rate of the observed unit hydrograph (m^3/s), $Q_{p[COM]}$ ($Q_{p[EHM]}$ or $Q_{p[HM]}$) = peak flow rate of the estimated unit hydrograph (m^3/s). Table 5.3 shows the observed, estimated peak flow rates and corresponding RE in peak flow rates for the two methods, and Fig. 5.8 compares the estimated and observed peak flow rates. It is observed from Table 5.3 that the relative error in peak flow rate due to EHM ($RE = -0.491$) is less than the relative error due to HM ($RE = -2.948$) for the largest catchment (Chaukhutia catchment, area = 452.25 km^2), showing EHM estimates the peak flow rate better than HM. However, both the models have negative REs, i.e. both models overestimate the peak flow rates. Similarly, for the smallest catchment (Shanchuan catchment, area = 21 km^2), RE due to HM is less than RE due to EHM, showing HM performs better than

EHM. However, in this case, both the models underestimate the peak flow rates. Fig. 5.9 shows the variation of relative errors in peak flow rates due to both models with the catchment area. It is observed that with increase in catchment area beyond 150 km², RE due to EHM is less than RE due to HM. This shows that EHM underestimates lesser than HM with the increase in catchment area, and vice versa.

Table 5.3. Goodness of fit in terms of RE (%)

Sl. No.	Catchment	Area (km ²)	Q _p [OBS] (m ³ /s)	Q _p [EHM] (m ³ /s)	Q _p [HM] (m ³ /s)	RE _[EHM]	RE _[HM]
1	Chaukhutia	452.25	51.13	51.38	52.64	-0.491	-2.948
2	Gormel Ermenek Creek	142.00	5.48	5.48	5.56	0.00	-1.530
3	Bridge catchment no.253	114.22	5.46	5.39	5.46	1.163	0.000
4	Kothuwatari	27.93	4.34	4.33	4.52	0.357	-3.929
5	Shanchuan	21.00	15.05	14.35	14.70	4.651	2.326

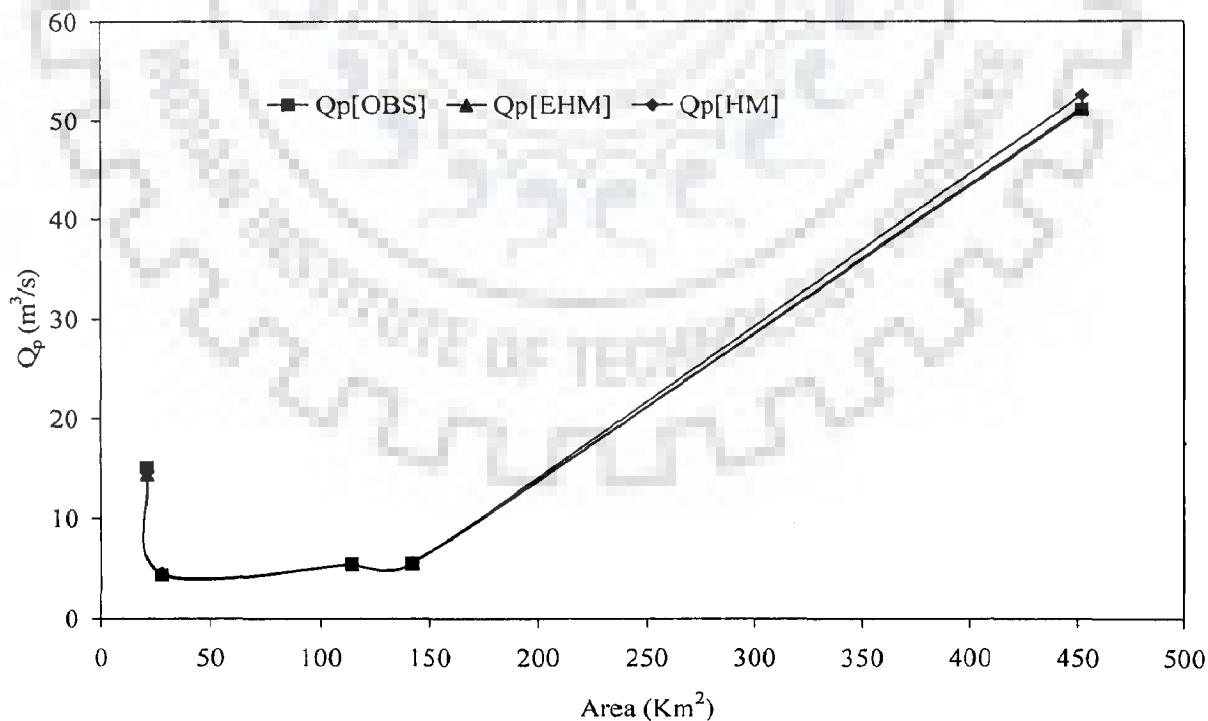


Fig. 5.8 Agreement between observed and estimated peak flow rates

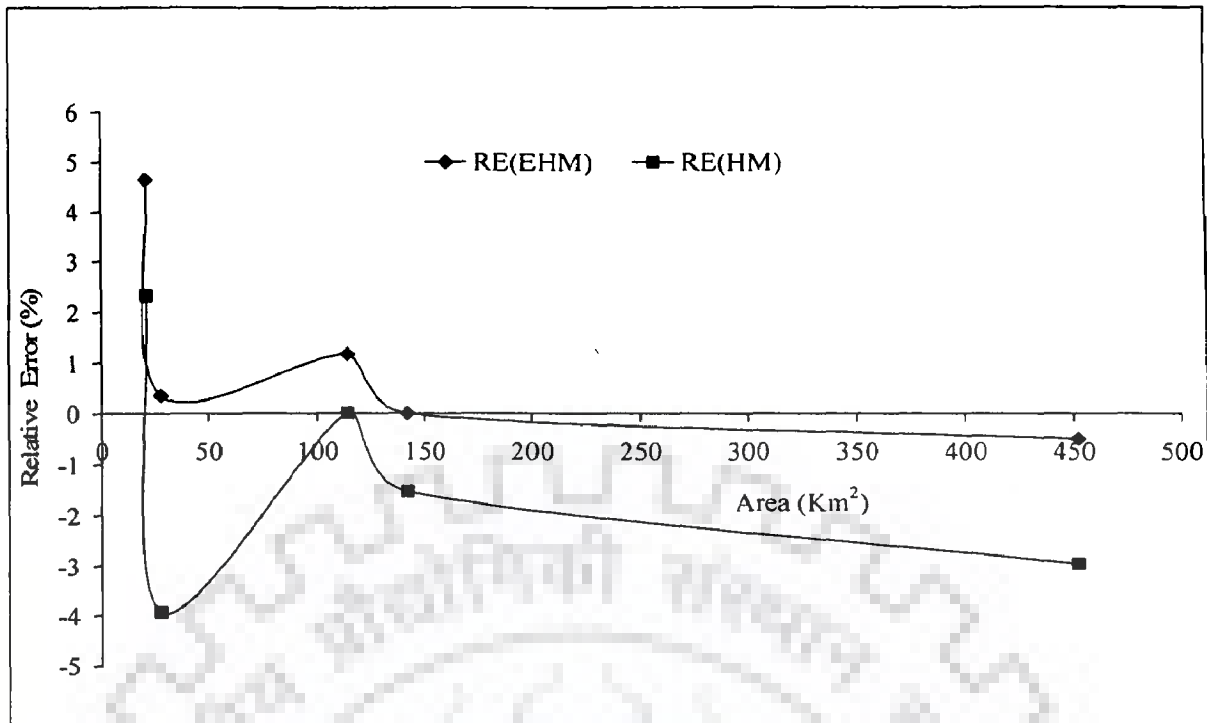


Fig. 5.9 Variation of relative error in peak flow rates with catchment area

5.4.2 Sensitivity Analysis

A sensitivity analysis was carried out for the parameters influencing the Q_p estimation, viz., T , K_1 and K_2 . While performing the sensitivity analysis, all the parameters were varied in a definite ratio (i.e. decreasing the parameters by 10%, 20%, 30%, and 40% to its estimated values). This percent variation is randomly chosen and any other variation could have been opted. The results of sensitivity analysis for the parameters T , K_1 and K_2 vs Q_p are listed in Tables 5.4 to 5.6. Where T_1 , T_2 , T_3 , and T_4 ; K_{11} , K_{12} , K_{13} , and K_{14} ; and K_{21} , K_{22} , K_{23} , and K_{24} are the values of the parameters T , K_1 and K_2 corresponding to 10%, 20%, 30% and 40% decrease in their estimated values, respectively. It is observed from Table 5.4 that Q_p - T plot falls sharply for catchments with smaller area rather than the large catchments. This may be attributed to the fact that translational component adds to the channel routing which was not considered in the Nash model. Thus the channel routing decreases the peak value or flattens the unit hydrograph. It appears that the channel routing is more effective in smaller catchments, and vice versa. It is observed from Tables 5.4 & 5.5 that for the same percent of variation

in the parameters T and K_1 , the percent variation in Q_p is more sensitive to K_1 . Similarly, it can be inferred from Tables 5.4, 5.5 & 5.6 that Q_p is sensitive to K_2 more than K_1 and T . Keeping K_1 and K_2 constant when T is increased, Q_p decreases up to a specific point in the graph (Fig. 5.10), and after the flat q_p - T line, it suddenly falls. It may also be inferred from Tables 5.5 & 5.6 that the estimated UHs become higher peaked as the values of K_1 and K_2 are decreased, consistent with the work of Singh (1964) that the UHs become higher peaked with decreasing K_2 .

Further, to justify the practical use of EHM and HM, these were compared with the Nash model (Eq. 2.54) for given q_p and t_p of a flood event. The Nash model parameters K and n were estimated by Eq. (2.66) and Eq. (2.76), respectively. When employed to the data of Gormel Ermenek Creek catchment, the Nash model underestimated the peak flow rates more than those due to EHM and HM, as seen in Fig. 5.11 depicting the resulting unit hydrographs. Based on the goodness-of-fit criteria of STDER and RE, for the Gormel Ermenek Creek application resulted, STDER equal to 0.42, 0.46, and 0.71, and RE equal to 0.00%, -1.53%, and 9.35% for EHM, HM and Nash models, respectively, indicating the EHM and HM to perform much better than the Nash model in UH derivation. In application to all other test catchments, similar results were obtained.

Table 5.4 Sensitivity of peak flow rate to translation

Sl. No.	Item	Catchments				
		Chaukhutia	G. Ermenek	B. C. no. 253	Kothuwatari	Shanchuan
1	(T, Q_p)	(0.119, 51.38)	(0.50, 5.48)	(0.10, 5.39)	(0.050, 4.33)	(0.005, 14.35)
2	(T_1, Q_{p1})	(0.107, 51.76)	(0.45, 5.42)	(0.09, 5.39)	(0.045, 4.35)	(0.004, 14.70)
3	(T_2, Q_{p2})	(0.095, 52.01)	(0.40, 5.56)	(0.08, 5.39)	(0.040, 4.38)	(0.0036, 14.7)
4	(T_3, Q_{p3})	(0.083, 52.26)	(0.35, 5.60)	(0.07, 5.39)	(0.035, 4.40)	(0.0031, 14.7)
5	(T_4, Q_{p4})	(0.071, 52.51)	(0.30, 5.64)	(0.06, 5.43)	(0.030, 4.42)	(0.0027, 14.7)

Table 5.5 Sensitivity of peak flow rate to K_1

Sl. No.	Item	Catchments				
		Chaukhutia	G. Ermenek	B. C. no. 253	Kothuwatari	Shanchuan
1	(K_1, Q_p)	(0.252, 51.38)	(1.250, 5.48)	(1.150, 5.39)	(0.275, 4.33)	(0.063, 14.35)
2	(K_{11}, Q_{p1})	(0.227, 52.76)	(1.125, 5.76)	(1.035, 5.68)	(0.248, 4.58)	(0.056, 15.40)
3	(K_{12}, Q_{p2})	(0.202, 54.02)	(1.000, 6.03)	(0.920, 6.03)	(0.220, 4.83)	(0.05, 16.10)
4	(K_{13}, Q_{p3})	(0.176, 55.15)	(0.875, 6.27)	(0.805, 6.31)	(0.193, 5.05)	(0.044, 16.80)
5	(K_{14}, Q_{p4})	(0.151, 56.15)	(0.750, 6.43)	(0.690, 6.54)	(0.165, 5.23)	(0.038, 17.50)

Table 5.6 Sensitivity of peak flow rate to K_2

Sl. No.	Item	Catchments				
		Chaukhutia	G. Ermenek	B. C. No. 253	Kothuwatari	Shanchuan
1	(K_2, Q_p)	(0.559, 51.38)	(1.65, 5.48)	(1.355, 5.39)	(0.480, 4.33)	(0.099, 14.35)
2	(K_{21}, Q_{p1})	(0.5031, 56.66)	(1.485, 5.88)	(1.2195, 5.74)	(0.432, 4.76)	(0.089, 15.75)
3	(K_{22}, Q_{p2})	(0.4472, 57.41)	(1.320, 6.23)	(1.084, 6.16)	(0.384, 5.21)	(0.079, 17.15)
4	(K_{23}, Q_{p3})	(0.3913, 62.69)	(1.115, 6.59)	(0.9485, 6.50)	(0.336, 5.68)	(0.070, 18.55)
5	(K_{24}, Q_{p4})	(0.3354, 65.45)	(0.990, 6.86)	(0.813, 6.82)	(0.288, 6.14)	(0.060, 19.95)

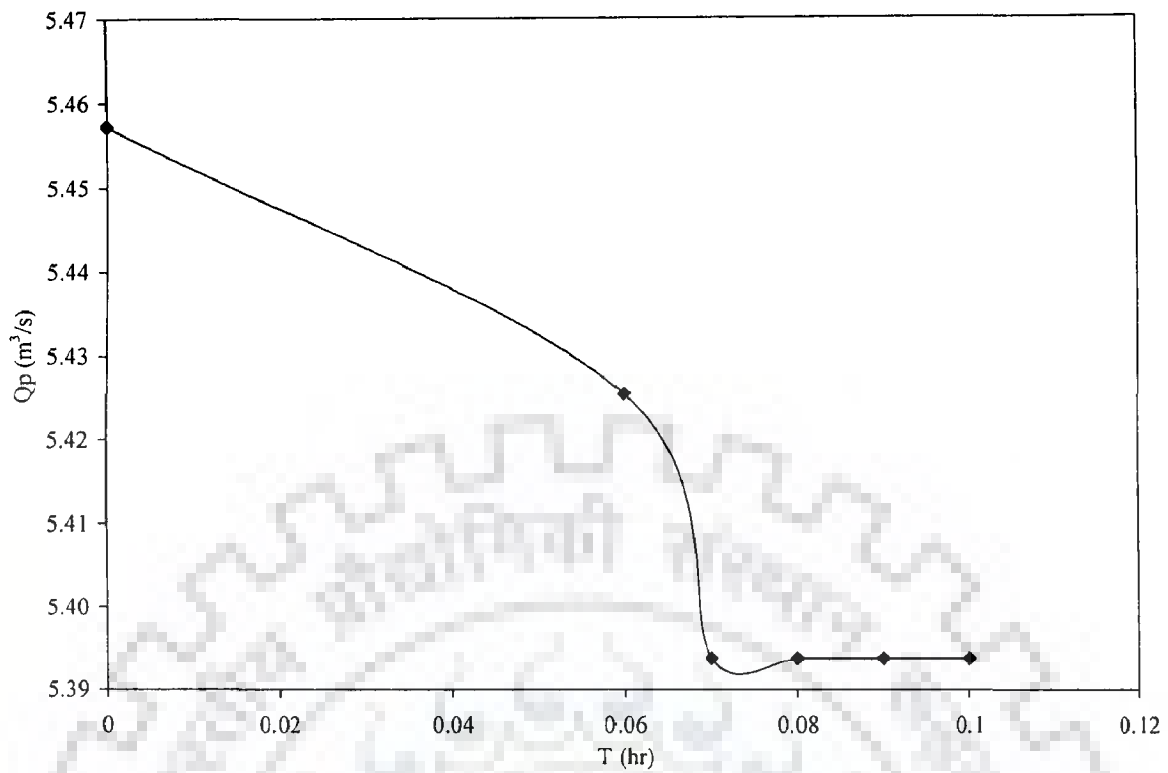


Fig. 5.10 Sensitivity of peak flow rates with translation

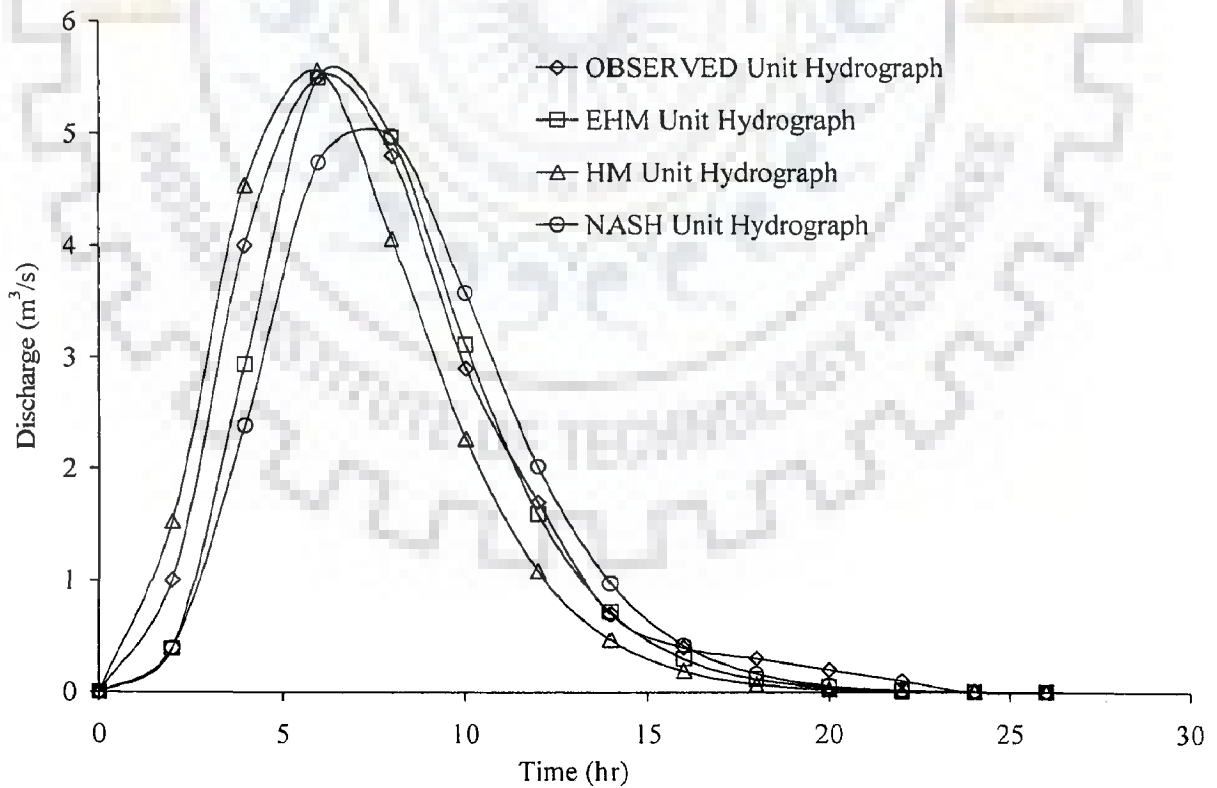


Fig.5.11 Agreement between observed and estimated two-hour-unit hydrographs for Gormel Ermenek Creek catchment

5.5 SUMMARY

In the present chapter, a conceptually sound and theoretically improved extended hybrid model (EHM) was proposed. The model considered (i) the cascaded approach of Nash (1957) and (ii) the hybrid approach of Bhunya et al. (2005). EHM is a generalized form of the Cascaded (Nash, 1957) and Hybrid (Bhunya et al., 2005) models. This shows that EHM is an improvement over the existing models such as Nash (1957) and Bhunya et al. (2005). The study generally revealed that the quantitative performance of the extended hybrid model (EHM) in terms of STDER and RE enhanced the hybrid model (HM) as the size of the catchments increased. However, regarding the peak flow rates (Q_p), both the models performed well. The study also revealed that the Nash model performed poorer than both EHM and HM. In sensitivity analysis, the peak flow rate was more sensitive to K_2 than either K_1 or T . In general, Q_p was less sensitive to translation for the smaller area, but more sensitive for the larger area; and more sensitive to both K_1 and K_2 than T (or $Q_p(K_2) > Q_p(K_1) > Q_p(T)$) for both smaller as well as larger areas.

CHAPTETR-6

CHI-SQUARE AND FRÉCHET DISTRIBUTIONS FOR SUH

DERIVATION

6.1 BACKGROUND

Various attempts have been made in the past to derive synthetic unit hydrograph (SUH) using the probability distribution functions (pdfs), as evident from chapter 2. In SUH derivation, one of the important steps is the estimation of one or two key points on UH (or IUH), through which the hydrograph is fitted. To achieve this objective, relationships are sought from the salient points of UH and selected catchment characteristics which can be measured from a topographic map, and generalized rainfall statistics. Further, linking of the salient points of the UH to the catchment characteristics provides a scientific basis for the hydrograph fitting to yield a smooth and single valued shape corresponding to unit runoff volume (Bhunya et al., 2007b).

The preferred technique for developing such relationships has invariably been multiple linear regression analysis (Hall et al., 2001). As discussed in chapter 2, Rosso (1984) parameterized the Nash model, which is a two-parameter gamma distribution (2PGD), using Horton order ratios. This chapter presents an extension of the earlier works in two ways: (i) it explores the potential of one-parameter Chi-square and the two-parameter Fréchet distributions for fitting UH, which has not been attempted in the past, where an analytical approach is followed to estimate the distribution parameters; (ii) the UH parameters, viz., peak discharge, time to peak, etc. are accomplished using Horton order ratios given by Rodriguez-Iturbe and Valdes (1979); (iii) it examines the similarity in behavior of parameters between the three distributions as SUH; and (iv) the workability of this approach in SUH derivation is demonstrated using data of two Indian catchments; and the results are compared with the existing Gamma synthetic method of Rosso (1984).

6.2 STATISTICAL DISTRIBUTIONS

6.2.1 One-Parameter Chi-Square Distribution

The one-parameter Chi-square distribution (CSD) (Fig. 6.1) is a special case of gamma distribution, and the pdf is given as (Montgomery and Runger, 1994):

$$h(t) = \frac{1}{2^{b/2} \Gamma(b/2)} t^{b/2-1} e^{-t/2} \quad \text{for } b > 0, t > 0 \quad (6.1)$$

The mean and variance are given by

$$\mu = b \text{ and } \sigma^2 = 2b \quad (6.2)$$

The salient properties of the Chi-square distribution are:

- (i) It is skewed to the right and its random variate is non-negative (Fig.1); as b tends to infinity, it approaches the normal distribution.
- (ii) $h(t) = 0$ at $t = 0$ and $h(t) \approx 0$ as $t \rightarrow \infty$.

- (iii) $\int_0^{\infty} h(t) dt = 1$

which makes this distribution fit for describing a UH shape.

In spite of its resemblance to the gamma pdf, the distribution was considered in this study because estimating a single parameter of the Chi-square distribution is simple and should involve less error compared to estimates of two parameters of the gamma distribution (Bhunya et al., 2007a).

Taking $\tau = b/2$, the form of the Chi-square distribution of Eq. (6.1) can be written as:

$$q(t) = \frac{1}{2^{\tau} \Gamma(\tau)} t^{\tau-1} e^{-\frac{t}{2}} \quad (6.3)$$

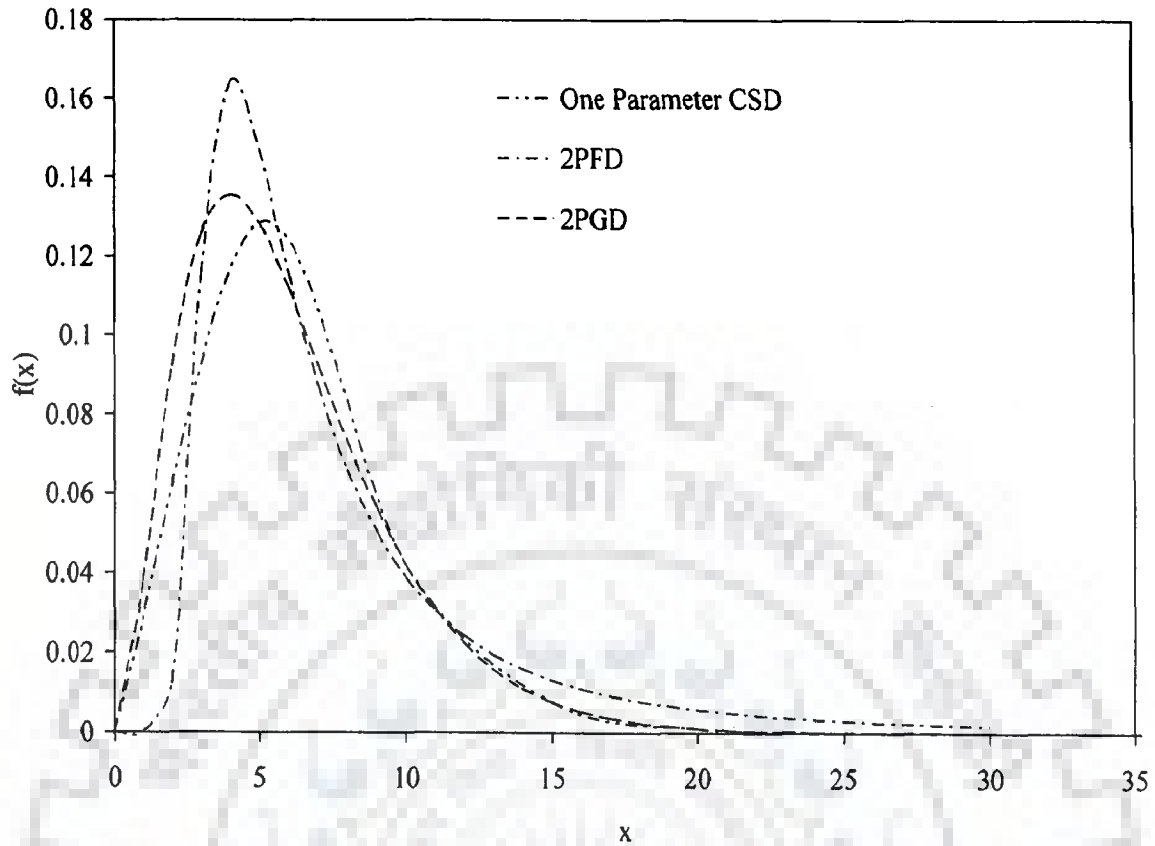


Fig. 6.1 pdf shapes for of One-parameter Chi-square distribution (CSD) ($\tau = 3$) and Two-parameter Fréchet distribution (2PFD) ($c = 2, \alpha = 5$), and Two parameter Gamma distribution (2PGD) ($n = 3, K = 2$)

Simplification of Eq. (6.3) at peak condition yields

$$t_p = 2(\tau - 1); \quad q_p t_p = \frac{(\tau - 1)^\tau e^{-(\tau - 1)}}{\Gamma(\tau)} \quad (6.4a)$$

A substitution of $m = \tau - 1$ yields

$$q_p t_p = \frac{m^{m+1} e^{-m}}{\Gamma(m+1)} \quad (6.4b)$$

Further, simplification to Eq. (6.4b) yields

$$q_p t_p = \frac{m^m e^{-m}}{\Gamma(m)} \quad (6.4c)$$

Defining the non dimensional term $\beta = q_p t_p$, Eq. (6.4c) reduces to

$$\beta = \frac{m^m e^{-m}}{\Gamma(m)} \quad (6.4d)$$

Solution of this can be approximately given as (Appendix E):

$$m = \pi\beta^2 \pm \beta\sqrt{(\pi^2\beta^2 + \pi/3)} \quad (6.4e)$$

Taking +ve sign only, Eq. (6.4e) reduces to

$$m = \pi\beta^2 + \beta\sqrt{(\pi^2\beta^2 + \pi/3)} \quad (6.5)$$

For given q_p and t_p , Eqs. (6.1) - (6.5) describe the complete shape of the SUH.

6.2.2 Two-Parameter Fréchet Distribution

The pdf of two-parameter Fréchet distribution (2PFD) (Fig. 6.1) is given as (Ayyub and McCuen, 1997):

$$f(x) = (c/\alpha)(\alpha/x)^{c+1} e^{-(\alpha/x)^c} \quad \text{for } x > 0 \quad (6.6)$$

The location parameter, $\alpha > 0$, and the shape parameter, $c > 0$.

The mean (μ) and variance (σ^2) for the distribution are, respectively, given by

$$\mu = \alpha \Gamma(1 - 1/c); \quad \sigma^2 = \alpha^2 [\Gamma(1 - 2/c) - \Gamma^2(1 - 1/c)] \quad (6.7)$$

and the cumulative distribution function (cdf) is given as:

$$F(x) = e^{-(\alpha/x)^c} \quad (6.8)$$

As $x \rightarrow \infty$, $F(x) = 1$. This condition meets the criterion for UH description (Sherman, 1932). Taking Fréchet distribution pdf (Eq. 6.6) as the discharge ordinates $q(t)$ of UH and x as time t , one gets

$$q(t) = (c/\alpha)(\alpha/t)^{c+1} e^{-(\alpha/t)^c} \quad \text{for } t > 0 \quad (6.9)$$

Now applying the condition at time to peak ($t = t_p$), $dq(t)/dt = 0$, one gets from Eq. (6.9) the following:

$$t_p = \alpha [c/(c+1)]^{1/c}; \quad \alpha = t_p \left(\frac{c+1}{c} \right)^{1/c}; \quad \text{and } q_p = (c/\alpha)(1+1/c)^{(1+1/c)} e^{-(1+1/c)} \quad (6.10 \text{ a, b, c})$$

Hence the nondimensional term β can simply be expressed as:

$$\beta = (1+c)e^{-(1+1/c)} \quad (6.11)$$

Since, for a given UH, the dimensionless factor β is always positive, the shape parameter of the Fréchet distribution is always greater than zero i.e. $c > 0$. On expanding the exponential term up to second order in Eq. (6.11), it simplifies to the following form:

$$c^3 + (1 - e\beta)c^2 - (e\beta)c - (e\beta)/2 = 0 \quad (6.12)$$

Following Abramowitz and Stegun (1964), the solution of Eq. (6.12) can be expressed as:

$$c = (u_1 + v_1) - A_1 / 3 \quad (6.13)$$

where A_1 , u_1 , and v_1 are the functions of β and are defined as follows:

$$A_1 = (1 - e \beta); B_1 = -e \beta; C_1 = -e \beta / 2, \text{ and } u_1 = \left[r_1 + (p_1^3 + r_1^2)^{1/2} \right]^{1/3}; v_1 = \left[r_1 - (p_1^3 + r_1^2)^{1/2} \right]^{1/3} \quad (6.14)$$

where $p_1 = B_1 / 3 - A_1^2 / 9$; $r_1 = (A_1 B_1 - 3 C_1) / 6 - A_1^3 / 27$. Thus, parameter c of the 2PFD can be estimated using Eq. (6.13), and corresponding to this α parameter can be estimated from Eq. (6.10b) for a known value of t_p . Estimated parameters are substituted in Eq. (6.9) to get the complete shape of UH.

6.3 VALIDITY OF ANALYTICAL ESTIMATION METHODS

The validity of the analytical parameter estimation methods for the one-parameter CSD and 2PFD was further checked as follows.

6.3.1 One-Parameter Chi-square Distribution

For one parameter CSD the validation test procedure is as follows:

- (i) Using random number generation scheme the parameter m was generated and corresponding τ is calculated as $\tau = m + 1$.
- (ii) Corresponding β for the value of m (or τ) obtained at (i) was estimated by Eq. (6.4d). These values of τ and β are the actual values.
- (iii) The β -values estimated at (ii) are used in Eq. (6.5) to get the corresponding values of m and then τ . These are the estimated values of τ .

For this experiment, m was generated using random number generation such that the corresponding β does not exceed 1.25 (as β varies from 0.35 to 1.25 (Singh, 2000)). Further, it is noted here that β -values less than 0.01 are seldom experienced in field and the maximum value is rarely found to be greater than one (Bhunya et al., 2004). The results of actual and computed values of τ are given in Table 6.1 and plotted in Fig. 6.2a, and a best-fit-line is fitted to the scatter plot to test the degree of resemblance. The regression coefficient, $R^2 = 0.9982$ indicates the high accuracy of the analytical parameter estimation method.

6.3.2 Two-Parameter Fréchet Distribution

In a similar way, for the 2PFD, the parameter c was generated using random number scheme and the corresponding β from Eq. (6.11). Corresponding to this β , the parameter c was computed analytically using Eq. (6.13) and the results are given in Table 6.2 and plotted in Figure 6.2b for which $R^2 = 0.999$. Since the value of t_p is a pre-requisite to compute α , its validity is checked taking arbitrarily $t_p = 1$ hour from Eq. (6.10b). The results are reported in Table 6.2, and plotted in Fig. 6.2c. The best fit line yields, $R^2 = 0.9980$, inferring that the proposed analytical method for 2PFD is quite suitable for parameter estimation.

6.4 SENSITIVITY OF DISTRIBUTION PARAMETERS

Since the dimensionless parameter $\beta (= q_p t_p)$ is one of the most important characteristics of a given UH, as it bears two most important flood characteristics, i.e. q_p and t_p of the UH. Hence, the sensitivity of β was examined with respect to the distribution parameters of CSD and 2PFD by evaluating the partial derivatives of β , i.e. $\partial\beta/\partial m$, or $\partial\beta/\partial\tau$, $\partial\beta/\partial c$, $\partial\beta/\partial\alpha$, for CSD and 2PFD, respectively, as follows.

6.4.1 One-Parameter Chi-square Distribution

Expression of $\partial\beta/\partial m$ for the CSD can be derived as:

Table 6.1 Validity of Analytical method for computing m or τ of one parameter Chi-square distribution

Actual m	Actual τ	β	Estimated m	Estimated τ	Error in m (%)	Error in τ (%)
0.916	1.916	0.35	0.91	1.91	0.87	0.42
1.288	2.288	0.43	1.28	2.28	0.54	0.31
1.428	2.428	0.45	1.42	2.42	0.49	0.29
2.065	3.065	0.55	2.06	3.06	0.24	0.16
3.245	4.245	0.70	3.24	4.24	0.15	0.12
4.705	5.705	0.85	4.70	5.70	0.09	0.07
6.445	7.445	1.00	6.44	7.44	0.08	0.07

Note: Error (%) = [(Actual value-Estimated Value)/Actual value]*100

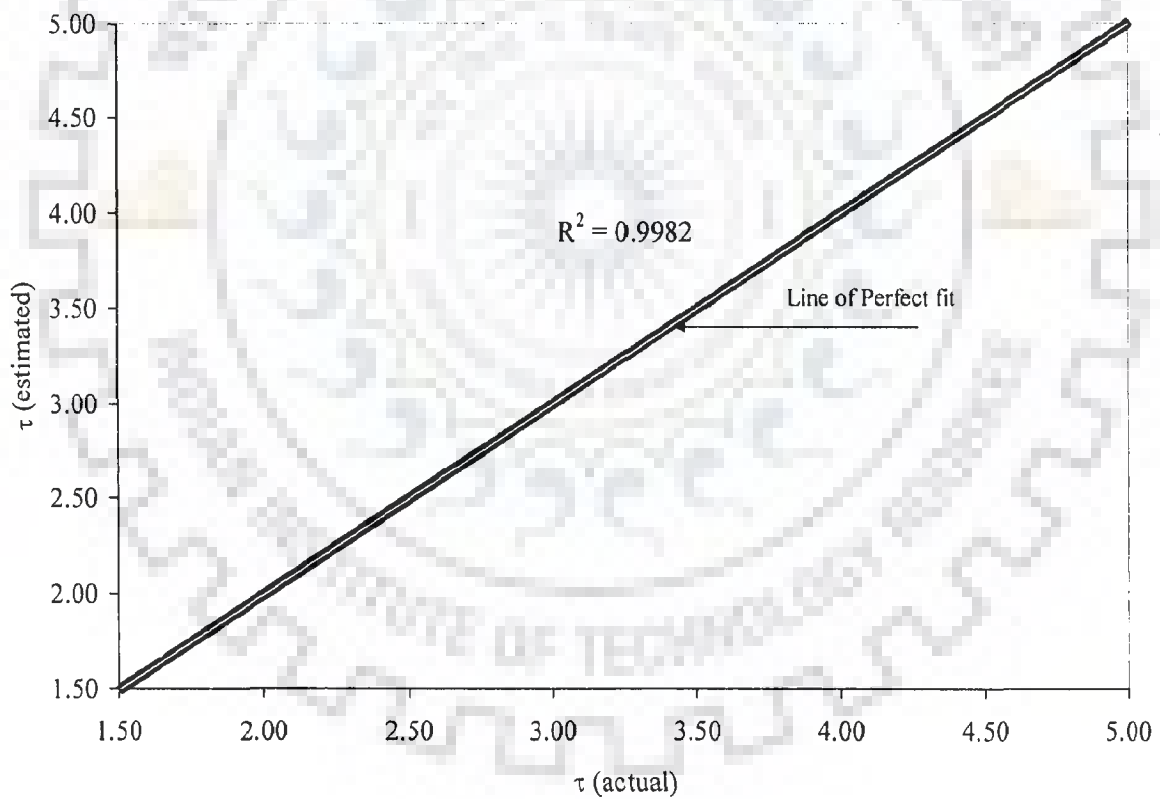


Fig. 6.2a. Best-fit-line between estimated and actual τ of one parameter CSD

Table 6.2 Validity of Analytical method for computing c and α of two parameter Fréchet distribution

Actual c	Actual α	β	Estimated c	Estimated α	Error in c (%)	Error in α (%)
1.25	1.60	0.372	1.20	1.65	3.84	-3.40
1.40	1.47	0.432	1.36	1.50	2.98	-2.14
1.60	1.35	0.512	1.57	1.37	2.19	-1.23
1.80	1.28	0.591	1.77	1.29	1.65	-0.75
2.05	1.21	0.689	2.03	1.22	1.20	-0.43
2.40	1.16	0.825	2.38	1.16	0.81	-0.22
2.60	1.13	0.900	2.58	1.14	0.66	-0.15
3.00	1.10	1.050	2.99	1.10	0.47	-0.08

Note: Error (%) = $[(\text{Actual value} - \text{Estimated Value}) / \text{Actual value}] * 100$

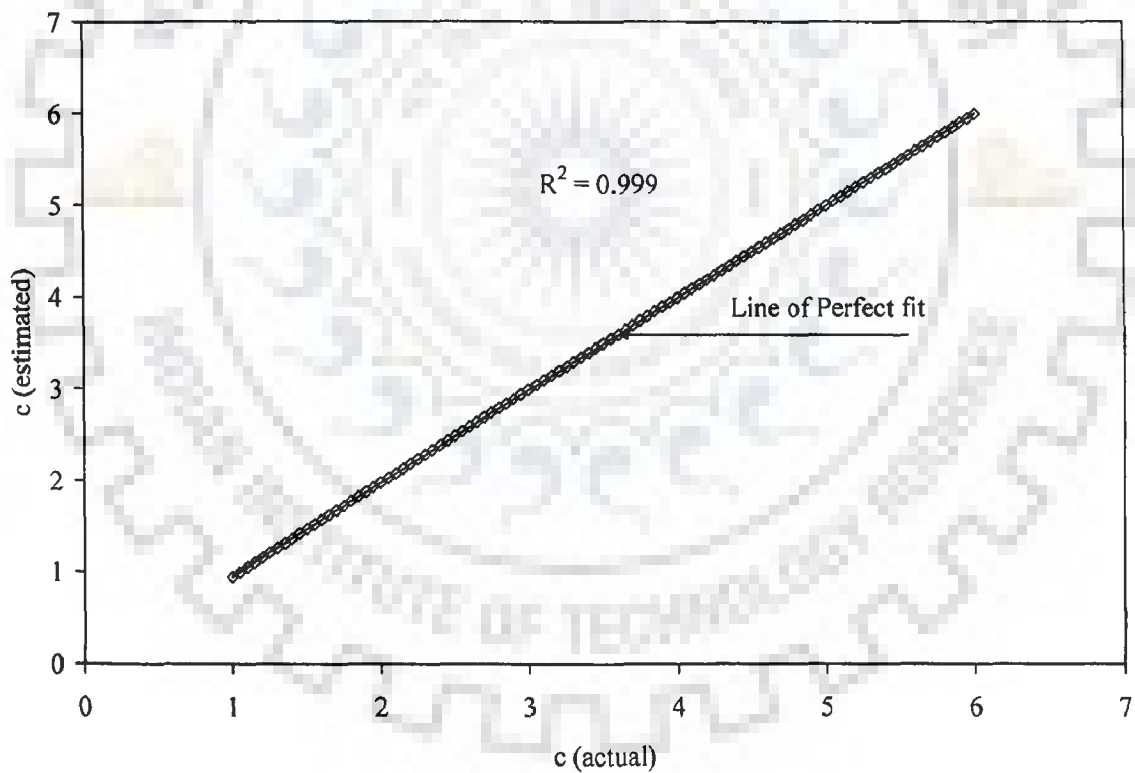


Fig. 6.2b Best-fit-line between estimated and actual c of 2PFD

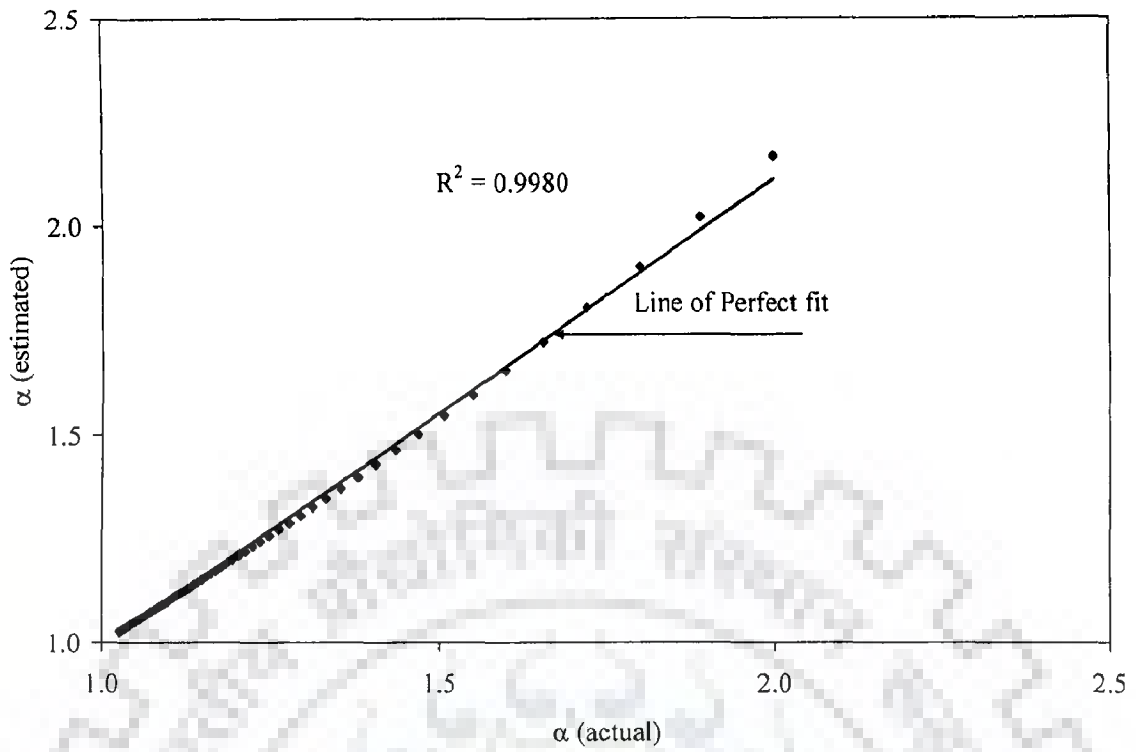


Fig. 6.2c Best-fit-line between estimated and actual α of 2PFD

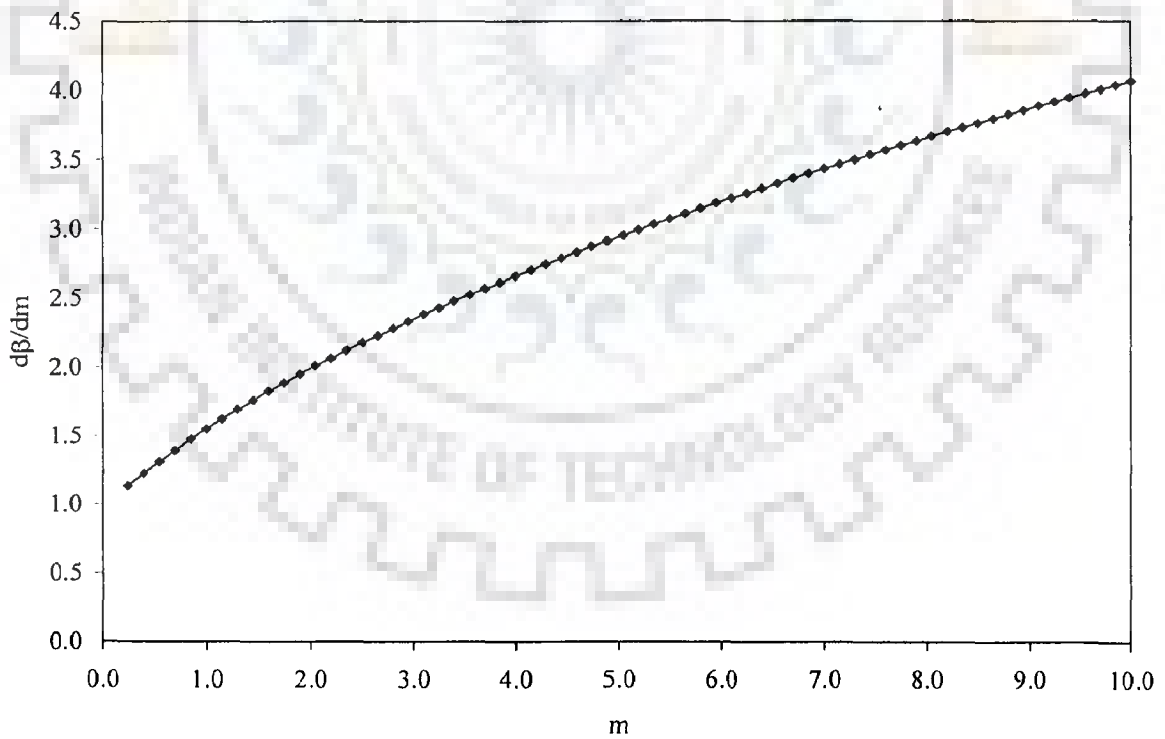


Fig. 6.3a Sensitivity to parameter m of one parameter CSD

$$\partial\beta / \partial m = \frac{m\pi + \pi/3}{\sqrt{(2\pi m + \pi/3)}} \quad (6.15)$$

Fig. 6.3a shows the variation of $\partial\beta / \partial m$ versus m . It can be observed from Fig. 6.3a that any increase in m (or τ) increases the rate of change of β , and vice versa.

6.4.2 Two-Parameter Fréchet Distribution

For 2PFD, the expressions for $\partial\beta / \partial c$ and $\partial\beta / \partial \alpha$ can be expressed as:

$$\partial\beta / \partial c = e^{-(1+1/c)} [(c^2 + c + 1)/c^2] \quad (6.16)$$

$$\partial\beta / \partial \alpha = (\partial\beta / \partial c)(\partial c / \partial \alpha) = -[(c^2 + c + 1)e^{-(1+1/c)}] / (1+1/c)^{1/e} [1/(1+c) + \ln(1+1/c)] \quad (6.17)$$

Figs. 6.3b & 6.3c show the variation of β with respect to c and α . Since α can be expressed in terms of c (Eq. 6.10b), the expression for $\partial\beta / \partial \alpha$ is also expressed in terms of c for simplicity reasons. As observed from Figs 6.3b & 6.3c, the non-dimensional parameter β is more sensitive to α than c .

6.5 SIMILARITY BETWEEN THE THREE DISTRIBUTIONS

Gamma distribution tends to a Chi-square distribution when $K = 2$ and n is equal to $1/2, 1, 3/2$, etc. In spite of resemblance to the Gamma distribution, the Chi-square distribution was considered in this study to compare its workability vis-à-vis Gamma method, when K and n differ from this special condition, i.e. $K \neq 2$ and $n \neq 1/2, 1, 3/2$. etc. Now comparing the 2PGD and 2PFD for peak flow condition i.e. when $(q_p)_{2PGD} = (q_p)_{2PFD}$, where $(q_p)_{2PGD}$ and $(q_p)_{2PFD}$ are the peak flow rates of 2PGD and 2PFD, respectively.

For 2PGD, the expression for (q_p) can be derived from Eq. (2.67) by coupling it with Eq. (2.66), as below:

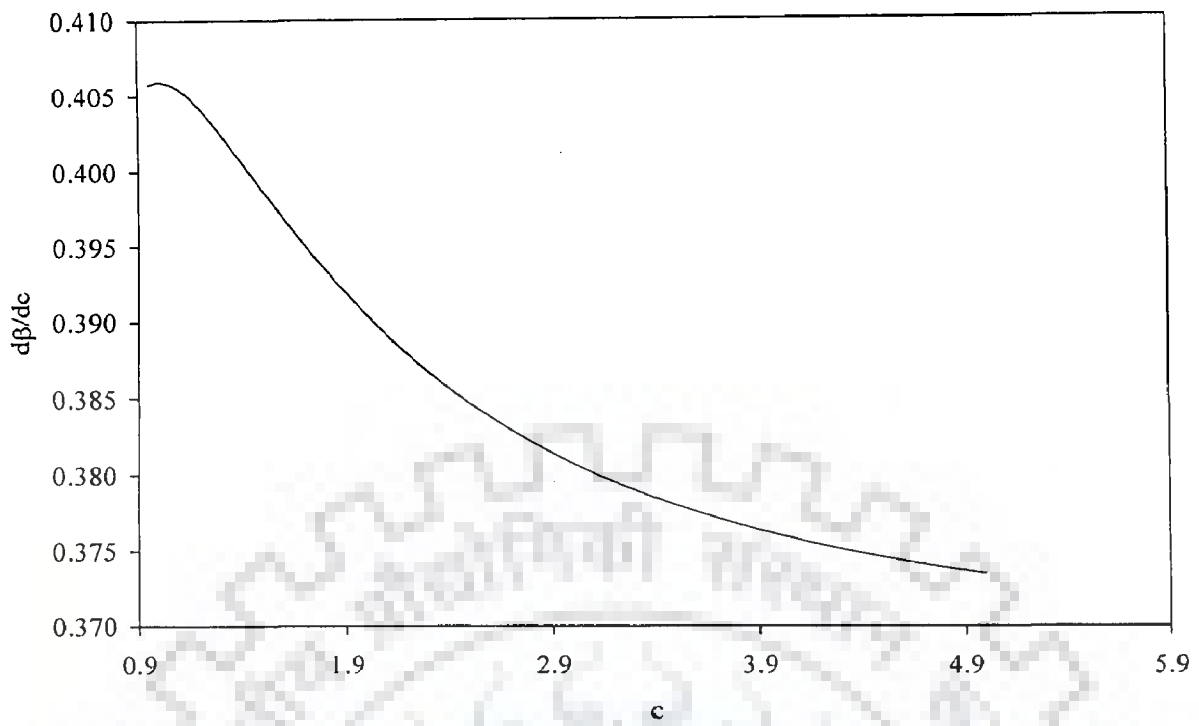


Fig. 6.3b Sensitivity to parameter c of 2PFDF

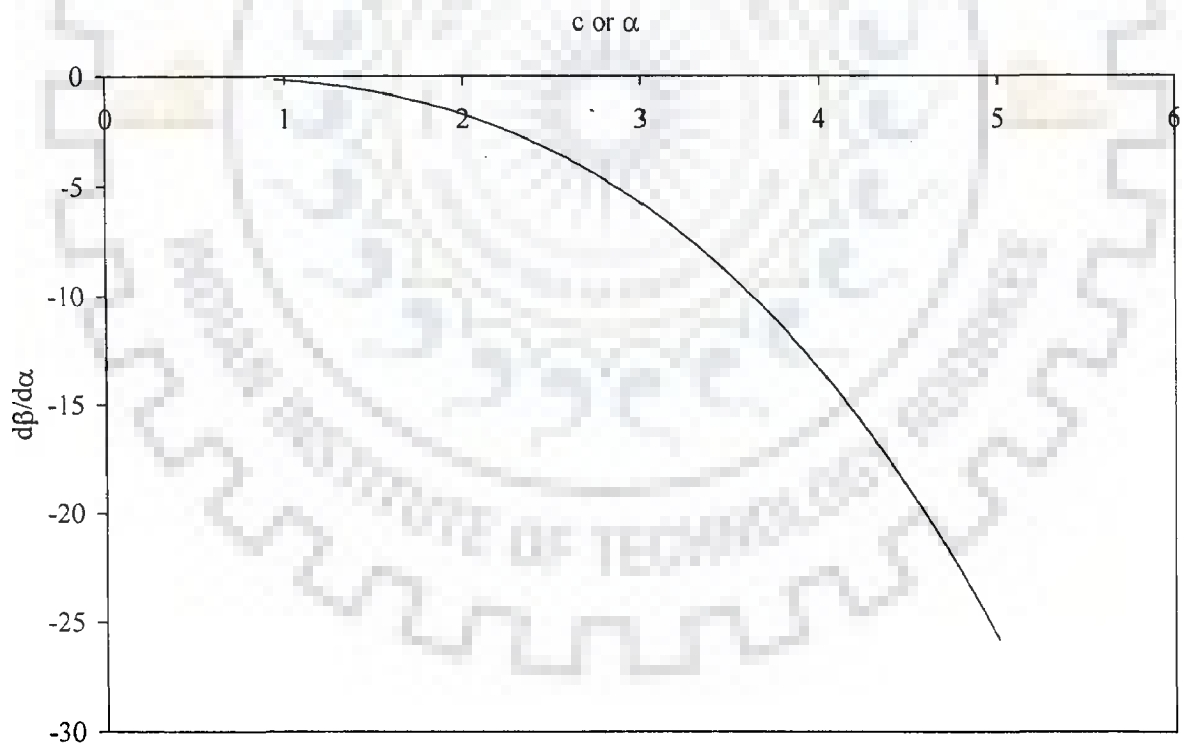


Fig. 6.3c Sensitivity to parameter alpha of 2PFDF

$$(q_p)_{2PGD} = \frac{(n-1)^{(n-1)} e^{-(n-1)}}{K\Gamma(n)} \quad (6.18)$$

Now applying the condition, i.e. $(q_p)_{2PGD} = (q_p)_{2PFD}$, we get

$$(n-1)^{n-1} e^{-(n-1)} / K\Gamma(n) = (c/\alpha)((c+1)/c)^{((c+1)/c)} e^{-((c+1)/c)} \quad (6.19)$$

Substituting $(c+1)/c = n-1$ on the right hand side of Eq. (6.19) yields $K = \alpha/c\Gamma(n)$. Thus the parameters of the two distributions are mapped as

$$(c+1)/c = n-1 \text{ or } n = 2 + 1/c; \text{ and } K = \alpha/c\Gamma(n). \quad (6.20)$$

To check the validity of the above mapping relationship, the catchment data given in Rosso (1984) were applied, and the results are given in Table 6.3. The dimensionless product β for each catchment was estimated by Eq. (2.62), and corresponding parameters of 2PFD were estimated by Eqs. (6.10) and (6.13) for a specific value of t_p . Since the location parameter α of 2PFD depends on both t_p and c , more than one values of α may be obtained for a given c , when t_p is changed. It can be inferred from Table 6.3 that the mapping of parameters is quite satisfactory. The workability of the proposed methods for deriving SUHs for limited data conditions is checked using real data, as discussed below.

6.6 APPLICATION OF MODELS

The workability of the proposed methods, i.e., one parameter CSD, and 2PFD for deriving a SUH for limited data conditions is checked in comparison with 2PGD model (Rosso, 1984), using real data, as discussed below. For this, the data of Bridge catchment No. 253 and Myntdu-Leska catchments are used here. These data were used by Bhunya et al. (2003, 2004). The characteristics of the catchments and the unit hydrographs are given in Table 3.3. The main aphorism of this application is to parameterize the one parameter CSD and 2PFD in Horton order ratio, and check their suitability in SUHs derivation in comparison

Table 6.3 Mapped Parameters of 2PGD for the data reported by Rosso (1984)

Catchment	Parameters of				Mapped Parameters of 2PGD (Eq. 6.20)	
	2PFD		2PGD			
	c	α	n	K	n	K
Ilice Creek	1.33	1.14	2.3	0.52	2.75	0.53
Virginio Creek	1.69	7.91	2.6	3.24	2.59	3.3
Bisenzio	1.71	14.4	1.6	6.02	2.58	5.98
Elsa	1.83	6.35	3.1	2.5	2.55	2.52
Sieve	1.87	8.81	3.9	3.49	2.54	3.45

with 2PGD model of Rosso (1984). The detailed steps followed in the procedure are listed below.

6.6.1 For Bridge Catchment

To derive SUHs for Bridge catchment, q_p is considered to be known, t_p , β , and the parameters of models are derived as follows:

- (i) At first step use Eq. (2.63) and substitute the value of q_p and R_L (from Table 3.3) to get the value of vL^{-1} as:

$$q_p = Q_p/A_w = (5.46 \times 1000 \times 3600)/(114.22 \times 10^6) = 0.172 \text{ mm/hr/mm} = 0.364 (1.907)^{0.43} v L^{-1}. \text{ Hence, } v L^{-1} = 0.172 / [0.364 (1.907)^{0.43}] = 0.358 \text{ hr}^{-1};$$

- (ii) Now substitute the values of vL^{-1} (step i) and R_A , R_B , and R_L (from Table 3.3) into Eq. (2.64) to get t_p as:

$$t_p = 1.584 (4.282/5.553)^{0.55} 1.907^{-0.38} v^{-1} L = 3.0 \text{ hrs};$$

- (iii) Get the dimensionless product $\beta = q_p \times t_p = 0.172 \times 3.0 = 0.516$.

- (iv) Taking these values (at steps i-iii), estimate the parameters of the one parameter CSD, 2PFD, and 2PGD (Rosso, 1984). For one parameter CSD, use Eq. (6.5) for m or τ , Eqs. (6.13) and (6.10) for c and α , and Eqs. (2.69) and (2.70) for n and K ,

respectively for 2PFD and 2PGD models. The estimated parameters values are given in Table 6.4.

- (v) Finally, derive the SUHs using the above three methods, viz., Eq. (6.3) for one parameter CSD, Eq. (6.9) for 2PFD, and Eq. (2.54) for 2PGD. The derived SUHs are shown in Fig. 6.4.

6.6.2 For Myntdu-Leska Catchment

Following the same procedure, as above, for the Myntdu-Leska catchment, the steps involved in SUHs derivation are given below.

- (i) At first step use Eq. (2.63) and substitute the value of q_p and R_L (from Table 3.3) to get the value of vL^{-1} as:

$$q_p = Q_p/A_w = (11.8 \times 1000 \times 3600)/(350 \times 10^6) = 0.122 \text{ mm/hr/mm} = 0.364 (2.12)^{0.43} v L^{-1}. \text{ Hence, } v L^{-1} = 0.122 / [0.364 (2.12)^{0.43}] = 0.243 \text{ hr}^{-1};$$

- (ii) Now substitute the values of vL^{-1} (step i) and R_A , R_B , and R_L (from Table 3.3) into Eq. (2.64) to get t_p as

$$t_p = 1.584 (4.27/4.61)^{0.55} 2.12^{-0.38} v^{-1} L = 4.72 \text{ hrs};$$

- (iii) Get the dimensionless product $\beta = q_p x t_p = 0.122 \times 4.72 = 0.574$.

- (iv) Taking these values (at steps i-iii), estimate the parameters of the one parameter CSD, 2PFD, and 2PGD (Rosso, 1984). For one parameter CSD, use Eq. (6.5) for m or τ , Eqs. (6.13) and (6.10) for c and α , and Eqs. (2.69) and (2.70) for n and K , respectively for 2PFD and 2PGD models. The estimated parameters values are given in Table 6.4.

- (v) Finally, derive the SUHs using the above three methods, viz., Eq. (6.3) for one parameter CSD, Eq. (6.9) for 2PFD, and Eq. (2.54) for 2PGD. The derived SUHs are shown in Fig. 6.5.

Table 6.4 Parameters of the three distributions for the partial data condition for the study areas

Catchments	Parameter estimates of				
	2PFD		CSD	2PGD	
	c	α	τ	n	K
Bridge Catch.No-253	1.58	4.10	2.82	2.81	1.62
Myntdu-Leska	1.73	6.15	3.22	3.27	2.09

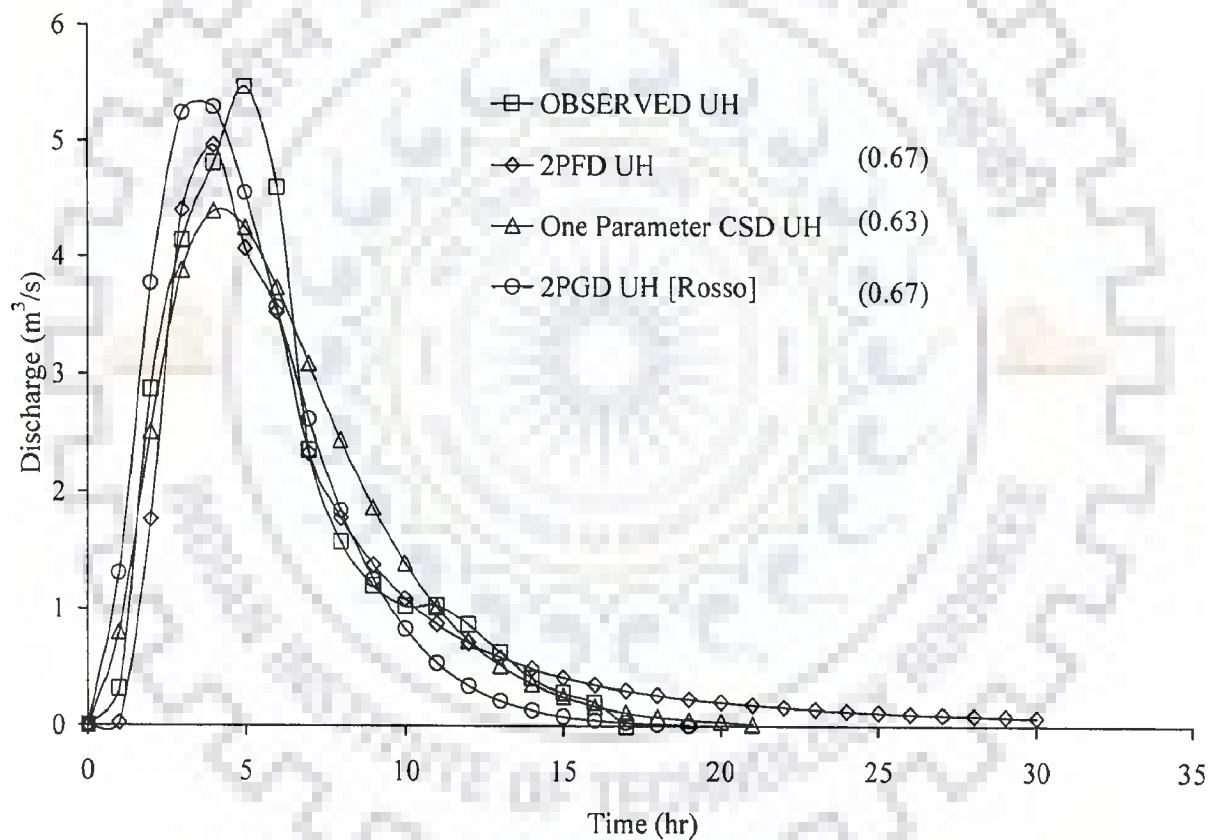


Fig. 6.4 Comparison of observed and computed UHs using three different pdfs for Bridge catchment no. 253. The figures in bracket give the corresponding STDER.

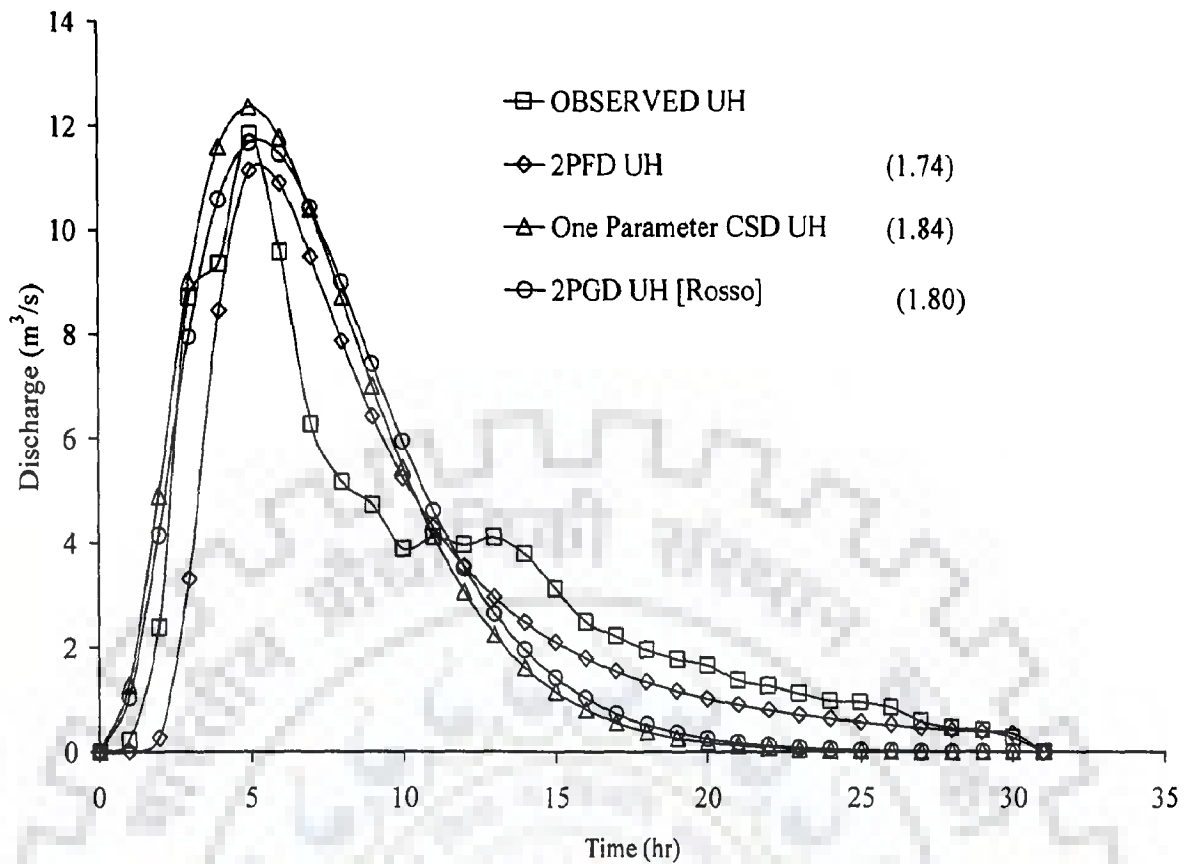


Fig 6.5 Comparison of observed and computed UHs using three different pdfs for Myntdu-Leska catchment. The figures in bracket give the corresponding STDER.

6.7 PERFORMANCE OF MODELS

To check the performance of the above three methods, the goodness-of-fit is further evaluated using the ratio (STDER) (Eqs. 5.23, 5.24) of the absolute sum of non-matching areas to the total hydrograph area. A low value of STDER-value represents a good-fit, and vice versa; and STDER equal to zero represents a perfect fit. It is observed from Fig. 6.4 that for the Bridge catchment no. 253 the STDERs due to three pdfs, i.e. one parameter CSD, 2PFD, and 2PGD are found to be 0.63, 0.67, and 0.67, respectively. It means that SUH derived by using one parameter CSD performs marginally better than 2PGD (Rosso, 1984),

and 2PFD. Similarly, for Myntdu-Leska catchment (Fig. 6.5) using one parameter CSD, 2PFD, and 2PGD, STDERs are found to be 1.84, 1.74, and 1.80, respectively. It means that SUH derived by using 2PFD performs marginally better than 2PGD, and better than one parameter CSD.

6.8 SUMMARY

In this chapter, the potential of one-parameter Chi-square distribution and two-parameter Fréchet distribution was explored for deriving an SUH. For this, an analytical procedure was developed to estimate the distribution parameters. For limited data conditions, SUH parameters, viz., peak discharge, time to peak, etc. were computed using Horton order ratios given by Rodriguez-Iturbe and Valdes (1979). Finally, the results of two pdfs were compared with the existing Gamma synthetic method of Rosso (1984). It was found that the two pdfs compared well with the popular 2PGD, indicating equal potential of both the considered distributions for SUH derivation.

CHAPTER-7

SCS-CN METHOD BASED SEDIMENT GRAPH MODELS

7.1 BACKGROUND

The sediment flow rate plotted as a function of time during a storm at a given location is known as a sediment graph. To determine these sediment graphs, simple conceptual models are used, which are based on spatially lumped form of continuity and linear storage-discharge equations. As discussed in sub-section 2.3.5, the simple conceptual models based on IUSG or (USG) concepts are placed on high priority to model the time distributed sediment yield from a watershed, as these are founded on a strong conceptual basis. Moreover, if simple but efficient time distributed sediment yield models are to be developed, then one has no choice other than the conceptual sediment graph models. As discussed in sub-section 2.3.5, the available sediment graph models have several inconsistencies. Similarly, the sediment yield models proposed by Mishra et al. (2006a) using SCS-CN method, DR concept, and USLE take care of various elements of rainfall-runoff process such as initial abstraction, initial soil moisture, and initial flush. However, these models are not suitable for sediment graph based applications.

Thus, this chapter proposes new conceptual sediment graph models based on the popular IUSG, SCS-CN method, and Power law. Briefly, the methodology comprises of the mobilized sediment estimation by SCS-CN method and Power law. The proposed approach is advantageous in the sense that it considers the rainfall intensity, soil type, land use, hydrologic condition, and antecedent moisture, and thus, physically more appreciable than the common and less accurate regression type relations. The mobilized sediment is routed through cascade of linear reservoirs similar to Nash (1957). Finally, sediment graphs are derived by convolution of IUSG with mobilized sediment. The workability of the proposed sediment graph models is checked using the sediment graph data of two real catchments. It is noteworthy here that the model does not explicitly account for the geometric configuration of a given watershed.

7.2 MATHEMATICAL FORMULATION

For formulating the sediment graph models, three popular existing methods are used: (i) Nash-based IUSG model, (ii) SCS-CN method, and (iii) Power law. The proposed sediment graph models are based on the following assumptions:

- (i) the bed load contributions to the total sediment yield are neglected since they are usually small; therefore the suspended sediment yield is considered as the total sediment yield of the watershed;
- (ii) the rainfall, P , grows linearly with time t , i.e. $P = i_0 t$, where i_0 is the uniform rainfall intensity;
- (iii) the inflow is assumed to be instantaneous and it occurs uniformly over the entire watershed producing a unit of mobilized sediment; and
- (iv) the process is linear and time invariant.

The three sub-models used for the formulation of the sediment graph models are discussed as follows:

7.2.1 Sub-models

7.2.1.1 Nash Based IUSG

The suspended sediment dynamics for a linear time-invariant watershed is represented by a spatially lumped form of continuity equation and a linear-storage discharge relationship. The schematic representation of this sub-model is given in Fig. 7.1 and described mathematically below:

The first linear reservoir is represented by

$$I_{sl}(t) - Q_{sl}(t) = dS_{sl}(t) / dt \quad (7.1)$$

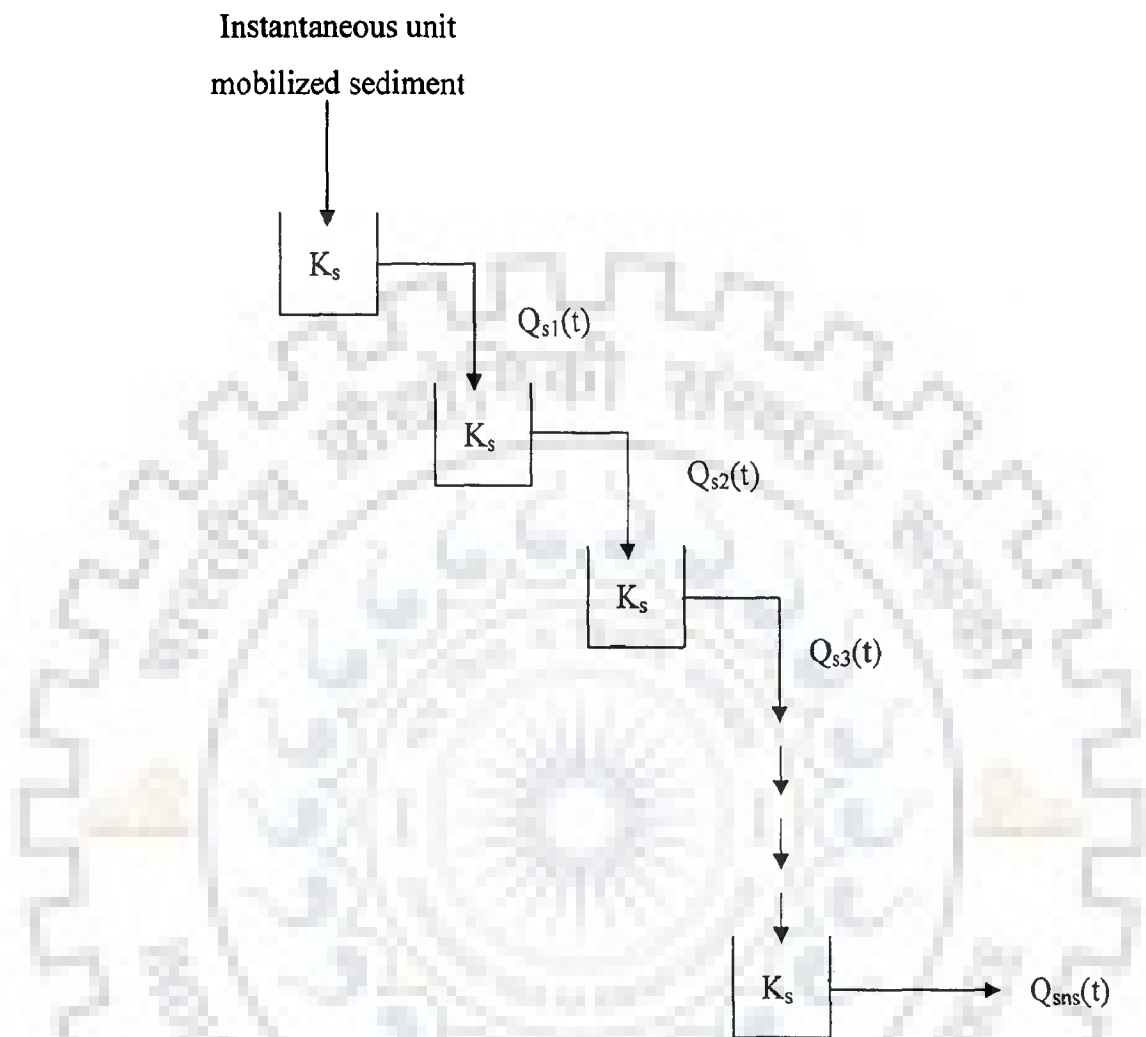


Fig. 7.1. Schematic representation of Nash-based IUSG sub-model

$$S_{si}(t) = K_s Q_{si}(t) \quad (7.2)$$

where $I_{si}(t)$ is the sediment input to the first reservoir (kN/hr), $Q_{si}(t)$ is the sediment outflow from the reservoir (kN/hr), $S_{si}(t)$ is the sediment storage within the reservoir (kN), and K_s is sediment storage coefficient (hr).

For an instantaneous inflow, i.e. $I_{si}(t) = 0$, which, on substituting into Eq. (7.1) yields

$$0 - Q_{si}(t) = dS_{si}(t)/dt \quad (7.3)$$

Substituting the value of $S_{si}(t)$ from Eq. (7.2) into Eq. (7.3) we get

$$0 - Q_{si}(t) = d(K_s Q_{si}(t))/dt \quad (7.4)$$

On rearranging Eq. (7.4) and performing integration operation, one gets

$$\int dQ_{si}(t)/Q_{si}(t) = -(1/K_s) \int dt \quad (7.5)$$

Simplification of Eq. (7.5) yields

$$-t/K_s + C_1 = \ln Q_{si}(t) \quad (7.6)$$

where C_1 is the constant of integration, which can be estimated by putting $t = 0$ in Eq. (7.6) to get $C_1 = -\ln Q_{si}(0)$, which, on substituting into Eq. (7.6) and on rearranging, gives

$$Q_{si}(t) = Q_{si}(0)e^{-t/K_s} \quad (7.7)$$

For $t = 0$, Eq. (7.2) can be expressed as:

$$S_{si}(0) = K_s Q_{si}(0) \quad (7.8)$$

If A_w is the watershed area (km^2), and Y is the mobilized sediment per storm per unit area (kN/km^2), then the total amount of mobilized sediment $Y_T = A_w Y$ (kN). If this occurs instantaneously and is one unit, i.e. at $t = 0$, $S_{s1}(0) = A_w Y = 1$ (kN). Substituting this into Eq. (7.8), we have

$$1 = K_s Q_{s1}(0) \quad (7.9)$$

Using Eqs. (7.7) and (7.9), a simpler form is deduced as:

$$Q_{s1}(t) = (1/K_s) e^{-t/K_s} \quad (7.10)$$

Eq. (7.10) gives the rate of sediment output from the first reservoir. This output forms the input to second reservoir and if it goes on up to n_s^{th} reservoir, the resultant output from the n_s^{th} reservoir can be derived as [Appendix F]:

$$Q_{sn_s}(t) = \frac{1}{K_s \Gamma(n_s)} (t/K_s)^{n_s-1} e^{-t/K_s} \quad (7.11)$$

where $\Gamma(\)$ is the Gamma function. Eq. (7.11) represents the IUSG ordinates (hr^{-1}) at time t . For the condition, $dQ_{sn_s}(t)/dt = 0$ at $t = t_{ps}$, where t_{ps} is the time to peak sediment flow rate. Therefore,

$$K_s = t_{ps} / (n_s - 1) \quad (7.12)$$

The coupling of Eqs. (7.11) & (7.12) yields

$$Q_{sn_s}(t) = (n_s - 1)^{n_s} / t_{ps} \Gamma(n_s) [(t/t_{ps}) e^{-(t/t_{ps})}]^{n_s-1} \quad (7.13)$$

Eq. (7.13) is simplified form of IUSG (Eq. 7.11) and has only one parameter n_s .

7.2.1.2 SCS-CN Method

Following Mishra et al. (2002) and Mishra and Singh (2003a, 2004b) for the condition, $f_c = 0$, the Horton's method (Horton, 1938) can be expressed mathematically as:

$$f = f_0 e^{-kt} \quad (7.14)$$

where f is the infiltration rate ($L T^{-1}$) at time t , f_0 is the initial infiltration rate ($L T^{-1}$) at time $t=0$, k is the decay constant (T^{-1}), and f_c is the final infiltration rate ($L T^{-1}$). It is to note that Eq. (7.14) is valid for t that is the time past ponding. An integration of Eq. (7.14) leads to deriving cumulative infiltration rate F at time t as:

$$F = \frac{f_0}{k} (1 - e^{-kt}) \quad (7.15)$$

Thus, it can be inferred from Eq. (7.15) that as $t \rightarrow \infty$, $F \rightarrow f_0/k$. Similarly, from Eq. (2.3), as $Q \rightarrow (P-I_a)$, $F \rightarrow S$, which is valid for time t approaching infinity. Therefore, the similarity yields

$$S = \frac{f_0}{k} \quad (7.16)$$

From the experience on infiltration tests (Mein and Larson, 1971) $f_0 = i_0$, where i_0 is the uniform rainfall intensity at time $t = 0$. Therefore, substituting this into Eq. (7.16) yields

$$f_0 = i_0 = kS \quad (7.17)$$

Eq. (7.17) describes the relationship among the three parameters f_0 , k , and S and defines Horton parameter k to be equal to the ratio of the uniform rainfall intensity, i_0 , to the potential maximum retention, S , implying that k increases as i_0 increases and decreases as S increases or CN decreases, and vice versa also holds. Thus, k depends on the magnitude of

the rainfall intensity and soil type, land use, hydrologic condition, antecedent moisture that affect S and it is consistent with the description of Mein and Larson (1971).

An assumption of rainfall P growing linearly with time t leads to

$$P = i_0 t \quad (7.18)$$

which is a valid and reasonable assumption for usually derived infiltration rates from field/laboratory tests (Mishra et al., 2002). It also asserts the general notion that P grows unbounded (Ponce and Hawkins, 1996). Now putting the value of i_0 from Eq. (7.17) into Eq. (7.18) gives

$$P = kSt \quad (7.19)$$

Such an analogy between Horton model and SCS-CN method can be found in detail in Mishra and Singh (2003a).

7.2.1.3 Power Law

Novotny and Olem (1994) used the Power law for deriving the relationship between runoff coefficient C and sediment delivery ratio DR as:

$$DR = \alpha C^\beta \quad (7.20)$$

where α and β are, respectively, the coefficient and exponent of power relationship; and DR is a dimensionless ratio of the sediment yield Y to the potential maximum erosion A :

$$DR = \frac{Y}{A} \quad (7.21)$$

The runoff coefficient, C , is a dimensionless ratio of actual runoff, Q , to total rainfall, P :

$$C = \frac{Q}{P} \quad (7.22)$$

On substituting the expressions of DR and C into Eq. (7.20), one gets

$$Y = \alpha A \left(\frac{Q}{P} \right)^{\beta} \quad (7.23)$$

7.2.2 Case Specific Formulations

The sub-models described above are used to develop the proposed sediment graph models (SGM) for four different cases, depending on the number of model parameters, and these are designated as SGM₁ through SGM₄, respectively. For SGM₁, both the initial soil moisture V_0 and initial abstraction I_a are assumed to be zero, i.e. $V_0 = 0$ and $I_a = 0$. For SGM₂, $V_0 = 0$, but $I_a \neq 0$. For SGM₃, $V_0 \neq 0$ and $I_a = 0$. Finally, for SGM₄, $V_0 \neq 0$ and $I_a \neq 0$. Here, a brief description of these conditions for their realization in field is in order. $V_0 = 0$ represents that the watershed is initially fully dry which can be realized in field if the antecedent precipitation (for 5 or more preceding no. of days) is zero. On the other hand, the condition $I_a = 0$ indicates an initially ponded situation (Chen, 1982), which implies that the storm under consideration has initially created a pond like situation, when the initial abstraction requirements are zero. Since both the conditions are separate from each other, i.e. one depends on the antecedent amount of precipitation and the other on the storm under consideration, any of the conditions, leading to the formulation of the following SGM₁ through SGM₄ models, can be realized in field.

7.2.2.1 SGM₁: Initial soil moisture (V_0) = 0 and Initial abstractions (I_a) = 0

Equating Eq. (2.3) with Eq. (2.5) for the condition $I_a = 0$, one gets

$$Q/P = P/(P+S) = F/S \quad (7.24)$$

Coupling Eqs. (7.23) & (7.24) yields the expression for Y as:

$$Y = \alpha A [P / (P + S)]^\beta \quad (7.25)$$

Substituting the value of P from Eq. (7.19) into Eq. (7.25), one gets

$$Y = \alpha A [kt / (1 + kt)]^\beta \quad (7.26)$$

Eq. (7.26) gives the amount of mobilised sediment per unit area due to an isolated storm event occurring uniformly over the watershed. The total amount of mobilized sediment is expressible as:

$$Y_T = \alpha A A_w [kt / (1 + kt)]^\beta \quad (7.27)$$

Coupling Eqs. (7.13) and (7.27) results in the following expression:

$$Q_s(t) = \left[\alpha A A_w [kt / (1 + kt)]^\beta (n_s - 1)^{n_s} / t_{ps} \Gamma(n_s) \left[(t / t_{ps}) e^{-(t / t_{ps})} \right]^{n_s - 1} \right] \quad (7.28)$$

where $Q_s(t)$ represents the ordinates of sediment graph model. Eq. (7.28) is the simplest expression of sediment graph model with parameters α , β , k , and n_s .

7.2.2.2 SGM₂: Initial soil moisture (V_0) = 0 and Initial abstractions $I_a \neq 0$

For the condition, when $I_a \neq 0$, Eq. (7.25) can be expressed as:

$$Y = \alpha A [(P - I_a) / (P - I_a + S)]^\beta, \quad (7.29)$$

Substituting the value of $I_a = \lambda S$ from Eq. (2.4) into Eq. (7.29) yields

$$Y = \alpha A[(P - \lambda S)/(P - \lambda S + S)]^\beta \quad (7.30)$$

Coupling Eqs. (7.19) and (7.30) yields

$$Y = \alpha A[(kt - \lambda)/(1 + kt - \lambda)]^\beta \quad (7.31)$$

Eq. (7.31) estimates the amount of mobilized sediment for the condition of initial abstractions ($I_a \neq 0$). The total amount of mobilized sediment is expressed as:

$$Y_T = \alpha A A_w [(kt - \lambda)/(1 + kt - \lambda)]^\beta \quad (7.32)$$

The coupling of Eq. (7.13) with Eq. (7.32) results

$$Q_s(t) = \left[\alpha A A_w [(kt - \lambda)/(1 + kt - \lambda)]^\beta (n_s - 1)^{n_s} / t_{ps} \Gamma(n_s) [(t/t_{ps}) e^{-(t/t_{ps})}]^{n_s - 1} \right] \quad (7.33)$$

Eq. (7.33) is the expression of sediment graph model with parameters α , β , k , λ , and n_s .

7.2.2.3 SGM₃: Initial Soil moisture (V_0) $\neq 0$ and Initial abstractions (I_a) = 0

For the condition $I_a = 0$, incorporating the initial soil moisture (V_0) in the basic proportionality concept (Eq. 2.3), the expression for mobilized sediment (Eq. 7.25) reduces to the following form:

$$Y = \alpha A[(P + V_0)/(P + S + V_0)]^\beta \quad (7.34)$$

A substitution of the expression of P from Eq. (7.19) into Eq. (7.34) reduces to

$$Y = \alpha A[(kSt + V_0)/(kSt + V_0 + S)]^\beta \quad (7.35)$$

Alternatively, Eq. (7.35) can be expressed as:

$$Y = \alpha A [(kt + V_0/S)/(1 + kt + V_0/S)]^\beta \quad (7.36)$$

From Eq. (7.36), the total amount of mobilized sediment can be expressed as:

$$Y_T = \alpha A A_w [(kt + V_0/S)/(1 + kt + V_0/S)]^\beta \quad (7.37)$$

Coupling Eq. (7.13) with Eq. (7.37) one gets

$$Q_s(t) = \left[\alpha A A_w [(kt + V_0/S)/(1 + kt + V_0/S)]^\beta (n_s - 1)^{n_s} / t_{ps} \Gamma(n_s) [(t/t_{ps}) e^{-(t/t_{ps})}]^{n_s - 1} \right] \quad (7.38)$$

For a given watershed and storm event, the ratio of V_0 and S (let θ) is constant and varies in the range of 0 and 1 (Michel et al., 2005). Hence putting $\theta = V_0/S$, Eq. (7.38) can be re-written as:

$$Q_s(t) = \left[\alpha A A_w [(kt + \theta)/(1 + kt + \theta)]^\beta (n_s - 1)^{n_s} / t_{ps} \Gamma(n_s) [(t/t_{ps}) e^{-(t/t_{ps})}]^{n_s - 1} \right] \quad (7.39)$$

Eq. (7.39) is the expression for sediment graph model with parameters α , β , k , λ , θ , and n_s .

7.2.2.4SGM₄: Initial soil moisture (V_0) \neq 0 and Initial abstractions (I_a) \neq 0

For the condition $I_a \neq 0$, and incorporating the initial soil moisture (V_0) in the basic proportionality concept (Eq. 2.3), the expression for mobilized sediment (Eq. 7.34) reduces to

$$Y = \alpha A [(P - I_a + V_0)/(P - I_a + V_0 + S)]^\beta \quad (7.40)$$

On substituting the expressions of I_a and P from Eqs. (2.4) & (7.19), respectively, Eq. (7.40) simplifies to the following form as:

$$Y = \alpha A [(kSt - \lambda S + V_0) / (kSt - \lambda S + V_0 + S)]^\beta \quad (7.41)$$

Alternatively, Eq. (7.41) can be expressed as:

$$Y = \alpha A [(kt - \lambda + V_0 / S) / (1 + kt - \lambda + V_0 / S)]^\beta \quad (7.42)$$

Hence, the total amount of mobilized sediment can be expressed as:

$$Y_T = \alpha A A_w [(kt - \lambda + V_0 / S) / (1 + kt - \lambda + V_0 / S)]^\beta \quad (7.43)$$

Coupling Eqs. (7.13) & (7.43), one gets

$$Q_s(t) = \left[\alpha A A_w [(kt - \lambda + V_0 / S) / (1 + kt - \lambda + V_0 / S)]^\beta (n_s - 1)^{n_s} / t_{ps} \Gamma(n_s) [(t / t_{ps}) e^{-(t / t_{ps})}]^{n_s - 1} \right] \quad (7.44)$$

Similar to Eq. (7.39), replacing $\theta = V_0 / S$, Eq. (7.44) simplifies to

$$Q_s(t) = \left[\alpha A A_w [(kt - \lambda + \theta) / (1 + kt - \lambda + \theta)]^\beta (n_s - 1)^{n_s} / t_{ps} \Gamma(n_s) [(t / t_{ps}) e^{-(t / t_{ps})}]^{n_s - 1} \right] \quad (7.45)$$

Eq. (7.45) is the expression of sediment graph model with parameters α , β , k , λ , θ , and n_s .

7.3 MODEL APPLICATION AND TESTING

The applicability of the proposed sediment graph models is tested using the sediment graph data of three storm events of Nagwan watershed (Tables 3.4 & 7.1). The model SGM_1 excludes the initial abstraction and initial soil moisture components, SGM_2 accounts only for

initial abstraction, SGM₃ accounts for initial soil moisture and excludes I_a, and SGM₄ accounts for both initial soil moisture and initial abstraction. The model SGM₁ is the simplest and SGM₄ is the most complex based on the criteria of the number of parameters involved in the model formulation.

7.3.1 Parameter Estimation

The shape parameter n_s of IUSG sub-model was estimated by the relationship given by Bhunya et al. (2003b) as:

$$\begin{aligned} n_s &= 5.53\beta_s^{1.75} + 1.04 && \text{for } 0.01 < \beta_s < 0.35 \\ n_s &= 6.29\beta_s^{1.998} + 1.157 && \text{for } \beta_s \geq 0.35 \end{aligned} \quad (7.46)$$

where β_s is a non dimensional parameter defined as the product of peak sediment flow rate (q_{ps}) (kN/hr/kN) and time to peak sediment flow rate (t_{ps}) (hr). The estimated values of n_s are given in Table 7.1. The rest of the parameters, whose numbers vary with the different models, were estimated using the non-linear Marquardt (1963) algorithm of the least squares. As discussed earlier, SGM₁ model (Eq. 7.28) is the simplest one with least numbers of parameters while SGM₄ (Eq. 7.45) has the maximum number of parameters. In the present application, the potential maximum erosion A was also taken as a parameter. However, if sufficient information regarding rainfall and watershed characteristics is available, it could be estimated by MUSLE (Williams, 1975). The estimated values of the parameters are given in Table 7.2.

7.3.2 Performance Analysis

The performance of the proposed sediment graph models was evaluated on the basis of (i) visual closeness of the observed and computed sediment graphs and (ii) goodness of fit

(GOF) in terms of Nash and Sutcliffe (NS) (1970) efficiency and relative error (RE) of the results defined as:

$$\text{NS Efficiency} = (1 - D_1 / D_0) \times 100 \quad (7.47)$$

where D_1 is the sum of the squares of deviations between computed and observed total sediment outflow, given as:

$$D_1 = \sum (Q_s - Q_{sc})^2 \quad (7.48)$$

and D_0 is the model variance which is the sum of the squares of deviations of the observed total sediment outflow about mean of the total observed sediment outflow, given as:

$$D_0 = \sum (Q_s - \bar{Q}_s)^2 \quad (7.49)$$

and relative errors (RE) are defined as:

$$\text{RE}_{(Q_s)} = \frac{Q_{sc} - Q_s}{Q_{sc}} \times 100; \quad (7.50)$$

$$\text{RE}_{(Q_{ps})} = \frac{Q_{psc} - Q_{ps}}{Q_{psc}} \times 100; \quad (7.51)$$

$$\text{RE}_{(t_{ps})} = \frac{t_{ps(c)} - t_{ps}}{t_{ps(c)}} \times 100 \quad (7.52)$$

where Q_s and $Q_{s(c)}$ = observed and computed total sediment outflow, respectively; and Q_{ps} and $Q_{ps(c)}$ = observed and computed peak sediment outflow rate, respectively; t_{ps} and $t_{ps(c)}$ = observed and computed time to peak sediment flow rates; and $RE_{[Q_s]}$, $RE_{[Q_{ps}]}$, and $RE_{[t_{ps}]}$ = relative errors in total sediment outflow, peak sediment flow rates, and time to peak sediment flow rates, respectively.

7.3.3 Sensitivity Analysis

To evaluate the dependence of the computed total sediment outflow and peak sediment flow rate on the various parameters of each model, the sensitivity analysis was carried out. Parameters were varied in a definite ratio, i.e. by increasing the parameters by 10%, 20%, and 30% to their estimated values. This percent variation was however chosen arbitrarily, and any other variation could have been opted. For each model the sensitivity analysis was carried out by comparing the percentage change in computed values of Q_s and Q_{ps} corresponding to percent increase in the estimated parameter value.

7.4 RESULTS AND DISCUSSION

7.4.1 Parameter Estimation

It is observed from Table 7.2 that the parameter α varies from 0.411 to 1.000, from 0.232 to 0.520, from 0.198 to 0.597, and from 0.226 to 0.579 for SGM₁-SGM₄, respectively. Similarly, β ranges from 0.451 to 1.000, from 0.325 to 0.450, from 0.336 to 0.972, and from 0.336 to 0.688 for respective models. k respectively varies from 0.012 to 0.021 h⁻¹, from 0.007 to 0.017 h⁻¹, from 0.01 to 0.027 h⁻¹, and from 0.01 to 0.012h⁻¹. Similarly, θ of SGM₃ varies from 0.0001 to 0.034, and θ of SGM₄ from 0.004 to 0.039. These values are in close agreement with the results obtained by Mishra et al. (2006a), and θ -values are also consistent with those due to Michel et al. (2005). Similarly, λ of SGM₂ was observed to vary from 0.01 to 0.018, and of SGM₄ from 0.01 to 0.027, close to recommendation of Hawkins et al. (2001), i.e. $0 \leq \lambda \leq 0.05$.

Table 7.1 Unit sediment graph characteristics of the storm events of Nagwan watershed

Watershed	Date of storm	q_{ps} (kN/hr/kN)	t_p (hr)	β_s	n_s
Nagwan	July 6, 1989	0.22	3.5	0.770	4.89
	July 20, 1989	0.16	4.5	0.720	4.42
	July 28, 1989	0.17	4.5	0.765	4.84

Table 7.2 Optimized parameter values for Nagwan watershed

Date of storm	Model	Model Parameters					
		α	β	k	θ	λ	A(kN/km ²)
July 6, 1989	SGM ₁	0.417	0.707	0.021	-	-	2905
	SGM ₂	0.332	0.325	0.012	-	0.018	1983
	SGM ₃	0.198	0.336	0.012	0.0001	-	2963
	SGM ₄	0.226	0.336	0.012	0.009	0.027	3042
July 20, 1989	SGM ₁	1.000	1.000	0.016	-	-	8464
	SGM ₂	0.520	0.450	0.007	-	0.017	7648
	SGM ₃	0.597	0.972	0.027	0.0001	-	8960
	SGM ₄	0.579	0.571	0.011	0.004	0.026	7779
July 28, 1989	SGM ₁	0.411	0.451	0.012	-	-	2867
	SGM ₂	0.233	0.345	0.017	-	0.010	3474
	SGM ₃	0.375	0.736	0.010	0.034	-	5615
	SGM ₄	0.372	0.688	0.010	0.039	0.010	5021

7.4.2 Comparative Performance of Models

For visual appraisal, the computed sediment graphs are compared with the observed sediment graphs and shown in Figs. 7.2-7.4. It can be inferred from the figures that the computed sediment graphs are close to the observed sediment graphs, except for peak

sediment flow rates which are underestimated. All models appear to have performed similarly.

The results were further tested with GOF criteria given by Eq. (7.47) and Eqs. (7.50-7.52) and the models NS efficiency (%) and RE (%) are shown in Table 7.3. The results indicate SGM₂ to give higher efficiency compared to others, except for the storm event of 28th July 1989, where SGM₃ has the highest efficiency, though the difference is negligible (0.44% to 2.69%). In general, the higher model efficiencies (more than 90%) due to all model applications support their credibility and workability. Table 7.3 also shows the models performance in terms of their RE in total sediment outflow, Q_s , peak sediment flow rates, Q_{ps} , and time to peak sediment flow rate, t_{ps} .

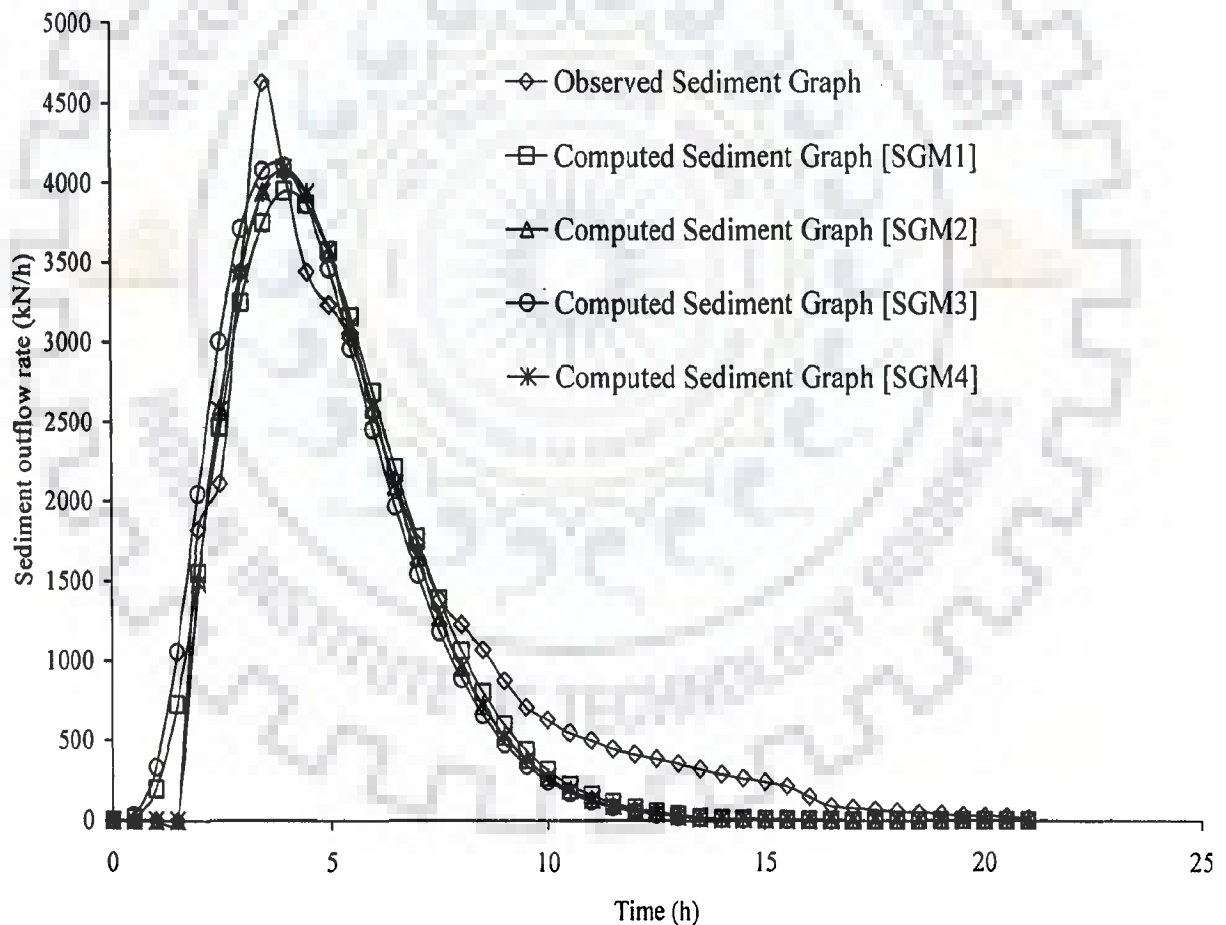


Fig. 7.2. Comparison of observed and computed sediment graphs for the storm of July 6, 1989

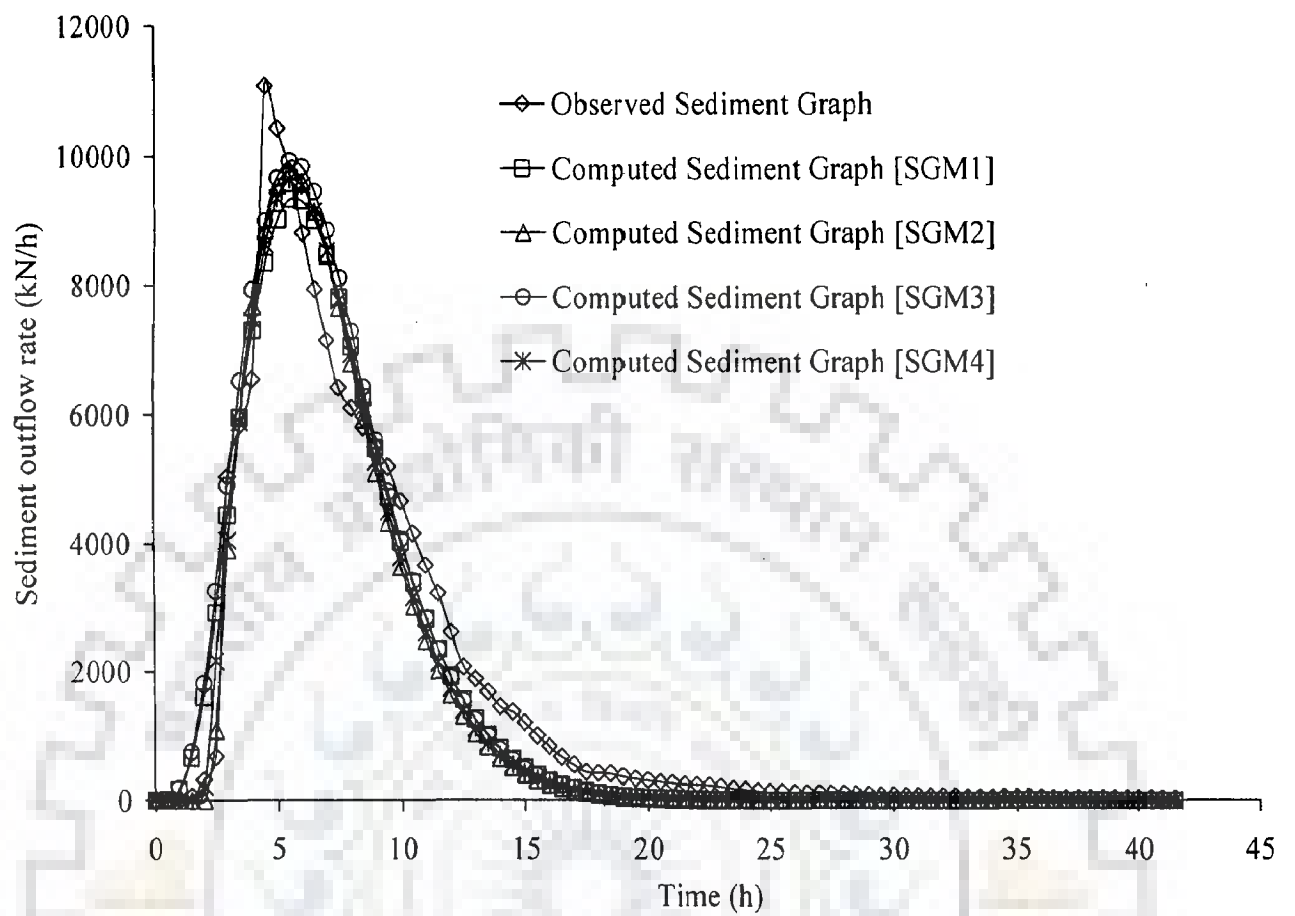


Fig. 7.3. Comparison of observed and computed sediment graphs for the storm of July 20, 1989

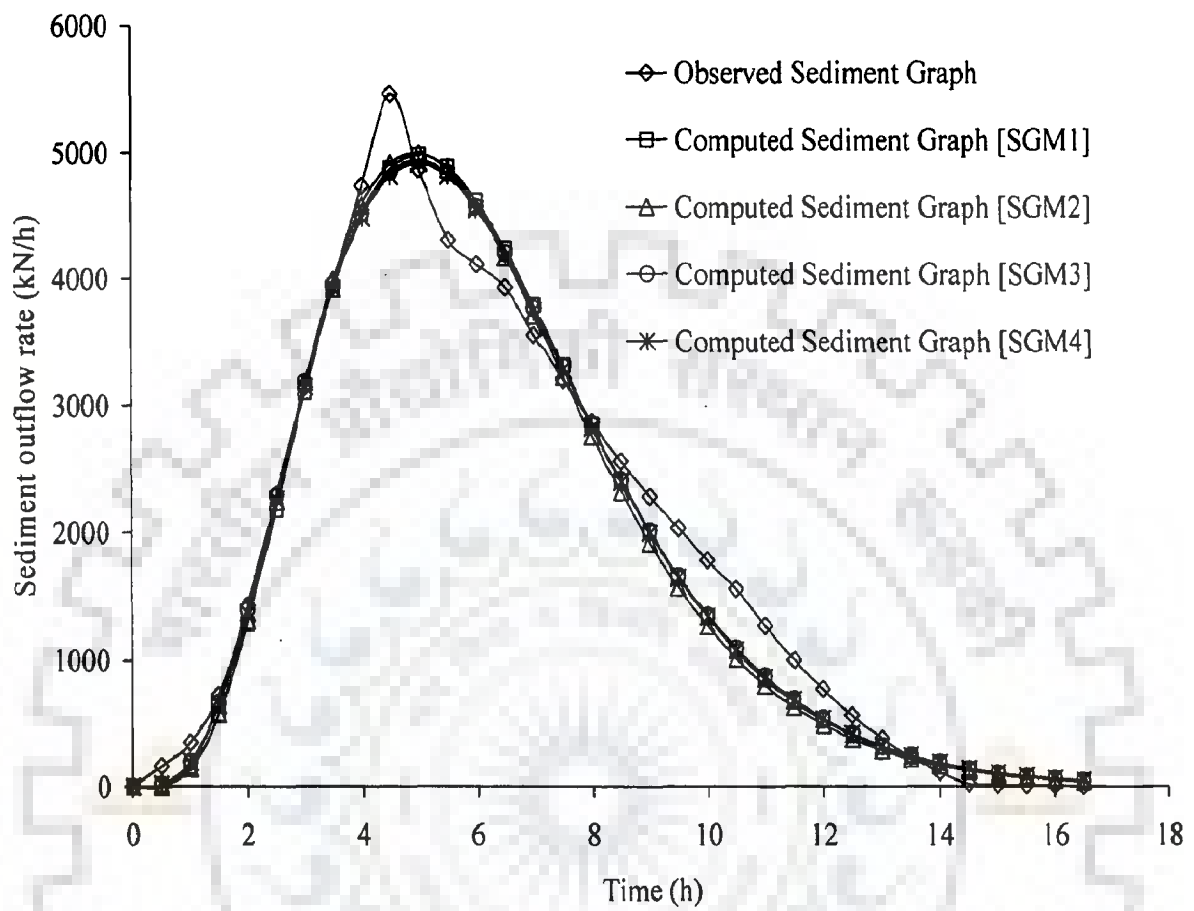


Fig. 7.4. Comparison of observed and computed sediment graphs for the storm of July 28, 1989

Table 7.3 Goodness of fit of models in terms of Model efficiency and Relative error

Date of storm	Model	Total sediment outflow (kN)		RE _{Q_s} (%)	Peak sediment outflow rate (kN/h)		RE _{Q_{ps}} (%)	Time to peak sediment outflow (h)		RE _{t_{ps}} (%)	NS Efficiency (%)
		Q _s	Q _{sc}		Q _{ps}	Q _{psc}		t _{ps}	t _{psc}		
July 6, 1989	SGM ₁	21315	19227	9.80	4621	3947	14.59	3.5	4.0	-14.29	95.16
	SGM ₂	21315	18555	12.95	4621	4083	11.65	3.5	4.0	-14.29	95.83
	SGM ₃	21315	19453	8.74	4621	4103	11.21	3.5	4.0	-14.29	93.14
	SGM ₄	21315	18610	12.69	4621	4090	11.49	3.5	4.0	-14.29	93.84
July 20, 1989	SGM ₁	70075	64915	7.36	11069	9326	15.75	4.5	5.5	-22.22	95.10
	SGM ₂	70075	61303	12.52	11069	9765	11.78	4.5	5.5	-22.22	95.68
	SGM ₃	70075	68096	2.82	11069	9920	10.38	4.5	5.5	-22.22	94.52
	SGM ₄	70075	62560	10.72	11069	9632	12.99	4.5	5.5	-22.22	95.53
July 28, 1989	SGM ₁	31833	30643	3.74	5459	4978	8.81	4.5	5.0	-11.11	97.55
	SGM ₂	31833	30320	4.75	5459	4990	8.59	4.5	5.0	-11.11	97.39
	SGM ₃	31833	30870	3.03	5459	4936	9.58	4.5	5.0	-11.11	97.83
	SGM ₄	31833	30640	3.75	5459	4910	10.06	4.5	5.0	-11.11	97.79

It is observed from Table 7.3 that SGM₃ yields lower values of RE_(Q_s) than the others. This may be attributed to incorporation of initial soil moisture in model formulation. Similar results were obtained for RE_(Q_{ps}), except for the storm event of July, 28, 1989, where SGM₁ has a lower RE value than the others, though the difference is negligible (0.22% to 5.37%). Albeit, the RE values in case of t_{ps} estimation is on higher side (-11 to -22%), however, the accuracy obtained is fair because even the more elaborate process-based soil erosion models are found to produce results with still larger errors (Vanoni 1975; Foster 1982; Hadley et al. 1985; Wu et al., 1993; Wicks and Bathurst 1996; and Jain et al., 2005). The results of total sediment yield computations using models SGM₁-SGM₄ for the three storm events are also depicted graphically in Fig. 7.5. Both the observed and computed data points falling close to the line of perfect fit indicate satisfactory performance of all models.

In brief, the proposed sediment graph models (SGM₁-SGM₄) compute sediment graphs and total sediment outflow reasonably well with efficiency greater than 90% and

relative error less than 12.95% and 15.75% for total sediment outflow and peak sediment flow rate, respectively. A close investigation of the results indicates that the GOF (Table 7.3) in terms of NS efficiency increases with incorporation of I_a in model formulation (SGM₂) and, on the other hand, REs for Q_s and Q_{ps} decrease with incorporation of V_0 (SGM₃). It follows that both components of hydrologic cycle do affect the sediment graph derivation. The following section tests the sensitivity of different model parameters.

7.4.3 Sensitivity of Parameters

The effect of variation in parameter α on Q_s and Q_{ps} due to all the models SGM₁-SGM₄ is shown in Fig. 7.6. All the models appear to show similar trends in variation of Q_s and Q_{ps} with variation in α . A similar percent variation in the values of Q_s and Q_{ps} was analyzed for β , and the results are depicted in Fig. 7.7, which shows that both Q_s and Q_{ps} tend to decrease (up to 130%) as β increases. Furthermore, SGM₃ is seen to be the most sensitive to parameter β followed by SGM₂, SGM₄, and SGM₁; and β is more sensitive than α . A similar analysis was carried out for parameter k and the results are shown in Fig. 7.8. SGM₂ appears to be most sensitive to k variation, followed by SGM₁, SGM₄, and SGM₃. The percent variation is however less than that due to β , and is of the order of α . The sensitivity results (Fig. 7.9) of θ -inclusion in SGM₃ and SGM₄ indicate SGM₄ to be more sensitive to θ than SGM₃. Similarly, λ is more sensitive (Fig. 7. 10) in SGM₄ than SGM₂. The sensitivity of shape parameter n_s (Fig. 7.11) indicates that the variation in Q_s is negative and less in magnitude than Q_{ps} for any variation in n_s . The variation in Q_{ps} is however positive. Fig. 7.11 also indicates that all models (SGM₁-SGM₄) have a similar response for Q_{ps} to any variation in n_s . Furthermore, the percent variation in this case is less than β , followed by α , and k . In brief, the results indicate that the variation in Q_s and Q_{ps} is most sensitive to β , followed by α , k , θ , λ , and n_s for SGM₁-SGM₄. A similar trend in parameter sensitivity was observed (not shown) with the other two events. The results also show a higher percent variation in Q_{ps} than Q_s , indicating Q_{ps} to be more parameter sensitive than Q_s .

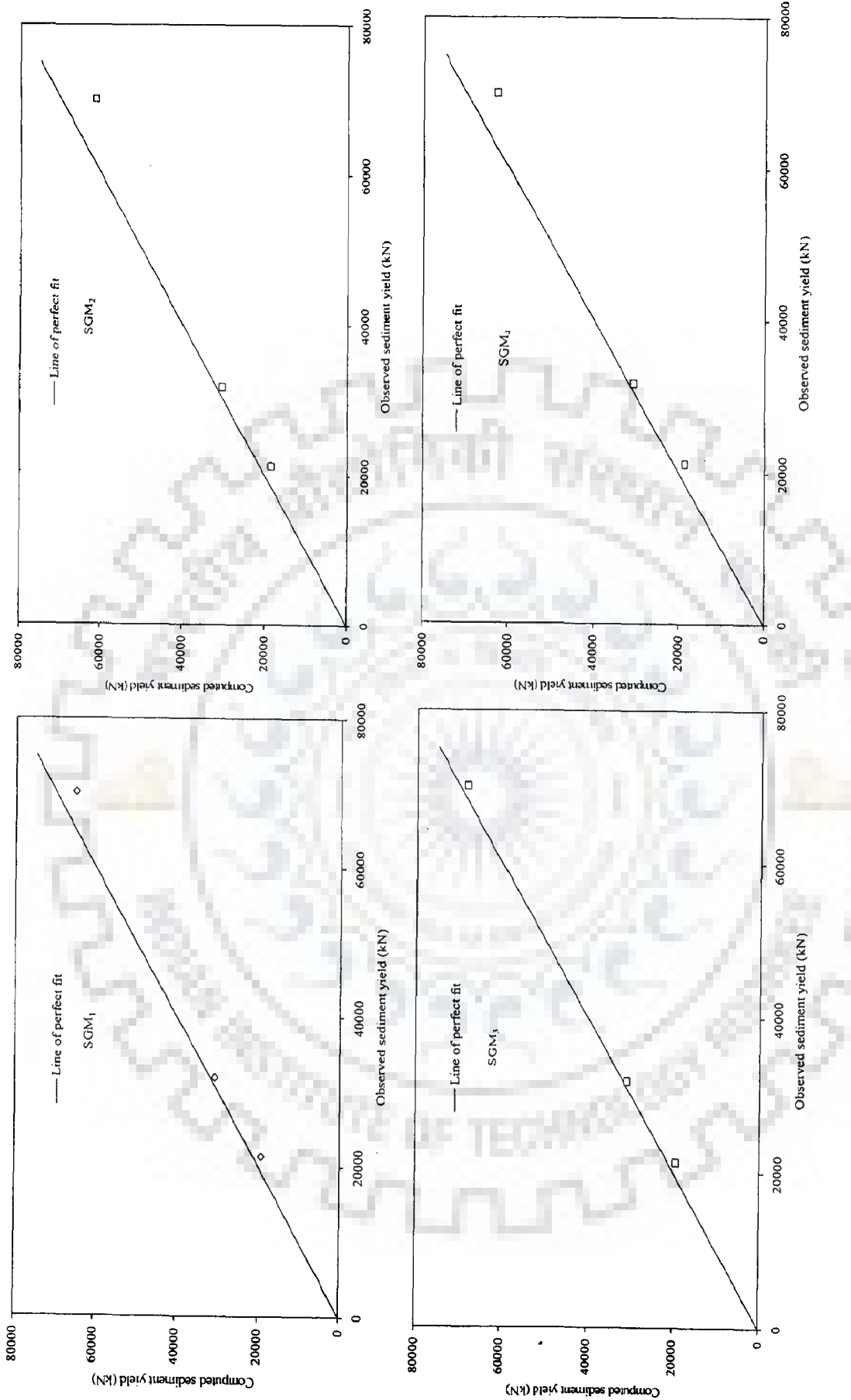


Fig. 7.5. Comparison between observed and computed sediment yield using SGM₁-SGM₄ for all storm events

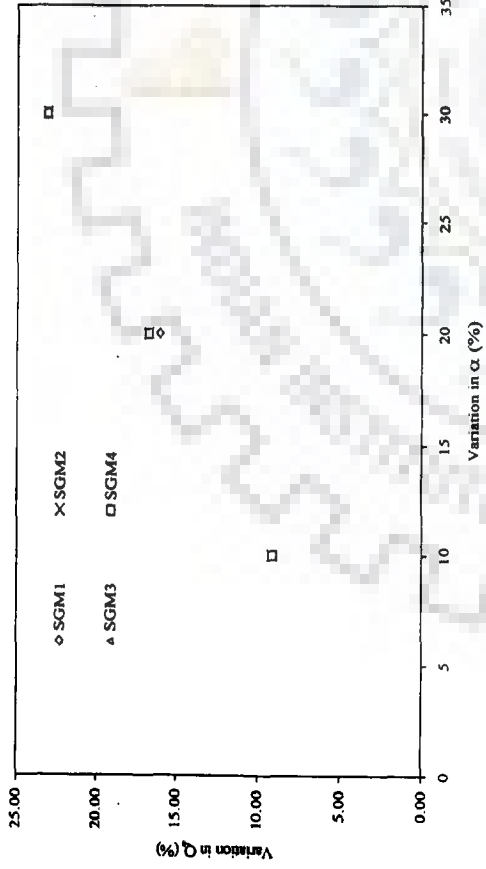


Fig.7.6. Models sensitivity to α

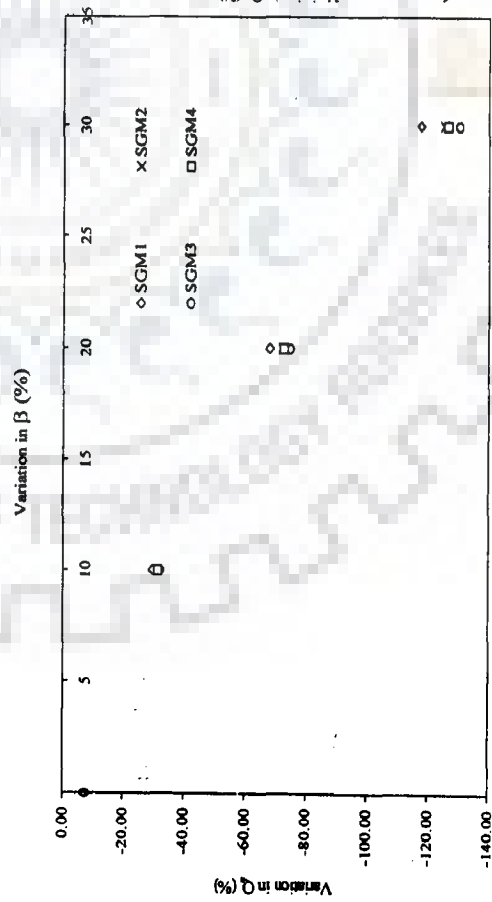
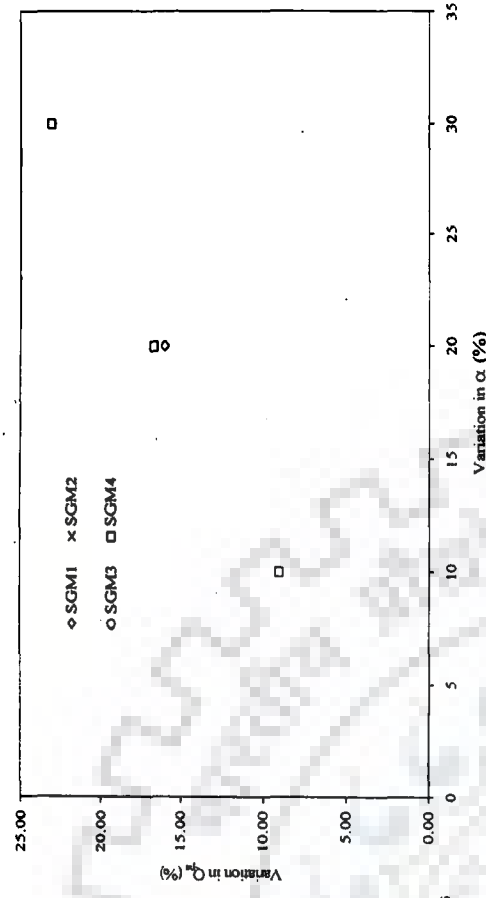


Fig. 7.7. Models sensitivity to β

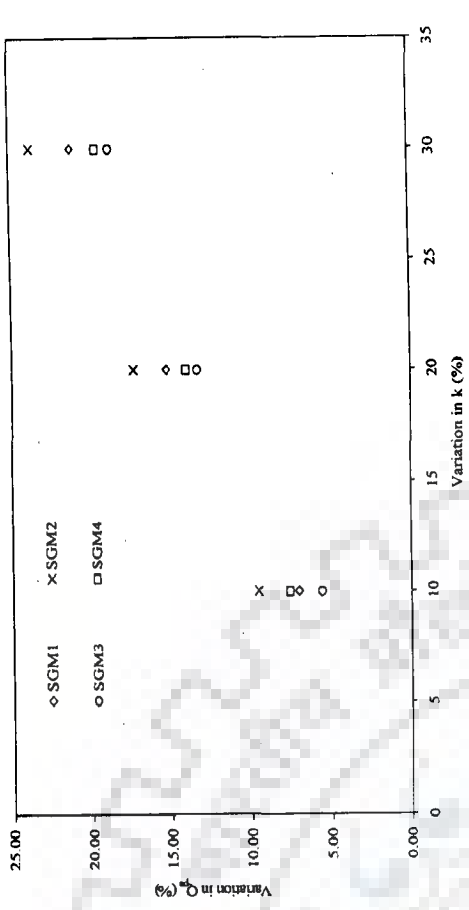


Fig.7.8. Models sensitivity to k

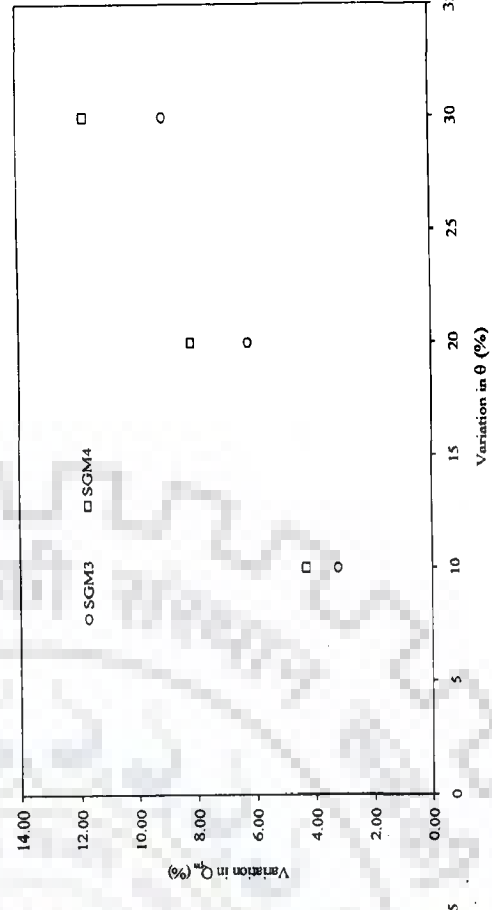


Fig.7.9. Models sensitivity to theta

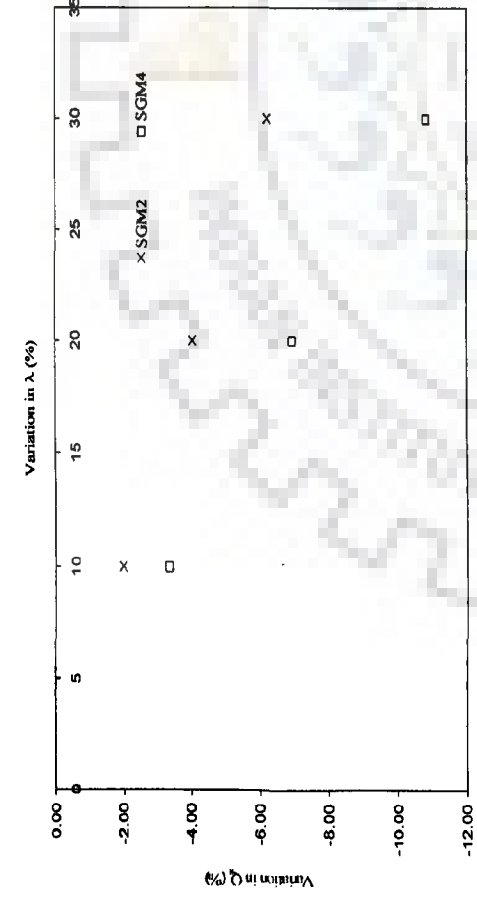
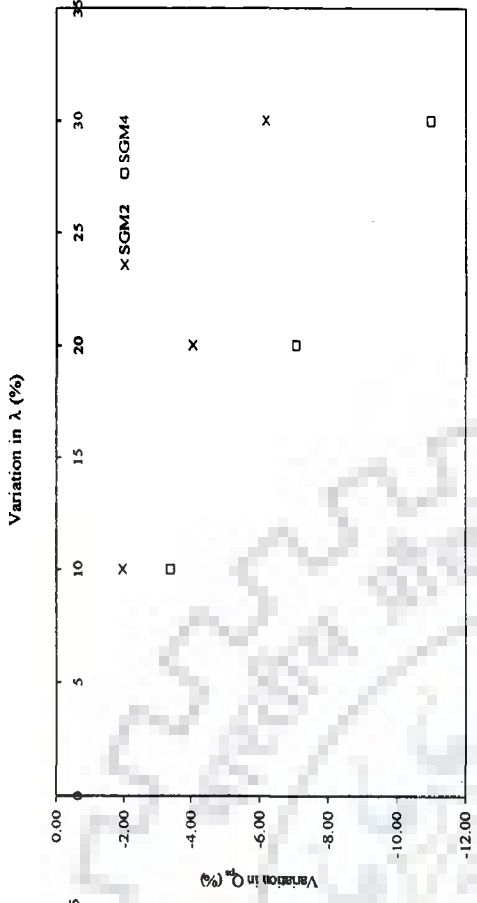


Fig.7.10. Models sensitivity to λ

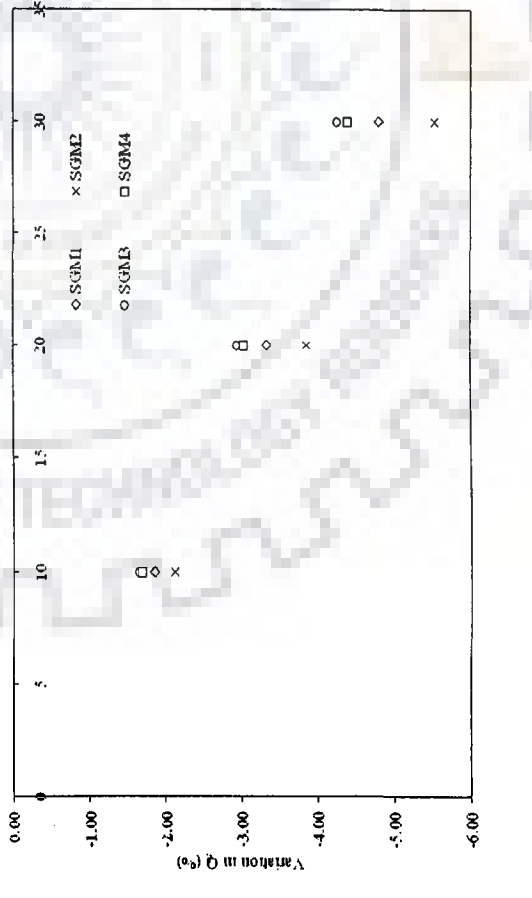
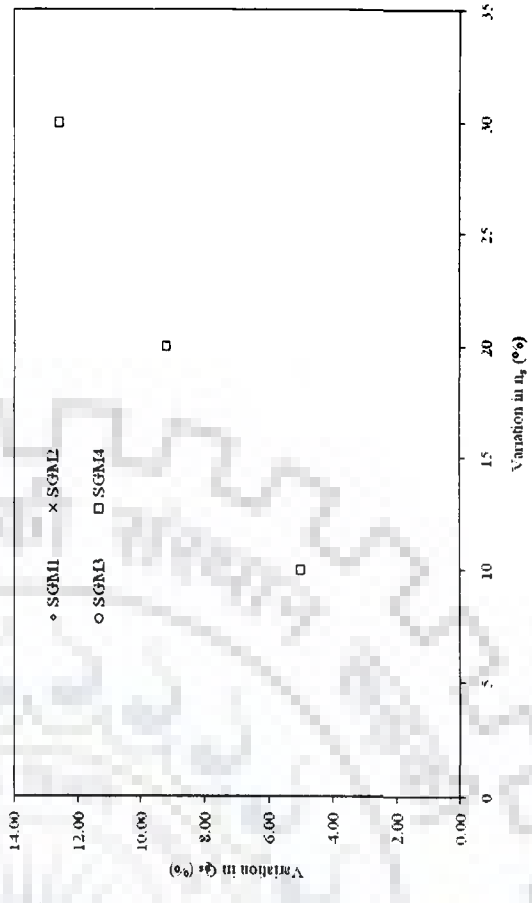


Fig.7.11. Models sensitivity to ν_s

7.5 FURTHER APPLICATION OF SGM₁

Since SGM₁ is the simplest of the four proposed sediment graph models, this model is further evaluated for its capability of sediment graph computations using the published data of Chaukhutia watershed of Ramganga reservoir catchment (Kumar and Rastogi, 1987; Raghuwanshi et al., 1994, 1996) . For application of SGM₁ model, six storm events were taken from the published data of Chaukhutia watershed of Ramganga reservoir catchment. The basic characteristics of sediment graph data are given in Table 3.5. Unit sediment graph data derived from Table 3.5 are given in Table 7.4. The SGM₁ model (Eq. 7.28) has the parameters α , β , k , and n_s . Eq. (7.46) was utilized to estimate the shape parameter (n_s) of IUSG sub-model for the selected events as given in Table 7.4. The rest of the parameters α , β , k , and A were estimated by using the non-linear Marquardt algorithm. The estimated optimum parameters values for Chaukhutia watershed are given in Table 7.5.

Similar to the above, the performance of SGM₁ model was evaluated on the basis of the (i) visual closeness of the observed and computed sediment graphs visually and (ii) goodness of fit (GOF) in terms of NS efficiency (Eq. 7.47) and relative error (RE) (Eqs. 7.50-7.52). For visual appraisal, the sediment graphs computed using SGM₁ model were compared with the observed sediment graphs as shown in Figs. (7.12)- (7.17). From these figures, it is observed that the computed sediment graph exhibits fair agreement with the observed graph. The results of total sediment yield computations for the six storm events are also depicted graphically in Fig. 7.18. Both the observed and computed data points falling close to the line of perfect fit indicate satisfactory model performance.

Further, the results of GOF criteria given by Eqs. (7.47) and (7.50)-(7.52) for all the events are shown in Table 7.6. The results indicate that RE for total sediment outflow and peak sediment flow rate estimates vary from 2.49 to 10.04% and 12.59 to 16.56%, respectively. Though, the error in peak sediment flow rate estimation is on higher side, it may be safely accepted because even the more elaborate process-based soil erosion models are found to produce results with still larger errors (Jain et al., 2005). Table 7.6 also shows the GOF in terms of NS efficiency for the considered storm events. NS efficiency varies from 90.52 to 95.41%, indicating a satisfactory performance of the model for sediment graph computations.

Table 7.4 Unit sediment graph characteristics of storm events of Chaukhutia watershed

Date of storm	q_{ps} (tons/hr/tons)	t_{ps} (hr)	β_s	n_s
July 17, 1983	0.380	2	0.760	4.79
August 21/22, 1983	0.418	2	0.836	5.55
July 15, 1984	0.397	2	0.794	5.12
August 18/19, 1984	0.404	2	0.810	5.27
September 1/2, 1984	0.390	2	0.780	4.99
September 17/18, 1984	0.410	2	0.820	5.39

Table 7.5 Optimized parameter values for Chaukhutia watershed

Date of storm	Model Parameters			
	α	β	k	A (tons/km ²)
July 17, 1983	0.530	0.351	0.029	26.66
August 21/22, 1983	0.727	0.701	0.030	40.78
July 15, 1984	0.735	0.721	0.030	62.69
August 18/19, 1984	0.714	0.663	0.030	38.14
September 1/2, 1984	0.388	0.425	0.030	19.64
September 17/18, 1984	0.587	0.781	0.030	29.34

Table 7.6 Goodness of fit statistics

Date of storm	Total Sediment out flow (tons)		RE _(Q_s) (%)	Peak sediment out flow rate (tons/hr)		RE _(Q_{ps}) (%)	NS Efficiency (%)
	Q _s	Q _{sc}		Q _{ps}	Q _{psc}		
July 17, 1983	2698	2481	8.04	1025	893	12.88	92.91
August 21/22, 1983	2070	1992	3.77	875	748	14.51	93.48
July 15, 1984	3145	2970	5.56	1250	1043	16.56	90.52
August 18/19, 1984	2105	2041	3.04	850	743	12.59	95.34
September 1/2, 1984	1205	1084	10.04	475	397	16.42	93.65
September 17/18, 1984	963	939	2.49	392	339	13.52	95.41

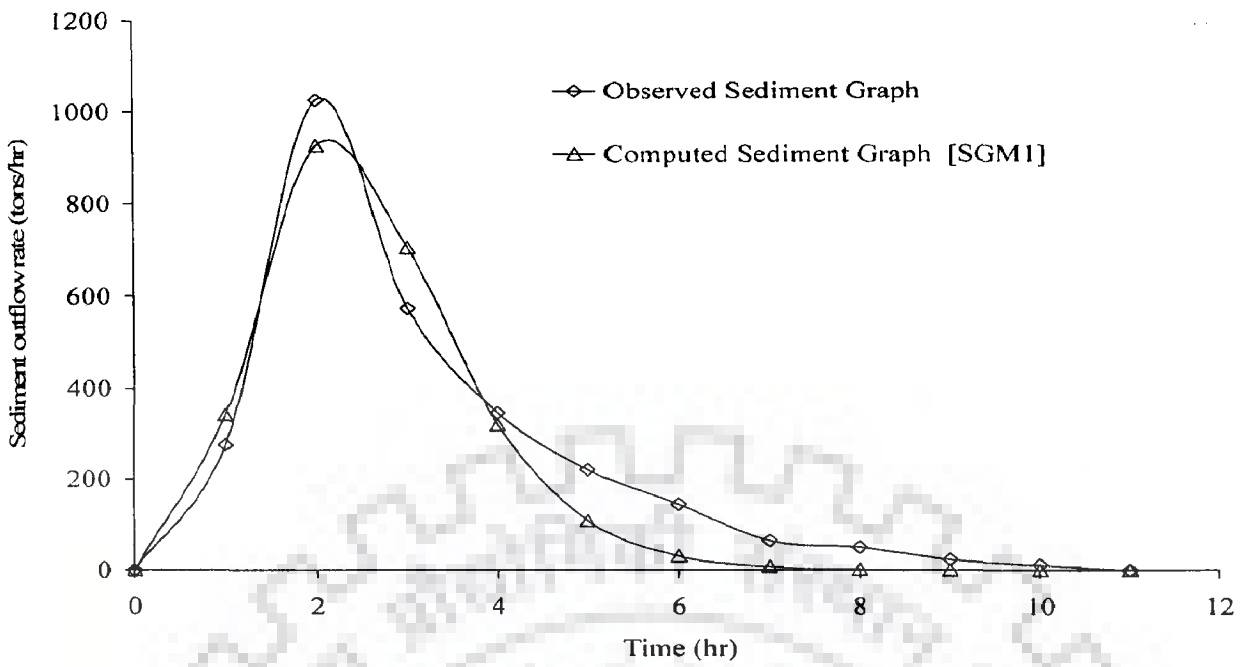


Fig. 7.12 Comparison of observed and computed sediment graphs for the storm of July 17, 1983.

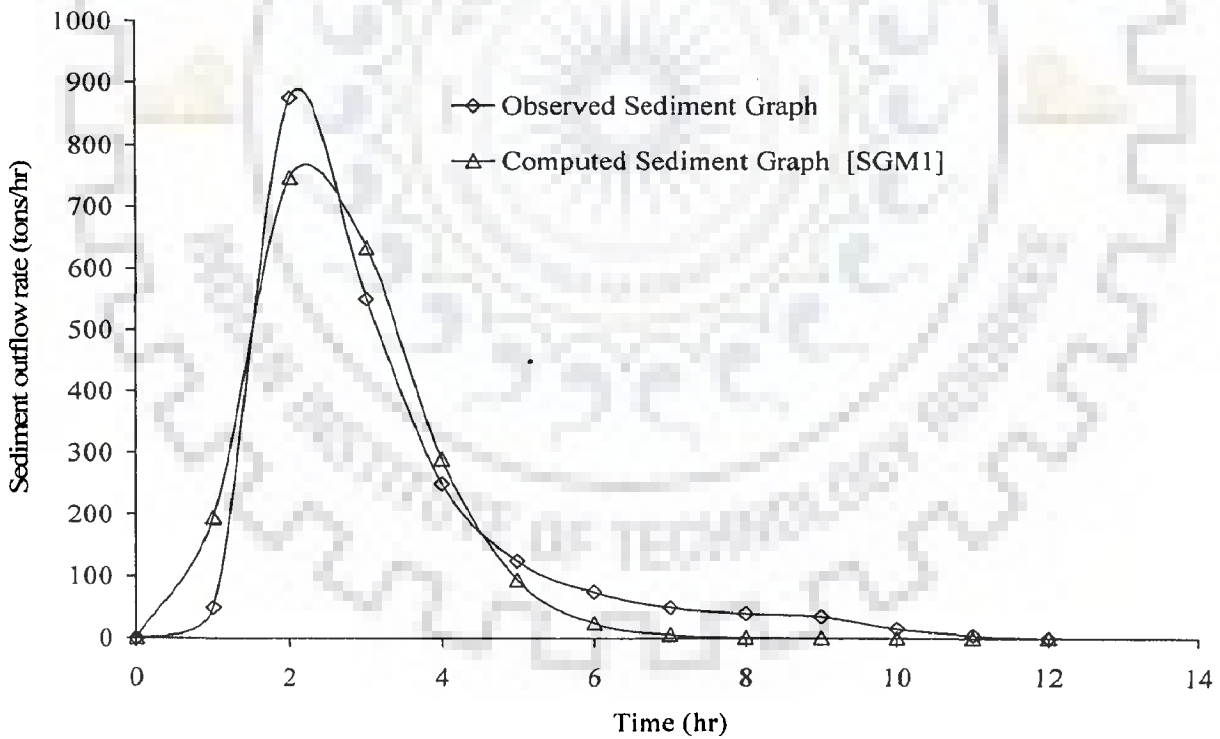


Fig. 7.13 Comparison of observed and computed sediment graphs for the storm of August 21/22, 1983.

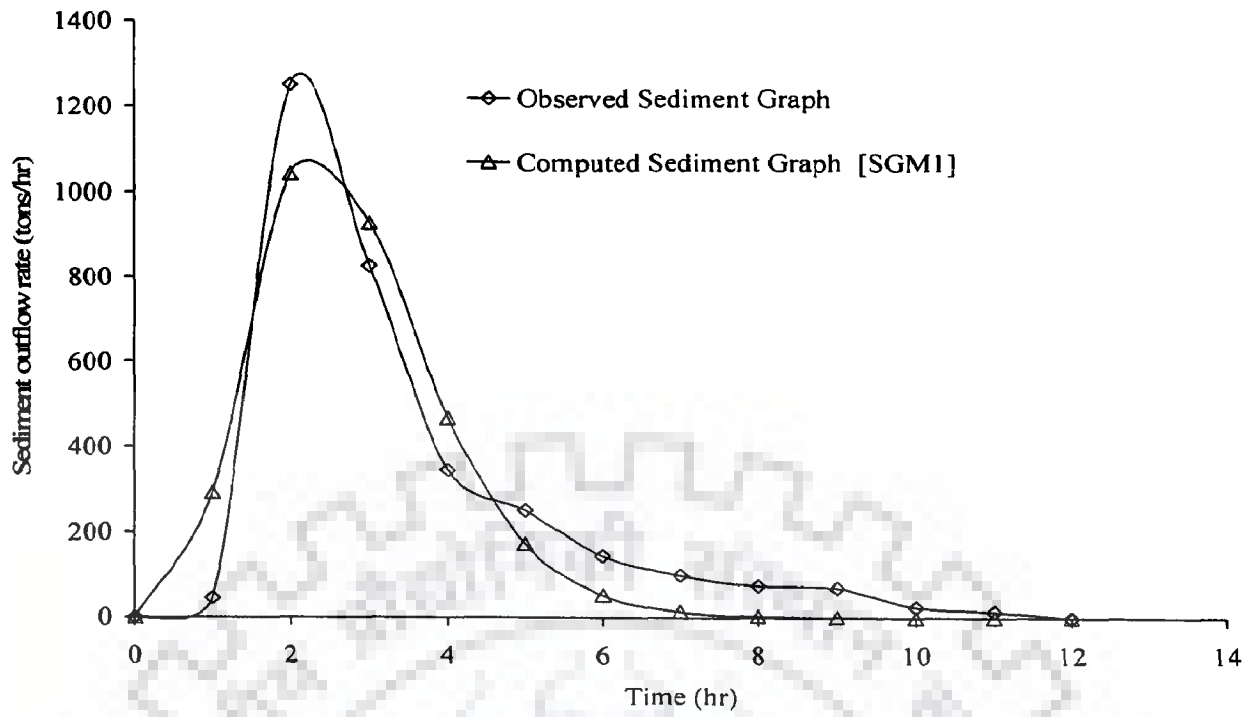


Fig. 7.14 Comparison of observed and computed sediment graphs for the storm of July 15, 1984

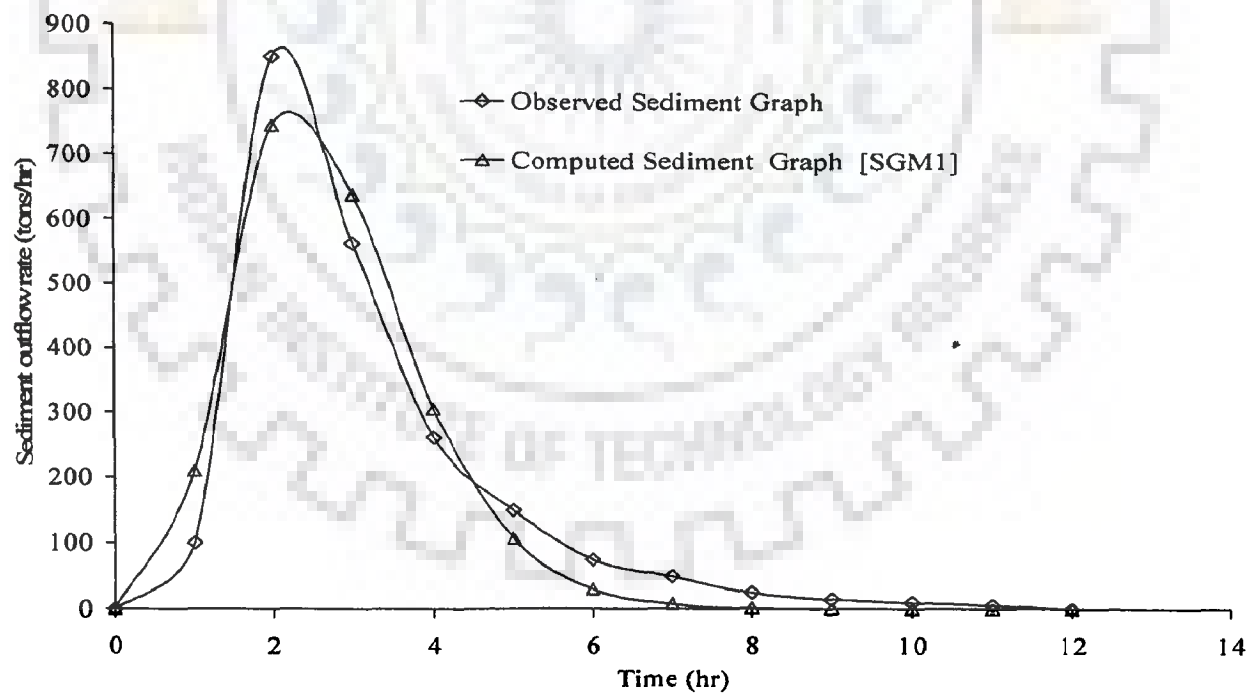


Fig. 7.15 Comparison of observed and computed sediment graphs for the storm of August 18/19, 1984.

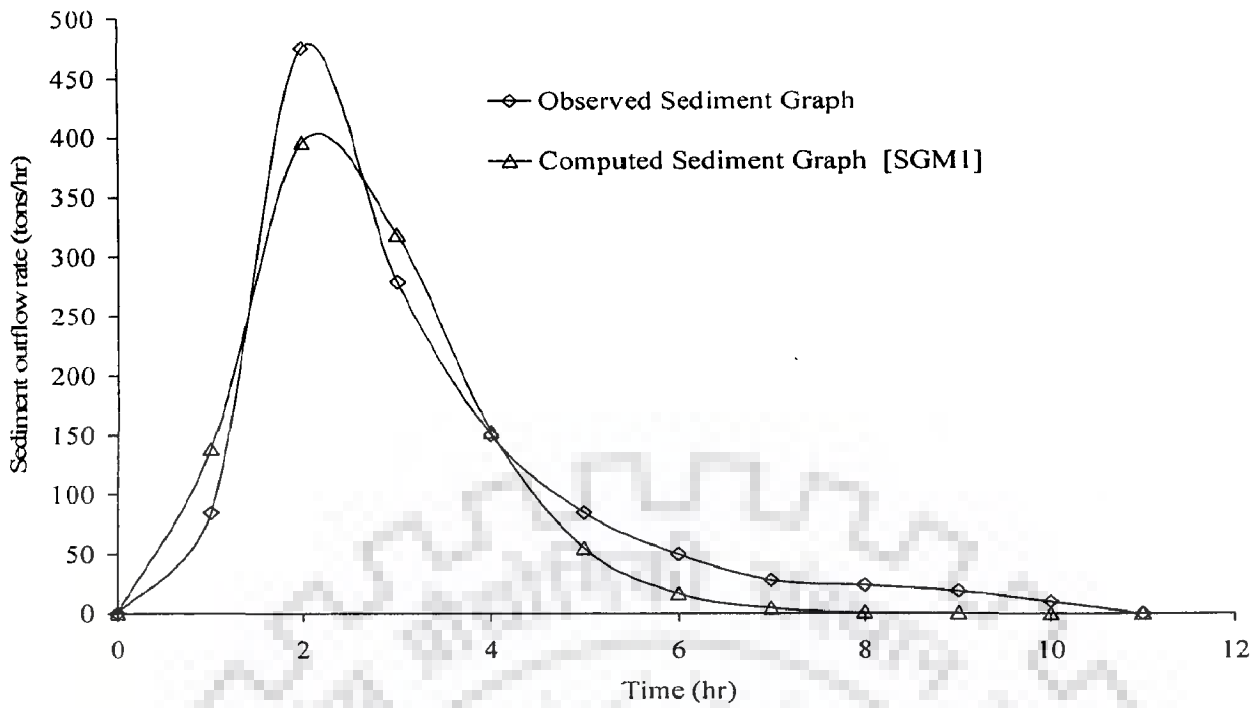


Fig. 7.16 Comparison of observed and computed sediment graphs for the storm of September 1/2, 1984

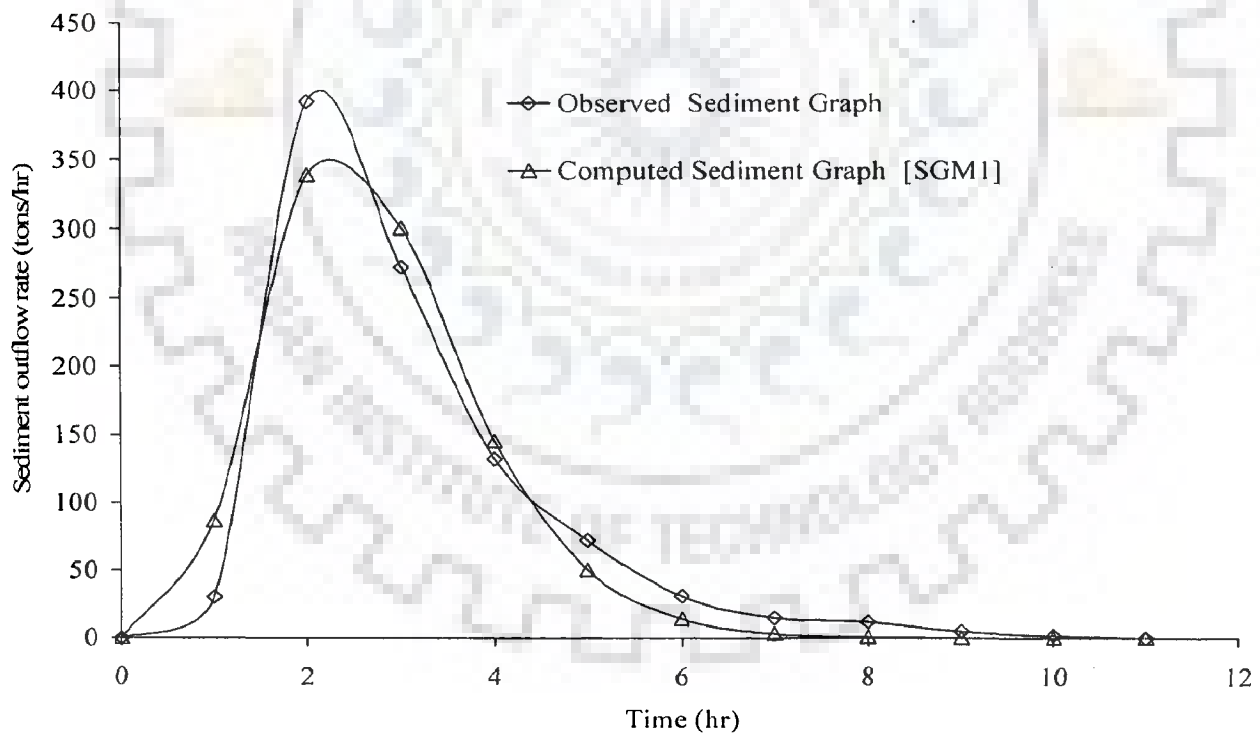


Fig. 7.17 Comparison of observed and computed sediment graphs for the storm of September 17-18, 1984

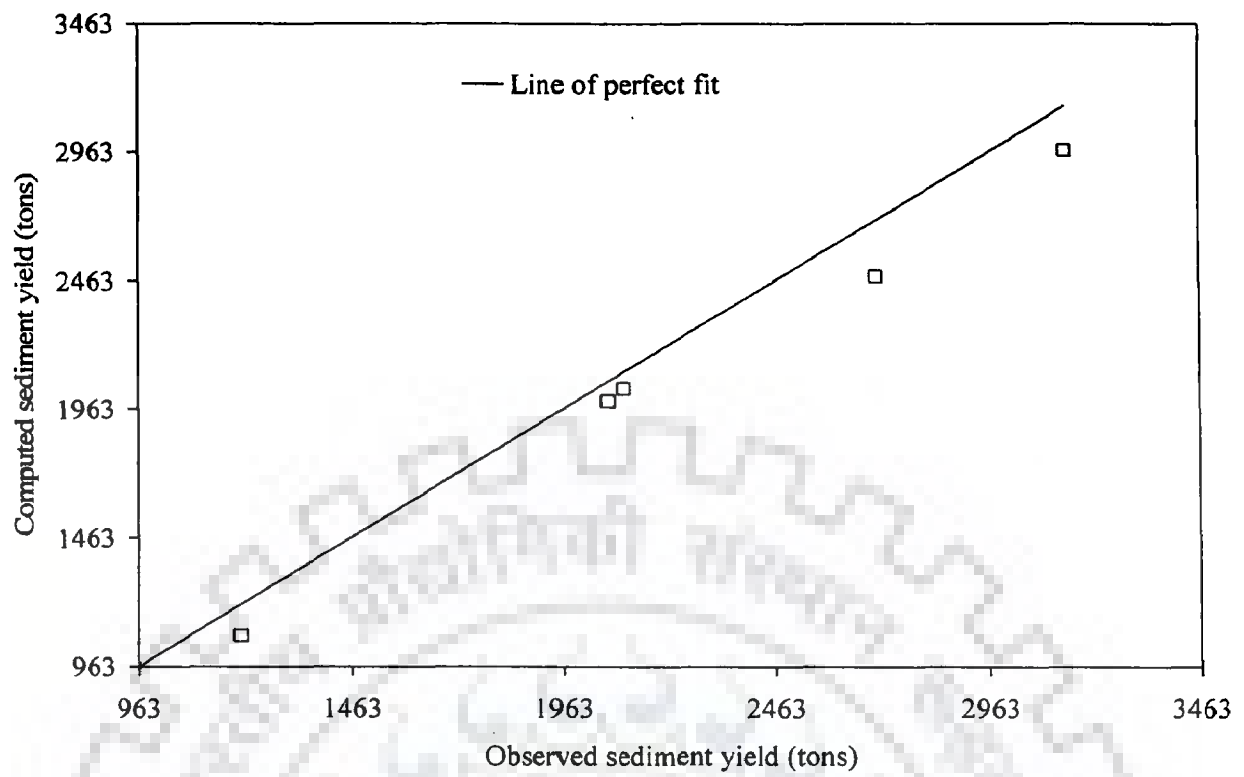


Fig. 7.18 Comparison between observed and computed total sediment outflow for all storm events.

7.6 SUMMARY

In the present study, conceptually sound and hydrologically improved sediment graph models were proposed based on (i) Nash model-based IUSG, (ii) SCS-CN method, and (iii) Power law. The proposed procedure eliminated the routine regression procedure to estimate the mobilized sediment. The proposed models explicitly considered the changes in soil type, land use, hydrologic condition, antecedent moisture in their formulation. The study revealed that the proposed models could be used for computing sediment graphs as well as the total sediment yield. Higher values of model's efficiencies and low relative errors further indicated the suitability of the proposed models for computation of sediment graphs and total sediment outflow from Nagwan watershed (India). These models also accounted for the initial soil moisture and initial abstraction coefficient, and the results indicated their significance in sediment graph based analysis in particular and sediment yield modeling in general. These models were however quite sensitive to parameter β . Further application of SGM₁ model showed its enhanced performance ($RE_{Q_s} < 10\%$, $RE_{Q_{ps}} < 17\%$, NS efficiency $> 91\%$). Higher values of model efficiency and low relative error further strengthened the suitability of model for computation of sediment graphs and total sediment outflow.

CHAPTER-8

SUMMARY AND CONCLUSIONS

Rainfall-runoff modeling is integral to water resources planning, development, and management; and a multitude of models are available in hydrologic literature to address the related issues. Among the popular event-based models, the SCS-CN method has experienced myriad applications in estimation of direct runoff for a given storm rainfall event. This is perhaps the only methodology available in hydrologic literature which considers the major runoff producing watershed characteristics in runoff computations. A literature review indicates that the methodology has been applied successfully to address various hydrologic problems including those which were not originally intended. Similarly, the SUH methods are placed at the apex among the hydrologic models available for estimation of flood hydrograph with limited data availability conditions, and for ungauged catchments. In a similar vein, the sediment graph models are widely used for estimation of time distributed sediment yield. These models play a significant role in water quality modeling. Further, these are useful in evaluation of the effectiveness of watershed management programs and study of depletion of lakes and reservoirs and non-point source pollution. The increased awareness of environmental quality and the desire to control non-point source pollution have significantly increased the need for time distributed sediment yield estimates, for sediment is not only a pollutant but also a carrier of pollutants, such as radioactive material, pesticides, and nutrients.

This study was undertaken to explore the new/modified or improved versions of SCS-CN methodology, SUH methods, and sediment graph models based on a stronger mathematical background and hydrologically more rational approach to perform their prescribed tasks successfully and efficiently. In this chapter, each of these methodologies/models is summarized and concluded briefly.

8.1 REVISED SOIL MOISTURE ACCOUNTING PROCEDURE IN SCS-CN METHODOLOGY

Various improvements/modifications to the existing SCS-CN methodology have been suggested in literature in the recent past. However, there are still some issues that need to be explored for better results. The accounting of soil moisture in the SCS-CN methodology is one of them. Though it was addressed earlier by Williams and LaSeur (1976) and Mishra et al. (2004a) to account for the variability of antecedent rainfall and associated soil moisture amount in terms of antecedent moisture condition (AMC), a concrete mathematical formulation and its inclusion in the existing SCS-CN methodology was provided by Michel et al. (2005) only. This work addresses not only the soil moisture accounting (SMA) procedure but also corrects the SCS-CN method for its parameterization. To overcome the inconsistencies associated with the existing SCS-CN method, they modified the SCS-CN method by introducing an intrinsic parameter S_a (a function of I_a and V_0) which is constant for a watershed. However, their model also inherits some structural inconsistencies, specifically the whole procedure relies on the existing SCS-CN method, which in itself does not account for the soil moisture directly in its basic proportionality concept or $C = S_r$ concept (Mishra and Singh, 2003a). Secondly, the methodology does not provide an expression for estimation of V_0 . Hence the present study revisited the existing SCS-CN method for its underlying SMA procedure, leading to a revised version of the Michel et al. model. Using the data of 35 watersheds of United States, the event-aggregated proposed model, Michel et al. model, and the original SCS-CN method were compared for their performance. In these applications the proposed procedure is found to be more accurate than the others, and the original SCS-CN method performed the poorest of all. The results indicated the appropriateness of inclusion of initial soil moisture in the $C = S_r$ concept in particular and in SCS-CN proportionality hypothesis in general. Based on this revised SMA procedure, the present study also proposes a continuous hydrologic simulation model parallel to Michel et al model. An application of both the models to daily rainfall-runoff data of Hemavati watershed (India) shows that both the models perform equally well in continuous hydrologic simulation; the proposed model however performs marginally better than the Michel et al. model.

8.2 SYNTHETIC UNIT HYDROGRAPH (SUH) METHODS

8.2.1 Extended Hybrid Model (EHM)

The notion of synthetic unit hydrograph (SUH) is of major interest in surface water hydrology. Probably it was the paucity of observed rainfall-runoff data which motivated the hydrologic community and practicing engineers towards the use of SUH methods. Of late, Bhunya et al. (2005) introduced a hybrid model (HM) for SUH derivation. Though the HM model is an improvement over the widely used Nash (1957) model, there are still some points of concern as follows: (i) it ignores the concept of translation, which is essential for describing a dynamic system; and (ii) it lacks for generality. The present study attempts to provide an improved version of HM model. Consequently, a conceptually sound and theoretically improved extended hybrid model (EHM), which is a generalized form of the Cascaded (Nash, 1957) and HM models, is proposed. The proposed EHM model explicitly considers the cascaded approach of Nash (1957) and the hybrid approach of Bhunya et al. The application of EHM and HM models to the short-term data of five catchments (small to medium) ranging from 21 km² to 452.25 km² reveals that the EHM performs better than the HM model in terms of both standard (STDER) and relative errors (RE), particularly for the larger watersheds. The Nash model performs poorer than both EHM and HM models. The sensitivity analysis of EHM for the dependability of peak flow rate (Q_p) on parameters T, K_1 and K_2 shows Q_p to be more sensitive to K_2 than either K_1 or T. Furthermore, Q_p is less sensitive to translation for smaller area, but more for the larger area, and more to both K_1 and K_2 than T (or $Q_p(K_2) > Q_p(K_1) > Q_p(T)$) for both smaller as well as larger catchments.

8.2.2 Chi-square and Fréchet Distributions for SUH derivation

The use of probability distribution functions (pdfs) as synthetic unit hydrographs (SUH) has a long successful history in surface water hydrology. The similarity between pdf of a distribution with area under the pdf curve to be unity and a conventional unit hydrograph are considered to be the important features of a pdf for derivation of SUH. Building on the idea that a functional relationship between the important points on instantaneous unit

hydrograph (IUH) and catchment characteristics exists, Rodriguez-Iturbe and Valdes (1979) developed analytical expressions for salient points of UH, viz., peak flow rate (q_p) and time to peak (t_p), coupling the catchment geomorphology using Horton order ratios. Utilizing these relationships, Rosso (1984) parameterized the Nash model, which represents Gamma pdf, in terms of Horton order ratios.

Based on the work of Rodriguez-Iturbe and Valdes (1979) and Rosso (1984), the present work parameterized one-parameter Chi-square and two-parameter Fréchet distributions in terms of Horton order ratios for SUH derivation. The study specifically proposes the analytical methods for parameter estimation of the two distributions. The suitability of proposed analytical methods to both the distributions was checked using the random number generation scheme and it was found that the proposed analytical methods could be used successfully for parameter estimation. Further, an attempt was made for the possible similarity among the three distributions, two-parameter Fréchet distribution (2PFD), one parameter Chi-square distribution (CSD), and two-parameter Gamma distribution (2PGD). Finally, the proposed models were applied to the short-term rainfall-runoff data of two Indian catchments for limited data availability conditions. The results show that SUHs obtained by 2PFD and one parameter CSD are comparable with those due to 2PGD method (Rosso, 1984). For one parameter CSD, the results of the sensitivity analysis show that the non-dimensional term β increases with an increase in m or τ , and vice-versa. Similarly, for 2PFD, it was found that the non-dimensional term β is more sensitive to location parameter α than the shape parameter c . An analytical diagnosis of 2PGD and 2PFD as SUH shows a similarity in behavior of the distribution parameters.

8.3 SCS-CN METHOD BASED SEDIMENT GRAPH MODELS

The sediment yield from a watershed is the output form of an erosion process, and is difficult to estimate as it arises from a complex interaction of various hydro-geological processes. However, the conceptual sediment graph models are widely used for the purpose. The sediment graph models provide not only the time distribution of sediment yield but also the total sediment yield due to a particular storm event from a catchment. The present study is a step ahead towards development of new conceptual sediment graph models based on

three popular models/methods (here termed as sub-models) as: (i) Nash based IUSG model; (ii) SCS-CN method; and (iii) Power law. The proposed sediment graph models implicitly consider the major runoff and, in turn, the sediment yield producing watershed characteristics such as soil type, land use, hydrologic condition, antecedent moisture, and rainfall characteristics. Four sediment graph models, SGM₁ through SGM₄ corresponding to $V_0 = 0$ (i.e. initially fully dry condition of the watershed, dependent on the antecedent rainfall) and $I_a = 0$ (i.e. initially ponded situation, dependent on the initial amount of rainfall of the storm under consideration), $V_0 = 0$ and $I_a \neq 0$, $V_0 \neq 0$ and $I_a = 0$, and $V_0 \neq 0$ and $I_a \neq 0$, respectively, were proposed and applied to the observed short-term sediment yield data of Nagwan watershed. In these models, SGM₁ is the simplest one, and SGM₄ the most complex on the basis of number of parameters. Based on goodness of fit (GOF) criteria, the results due to the proposed sediment graph models matched closely with the observed sediment graphs. Similarly, the total sediment yield computed by the models SGM₁-SGM₄ was in close agreement with the observed sediment yield for the three storm events, showing a satisfactory model performance.

Further, the efficiency of models increased with incorporation of initial abstraction in model formulation, but the relative error in Q_s and Q_{ps} decreased with incorporation of initial soil moisture. In general, the results indicated both the initial soil moisture and initial abstractions to play a significant role in such sediment graph based studies. The sensitivity analysis of these models showed that Q_s and Q_{ps} were most sensitive to parameter β , followed by α , k , n , θ , and λ . The workability of simplest SGM₁ model was further evaluated using the short-term sediment yield data of Ramganga catchment. The resulting higher values of model efficiencies and lower values of RE of Q_{ps} and Q_s further strengthened the suitability of the proposed model for computation of time distributed sediment yield and total sediment yield.

8.4 MAJOR RESEARCH CONTRIBUTIONS OF THE STUDY

Popular and extensively used SCS-CN method, SUH methods, and sediment graph models were critically reviewed for their behavior, structure, and realm of applications, and the inconsistencies identified. Consequently, the study attempted to propose the

improved/modified versions of SCS-CN method, SUH methods, and sediment graph models based on stronger mathematical foundation and hydrologically more realistic perception. The major research contributions of the present study can be summarized as follows:

1. The revised SMA procedure of SCS-CN methodology led to the development of (i) an event-based SMA-inspired SCS-CN model and (ii) a long-term SMA-inspired SCS-CN model. The revised procedure has SMA accountability in its basic proportionality concept or $C = S_r$ concept, and it performed much better than those of Michel et al. and existing SCS-CN method.
2. The proposed EHM model incorporates the concept of translation and considers the cascaded approach of Nash (1957) and hybrid approach of Bhunya et al. (2005) for SUH derivation. The diagnosis of the proposed general expression of EHM model shows that the Nash (1957) and HM (Bhunya et al., 2005) models are special cases of the EHM model, and thus, EHM is an improvement over the widely used Nash and HM models.
3. Two probability distribution functions (pdf), viz., one-parameter Chi-square distribution (CSD) and two-parameter Fréchet distribution (2PFD) are explored for SUH derivation using Horton order ratios for limited data availability condition. An analytical but simple procedure is developed for parameter estimation of pdfs. The two pdfs are analyzed for their possible similarity with two-parameter Gamma distribution (2PGD) model. Both the pdfs and the widely used (2PGD) model performed equally well.
4. Four new sediment graph models (SGM_1 - SGM_4) based on Nash model-based IUSG, SCS-CN method, and Power law are proposed for computing sediment graphs (temporal sediment flow rate distribution) as well as total sediment yield. The models comprise of the mobilized sediment estimation by SCS-CN method and Power law and consider the rainfall intensity, soil type, land use, hydrologic condition, and

antecedent moisture, and thus, physically more plausible than the common and less accurate regression type relations. The proposed SGM_2 is recommended for field use.

8.5 FUTURE SCOPE

In spite of present research endeavors, there exists a scope for future research. For example, the revised SMA procedure can be attempted for sediment yield modeling; the expressions for V_0 and S_a of the revised SMA-inspired event-based and long-term SCS-CN models can be further refined on the basis of rainfall and soil characteristics; the extended hybrid model (EHM) with hybrid units > 2 , a parallel combination of hybrid units of EHM model, and EHM model coupled with GIUH approach can be attempted for SUH derivation. The last can be applied for sediment graph based studies. More pdfs, viz., two parameter inverse gamma distribution, three parameter beta distribution, three parameter two sided power distribution, two parameter Weibull distribution can be explored for SUH derivation and the proposed sediment graph models can be attempted for modeling sediment yield from ungauged watersheds. Furthermore, the pdfs can be explored for their possible use in synthetic sediment graph derivation for ungauged catchments.

REFERENCES

1. Abbott, M. B., Bathurst, J. C., Cunge, J. A., O'Connell, P. E., and Rasmussen, J. (1986b). An introduction to the European Hydrologic System-Systeme Hydrologique Europeen, SHE, 2: Structure of a physically-based, distributed modeling system. *J. Hydrology*, **87**, 61– 77.
2. Abbott, M. B., Bathurst, J. C., Cunge, J. A., O'Connell, P. E., and Rasmussen, J. (1986a). An introduction to the European Hydrologic System-Systeme Hydrologique Europeen, SHE, 1: History and philosophy of a physically-based, distributed modeling system. *J. Hydrology*, **87**, 45–59.
3. Abramowitz, M., and Stegun, I. A. (1964). *Handbook of Mathematical Functions*, Dover, New York.
4. Aksoy, H., and Kavvas, M. L. (2005). A review of hillslope and watershed scale erosion and sediment transport models. *CATENA*, **64**, 247-271.
5. Allam, M. N., and Balkhair, K. S. (1987). Case study evaluation of geomorphologic instantaneous unit hydrograph. *Water Resources Management*, **1**, 267-291.
6. Al-Wagdany, A. S., and Rao, A. R. (1997). Estimation of velocity parameter of geomorphologic instantaneous unit hydrograph. *Water Resources Management*, **11**, 1-16.
7. Anderson, H. W. (1954). Suspended sediment discharge as related to stream flow, topography, soil and land use. *Trans. American Geophysical Union*, **35** (2), 268-281.
8. Anderson, H. W. (1962). Current research on sedimentation and erosion in California wildlands. *International Association of Scientific Hydrology*, **59**, 173-183.
9. Andrews, R. G. (1954). The use of relative infiltration indices in computing runoff (unpublished), Soil Conservation Service, Fort Worth, Texas, p. 6.
10. Arnold, J. R., Srinivassan, R., Mutiah, R. S., and Williams, J. R. (1998). Large area hydrologic modeling and assessment Part I: Model development. *J. American Water Resources Association*, **34**, 73-89.
11. Aron, G., and White, E. L. (1982). Fitting a gamma distribution over a synthetic unit hydrograph. *Water Resources Bulletin*, **18** (1), 95–98.

12. Aron, G., Miller, A. C. Jr., and Lakatos, D. F. (1977). Infiltration formula based on SCS curve number. *J. Irrigation and Drainage Division, ASCE*, **103** (IR4), 419-427.
13. ASCE (1970). Sediment sources and sediment yields. *J. Hydraulics Division, ASCE*, **96** (HY6), 1283– 1329.
14. ASCE (1996). *Handbook of Hydrology*, ASCE Manual and Report on Engineering Practice No. 28, New York.
15. Ayyub, B. M., and McCuen, R.H. (1997). *Probability, Statistics and Reliability for Engineers and Scientists*, CRC Press, Boca Raton, New York.
16. Beasley, D. B., Huggins, L. F., and Monke, E. J. (1980). ANSWERS—A model for watershed planning. *Trans. American Society of Agricultural Engineers*, **23**, 938–944.
17. Bennett, J. P. (1974). Concepts of mathematical modelling of sediment yield. *Water Resources Research*, **10**, 485–492.
18. Bernard, M. (1935). An approach to determinate stream flow. *Trans. ASCE*, **100**, 347–362.
19. Bérod, D. D., Singh, V. P., Devred, D., and Musy, A. (1995). A geomorphologic non-linear cascade (GNC) model for estimation of floods from small alpine watersheds. *J. Hydrology*, **166**, 147–170.
20. Bhaskar, N. R., Parida, B. P., and Nayak, A. K. (1997). Flood estimation for ungauged catchments using the GIUH. *J. Water Resources Planning and Management, ASCE*, **123** (4), 228-238.
21. Bhunya, P. K., Mishra, S. K., and Berndtsson, R. (2003b). Simplified two parameter gamma distribution for derivation of synthetic unit hydrograph. *J. Hydrologic Engineering, ASCE*, **8** (4), 226-230.
22. Bhunya, P. K. (2005). *Statistical Approach for estimation of Design Flood in Ungauged catchments*. Unpublished Ph.D. Thesis, Dept. of Civil Engg., Indian Institute of Technology Roorkee, India.
23. Bhunya, P. K., Berndtsson, R., Ojha, C. S. P., and Mishra, S. K. (2007a). Suitability of Gamma, Chi-square, Weibull and Beta distributions as synthetic unit hydrographs. *J. Hydrology*, **334**, 28-38.

24. Bhunya, P. K., Ghosh, N. C., Mishra, S. K., Ojha, C. S. P. and Berndtsson, R. (2005). Hybrid model for derivation of synthetic unit hydrograph. *J. Hydrologic Engineering, ASCE*, **10** (6), 458-467.
25. Bhunya, P. K., Mishra, S. K., and Berndtsson, R. (2003a). Discussion of approach to confidence interval estimation for curve numbers” by McCuen, R. H., *J. Hydrologic Engineering, ASCE*, **8** (4), 232-235.
26. Bhunya, P. K., Singh, P. K., and Mishra, S. K. (2007b). Fréchet and chi-square distributions combined with Horton order ratios to derive a synthetic unit hydrograph. *Hydrological Sciences J.* (Accepted).
27. Bhunya, P.K, Mishra, S. K., Ojha, C. S. P., and Berndtsson, R. (2004) Parameter estimation of beta distribution for unit hydrograph derivation. *J. Hydrologic Engineering, ASCE*, **9** (4), 325-332.
28. Bonta, J. V. (1997). Determination of watershed curve number using derived distributions. *J. Irrigation and Drainage Engineering, ASCE*, **123** (1), 234-238
29. Boszany, M. (1989). Generalization of SCS curve number method. *J. Irrigation and Drainage Engineering, ASCE*, **115** (1), 139-144.
30. Box, G. E. P. and Jenkins, G. M. (1976). *Time Series Analysis-Forecasting and Control*. Holden-Day, San Francisco, California.
31. Boyd, M. J., Bates, B. C., Pilgrim, D. H., and Cordery, I. (1987). WBNM: A general runoff routing model—Programs and user manual, Water Research Laboratory Rep. No. 170, Univ. of New South Wales, Kensington, Australia.
32. Boyd, M. J., Pilgrim, D. H., and Cordery, I. (1979). A storage routing model based on catchment geomorphology. *J. Hydrology*, **42** (3-4), 209-330.
33. Bras, R. L. (1990). *Hydrology: An Introduction to Hydrologic Science*, Addison-Wesley Publishing Co., N.Y.
34. Bruce, R. R., Harper, L. A., Leonard, R. A., Snyder, W. M., and Thomas, A. W. (1975). Model for runoff of pesticides from small upland watersheds. *J. Environmental Quality*, **4** (4), 541-548.
35. Cazier, D. J., and Hawkins, R. H. (1984). Regional application of the curve number method, *Water Today and Tomorrow, Proc. ASCE, Irrigation and Drainage Division Special Conference, ASCE, New York, N. W.*, p. 710.

36. Chaves, P., and Kojiri, T. (2007). Deriving reservoir operational strategies considering water quantity and quality objectives by stochastic fuzzy neural networks. *Advances in Water Resources*, **30** (5), 1329-1341.
37. Chen, C. (1982). An evaluation of the mathematics and physical significance of the Soil Conservation Service Curve Number procedure for estimating runoff volume. Proc., Int. Symp. on Rainfall-Runoff Relationship, V. P. Singh (Ed.), water Resources Publications, Littleton, Colo., pp. 387-418.
38. Chen, V. J. and Kuo, C. Y. (1986). A study of synthetic sediment graphs for ungauged watersheds. *J. Hydrology*, **84**, 35-54.
39. Choi, J.-Y., Engel, B. A., and Chung, H. W. (2002). Daily stream flow modeling and assessment based on curve number technique. *Hydrological Processes*, **16**, 3131-3150.
40. Chow, V. T., Maidment, D. R., and Mays, L. W. (1988). *Applied Hydrology*, McGraw Hill, Inc., New York, p. 572.
41. Chow, V.T. (1964). *Handbook of Applied Hydrology*, McGraw-Hill Book Co. Inc., New York.
42. Chutha, I., and Dooge, J. C. I. (1990). The shape parameters of the geomorphologic unit hydrograph. *J. Hydrology*, **117** (4), 81-97.
43. Clark, C. O. (1945). Storage and unit hydrograph. *Trans. ASCE*, **110**, 1419-1446.
44. Collins, W. T. (1939). Runoff distribution graphs from precipitation occurring in more than one time unit. *Civil Engineering (N. Y.)*, **9** (9), 559-561.
45. Croley II, T.E. (1977). Hydrologic and hydraulic computations on small programmable calculators. Iowa Inst. Hydraul. Res., Univ. Iowa, Iowa City, Iowa, 837 pp.
46. Croley, T.E., II. (1980). Gamma synthetic hydrographs. *J. Hydrology*, **47**, 41-52.
47. Cudennec, C., Fouad, Y., Gatot, I. S., and Duchesne, J. (2004). A geomorphological explanation of the unit hydrograph concept. *Hydrological Processes*, **18** (4), 603-621.
48. Das G., and Agarwal, A. (1990). Development of a conceptual sediment graph model. *Trans. ASAE*, **33** (1), 100-104.
49. De Vito, L. (1975). Valutazione delle portate di piena a bassa frequenza probabile nei corsi d'acqua abruzzesi con il metodo dell'idrogramma unitario. *Energ. Elettr.*, **52** (12), 661-682.

50. Doetsch, G. (1961). Guide to the Applications of Laplace Transform. D. Van Nostrand Company Ltd. London.
51. Dooge, J. C. I. (1959). A general theory of the unit hydrograph. *J. Geophysical Research*, **64** (2), 241–256.
52. Edson, C. G. (1951). Parameters for relating unit hydrograph to watershed characteristics. *Trans. American Geophysical Union*, **32** (4), 591–596.
53. Einstein, H. A. (1964). Sedimentation, Part II. River sedimentation. In: V.T. Chow (Ed.), *Handbook of Applied Hydrology*. McGraw-Hill, New York, N.Y., pp. 17-35-17-67.
54. Eldho T.I., A. Jha, and Singh, A. K. (2006). Integrated Watershed Modelling using A Finite Element Method and a GIS Approach. *International Journal of River Basin Management, IAHR*, **4** (1), 1-9, 2006.
55. Espey, W. H. Jr., and Winslow, D.E. (1974). Urban flood frequency characteristics. *Proc. ASCE*, **100** (HY2), 179-293.
56. Fleurant, C., Kartiwa, B., and Roland, B. (2006). Analytical model for a geomorphologic instantaneous unit hydrograph. *Hydrological processes*, **20**, 3879-3895.
57. Foster, G. R. (1982). Modeling the erosion processes. In: C.T. Hann, Johnson, H., and Brakensiek, D.L. (Eds.), *Hydrological modelling of small watersheds*, ASAE Monograph No. 5, ASAE, St. Joseph, Mich., 297–380.
58. Foster, G.R., Meyer, L.D. (1975). Mathematical simulation of upland erosion by fundamental erosion mechanics. In: *Present and Prospective Technology for Predicting Sediment Yields and Sources*. Agricultural Research Service, USDA, Washington, DC, pp. 190– 207.
59. Garen, D., and Moore, D. S. (2005). Curve number hydrology in water quality modeling: use, abuse, and future directions. *J. American Water Resources Association*, **41** (2), 377-388.
60. Geetha, K., Mishra, S. K., Eldho, T.I., Rastogi, A. K., and Pandey, R. P. (2007). SCS-CN based continuous model for hydrologic simulation. *Water Resources Management J.* (Published on line).
61. Gosain, A. K., Rao, S., and Basuray, D. (2006). Climate change impact assessment on hydrology of Indian river basins. *Current Science*, **90** (3), 346-353.

62. Graf, W. H. (1971). *Hydraulics of Sediment Transport*. McGraw-Hill, New York, N.Y., 513 pp.
63. Gray, D. M. (1961). Synthetic unit hydrographs for small drainage areas. *J. Hydraulics Division, ASCE*, **87** (4), 33-54.
64. Grove, M., Harbor, J., and Engel, B. (1998). Composite vs. distributed curve numbers: Effects on estimates of storm runoff depths. *J. American Water Resources Association*, **34** (5), 1015-1033.
65. Güldal, V, and Müftüoğlu, R. F. (2001). 2D Unit sediment Graph theory. *J. Hydrologic Engineering, ASCE*, **6** (2), 132-140.
66. Gupta, V. K., C. T. Wang, and Waymire, E. (1980). A representation of an instantaneous unit hydrograph from geomorphology. *Water Resources Research*, **16** (5), 855-862.
67. Haan, C. T., Barfield, B. J., and Hayes, J. C. (1994). *Design hydrology and sedimentology for small catchments*. Academics, New York.
68. Hadley, R. F., Lal, R., Onstad, C. A., Walling, D. E., and Yair, A. (1985). Recent developments in erosion and sediment yield studies. IHP-II Project A.1.3.1, United Nations Educational Scientific and Cultural Organization, Paris.
69. Haktanir, T., and Sezen, N. (1990). Suitability of two-parameter gamma distribution and three-parameter beta distribution as synthetic hydrographs in Anatolia. *Hydrological Sciences J.*, **35** (2), 167-184.
70. Hall, M. J, Zaki, A. F., and Shahin, M. M. A. (2001). Regional analysis using the geomorphoclimatic instantaneous unit hydrograph. *Hydrology and Earth System Sciences J., EGS*, **5** (1), 93-102.
71. Hawkins, R. H. (1975). The importance of accurate curve numbers in the estimation of storm runoff. *Water Resources Bulletin*, **11** (5), 887-891.
72. Hawkins, R. H. (1978). Runoff curve numbers with varying site moisture. *J. Irrigation and Drainage Division, ASCE*, **104** (IR4), 389-398.
73. Hawkins, R. H. (1979). Runoff curve numbers from partial area watersheds. *J. Irrigation and Drainage Division, ASCE*, **105** (IR4), 375-389.
74. Hawkins, R. H. (1984). A comparison of predicted and observed runoff curve numbers. *Proc., ASCE, Irrigation and Drainage Division Special Conference, ASCE, New York, N. W.*, 702-709.

75. Hawkins, R. H. (1993) Asymptotic determination of Runoff curve numbers from data. *J. Irrigation and Drainage Engineering*, **119** (2), 334-345.
76. Hawkins, R. H. (1996). Discussion on 'SCS-runoff equation revisited for variable-source runoff areas' by Steenhuis et al. (1995). *J. Irrigation and Drainage Engineering*, **122**, (5), 319-322.
77. Hawkins, R. H., Hjelmfelt, A. T. Jr., and Zevenbergen, A. W. (1985). Runoff probability, storm depth and curve numbers. *J. Irrigation and Drainage Engineering*, **111** (4) 330-340.
78. Hawkins, R. H., Woodward, D. E., and Jiang, R. (2001). Investigation of the runoff curve number abstraction ratio. Paper presented at USDA-NRCS Hydraulic Engineering Workshop, Tucson, Arizona.
79. HEC-1 (1990). Flood hydraulics package User's Manual, CPD-1A Version 4.0, US Army Corps of Engineers, Washington, DC.
80. Hjelmfelt, A. T. Jr. (1980). Empirical investigation of curve number technique. *J. Hydraulics Division, ASCE*, **106**, (9), 1471-1477.
81. Hjelmfelt, A. T. Jr. (1991). Investigation of curve number procedure. *J. Hydraulic Engineering*, **117** (6), 725-737.
82. Hjelmfelt, A. T. Jr., Kramer, L. A., and Burwell, R. E. (1982). Curve numbers as random variable. *Proc. Int. Symp. on Rainfall-Runoff Modeling*, V. P. Singh, (Ed.), Water Resour. Publ., Littleton, Colo., pp. 365-373.
83. Holtan, H. N., and Lopez, N. C. (1971). USDHAL-70 model of watershed hydrology, USDA, Tech. Bull., 1435.
84. Horton, R. E. (1945). Erosional development of streams and their drainage basins: Hydrophysical approach to quantitative morphology. *Bulletin Geological Society of America*, **56** (3), 275-370.
85. Horton, R. I. (1938). The interpretation and application of runoff plot experiments with reference to soil erosion problems. *Proc., Soil Science Society of America*, **3**, 340-349.
86. <http://hydrolab.arsusda.gov/arswater.html>
87. <http://www.ars.usda.gov/arsdb.html>
88. Huber, W. C., Heaney, J. P., Bedient, B. P., and Bender, J. P. (1976). Environmental resources management studies in the Kissimmee river basin, Report No. ENV-05-76-3,

Department of Environmental Engineering Science, University of Florida, Gainesville, F.L.

89. Hydrologic Engineering Center (HEC). (2000). Hydrologic modeling system HEC-HMS user's manual, version 2.' Engineering, U. S. Army Corps of Engineers, Davis, Calif.
90. Hydrology. (1985). National engineering handbook, Supplement A, Sect. 4, Chapter 10, Soil Conservation Service, USDA, Washington, D.C.
91. Jain, M. K., Kothyari, U.C., and Ranga Raju, K. G. (2005). GIS based distributed model for soil erosion and rate of sediment outflow from catchments. *J. Hydraulic Engineering, ASCE*, **131** (9), 755-769.
92. Jain, S. K., Singh, R. D., and Seth, S. M. (2000). Design flood estimation using GIS supported GIUH, *Water Resources Management*, **14**, 369-376.
93. Jain, V., and Sinha, R. (2003). Derivation of unit hydrograph from GIUH: Analysis for a Himalayan river. *Water Resources Management*, **17**, 355-375.
94. Jeng, R. I., and Coon, G. C. (2003). True form of instantaneous unit hydrograph of linear reservoirs. *J. Irrigation and Drainage Engineering*, **129** (1) 11-17.
95. Johnson, J. W. (1943). Distribution graphs for suspended matter concentration. *Trans. ASCE*, **108**, 2199.
96. Juyal G. P., and Katiyar V. S. (1991). Water resources development and management in small hilly watershed. **11** (4), *J. of Indian Water Resources Society*, 14-17.
97. Juyal, G. P., and Shastry, G. (1991). Erosion losses and process studies for spurs for stream bank erosion control. Annual Rep. 1990-1991, Central Soil and Water Conservation Research and Training Institute (CSWCRTI), Dehradun, India, 88-90.
98. Kafarov, V. (1976). *Cybernetic methods in Chemistry and Chemical Engineering*. English translation, Mir Publishers, Moscow, 483p.
99. Kavvas, M. L., Chen, Z. Q., Dogrul, C., Yoon, J. Y., Ohara, N., Liang, L., Aksoy, H., Anderson, M. L., Yoshitani, J., Fukami, K., and Matsuura, T. (2004). Watershed environmental hydrology (WEHY) model based on upscaled conservation equations: hydrologic module. *J. Hydrologic Engineering, ASCE*, **9** (6), 450-464.
100. Kavvas, M. L., Yoon, J. Y., Chen, Z. Q., Liang, L., Dogrul, C., Ohara, N., Aksoy, H., Anderson, M. L., Reuters, J., and Hackley, S. (2006). Watershed environmental

- hydrology model: Environmental module and its application to a California watershed. *J. Hydrologic Engineering*, ASCE, **11** (3), 261-272.
101. Kinnell, P., and Risse, L. (1998). USLE-M: Empirical modelling rainfall erosion through runoff and sediment concentration. *Soil Science Society of America*, **62** (6), 1667–1672.
102. Kirshen, D. M., and Bras, R. L. (1983). The linear channel and its effect on geomorphologic IUH. *J. Hydrology*, **653**, 175-208.
103. Kisi, O., Karahan, M. E., and Sen, Z. (2006). River suspended sediment modeling using a fuzzy logic approach. *Hydrological Processes*, **20**, 4351-4362.
104. Knisel, W. G. (1980). CREAMS: A field scale model for chemicals, runoff, and erosion from agricultural management systems, Conservation Research Report, USDA, 26, 643 pp.
105. Kothiyari, U. C., Tiwari, A. K., and Singh, R. (1994). Prediction of sediment yield. *J. Irrigation and Drainage Engineering*, ASCE, **120** (6), 1122-1131.
106. Kothiyari, U. C., Tiwari, A. K., and Singh, R. (1997). Estimation of temporal variation of sediment yield from small catchments through the kinematic method. *J. Hydrology* **203**, 39–57.
107. Kothiyari, U. C., Tiwari, A. K., Singh, R. (1996). Temporal variation of sediment yield. *J. Hydrologic Engineering*, **1**, (4), 169-176.
108. Kreyszig, E. (1993). *Advanced Engineering Mathematics*. John Wiley & Sons, Inc., Singapore.
109. Kull, D. W. and Feldman, A. D. (1998). Evaluation of Clark's unit hydrograph method to spatially distributed runoff. *J. Hydrologic Engineering*, **3** (1), 9-19.
110. Kumar, R., Chatterjee, C., Lohani, A. K., Kumar, S., and Singh, R. D. (2002). Sensitivity analysis of the GIUH based Clark model for a catchment. *Water Resources Management*, **16** (4), 263 – 278.
111. Kumar, R., Chatterjee, C., Singh, R. D., Lohani, A. K., Kumar, S. (2007). Runoff estimation for an ungauged catchment using geomorphological instantaneous unit hydrograph (GIUH) models. *Hydrological Processes*, **21**, 1829-1840.
112. Kumar, S., and Rastogi, R. A. (1987). Conceptual catchment model for estimation of suspended sediment flow. *J. Hydrology*, **95**, 155-163.

113. Langbein, W. B. (1947). Topographic characteristics of drainage basins. U S Geological Water Survey- Water supply paper 968-C, 125-155.
114. Lee, Y. H., and Singh, V. P. (1999). Prediction of sediment yield by coupling Kalman filter with Instantaneous Unit Sediment Graph. *Hydrological Processes*, **13**, 2861-2875.
115. Lee, Y. H., and Singh, V. P. (2005). Tank model for sediment yield. *Water Resources Management*, **19**, 349-362.
116. Linsley, R. K. (1982). Rainfall-runoff models—an overview. In: Proc., Int. Symp. on Rainfall-Runoff Modelling, Singh, V. P. (Ed.), Water Resources Publications, Littleton, CO.
- 116b. Levenberg, k. (1944). A method for the solution of certain non-linear problems in least squares. *Quart. Appl. Math.*, **2**, 164-168.
117. Linsley, R.K., Kohler, M.A., and Paulhus, J. L. H. (1975). *Hydrology for Engineers*. McGraw Hill, New York.
118. Marquardt, D. W. (1963). An algorithm for least squares estimation of non linear parameters. *J. Society for Industrial and Applied Mathematics*, **11** (2), 431-441.
119. McCuen, R. H. (1982). *A Guide to Hydrologic Analysis Using SCS Methods*. Prentice-Hall Inc., Englewood Cliffs, N.J.
120. McCuen, R. H. (1989). *Hydrologic Analysis and Design*, Prentice Hall, Englewood Cliffs, New Jersey.
121. McCuen, R. H., Knight, Z., and Cutter, A. G. (2006). Evaluation of the Nash-Sutcliffe efficiency index. *J. Hydrologic Engineering*, ASCE, **11** (6), 597-602.
122. McCuen, R.H. (2002). Approach to confidence interval estimation for curve numbers. *J. Hydrologic Engineering*, **7**, 1, 43-48.
123. McCuen, R.H., and Bondelid, T.R. (1983). Estimating unit hydrograph peak rate factors. *J. Irrigation and Drainage Engineering*, ASCE, **110** (7): 887-904.
124. Mein, G. R. and Larson, C. L. (1971). Modeling the infiltration component of the rainfall-runoff process, Water Resources Research Center, University of Minnesota, Minneapolis, Minnesota.
125. Merritt, W. S., Letcher, R. A., and Jakeman, A. J. (2003). A review of erosion and sediment transport models. *Environmental Modelling & Software*, **18**, 761-799.
126. Michel, C., Andreassian, V., and Perrin, C. (2005). Soil Conservation Service Curve Number Method: How to mend a wrong Soil Moisture Accounting procedure. *Water Resources Research*, **41**, W02011, doi: 10.1029/2004WR003191.

127. Miller, N., and Cronshey, R. (1989). Runoff curve numbers, the next step, Proc., Int. Conf. on Channel Flow and Catchment Runoff, University of Virginia, Charlottesville, Va.
128. Mishra, S. K., and Singh, V. P. (1999a) Another look at SCS-CN method. *J. Hydrologic Engineering*, ASCE, **4** (3), 257-264.
129. Mishra, S. K., and Singh, V. P. (1999b). Hysteresis-based flood wave analysis. *J. Hydrologic Engineering*, ASCE, **4** (4), 358-365.
130. Mishra, S. K., and Singh, V. P. (2002a). SCS-CN method: Part I: Derivation of SCS-CN based models, *Acta Geophysica Polonica*, **50** (3), 457-477.
131. Mishra, S. K., and Singh, V. P. (2002b). SCS-CN based hydrologic simulation package, *Mathematical models in small watershed hydrology*, Singh, V. P., and Frevert, D. K., (Eds.) Water Resources Publication, Littleton, Co, 391-464.
132. Mishra, S. K., and Singh, V. P. (2003a). Soil conservation service curve number (SCS-CN) methodology, Kluwer Academic Publishers, P. O. Box 17, 3300 AA Dordrecht, The Netherlands.
133. Mishra, S. K., and Singh, V. P. (2003b). SCS-CN method Part II: Analytical Treatment, *Acta Geophysica Polonica*, **51** (1), 107-123.
134. Mishra, S. K., and Singh, V. P. (2004a). Long-term hydrologic simulation based on the Soil Conservation Service curve number. *Hydrological Processes*, **18**, 1291-1313.
135. Mishra, S. K., and Singh, V. P. (2004b). Validity and extension of the SCS-CN method for computing infiltration and rainfall-excess rates. *Hydrological Processes*, **18**, 3323-3345.
136. Mishra, S. K., and Singh, V. P. (2006). A re-look at NEH-4 curve number data and antecedent moisture condition criteria, *Hydrological Processes*, **20**, 2755-2768.
137. Mishra, S. K., Jain, M. K., and Singh, V. P. (2004a). Evaluation of the SCS-CN based model incorporating antecedent moisture. *Water Resources Management*, **18**, 567-589.
138. Mishra, S. K., Jain, M. K., Pandey, R. P., and Singh, V. P. (2003a). Evaluation of AMC dependent SCS-CN models using large data of small watersheds. *Water and Energy International*, **60** (3), 13-23.

139. Mishra, S. K., Jain, M. K., Pandey, R. P., and Singh, V. P. (2005). Catchment area-based evaluation of the AMC-dependent SCS-CN-based rainfall-runoff models. *Hydrological Processes*, **19**, 2701-2718.
140. Mishra, S. K., Sahu, R. K., Eldho, T. I., and Jain, M. K. (2006b). An improved I_a -S relation incorporating antecedent moisture in SCS-CN methodology. *Water Resources Management*, **20**, 643-660.
141. Mishra, S. K., Sansalone, J. J., and Singh, V. P. (2004b). Partitioning analog for metal elements in urban rainfall-runoff overland flow using the soil conservation service curve number concept. *J. Environmental Engineering, ASCE*, **130** (2), 145-154.
142. Mishra, S. K., Sansalone, J. J., Glenn III, D., W., and Singh, V. P. (2004c). PCN based metal partitioning in urban snow melt, rainfall/runoff, and river flow systems. *J. American Water Resources Association*, Paper No. 01043, 1315-1337.
143. Mishra, S. K., Singh, V. P., Ojha, C. S. P., Aravamuthan, V., and Sansalone, J. J. (2002). An SCS-CN based time distributed runoff model. *Water and Energy International J., Central Board of Irrigation and Power, New Delhi*, **59** (2), 34-51.
144. Mishra, S. K., Singh, V. P., Sansalone, J. J., and Aravamuthan, V. (2003b). A modified SCS-CN method: Characterization and Testing. *Water Resources Management*, **17**, 37-68.
145. Mishra, S. K., Tyagi, J. V., Singh, V. P., and Singh, R. (2006a). SCS-CN-based modeling of sediment yield. *J. Hydrology*, **324**, 301-322.
146. Mockus, V. (1949). Estimation of total (peak rates of) surface runoff for individual storms, Exhibit A of Appendix B, Interim Survey Report Grand (Neosho) River Watershed, USDA, Dec. 1.
147. Moglen, G. E. (2000). Effect of orientation of spatially distributed curve numbers in runoff calculations. *J. American Water Resources Association*, **36** (6), 1391-1400.
148. Montgomery, D. C., and Runger, G. C. (1994). *Applied Statistics and Probability for Engineers*. John Wiley Sons Inc., New York.
149. Moore, R. J. (1984). A dynamic model of basin sediment yield. *Water Resources Research*, **20**, 89-103.
150. Moore, R. J., and Clarke, R. T. (1983). A distribution function approach to modeling sediment yield. *J. Hydrology*, **65**, 239-257.

151. Nadarajah, S. (2007). Probability models for unit hydrograph derivation. *J. Hydrology*, **344**, 185-189.
152. Nash, J. E. (1957). The form of the instantaneous unit hydrograph. *Hydrological Sciences Bulletin*, **3**, 114– 121.
153. Nash, J. E. (1958). Determining runoff from rainfall. *Proc. Institution of Civil Engineers, Ireland*, **10**, 163-184.
154. Nash, J. E. (1959). Systematic determination of unit hydrograph parameters. *J. Geophysical Research*, **64** (1), 111–115.
155. Nash, J. E. (1960). A unit hydrograph study with particular reference to British catchments. *Proc. Institution of Civil Engineers, London*, **17**, 249–282
156. Nash, J. E., and Sutcliffe, J.V. (1970). River flow forecasting through conceptual models, Part I-A discussion of principles. *J. Hydrology*, **10**, 282-290.
157. Neitsch, S. L., Arnold, J. G., Kiniry, J. R., Williams, J. R., and King, K. W. (2002). *Soil and Water Assessment Tool (SWAT): Theoretical documentation, Version 2000'*, Texas water Resources Institute, College Station, Texas, TWRI Report TR-191.
158. Nippes, K. R. (1971). A new method of computation of the suspended sediment load. *Proc. Symp. Mathematical Models in Hydrology, Vol. II*, pp. 659-666.
159. Novotny, V. and Olem, H. (1994). *Water Quality: Prevention, Identification, and Management of Diffuse Pollution*. John Wiley & Sons, New York, N.Y.
160. Ogrosky, H. O. (1956). *Service objectives in the field of Hydrology*, Unpublished, Soil Conservation Service, Lincoln, Nebraska, 5 pp.
161. Oppenheim, A. V., Willsky, A. S., and Nawab, S. H. (2003). *Signals and Systems*. Pearson Education (Singapore) Pvt. Ltd., Indian Branch, Delhi, India.
162. Pandit, A., and Gopalakrishnan, G. (1996). Estimation of annual storm runoff coefficients by continuous simulation. *J. Irrigation and Drainage Engineering, ASCE*, **122** (40), 211-220.
163. Park, J., Kojiri, T., and Tomosugi, K. (2004). Proposal of Comparative hydrology using GIS based distributed model. *J. Japan Society of Hydrology and Water Resources*, **17** (4).
164. Ponce, V. M. (1989). *Engineering Hydrology: Principles and practice*, Prentice-Hall, Englewood Cliffs, N. J.

165. Ponce, V. M., and Hawkins, R. H. (1996). Runoff Curve Number: Has it reached maturity?. *J. Hydrologic Engineering*, **1** (1), 11-19.
166. Quimpo, R. G. (1967). Stochastic Model of Daily River Flow Sequences. Hydrology Paper 18, Colorado State University: Fort Collins, Co.
167. Raghuvanshi, N. S., Rastogi, R. A., and Kumar, S. (1996). Application of Linear system models for estimation of wash load. Proc. Int. Conf. Hydrology & Water Resources, Singh, V. P., and Kumar, B., (Eds.), **3**, New Delhi, India, pp. 113-123.
168. Raghuvanshi, N. S., Rastogi, R. A., and Kumar S. (1994). Instantaneous unit sediment graph. *J. Hydraulic Engineering*, **120** (4), 495-503.
169. Raghuvanshi, N. S., Singh, R., and Reddy, L. S. (2006). Runoff and sediment yield modeling using artificial neural networks: Upper Siwane river, India. *J. Hydrologic Engineering*, **11** (1), 71-79.
170. Rallison, R. E. (1980). Origin and evaluation of the SCS runoff equation. Proc., Symp. Watershed Management, ASCE, Idaho, July, 1980, 912-924.
171. Rallison, R. E., and Miller, N. (1982). Past, present, and future. Proc., Int. Symp. Rainfall-Runoff Relationship, Singh, V. P. (Ed.), Water Resources Pub., P.O. Box 2841, Littleton, Colorado.
172. Ramasastry, K. S., and Seth, S. M. (1985). Rainfall-runoff relationships. Rep. RN-20, National Institute of Hydrology, Roorkee, India.
173. Raudkivi, A. J. (1979). *Hydrology: An advanced introduction to hydrological processes and modeling*, Pergamon, Tarrytown, N.Y.
174. Renard, K. G. (1980). Estimating erosion and sediment yield from rangeland. Proc., ASCE Symp. Watershed management, Australia, Institution of Engineers, pp. 162-175.
175. Renard, K. G., and Laursen, E. M. (1975). Dynamic behavior model of ephemeral stream. *J. Hydraulics Division, ASCE*, **101** (5), 511-528.
176. Renard, K. G., Foster, G. R., Weesies, G. A., and Porter, J. P. (1991). RUSLE: Revised universal soil loss equation. *J. Soil and Water Conservation*, **46** (1), 30-33.
177. Renard, K. G., Foster, G. R., Yoder, D. C., McCool, D. K. (1994). RUSLE revisited: status, questions, answers, and the future. *J. Soil and Water Conservation*, 213-220 (May-June).

178. Rendon-Herrero, O. (1974). Estimation of wash load produced on certain small watersheds. *J. Hydraulics Division, Proc., ASCE*, **100** (HY7), 835–848.
179. Rendon-Herrero, O. (1978). Unit Sediment Graph. *Water Resources Research*, **14** (5), 889-901.
180. Rinaldo, A., and Rodriguez-Iturbe, I. (1996). Geomorphological theory of the hydrological response. *Hydrological Processes*, **10** (6), 803–829.
181. Rodriguez-Iturbe, I., and Rinaldo, A. (1997). *Fractal River Basins: Chance and Self-organization*. Cambridge University Press: Cambridge.
182. Rodriguez-Iturbe, I., and Valdés, J. B. (1979). The geomorphologic structure of the hydrologic response. *Water Resources Research*, **15** (6), 1409-1420.
183. Rodriguez-Iturbe, I., Devoto, G., and Valdes, J. B. (1979). Discharge response analysis and hydrologic similarity: The interrelation between the geomorphologic IUH and the storm characteristics. *Water Resources Research*, **15** (6), 1435–1444.
184. Rosso, R. (1984). Nash model relation to Horton Order Ratios. *Water Resources Research*, **20** (7), 914-920.
185. Sahoo, B., Chatterjee, C., Raghuwanshi, N. S., Singh, R., and Kumar, R. (2006). Flood estimation by GIUH based Clark and Nash models. *J. Hydrologic Engineering, ASCE*, **11** (6), 515-525.
186. Sahu, R. K., Mishra, S. K., Eldho, T. I., and Jain, M. K. (2005). A SCS-CN based model incorporating direct use of antecedent rainfall in runoff equation. *Proc., XXXI, IAHR Congress on 'Water For the future-Choices and Challenges, Seoul, Korea*, pp. 3727-3736.
187. Sahu, R. K., Mishra, S. K., Eldho, T. I., and Jain, M. K. (2007). An advanced soil moisture accounting procedure for SCS curve number method. *Hydrological Processes*, **21** (21), 2872-2881.
188. Sarkar, S., and Singh, S. R. (2007). Interactive effect of tillage depth and mulch on soil temperature, productivity and water use pattern of rainfed barley (*Hordium Vulgare L.*). *Soil and Tillage Research*, **92**, 79-86.
189. SCD. (1972). *Handbook of Hydrology*, Soil Conservation Department, Ministry of Agriculture, New Delhi, India.

190. Schneider, L. E., and McCuen, R. H. (2005). Statistical guidelines for curve number generation. *J. Irrigation and Drainage Engineering*, ASCE, **131** (3), 282–290.
191. SCS. (1956, 1964, 1971, 1972, 1993). Hydrology, National Engineering Handbook, Supplement A, Section 4, Chapter 10, Soil Conservation Service, USDA, Washington, D. C.
192. SCS. (1957). Use of storm and watershed characteristics in synthetic hydrograph analysis and application. U. S. Department of Agriculture, Soil Conservation Service, Washington, D. C.
193. SCS. (1986). Urban hydrology for small watersheds. Technical Release No. 55, Soil Conservation Service, USDA, Washington, D. C.
194. Sharda, V.N., Juyal, G.P., and Singh, P.N. (2002). Hydrologic and Sedimentologic behavior of a conservation bench terrace in a sub-humid climate. *Transactions of the ASAE*, **45** (5), 1433-1441.
195. Sharma, K. D., and Murthy, J. S. R. (1996). A conceptual sediment transport model for arid regions. *J. Arid Environments*, **33**, 281-290.
196. Shen, H.W. (1971). *River Mechanics*, Vol. I. Colorado State University, Fort Collins, Colo., pp. 13-1-13-26.
197. Sherman, L. K. (1932). Stream flow from rainfall by unit-graph method. *Engineering News Record*, Vol. 108, April 7, pp. 501-505.
198. Sherman, L. K. (1949). The unit hydrograph method, In: O. E. Meinzer (Ed.), *Physics of the Earth*, Dover Publications, Inc., New York, N. Y., 514-525.
199. Simanton, J. R., Hawkins, R. H., Mohseni-Saravi, M., and Renard, K. G. (1996). Runoff curve number variation with drainage area, Walnut Gulch, Arizona, Soil and Water Division, *Trans. ASAE*, **39** (4), 1391-1394.
200. Singh, K. P. (1964). Nonlinear instantaneous unit hydrograph theory. *J. Hydraulics Division, Proc., ASCE*, **90** (HY2), 313-347.
201. Singh, P. K. (2003). A conceptual model based on unit-step function approach with variable storage coefficient for estimation of direct runoff from a watershed of Tilaiya dam catchment in Upper Damodar Valley. Unpublished Thesis, M.Tech. (Soil and Water Conservation Engineering), G. B. Pant University of Agriculture and Technology, Pantnagar, India.

202. Singh, P. K., Bhunya, P. K., Mishra, S. K., and Chaube, U. C. (2007). An extended hybrid model for synthetic unit hydrograph derivation. *J. Hydrology*, **336**, 347-360.
203. Singh, S. K. (2000). Transmuting synthetic hydrographs into gamma distribution. *J. Hydrologic Engineering*, ASCE, **5** (4), 380-385.
204. Singh, V. P. (1988). *Hydrologic Systems, Vol. 1: Rainfall-Runoff Modeling*, Prentice-Hall, Englewood Cliffs, N. J.
205. Singh, V. P. (1989). *Hydrologic Systems: Vol. 2: Watershed Modeling*, Prentice Hall, Englewood Cliffs, N. J.
206. Singh, V. P. (1992). *Elementary Hydrology*, Prentice Hall, Englewood Cliffs, N. J.
207. Singh, V. P. (1995). Chapter 1: Watershed modeling, In: *Computer models of watershed hydrology*, V. P. Singh, (Ed.), Water Resources Publications, Littleton, Colo., 1-22.
208. Singh, V. P., and Frevert, D. K. (2002) *Mathematical Models of Small Watershed Hydrology and Applications*, Water Resources Publications, Highlands Ranch, Colo.
209. Singh, V. P., and Woolhiser, D. A. (2002). Mathematical modeling of watershed hydrology. 150th Anniversary paper. *J. Hydrologic Engineering*, ASCE, **7** (4), 271-292.
210. Singh, V. P., Baniukiwicz, A., and Chen V. J. (1982). An instantaneous unit sediment graph study for small upland watersheds, *Modeling Components of Hydrologic Cycle*, Singh, V. P. (Ed.), Water Resources Publications, Littleton, Colorado.
211. Singh, V. P., Krastanovic, P. F., and Lane, L. J. (1988). Stochastic models of sediment yield, In: *Modeling Geomorphological Systems*, Anderson, M. G. (Ed.), London, John Wiley.
212. Smith, R. E., and Eggert, K. G. (1978). Discussion on 'Infiltration formula based on SCS curve number. *J. Irrigation and Drainage Division*, ASCE, **104**, 462-464.
213. Snyder, F. F. (1938). Synthetic unit-graphs. *Trans. Am. Geophysical Union*, **19**, 447-454.
214. Sobhani, G. (1975). A review of selected small watershed design methods for possible adoption to Iranian conditions, M. S. Thesis, Utah State University, Logan, Utah.
215. Soil and Water Conservation Division (SWC&D). (1991-1996). *Evaluation of hydrological data*, Vols. I and II, Ministry of Agriculture, Government of India, New Delhi, India.

216. Sokolov, A. A., Rantz, S. E., and Roche, M. (1976). Methods of developing design flood hydrographs. Flood computation methods compiled from world experience, UNESCO, Paris
217. Sorman, A. U. (1995). Estimation of peak discharge using GIUH model in Saudi Arabia. *J. Water Resources Planning and Management, ASCE*, **121** (4), 287-293.
218. Springer, E. P., McGurk, B. J., Hawkins, R. H., and Goltharp, G. B. (1980). Curve numbers from watershed data. *Proc., Irrigation and Drainage Symp. on Watershed Management, ASCE, New York, N. Y.*, 938-950.
219. Steefel, C. I., Van Cappellan, P. (1998). Reactive transport modelling of natural systems. *J. Hydrology*, **209**, 1-7.
220. Steenhuis, T. S., Winchell, M., Rossing, J., Zollweg, J. A., and Walter, M. F. (1995). SCS runoff equation revisited for variable-source runoff areas. *J. Irrigation and Drainage Engineering*, **121** (3), 234-238.
221. Strahler, A. N. (1957). Quantitative analysis of watershed geomorphology. *Trans. Am. Geophysical Union*, **38** (6), 913-920.
222. Tayfur, G., Ozdemir, S., and Singh, V. P. (2003). Fuzzy logic algorithm for runoff-induced sediment transport from bare soil surfaces. *Advances in Water Resources*, **26**, 1249-1256.
223. Taylor, A. B., and Schwarz, H. E. (1952). Unit hydrograph lag and peak flow related to basin characteristics. *Trans. Am. Geophysical Union*, **33** (2), 235-246.
224. Todini, E. (1988). Rainfall-runoff modeling—past, present and future. *J. Hydrology*, **100**, 341-352.
225. U. S. Army Corps of Engineers (USACE). (1940). Engineering construction-flood control, Fort Belvoir, VA: Engineering School, USACE.
226. U. S. Army Corps of Engineers (USACE). (1990). Flood hydraulics package. User's Manual for HEC-1, CPD-1A, Version 4.0, USACE, Washington, D.C.
227. Valdes, J. B., Fiallo, Y., and Rodriguez-Iturbe, I. (1979). A rainfall-runoff analysis of the geomorphologic IUH. *Water Resource Research*, **15** (6), 1421-1434.
228. Van-Mullem, J. A. (1989). Runoff and peak discharges using Green-Ampt model. *J. Hydraulic Engineering, ASCE*, **117** (3), 354-370.
229. Vanoni, V. A. (Ed.) (1975). *Sedimentation Engineering*, ASCE, New York.

230. Verma, M. P. and Rastogi, R. A. (2002). Development of Clark unit hydrograph for a Himalayan watershed. *Indian J. Soil Conservation*, **30** (1), 16-20.
231. Wang, G. T., Singh, V. P., and Yu, F. X. (1992). A rainfall-runoff model for small watersheds. *J. Hydrology*, **138**, 97-117.
232. Wang, R.Y., and Wu, I. P. (1972). Characteristics of short duration unit hydrograph. *Trans. ASAE*, **15**, 452-456.
233. White, D. (1988). Grid based application of runoff curve numbers. *J. Water Resources Planning and Management, ASCE*, **114** (6), 601-612.
234. Wicks, J. M., and Bathurst, J. C. (1996). SHESED: A physically based, distributed erosion and sediment yield component for the SHE hydrological modeling system. *J. Hydrology*, **175**, 213-238.
235. Williams, J. R. (1975). Sediment routing for agriculture watersheds. *Water Resources Bulletin*, **11** (5), 965-974.
236. Williams, J. R. (1978). A sediment graph model based on an instantaneous unit sediment graph. *Water Resources Research*, **14** (4), 659-664.
237. Williams, J. R. (1981). Mathematical modeling of watershed sediment yield. Paper presented at the Int. Symp. on Rainfall-Runoff Modeling, May 18-21, at Mississippi State University, Mississippi State, Miss.
238. Williams, J. R., and LaSeur, W. V. (1976). Water yield model using SCS curve numbers. *J. Hydraulics Division, ASCE*, **102**, (HY9), Proc. Paper 12377, 1241-1253.
239. Wilson, B. N., Barfield, B. J., Moore, I. D., and Warner, R. C. (1984). A hydrology and sedimentology watershed model. II: Sedimentology component. *Trans. ASAE*, **17**, 1378-1384.
240. Wischmeier, W. H. and Smith, D. D. (1978). Predicting rainfall-erosion losses-A guide to conservation planning. Agricultural Handbook No. 537, Science and Education Administration, U.S. Department of agriculture, Washington D.C
241. Woodward, D. E., and Gburek, W. J. (1992). Progress report ARS/SCS curve number work group, Proc., ASCE, Water Forum 92, ASCE, New York, 378-382.
242. Woolhiser, D. A., and Renard, K. G. (1980). Stochastic aspects of watershed sediment yield. In: *Application of Stochastic Processes in Sediment Transport*, Shen, H. W., and Kikkawe, H. (Eds.), Chap. 3, Water Resources Publications, Littleton, Colo.

243. Woolhiser, D. A., Smith, R. E., and Goodrich, D. C. (1990). KINEROS-A kinematic runoff and erosion model, Documentation and user Manual. U. S. Department of Agriculture, Agricultural Research Service, ARS-77.
244. Wu, I. P. (1963). Design hydrographs for small watersheds in Indiana. J. Hydraulics Division, Proc., ASCE, **89** (HY6), 35-66.
245. Wu, I. P. (1969). Flood hydrology of small watersheds: Evaluation of time parameters and determination of peak discharge. Trans. ASAE, **12**, 655-660.
246. Wu, T. H., Hall, J. A., and Bonta, J. V. (1993). Evaluation of runoff and erosion models. J. Irrigation and Drainage Engineering, ASCE, **119** (4), 364-382.
247. Yen, B. C., and Lee, K. T. (1997). Unit hydrograph derivation for ungauged watersheds by stream-order laws. J. Hydrologic Engineering, ASCE, **2** (1), 1-9.
248. Yu, B. (1998). Theoretical justification of SCS method for runoff estimation. J. Irrigation and Drainage Engineering, **124** (6), 306-310.
249. Yuan, Y., Mitchell, J. K., Hirschi, M.C., Cooke, R. A. C. (2001). Modified SCS curve number method for predicting sub-surface drainage flow. Trans. ASAE, **44** (6), 1673-1682.
250. Yue, S., Taha, B. M. J., Bobee, B., Legendre, P., and Bruneau, P. (2002). Approach for describing statistical properties of flood hydrograph. J. Hydrologic Engineering, ASCE, **7** (2): 147-153, 2002.

Appendix A

Rainfall-runoff and P₅ data for the watershed no. 9004 (Source: <http://hydrolab.arsusda.gov/arswater.html>)

Event No.	P (mm)	Q (mm)	P ₅ (mm)	Event No.	P (mm)	Q (mm)	P ₅ (mm)	Event No.	P (mm)	Q (mm)	P ₅ (mm)	Event No.	P (mm)	Q (mm)	P ₅ (mm)
1	25.91	2.92	1.78	27	36.07	3.41	3.05	53	20.32	0.36	40.89	79	34.04	2.48	0.00
2	21.59	2.77	28.96	28	40.13	2.12	9.14	54	24.13	0.29	11.94	80	28.45	2.97	6.86
3	8.64	0.54	42.16	29	34.29	1.03	60.45	55	16.00	0.53	36.07	81	38.35	4.20	1.78
4	77.98	7.69	6.60	30	19.30	0.73	17.53	56	23.37	1.15	10.67	82	28.93	0.83	2.03
5	103.63	8.39	0.00	31	18.03	0.32	35.05	57	45.21	2.39	0.00	83	37.34	0.94	0.00
6	24.89	0.86	0.00	32	11.43	0.53	54.61	58	62.48	3.74	0.00	84	30.48	4.73	16.26
7	33.02	1.59	0.00	33	39.37	0.54	0.00	59	38.35	1.17	0.00	85	29.72	1.87	6.35
8	20.32	0.48	4.06	34	25.65	1.00	33.53	60	54.86	2.22	0.00	86	32.26	1.93	0.00
9	21.84	1.06	30.99	35	81.79	6.73	4.32	61	78.31	11.20	0.00	87	20.07	0.94	0.51
10	20.32	1.15	35.05	36	72.75	5.78	0.00	62	9.65	0.48	99.82	88	49.78	4.17	20.57
11	16.00	0.28	24.38	37	31.01	0.31	0.00	63	40.89	10.29	111.00	89	70.36	8.22	3.05
12	12.45	0.61	21.59	38	21.59	0.65	17.53	64	16.74	0.35	0.00	90	29.16	3.13	72.39
13	12.95	0.50	0.00	39	20.57	0.53	9.65	65	11.71	0.31	16.76	91	91.49	32.58	101.60
14	74.30	9.14	12.95	40	39.80	0.38	0.00	66	25.91	3.11	28.45	92	26.92	0.85	0.00
15	47.52	7.12	75.44	41	21.59	0.38	5.59	67	20.83	0.55	0.00	93	33.71	0.50	0.00
16	46.74	10.33	123.19	42	18.29	0.92	48.01	68	23.88	0.31	2.29	94	39.37	3.04	14.22
17	11.68	1.04	169.93	43	13.21	0.33	62.48	69	24.89	0.48	23.88				
18	49.78	2.09	0.00	44	23.37	1.30	53.34	70	13.46	2.40	24.89				
19	7.62	0.36	49.78	45	11.68	1.61	34.29	71	24.13	1.56	0.00				
20	7.37	0.26	60.96	46	17.53	0.46	0.00	72	35.81	8.46	0.00				
21	12.70	0.36	16.00	47	43.18	0.47	3.05	73	30.73	0.26	0.00				
22	13.21	0.54	0.00	48	42.16	1.18	46.23	74	25.48	1.43	6.10				
23	15.24	0.31	0.00	49	19.05	0.36	0.00	75	18.54	1.51	35.05				
24	11.43	0.31	19.81	50	32.00	0.42	41.15	76	14.43	0.52	0.00				
25	29.21	0.67	19.81	51	28.45	1.75	73.15	77	9.53	0.69	19.05				
26	26.67	0.59	29.21	52	40.89	5.24	2.79	78	21.34	0.86	36.83				

Appendix B

Daily rainfall-runoff and evaporation data for the year 1975 for Hemawati catchment

Day	Rainfall (mm)	Runoff (mm)	Evap. (mm)	Day	Rainfall (mm)	Runoff (mm)	Evap. (mm)	Day	Rainfall (mm)	Runoff (mm)	Evap. (mm)	Day	Rainfall (mm)	Runoff (mm)	Evap. (mm)
1	0	1.15	4	26	0	0.65	4	51	0	0.5	5.6	76	0	0.43	6.4
2	0	1.12	3	27	0	0.63	4.5	52	0	0.5	5	77	0	0.43	7.5
3	0	1.09	1.8	28	0	0.63	4.5	53	0	0.49	7	78	0	0.43	8.6
4	0	1.07	2.1	29	0	0.6	4.2	54	0	0.49	7.5	79	0	0.43	8
5	0	1.04	4	30	0	0.6	4	55	0	0.49	6.8	80	0	0.42	7.8
6	0	1.04	4	31	0	0.62	3	56	0	0.49	7.8	81	0	0.42	6.6
7	0	1.02	3.5	32	0	0.63	2.8	57	0	0.48	7	82	0	0.42	8
8	0	0.98	3.6	33	0	0.62	3.6	58	0	0.48	6.8	83	0	0.42	8
9	0	0.96	3.9	34	0	0.58	4.5	59	0	0.48	7.4	84	0	0.42	7.4
10	0	0.92	3	35	0	0.58	3.5	60	0	0.48	6	85	0	0.42	6
11	0	0.88	2.7	36	0	0.58	4.4	61	0	0.46	7	86	0.1	0.42	7.6
12	0	0.86	3.8	37	0	0.58	3.1	62	0	0.46	4	87	0	0.42	8
13	0	0.85	3.6	38	0	0.56	4.4	63	0	0.46	7.4	88	0	0.4	8.1
14	0	0.84	4	39	0	0.56	4.5	64	0	0.46	7.4	89	0	0.4	8
15	0	0.84	4	40	0	0.55	4	65	0	0.46	7.1	90	0	0.4	7.2
16	0	0.84	3.5	41	0	0.55	4.4	66	0	0.45	6.8	91	10.66	0.4	6
17	0	0.82	3.2	42	0	0.55	4.4	67	0	0.45	7.8	92	19.28	0.45	5.2
18	0	0.81	2.7	43	0	0.53	4.2	68	0	0.45	5.4	93	2.09	0.53	3
19	0	0.81	3.1	44	0	0.53	5.2	69	0	0.45	7	94	10.08	0.55	3
20	0	0.79	3	45	0	0.53	4.8	70	0	0.45	6.8	95	0	0.62	5.3
21	0	0.78	5	46	0	0.52	5.2	71	0	0.45	4	96	3.05	0.62	3.4
22	0	0.76	3.2	47	0	0.52	4.8	72	0	0.45	8.4	97	3	0.62	7
23	0	0.75	4.4	48	0	0.5	5.2	73	0	0.43	7.5	98	0.2	0.53	4.3
24	0	0.69	3.6	49	0	0.5	4.5	74	0	0.43	6.5	99	2.41	0.49	4
25	0	0.68	4	50	0	0.5	7.4	75	0	0.43	8	100	4.1	0.49	4.4

Appendix B. Contd...

Day	Rainfall (mm)	Runoff (mm)	Evap. (mm)	Day	Rainfall (mm)	Runoff (mm)	Evap. (mm)	Day	Rainfall (mm)	Runoff (mm)	Evap. (mm)	Day	Rainfall (mm)	Runoff (mm)	Evap. (mm)
101	2.5	0.48	5.2	126	0	0.39	5.2	151	1.15	0.37	8	176	3.95	0.53	5.6
102	0.3	0.48	6.6	127	0	0.39	5.9	152	2.92	0.37	8	177	23.92	0.53	2.9
103	0	0.46	5.4	128	0	0.39	5.4	153	16.07	0.39	5.1	178	34.42	1.56	4.4
104	0	0.46	6.6	129	0	0.39	5.6	154	13.03	0.46	5.8	179	21.52	4.65	6.5
105	0	0.45	7	130	0	0.37	5	155	23.1	0.62	6.3	180	11.86	3.54	4.4
106	14.01	0.43	5.8	131	2.1	0.37	6.8	156	19.9	1.24	5.2	181	4.37	2.66	3
107	0	0.43	6.8	132	0.6	0.37	4.2	157	11.85	1.64	5.6	182	2.19	2.12	4.8
108	3.27	0.43	5.9	133	0.43	0.37	4	158	36.09	1.12	5.6	183	12.22	2.35	4.1
109	0.85	0.45	6	134	2.3	0.39	1.7	159	39.81	3.37	6.6	184	20.28	1.45	5.7
110	0	0.46	6	135	3.91	0.4	9	160	63.92	8.5	5.9	185	5.94	1.93	3.2
111	0	0.48	6.2	136	0	0.42	3.8	161	9.71	7.46	4.8	186	23.86	3.8	1.2
112	0	0.49	7.5	137	0	0.4	5	162	9.07	3.34	4.8	187	10.43	5.33	0.9
113	6	0.53	9	138	0	0.39	4.5	163	7.06	2.16	5.8	188	12.33	4.44	4.2
114	5.59	0.55	7	139	0	0.39	5.4	164	2.54	1.89	6.3	189	16.44	5.3	3.7
115	4.83	0.56	9.4	140	0	0.39	5.6	165	12.95	1.32	5.2	190	15.94	5.26	3.7
116	6.6	0.53	5.3	141	0	0.39	4.8	166	0.85	1.02	6	191	55.67	9.82	3.5
117	0	0.53	5.3	142	0	0.39	5.8	167	0.55	0.82	6.5	192	49.02	14.44	0.9
118	0.76	0.53	4.2	143	0	0.37	7.4	168	0.51	0.76	6.6	193	31.33	15.75	3
119	0	0.52	2.6	144	0	0.37	6.4	169	0.4	0.69	5.7	194	27.39	10.34	5.2
120	0	0.49	4	145	0	0.37	6.2	170	0.18	0.58	5	195	14.07	9.55	4.6
121	0	0.46	4.8	146	0	0.37	6.4	171	0	0.56	4	196	24.52	10.84	3.6
122	0	0.4	6.2	147	0	0.37	6.2	172	0	0.56	3.8	197	21.63	11.06	1.8
123	0	0.4	7.2	148	0	0.37	6	173	0.99	0.55	7.5	198	33.95	16.3	4
124	0	0.4	6.8	149	0	0.37	6	174	0	0.55	5	199	67.28	22.97	4
125	0	0.39	6	150	0	0.37	6.1	175	2.88	0.55	5	200	101.02	49.32	4.8

Appendix B. Contd...

Day	Rainfall (mm)	Runoff (mm)	Evap. (mm)	Day	Rainfall (mm)	Runoff (mm)	Evap. (mm)	Day	Rainfall (mm)	Runoff (mm)	Evap. (mm)	Day	Rainfall (mm)	Runoff (mm)	Evap. (mm)
201	20.52	34.96	3.2	226	3.46	7.42	4	251	0	16.33	4.4	276	0	4.42	6.2
202	30.6	24	3.8	227	1.54	7.07	4.6	252	0	13.02	2.4	277	0.75	3.8	3.9
203	25.34	19.17	4	228	15.16	7.86	5.3	253	0	10.73	3.7	278	6.67	3.76	5.2
204	78.09	35.48	4.6	229	25.95	9.26	2.7	254	0	9.27	4.1	279	0	3.64	3.4
205	69.83	52.78	3	230	5.81	8.24	1.3	255	1.66	8.12	3.5	280	1.32	3.23	6
206	9.67	23.37	3.1	231	2.05	8.51	3.8	256	12.79	8.76	2.6	281	0	3.15	3.8
207	11.31	20	3.1	232	0.34	6.91	2	257	4.63	8.7	2.8	282	0	2.82	6
208	23.31	15.41	3.2	233	3.42	6.32	2.5	258	5.21	8.31	3	283	0	2.66	4
209	23.65	16.14	3.6	234	3.37	6.21	3.2	259	2.87	8.67	3.8	284	5.13	2.43	3.4
210	23.5	16.68	3.4	235	7.65	6.13	3.6	260	4.66	8.06	4	285	0.22	2.3	5.3
211	18.07	15.29	3	236	5.67	7.16	3	261	0.42	7.23	3.6	286	0	2.22	4
212	29.61	16.46	2.9	237	22.93	12.25	1	262	4.25	6.55	3.7	287	0	2.04	5.2
213	69.86	31.75	3.2	238	30.56	13.31	3.7	263	0.33	5.96	4.6	288	0	1.96	4.5
214	71.16	51.98	4.3	239	11.63	13.91	1.7	264	1.22	5.36	4.2	289	0	1.93	4.5
215	52.54	70.5	2.5	240	14.82	11.43	1.7	265	0.3	5.01	5.3	290	0.02	1.8	4
216	27.18	51.91	3.8	241	15.62	11.95	2.6	266	1.19	4.56	3.6	291	0	1.63	0.8
217	34.06	34.44	4.6	242	18.46	11.88	3.8	267	0	4.31	4.6	292	0.42	1.53	1.2
218	31.43	27.65	2.6	243	26.53	12.83	3.2	268	1.19	4.12	5	293	2.28	1.67	1.1
219	18.18	26.06	2.6	244	28.83	16.72	3.4	269	0.75	3.96	3.1	294	0	1.89	4.4
220	1.09	18.53	2.2	245	44.97	19.53	3.5	270	0.34	3.89	1.6	295	0.58	1.71	2
221	0.43	14.4	3	246	41.02	23.93	1.9	271	1.82	4.16	3.8	296	0	1.7	4
222	0.66	12.95	6.1	247	43.46	27.84	3	272	3.93	3.89	4.4	297	0	1.63	4.6
223	1.57	10.32	2.6	248	56.96	32.33	2.5	273	3.18	3.7	4.8	298	0	1.5	4
224	1.38	8.9	1.5	249	29.36	36.06	2.5	274	35.76	6.25	1.1	299	0	1.4	4
225	1.99	8.09	4.4	250	14.78	24.05	4	275	9.9	6.13	4	300	0.35	1.32	3.2

Appendix B. Contd...

Day	Rainfall (mm)	Runoff (mm)	Evap. (mm)	Day	Rainfall (mm)	Runoff (mm)	Evap. (mm)	Day	Rainfall (mm)	Runoff (mm)	Evap. (mm)
301	3.9	1.35	2.6	326	23.83	18.06	1.6	351	0	0.98	4
302	8.33	1.63	4	327	15.09	7.53	2	352	0	0.89	4.4
303	0.69	1.86	4.8	328	13.35	5.63	1.6	353	0	0.84	3.6
304	0	1.45	4.3	329	3.67	4.56	2.3	354	0	0.82	2
305	0	1.2	4	330	0.86	3.54	0.7	355	0	0.81	3.2
306	0	1.07	3.6	331	2.46	3	0.5	356	0	0.79	4.2
307	1.39	0.99	3	332	0.24	2.55	0.7	357	0	0.78	3.5
308	0.31	0.98	3.1	333	0	2.15	1.2	358	0	0.73	3
309	0	0.98	2.7	334	0	1.93	2.6	359	0	0.71	4
310	0	0.89	2.8	335	0	1.77	3.9	360	0	0.69	3.2
311	13.29	0.96	4	336	5.1	3.2	3.8	361	0	0.69	4.5
312	18.63	2.52	3.2	337	0	5.01	1.8	362	0	0.66	4
313	16.11	4.28	2.6	338	1.41	4.51	2.5	363	0	0.65	4.4
314	17.62	4.39	0.9	339	0	4.13	4	364	0	0.63	4.3
315	0	3.73	1.4	340	0.63	3.92	3.2	365	0	0.63	4.4
316	1.67	2.45	1.5	341	0.49	3.67	4.4				
317	4.64	1.96	1.7	342	0	3.44	3.5				
318	0.5	1.92	1	343	0	2.38	2.5				
319	3.74	1.64	2.6	344	0	1.34	0.8				
320	0.36	1.4	2.8	345	0	1.2	3.2				
321	0	1.28	2.8	346	0	1.15	4				
322	0	1.11	3.4	347	0	1.09	3.4				
323	0	1.04	2.8	348	0	1.07	2.9				
324	26.35	1.79	1.6	349	0	1.01	2.9				
325	38.76	15.84	2.3	350	0	0.98	2.9				

APPENDIX C

Derivation of the General Equation of EHM

The Laplace transform of the output from the n^{th} hybrid unit can be expressed as:

$$Q_n(s) = \frac{(e^{-Ts})^n}{(1 + K_1s)^n (1 + K_2s)^n} \quad (C1)$$

Alternatively Eq. (C1) can be expressed as:

$$Q_n(s) = \frac{(e^{-nTs})}{(1 + K_1s)^n (1 + K_2s)^n} \quad (C2)$$

An inverse Laplace transform of Eq. (C2) can be expressed as:

$$Q_n(t) = L^{-1} \frac{(e^{-nTs})}{(1 + K_1s)^n (1 + K_2s)^n} \quad (C3)$$

Solution of Eq. (C3) will provide the IUH of the outflow from the drainage basin represented by series of hybrid units. The Eq. (C3) can be re-written as:

$$Q_n(t) = L^{-1} \frac{1}{K_1^n K_2^n} \left[\frac{e^{-nTs}}{\left(s + \frac{1}{K_1}\right)^n \left(s + \frac{1}{K_2}\right)^n} \right] \quad (C4)$$

The solution of Eq. (C4) is given as follows:

Alternatively, Eq. (C4) can be expressed as:

$$Q_n(t) = \frac{1}{K_1^n K_2^n} L^{-1} \left\{ (e^{-nTs}) (F(s)) \right\} \quad (C5)$$

where $F(s) = \frac{1}{\left(s + \frac{1}{K_1}\right)^n \left(s + \frac{1}{K_2}\right)^n}$, its inverse Laplace transform $f(t)$ can be expressed

through the expression

$$f(t) = L^{-1}(F(s)) \quad (C6)$$

or

$$f(t) = L^{-1} \left[\frac{1}{\left(s + \frac{1}{K_1}\right)^n \left(s + \frac{1}{K_2}\right)^n} \right] \quad (C7)$$

On expanding Eq. (C7) by partial fractions yields

$$f(t) = L^{-1} \left[\frac{A_{11}}{\left(s + \frac{1}{K_1}\right)} + \frac{A_{12}}{\left(s + \frac{1}{K_1}\right)^2} + \dots + \frac{A_{1n}}{\left(s + \frac{1}{K_1}\right)^n} + \frac{A_{21}}{\left(s + \frac{1}{K_2}\right)} + \frac{A_{22}}{\left(s + \frac{1}{K_2}\right)^2} + \dots + \frac{A_{2n}}{\left(s + \frac{1}{K_2}\right)^n} \right] \quad (C8)$$

Eq. (C8) can be re-written as:

$$f(t) = L^{-1} \left[\left\{ \sum_{k=1}^n \frac{A_{1k}}{\left(s + \frac{1}{K_1}\right)^k} \right\} + \left\{ \sum_{k=1}^n \frac{A_{2k}}{\left(s + \frac{1}{K_2}\right)^k} \right\} \right] \quad (C9)$$

Where A_{1k} and A_{2k} are the partial fraction coefficients, can be calculated from the expressions (Doetsch G. 1961 and Oppenheim et. al., 2003) as follows:

$$A_{1k} = \frac{1}{(n-k)!} \left| \frac{d^{n-k}}{ds^{n-k}} \frac{1}{\left(s + \frac{1}{K_2}\right)^n} \right|_{s=-\frac{1}{K_1}} \quad \text{and} \quad A_{2k} = \frac{1}{(n-k)!} \left| \frac{d^{n-k}}{ds^{n-k}} \frac{1}{\left(s + \frac{1}{K_1}\right)^n} \right|_{s=-\frac{1}{K_2}}$$

Finally an expression for $f(t)$ can be given as:

$$f(t) = \sum_{k=1}^n \frac{t^{k-1}}{(n-k)!(k-1)!} \left[\left(e^{-\frac{t}{K_1}} \left| \frac{d^{n-k}}{ds^{n-k}} \frac{1}{\left(s + \frac{1}{K_2}\right)^n} \right|_{s=-\frac{1}{K_1}} \right) + \left(e^{-\frac{t}{K_2}} \left| \frac{d^{n-k}}{ds^{n-k}} \frac{1}{\left(s + \frac{1}{K_1}\right)^n} \right|_{s=-\frac{1}{K_2}} \right) \right] \quad (C10)$$

Using property of inverse Laplace transform (Kreyszig, 1993)

$$L^{-1} \left\{ e^{-nTs} F(s) \right\} = f(t - nT) u(t - nT) \quad \text{for } t \geq nT \quad (C11)$$

Where $u(t - nT)$ is the unit step function, which is equal to 1 for $t \geq nT$

Coupling of Eqs. (C5), (C10), and (C11) yields

$$Q_n(t) = \frac{1}{K_1^n K_2^n} \sum_{k=1}^n \frac{(t - nT)^{k-1}}{(n-k)!(k-1)!} \left[\left(e^{-\frac{(t-nT)}{K_1}} \left| \frac{d^{n-k}}{ds^{n-k}} \frac{1}{\left(s + \frac{1}{K_2}\right)^n} \right|_{s=-\frac{1}{K_1}} \right) + \left(e^{-\frac{(t-nT)}{K_2}} \left| \frac{d^{n-k}}{ds^{n-k}} \frac{1}{\left(s + \frac{1}{K_1}\right)^n} \right|_{s=-\frac{1}{K_2}} \right) \right] \quad (C12)$$

for $t \geq nT$
 otherwise

= 0

Eq. (C12) represents a generalized expression of the outflow (IUH) from the extended hybrid model due to unit impulse excitation at the inlet of first hybrid unit. The generalized form of the proposed model (Eq.C12) is an improved form of the widely used model of IUH in surface hydrology for derivation of synthetic unit hydrograph i.e. Nash (1957), as analyzed below.

The differentiation of Eq. (C12) with respect to 't' for the condition at $t = t_p$ $Q_n(t) = Q_p(t)$, after little algebraic simplification yields the following general expression for the time to peak $t_p(n)$ as

$$\sum_{k=1}^n \frac{1}{(k-1)!} \left\{ \begin{array}{l} (t_p - nT)^{k-2} e^{-\frac{(t_p - nT)}{K_1}} \left[(k-1) - \frac{(t_p - nT)}{K_1} \right] D_{1k} + \\ (t_p - nT)^{k-2} e^{-\frac{(t_p - nT)}{K_2}} \left[(k-1) - \frac{(t_p - nT)}{K_2} \right] D_{2k} \end{array} \right\} = 0 \quad (C13)$$

where, $D_{1k} = \left. \frac{d^{n-k}}{ds^{n-k}} \frac{1}{\left(s + \frac{1}{K_2}\right)^n} \right|_{s=-\frac{1}{K_1}}$ and $D_{2k} = \left. \frac{d^{n-k}}{ds^{n-k}} \frac{1}{\left(s + \frac{1}{K_1}\right)^n} \right|_{s=-\frac{1}{K_2}}$

APPENDIX D

Nash Model vs EHM

If there are n hybrid units in series (i.e. $k = n$), the Eq. (C12) yields

$$Q_n(t) = \frac{1}{K_1^n K_2^n} \sum_{k=1}^n \frac{(t - nT)^{n-1}}{(0)!(n-1)!} \left[\left(e^{-\frac{(t-nT)}{K_1}} \left| \frac{d^{n-n}}{ds^{n-n}} \frac{1}{\left(s + \frac{1}{K_2}\right)^n} \right|_{s=-\frac{1}{K_1}} \right) + \left(e^{-\frac{(t-nT)}{K_2}} \left| \frac{d^{n-n}}{ds^{n-n}} \frac{1}{\left(s + \frac{1}{K_1}\right)^n} \right|_{s=-\frac{1}{K_2}} \right) \right] \quad (D1)$$

This on further simplification can be expressed as

$$Q_n(t) = \left(\frac{(t - nT)}{(n-1)!} \right) \left[\frac{e^{-\frac{(t-nT)}{K_1}}}{(K_1 - K_2)^n} + \frac{e^{-\frac{(t-nT)}{K_2}}}{(K_2 - K_1)^n} \right] \quad (D2)$$

On putting $T = 0$, $K_1 = K$ and $K_2 = 0$ in Eq. (D2) results

$$Q_n(t) = \frac{1}{K\Gamma(n)} \left(\frac{t}{K} \right)^{n-1} e^{-\frac{t}{K}} \quad (D3)$$

which is the general expression of the IUH from the cascade of n identical linear reservoirs (Nash model) (Eq. 2.54). The above analysis shows that Nash model is only the part of the whole procedure.

APPENDIX E

Simplification for β

Using, Stirling's formula (Abramowitz and Stegun, 1964) for expansion of gamma function is expressed as:

$$\Gamma(m) = \sqrt{2\pi m} (m^{m-1} e^{-m}) \left(1 + \frac{1}{12m} + \frac{1}{288m^2} - \frac{139}{51840m^3} - \frac{571}{2488320m^4} \dots \right) \quad (E1)$$

Considering first two terms of Eq. (E1) in the parenthesis, Eq. (6.4d) simplifies to the following form

$$\beta = \frac{m^m e^{-m}}{e^{-m} m^{m-1} \left(1 + \frac{1}{12m} \right) \sqrt{2\pi m}} \quad (E2)$$

$[1+1/(12m)]$ in the denominator of (E2) can be approximated to $[1+1/(6m)]^{1/2}$. In such case (E2) simplify to the following form

$$\beta^2 \cong \frac{m^2}{(2\pi m + \pi/3)} \quad (E3)$$

Alternatively Eq. (E3) can be expressed as

$$3m^2 - 6\pi m\beta^2 - \pi\beta^2 = 0 \quad (E4)$$

Since, Eq. (E4) is a quadratic expression in m , the roots of Eq. (E4) can be expressed as

$$m = \pi\beta^2 \pm \beta\sqrt{(\pi^2\beta^2 + \pi/3)} \quad (E5)$$

APPENDIX F

Derivation of Nash Based IUSG Sub-model

Second Linear Reservoir:

The continuity equation and storage discharge relationships for the second reservoir are expressed as:

$$I_{s2}(t) - Q_{s2}(t) = dS_{s2}(t) / dt \quad (F1)$$

$$S_{s2}(t) = K_s Q_{s2}(t) \quad (F2)$$

Since the output from the first reservoir acts as input to the second reservoir, a substitution of $I_{s2}(t) = Q_{s1}(t)$ (Eq. 7.10) into Eq. (F1) yields

$$e^{-t/K_s} / K_s - Q_{s2}(t) = dS_{s2}(t) / dt \quad (F3)$$

Coupling of Eqs. (F2) and (F3), after rearranging, yields

$$dQ_{s2}(t) / dt + Q_{s2}(t) / K_s = e^{-t/K_s} / K_s^2 \quad (F4)$$

Solution of Eq. (F4) can be expressed as

$$Q_{s2}(t) = e^{-t/K_s} \left[\int dt / K_s^2 + C_2 \right] \quad (F5)$$

where C_2 is constant of integration. For the condition at $t = 0$, $Q_{s2}(t) = 0$ gives $C_2 = 0$.

Substituting the value of C_2 in Eq. (F5) we have

$$Q_{s2}(t) = (t/K_s^2)e^{-t/K_s} \quad (F6)$$

Eq. (F6) represents the sediment output from the second reservoir. It will act as input to the third reservoir.

Third Linear Reservoir:

For the third reservoir, the continuity equation and storage discharge relationships are expressed as

$$I_{s3}(t) - Q_{s3}(t) = dS_{s3}(t)/dt \quad (F7)$$

$$S_{s3}(t) = K_s Q_{s3}(t) \quad (F8)$$

Since the output from the second reservoir acts as input to the third reservoir, putting $I_{s3}(t) = Q_{s2}(t)$ (Eq. F6) in Eq. (F7) we have

$$t/K_s^2 e^{-t/K_s} - Q_{s3}(t) = dS_{s3}(t)/dt \quad (F9)$$

Coupling of Eqs. (F8) and (F9), after rearranging, yields

$$dQ_{s3}(t)/dt + Q_{s3}(t)/K_s = (t/K_s^3)e^{-t/K_s} \quad (F10)$$

The solution of Eq. (F10) can be expressed in the form

$$Q_{s3}(t) = e^{-t/K_s} \left[\int (t/K_s^3) dt + C_3 \right] \quad (F11)$$

where C_3 is constant of integration. For the condition, at $t=0, Q_{s3}(t) = 0$ gives $C_3=0$. On substituting the value of $C_3 = 0$ into Eq. (F11) we have

$$Q_{s3}(t) = (t^2 / 2K_s^3) e^{-t/K_s} \quad (F12)$$

Alternatively, Eq. (F12) can be expressed in the form:

$$Q_{s3}(t) = (1 / K_s \Gamma(3)) (t / K_s)^{3-1} e^{-t/K_s} \quad (F13)$$

Eq. (F13) represents the sediment output from the third reservoir.

Fourth Linear Reservoir:

In a similar fashion, for the fourth reservoir, the continuity equation and storage discharge relationship are expressed as

$$I_{s4}(t) - Q_{s4}(t) = dS_{s4}(t) / dt \quad (F14)$$

$$S_{s4}(t) = K_s Q_{s4}(t) \quad (F15)$$

The output from the third reservoir acts as input to the fourth reservoir. Therefore, substituting $I_{s4}(t) = Q_{s3}(t)$ (Eq. F13) into Eq. (F14), we have

$$(1 / K_s \Gamma(3)) (t / K_s)^2 e^{-t/K_s} - Q_{s4}(t) = dS_{s4}(t) \quad (F16)$$

Coupling Eqs. (F15) and (F16), after rearranging, yields

$$dQ_{s4}(t) / dt + Q_{s4}(t) / K_s = (t^2 / 2K_s^4) e^{-t/K_s} \quad (F17)$$

The solution of Eq. (F17) can be expressed in the form

$$Q_{s4}(t) = e^{-t/K_s} \left[\int (t^2 / 2K_s^4) dt + C_4 \right] \quad (F18)$$

where C is the constant of integration. For the condition at $t=0$, $Q_{s4}(t) = 0$ gives $C_4=0$. On substituting the value of $C_4 = 0$ into Eq. (F18), we have

$$Q_{s4}(t) = (t^3 / 6K_s^4) e^{-t/K_s} \quad (F19)$$

On rearranging, Eq. (F19) can be expressed as

$$Q_{s4}(t) = (1 / K_s \Gamma(4)) (t / K_s)^{4-1} e^{-t/K_s} \quad (F20)$$

n_s^{th} Linear Reservoir:

Similarly, for the n_s^{th} reservoir, the expression for the sediment output can be expressed as:

$$Q_{sn_s}(t) = (1 / K_s \Gamma(n_s)) (t / K_s)^{(n_s-1)} e^{-t / K_s} \quad (F21)$$

where n_s is the number of linear reservoirs, K_s is the storage coefficient, and Γ is Gamma function argument. Eq. (F21) represents the instantaneous unit sediment graph (IUSG) ordinates at time t in (T^{-1}) .

APPENDIX G

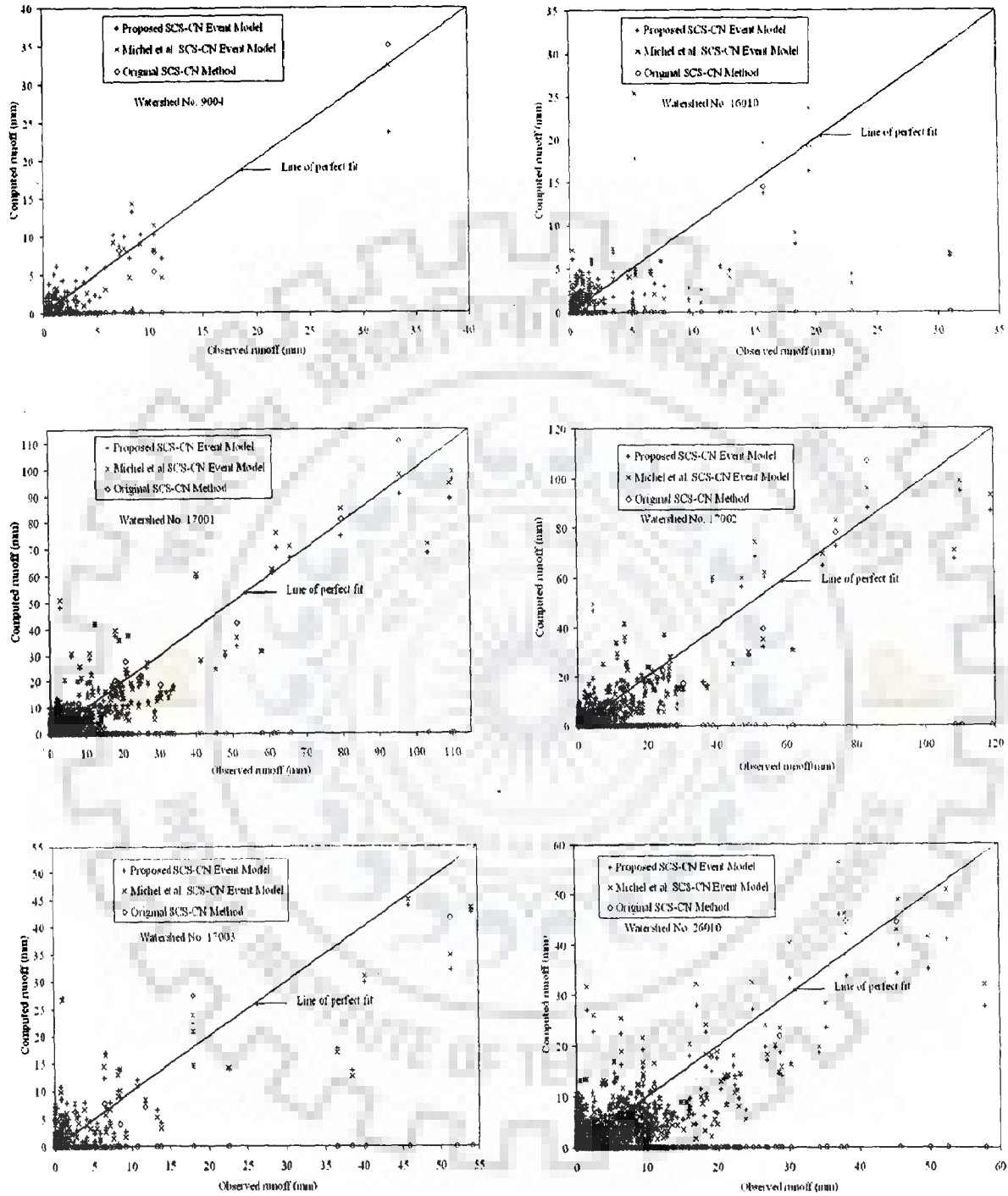


Fig. G.1: Fitting of SMA based event-aggregated and original SCS-CN models to the data of watershed nos. 9004, 16010, 17001, 17002, 17003, and 26010

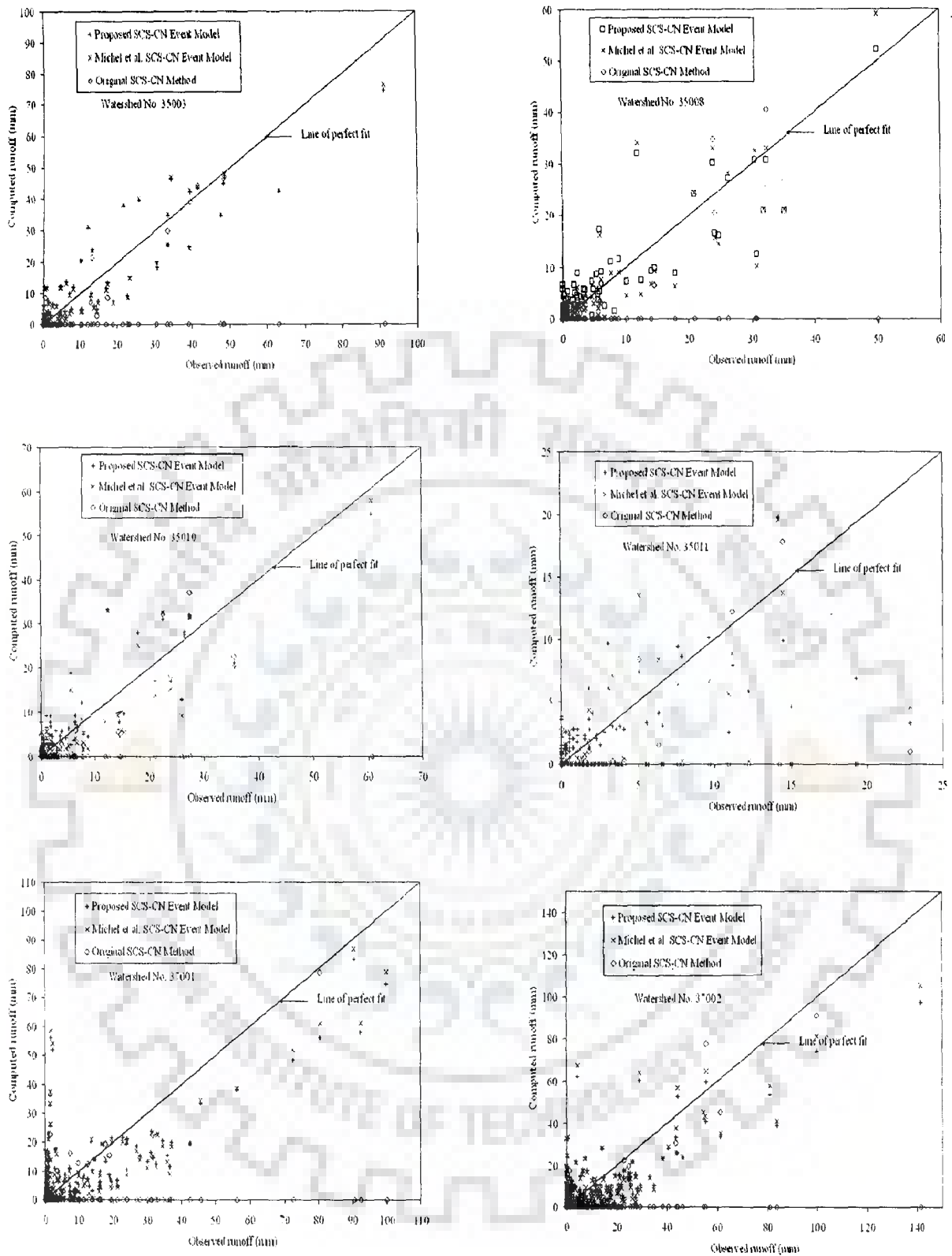


Fig. G.4: Fitting of SMA based event-aggregated and original SCS-CN models to the data of watershed nos. 35003, 35008, 35010, 35011, 37001, and 37002

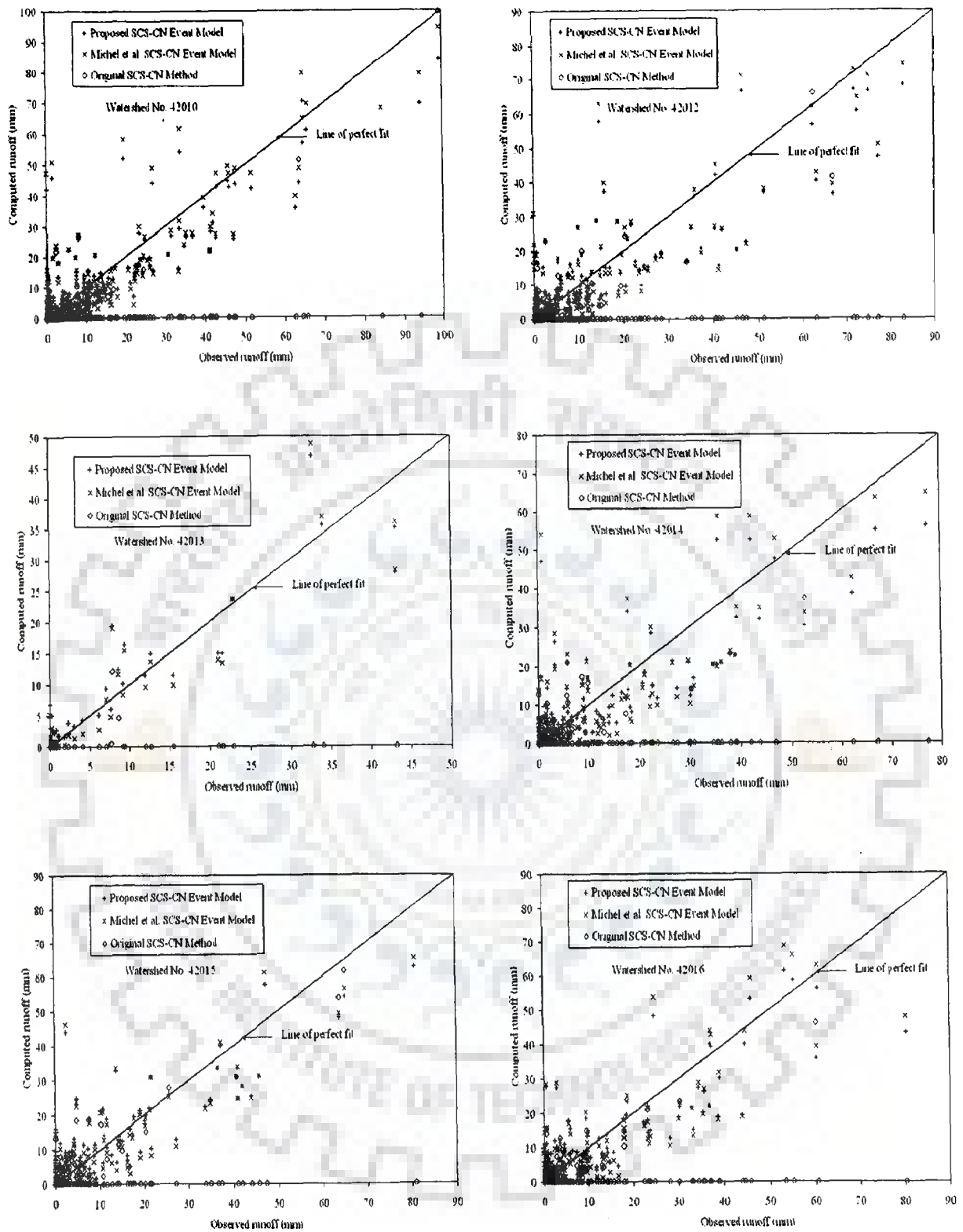


Fig. G.5: Fitting of SMA based event-aggregated and original SCS-CN models to the data of watershed nos. 42010, 42012, 42013, 42014, 42015, and 42016

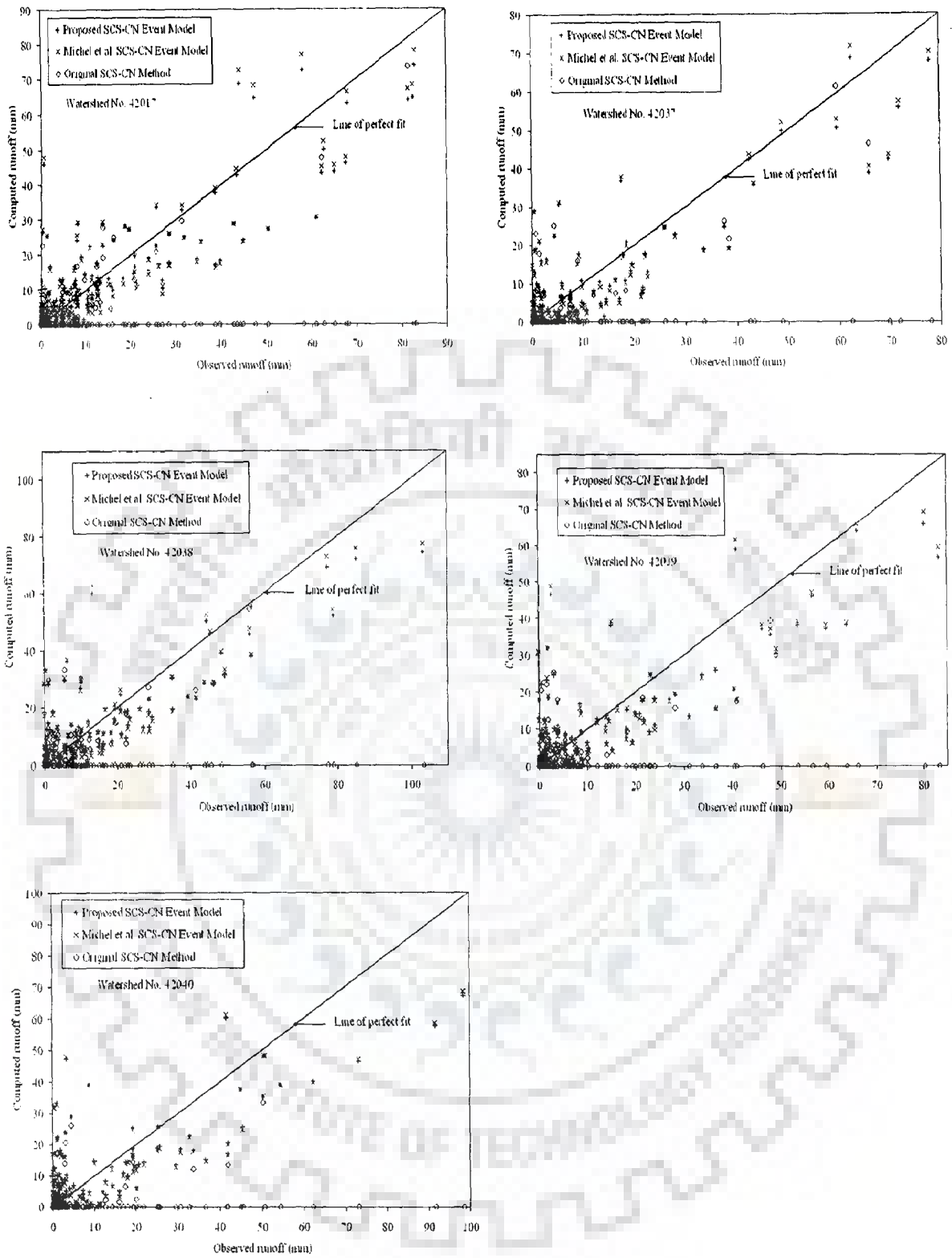


Fig. G.6: Fitting of SMA based event-aggregated and original SCS-CN models to the data of watershed nos. 42017, 42037, 42038, 42039, and 42040

PUBLICATIONS FROM THE THESIS

International Journals

1. **Singh, P. K.**, Bhunya, P. K., Mishra, S. K., and Chaube, U. C. (2007). An extended hybrid model for synthetic unit hydrograph derivation. **J. Hydrology**, **336**, 347-360.
2. **Singh, P. K.**, Bhunya, P. K., Mishra, S. K., and Chaube, U. C. (2007). A sediment graph model based on SCS-CN method. **J. Hydrology** (Available online; In Press).
3. Bhunya, P. K., **Singh, P. K.**, Mishra, S. K., and Chaube, U. C. (2007). Fréchet and Chi-square Distributions Combined with Horton Ratios to Derive a Synthetic Unit Hydrograph (SUH). **Hydrological Sciences Journal** (Accepted).
4. **Singh, P. K.**, Bhunya, P. K., Mishra, S. K., and Chaube, U. C. (2007). A simple conceptual model of sediment yield. **Water Resources Management** . (Under review).
5. **Singh, P. K.**, Mishra, S. K., Chaube, U. C. (2007). A relook Look at the Soil Moisture Accounting Procedure in SCS-CN Methodology. **Hydrological Sciences Journal** (Communicated).